Influence of admixtures on the plastic shrinkage cracking of concrete

by
Burgert Daniel Le Roux

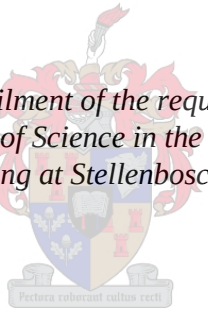

Thesis presented in fulfilment of the requirements for the degree of Master of Science in the Faculty of Engineering at Stellenbosch University

Supervisor: Mr Riaan Combrinck

March 2016

Declaration

I herewith declare that the work contained in this dissertation is my own, original work, and I am the titleholder of the copyright thereof. I have not previously submitted this dissertation in its entirety or in part for the purpose of receiving any qualification.

Date: March 2016

Summary

Plastic shrinkage cracking (PSC) is a well-known form of cracking in concrete at early ages and causes major concerns with regard to durability and aesthetical appearance of concrete structures. PSC is mainly attributed to tensile stresses arising in concrete due to a combination of capillary pressure and restraints provided by reinforcement and formwork. Concrete elements with large exposed surfaces, sited in areas with high evaporation rates, are prone to PSC. Although the phenomenological behaviour of PSC is well documented for normal concrete, the addition of admixtures to modern day concrete has resulted in unexpected and uncommon PSC behaviour. Therefore, the main objectives of this study are to determine both the phenomenological and fundamental influences of a wide range of admixtures at different dosages on the PSC of concrete.

Crack area measurements are used to determine the phenomenological influence of admixtures while measurement of surface tension, capillary pressure, bleeding, setting time, evaporation, shrinkage, and settlement are used to investigate the fundamental influences of admixtures. The experimental tests were conducted in a climate chamber with an ambient temperature of 40 °C, relative humidity of 10 % and a wind speed of 20.2 km/h. The associated admixtures include a minimum and maximum dosage of a glucose based retarder, calcium chloride based accelerator, chloride free air entraining agent, lignosulphonate plasticiser, shrinkage reducing admixture (SRA), poly carboxylate ethers (PCE) based super-plasticiser, and a sulphonated melamine formaldehyde (SMF) based super-plasticiser. A high flow concrete mix is used to accommodate the respective super-plasticisers whereas a conventional concrete mix is used to accommodate the remaining admixtures.

The influences of admixtures on PSC are determined by comparing the experimental results of mixes containing admixtures to a corresponding reference mix devoid from admixtures. The addition of the associated admixtures at different dosages altogether display a reduction in the severity of PSC compared to the reference mixes. The different dosage limits of the retarder and SMF-based super-plasticiser displayed a similar reduction in the severity of PSC. The addition of air entrainer, SRA and PCE-based super-plasticiser progressively reduced the severity of PSC since a higher dosage corresponds to a more profound reduction in cracking. Lastly, the minimum dosage of plasticiser and accelerator respectively exhibited a more substantial reduction in the severity of PSC compared to the maximum dosage. The associated phenomenological behaviour of admixtures is explained by referring to the underlying fundamental influences. Differences in the severity of PSC are mainly attributed to a reduction in surface tension and shrinkage with increasing content of the associated admixtures.

Opsomming

Plastiese krimp krake (PKK) is ‘n bekende vorm van krake wat ontstaan gedurende die eerste paar ure nadat beton gegiet is. PKK het ‘n nadelige gevolg aangaande die estetiese voorkoms van strukture en kan moontlik probleme veroorsaak in verband met die duursaamheid van beton. PKK word hoofsaaklik toegeskryf aan trekspannings wat voortspruit in beton as gevolg van kapilêre druk wat ontstaan weens hoë verdamping van samestellende water in die beton meng. Beton konfigurasies met ‘n groot oppervlakte wat blootgestel is aan verdamping is hoofsaaklik vatbaar vir die ontstaan van PKK. Die tipiese gedrag van PKK in beton is goed gedokumenteer alhoewel die invloed van bymiddels dikwels lei tot ongewone gedrag. Die doel van die studie is om die fenomenologiese - en fundamentele invloed van bymiddels op die plastiese krimp gedrag van beton te bepaal.

Die fenomenologiese invloed van bymiddels is vasgestel deur die uitvoer van kraak area toetse terwyl die oppervlakspanning, kapilêre druk, bloei, set tye, verdamping, krimp en versakking van beton onderskeidelik gemeet is om die fundamentele invloed van bymiddels te onsersoek. Die voorgenome toetse was uitgevoer in klimaat-beheerde toestande om ‘n hoë tempo van verdamping te bewerkstellig. Die verskeie toetse was blootgestel aan uiterste toestande vir verdamping met ‘n temperatuur van 40 °C, ‘n relatiewe humiditeit van 10 % en ‘n windspoed van 20.2 km/h. Die fenomenologiese - en fundamentele invloed van die volgende bymiddels is ondersoek in die studie: glukose-gebaseerde vertrager, klasium chloried versneller, “chloride free air entrainer”, “poly carboxylate ethers (PCE) based super-plasticiser”, “sulphonated melamine formaldehyde (SMF) based super-plasticiser”, “lignosulphonate based plasticiser” asook ‘n krimp-verlagende bymiddel. ‘n Hoë vloei beton meng is gebruik om die verskeie super-plastiseerders te akkommodeer terwyl ‘n konvensionele beton meng gebruik is om die oorblywende bymiddels te akkommodeer.

Die fenomenologiese - en fundamentele gedrag van die menge wat bymiddels bevat is vergelyk met ‘n verwysings mengsel wat geen bymiddels bevat nie om sodoende die invloed van die verskeie bymiddels vas te stel. Die toevoer van die voorgenome bymiddels het ‘n algehele afname in PKK tot gevolg gehad. Die toevoer van beide ‘n hoë en lae dosis van die vertrager asook die “SMF based super-plasticiser” het ‘n soortgelyke afname in PKK opgelewer. Die krimp-verlagende bymiddel, “air entrainer” asook die “PCE based super-plasticiser” het ‘n progressiewe mate van afname in PKK tot gevolg gehad. Die toevoegging van die minimum dosis van beide plastiseerder en versneller het ‘n meer noemenswaardige afname in PKK opgelwer in vergelyking met die toevoegging van ‘n ooreenstemmende maksimum dosis. Die voorgenome fenomenologiese gedrag van die verskeie menge is verklaar deur te verwys na die onderliggende fundamentele gedrag. Die verskil in fenomenologiese gedrag is hoofsaaklik toegeskryf aan die verlaging van oppervlakspanning en krimp weens die toevoer van die verskeie bymiddels.

Acknowledgements

I would like to thank the following people for their assistance and support throughout the course of this study:

- Firstly, I would like to thank my promoter, Riaan Combrinck, for his endless guidance and support throughout this study. I have learned and grown a lot under his supervision.
- I would like to thank the staff in the laboratory and workshop at the Civil Engineering Department of Stellenbosch University for their assistance during my experimental work. I especially would like to thank Peter and Chalton for their endless assistance and support.
- I would like to thank Chryso SA for the supply of admixtures. Their cooperation is greatfully acknowledged.
- I would like to thank my family and friends for their unconditional support and much needed distraction during the course of this study.
- Lastly, I would to thank my Creator for giving me the opportunity and ability to complete this study.

Table of Contents

List of figures

List of Tables

List of equations

List of Appendices

List of acronyms

AC_Min	Concrete mix containing a minimum dosage calcium chloride accelerator
AC_Max	Concrete mix containing a maximum dosage calcium chloride accelerator
AIR_Min	Concrete mix containing a minimum dosage chloride free air entrainer
AIR_Max	Concrete mix containing a maximum dosage chloride free air entrainer
ASTM	American Standard Testing Methods
C-S-H	Calcium silicate hydrates
FM	Fineness modulus
PCE	Poly carboxylate ethers
PCE_Min	Concrete mix containing a minimum dosage PCE-based super-plasticiser
PCE_Max	Concrete mix containing a maximum dosage PCE-based super-plasticiser
PL_Min	Concrete mix containing a minimum dosage glucose based plasticiser
PL_Max	Concrete mix containing a maximum dosage glucose based plasticiser
PPC	Pretoria portland cement
PSC	Plastic shrinkage cracking
PVC	Polyvinylchloride
RD	Relative density
REF	Reference mix
RET_Min	Concrete mix containing a minimum dosage glucose based retarder
RET_Max	Concrete mix containing a maximum dosage glucose based retarder
SANS	South Africa National Standards
SCC	Self-compacting concrete
SMF	Sulphonated melamine formaldehyde
SMF_Min	Concrete mix containing a minimum dosage SMF-based super-plasticiser
SMF_Max	Concrete mix containing a maximum dosage SMF-based super-plasticiser

S_Min	Concrete mix containing a minimum dosage SRA
S_Max	Concrete mix containing a maximum dosage SRA
SP	Super-plasticiser
SRA	Shrinkage reducing admixture
USA	United States of America

List of notations

C_2S	Dicalcium silicate
C_3S	Tricalcium silicate
C_3A	Tricalcium aluminate
C_4FA	Tetracalcium aluminoferrite
E	Evaporation rate [kg/m^2/h]
F	Magnitude of surface tension force [N]
L	Length of the line over which surface tension force acts [m]
P	Capillary pressure
r	Relative humidity [%]
R_1	Maximum radius of water menisci
R_2	Minimum radius of water menisci
T_{bt}	Concrete temperature [°C]
T_{kk}	Air temperature [°C]
V	Wind velocity [km/h]
γ	Surface tension

CHAPTER 1

Introduction

The term plastic shrinkage cracking (PSC) is used to describe cracks that form between the time of placement and final setting time of concrete. Concrete elements with large exposed surfaces, sited in areas with high evaporation rates, are prone to PSC. High evaporation rates are commonly encountered in South Africa being associated with high ambient temperatures, high wind speeds and a low relative humidity. Common examples of structural elements susceptible to PSC include bridge decks, industrial and residential floors, parking structures, wharves, podiums, and highway pavements amongst others. In addition to being unsightly, these cracks may reduce the durability of the concrete by acting as conduits for accelerated ingress of moisture and aggressive agents (Lura et al., 2007). This reduces the service life of concrete structures which gives PSC considerable economic significance in the construction industry (Dao et al., 2011).

PSC is mainly attributed to tensile stresses arising in concrete due to a combination of capillary pressure and restraints provided by reinforcement and formwork (Combrinck & Boshoff, 2013; Slowik et al., 2008). The capillary pressure is caused by evaporation of concrete pore water which causes menisci to form between adjacent solid particles on the surface of the concrete paste. These water menisci induce a negative capillary pressure in the concrete pore water which causes settlement and shrinkage of the plastic concrete. After reaching a certain pressure, menisci reach a break-through radius causing air to locally penetrate the pore system (Slowik et al., 2008). Capillary pressure in regions adjacent to the location of air entry is relieved through horisontal shrinkage until a plastic shrinkage crack is formed.

There are a number of effective measures to prevent or mitigate PSC, especially since PSC occurs in a relatively short time period. These measures generally focus on reducing the evaporation rate of the ambient environment. A widely used guideline is to ensure an evaporation rate less than 1 kg/m^2/h by implementing effective curing practices, wind breaks, and sunshades amongst other methods. The addition of low volume polymeric synthetic fibres to concrete is used as an internal method to reduce the risk of PSC to occur (Qi et al., 2003; Boshoff & Combrinck, 2013). However, preventative measures are often neglected or ineffective due to a lack of guidance and knowledge of PSC.

Application requirements, optimisation of construction periods, and complex design layouts of structural elements in modern day construction ensures the use of admixtures in concrete. Accordingly, it is of great significance to determine the influence of admixtures on PSC of concrete.

1.1 Problem statement

The influence of admixtures on fresh and hardened properties of concrete is well documented. However, research regarding the influence of admixtures on PSC is limited and although studies have been conducted to determine the influence of certain admixtures on PSC (Lura et al., 2007; Passuello et al., 2009; Leeman et al., 2014; Löfgren & Esping, 2014; Combrinck, 2012; Louw, 2014), the influence of the majority of admixtures on PSC remains unclear. Accordingly, various experimental tests are performed to provide a comprehensive understanding of the influence of a wide range of admixtures on PSC of concrete. The admixtures that are used to perform the experimental tests include a glucose based retarder, calcium chloride accelerator, chloride free air entraining agent, lignosulphonate based plasticiser, poly carboxylate ethers (PCE) based super-plasticiser, sulphonated melamine formaldehyde based super-plasticiser and a shrinkage reducing admixture.

1.2 Test objectives

Various experimental tests are used to investigate the phenomenological and fundamental influences of admixtures on the PSC of concrete. Phenomenological influence of admixtures refers to a physical increase or reduction in the severity of PSC whereas fundamental influences assist in explaining the phenomenological influence. In connection herewith, this study has the following test objectives:

- Determine the phenomenological influence of a wide range of admixtures at different dosages on the PSC of concrete, i.e. determine the physical increase or reduction in PSC.
- Determine the fundamental influence of the respective admixtures at different dosages on PSC of concrete to explain the corresponding phenomenological influence.

1.3 Methodology

Various experimental tests are performed to investigate the phenomenological and fundamental influences of the aforementioned admixtures on PSC of concrete. Crack area measurements are performed to determine the phenomenological influence of admixtures while tests for the measurement of surface tension, capillary pressure, bleeding, setting time, evaporation, unrestrained shrinkage, and settlement are performed to investigate the fundamental influences of admixtures.

Minimum and maximum dosages of the respective admixtures are used to perform the aforementioned tests to provide a progressive influence of admixtures on the PSC of concrete. The minimum dosages correspond to the recommended minimum dosage limits as prescribed by suppliers whereas the maximum dosages correspond to the maximum dosage permitted by the concrete mix without segregation. In addition, two different concrete mixes are respectively used to accommodate the wide range of admixtures. A conventional concrete mix is used to accommodate the addition of retarders, accelerators, air entrainers, plasticisers, and shrinkage reducing admixtures, respectively, whereas a high flow concrete mix is used to accommodate the addition of super-plasticisers.

The influence of admixtures on PSC is determined by comparing the experimental results of mixes containing admixtures to a corresponding reference mix. The respective reference mixes do not contain admixtures, although having the same mix design proportions than the mixes containing admixtures. Considering the fact that two different concrete mixes are used, test results are divided into two groups; phenomenological and fundamental influences of retarders, accelerators, air entraining agents, plasticisers, and SRA, respectively, are compared to that of the conventional concrete reference mix whereas corresponding influences of super-plasticisers are compared to that of the high flow concrete reference mix. Comparison of the fundamental influences is used to explain the related phenomenological behaviour of mixes containing the same admixture at different dosages.

1.4 Report layout

Chapter 2 provides a comprehensive background study on the PSC of concrete to provide the fundamental knowledge required to understand PSC. The various factors and mechanisms influencing PSC are discussed accordingly. The development process of PSC and preventative measures to inhibit or mitigate PSC are also discussed.

Chapter 3 provides the experimental framework. Relevant information regarding the test procedures, test setups, material specifications, and mix design proportions are discussed accordingly.

Chapter 4 provides the results and discussions of the conventional concrete mix with the addition of retarders, accelerators, air entrainers, plasticisers, and shrinkage reducing admixtures, respectively. The phenomenological behaviour of the associated admixtures are provided and discussed accordingly. Comparison of the fundamental influences is used to explain the related phenomenological behaviour of mixes containing the same admixture at different dosages.

Chapter 5 provides the results and discussions of the high flow concrete mix with the addition of super-plasticisers. The phenomenological behaviour of the associated super-plasticisers are provided and discussed accordingly. Comparison of the fundamental influences is used to explain the related phenomenological behaviour of mixes containing the same admixture at different dosages.

Chapter 6 provides the conclusions that are drawn concerning the phenomenological and fundamental influences of the respective admixtures on PSC, followed by relevant and feasible recommendations for future studies.

CHAPTER 2

Literature review

This chapter provides an introduction to plastic shrinkage cracking (PSC), followed by mechanisms required for PSC to occur. Thereafter, the development process of PSC is discussed, followed by factors influencing PSC. Although the addition of admixtures is regarded as a factor influencing PSC, it is reported in a separate section to signify the importance thereof. Lastly, preventative measures to inhibit or mitigate PSC are discussed.

2.1 Introduction to PSC

The term plastic shrinkage cracking is used to describe early age cracks that form between the time of concrete placement and final setting time (Boshoff & Combrinck, 2013). Concrete elements with large exposed surfaces, sited in areas with high evaporation rates, are prone to plastic shrinkage cracking. PSC is particularly of concern in countries with high evaporation rates such as Australia, South Africa, USA and the Middle East. In South Africa, high evaporation rates are associated with a high ambient temperature, high wind speed, and a low relative humidity. Common examples of structural elements susceptible to PSC include bridge decks, industrial and residential floors, parking structures, podiums, wharves, and highway pavements amongst others (Dao et al., 2010).

Figure 2.1 "Crazed" pattern of plastic shrinkage cracks in unreinforced concrete (Dao et al., 2011)

As illustrated in Figure 2.1, plastic shrinkage cracks typically exhibit a “crazed” pattern in unreinforced concrete whereas corresponding cracks typically mirror the layout of reinforcement in steel reinforced concrete (Boshoff, 2012). Crack lengths of shrinkage cracks typically vary between 50 and 1000 mm with crack spacings between 50 and 700 mm. The corresponding crack widths may reach 2 mm (Dao et al., 2011).

In addition to being unsightly, these cracks may reduce durability of concrete by acting as conduits for accelerated ingress of moisture and aggressive agents (Lura et al., 2007). The associated deterioration is predominantly attributed to carbonation and corrosion of reinforcement. PSC is of considerable economic significance in the construction industry as this phenomenon reduces the service life of concrete structures (Dao et al., 2011).

2.2 Mechanisms required for PSC

PSC is mainly attributed to tensile stresses arising in concrete due to a combination of capillary pressure and restraints provided by the reinforcement and formwork (Combrinck & Boshoff, 2013). It should be noted that PSC will not occur in the absence of restraint, capillary pressure build-up or air entry. These components are identified as the mechanisms required for PSC to occur, and are discussed accordingly.

2.2.1 Restraint

Restraint is regarded as one of the primary requirements for PSC to occur. In the absence of restraint, the concrete paste will shrink freely without any cracking (Boshoff & Combrinck, 2013). Restraints are, however, predominantly unavoidable in practice and include, amongst others:

- Friction provided by formwork
- Friction provided by the sub-grade (applicable to slabs on grade)
- Restraint provided by reinforcement steel
- Change in sectional depth
- Deformation gradient, i.e. the top surface of the concrete experiences higher shrinkage when compared to the lower part of the concrete

2.2.2 Capillary pressure

Capillary pressure is commonly referred to as matric suction, capillary tension, capillary suction, or sometimes simply suction (Dao et al., 2010). Capillary pressure in concrete is dependent on the rate of water loss, particle size distribution and surface tension of the pore fluid. The rate of water loss, in turn, relies on the rate of bleeding and evaporation. The aforementioned factors influencing capillary pressure is discussed accordingly in Section 2.4.

Initially, after concrete is placed, the bleeding rate typically exceeds the evaporation rate causing an accumulation of bleed water on the concrete surface. The accumulated bleed water temporarily inhibits capillary pressure build-up as the system of interconnected pores is completely filled with water (Slowik et al., 2008). Once the evaporation rate exceeds the bleeding rate, the accumulated bleed water is reduced until drying time is reached. Drying time of concrete is defined as the time when concrete pore water starts to evaporate (Boshoff & Combrinck, 2013). The onset of drying time causes the formation of water menisci between adjacent solid particles on the surface of the concrete paste. The curvature of water menisci surface induces negative capillary forces in the pore water which is commonly referred to as capillary pressure. As illustrated in Figure 2.2, the aforementioned forces act on the solid particles in both the vertical and horisontal direction resulting in settlement and shrinkage of the still plastic concrete (Slowik et al., 2008).

With reference to the Gauss-Laplace equation shown in below, capillary pressure in concrete is directly proportional to the surface tension of pore fluid and inversely proportional to radii of pores being emptied (Lura et al., 2007). Accordingly, a reduction in surface tension results in lower capillary pressure whereas smaller radii of menisci results in larger capillary pressure. Figure 2.2 illustrates how the respective radii are measured to calculate the capillary pressure.

illust tes ow th

$$P = -\gamma\left[\frac{1}{R1}\right]$$ Equation 2.1

where P is the capillary pressure [10^{-3} Pa]; R_1 is the radius of the meniscus [m]; and γ is the surface tension [mN/m].

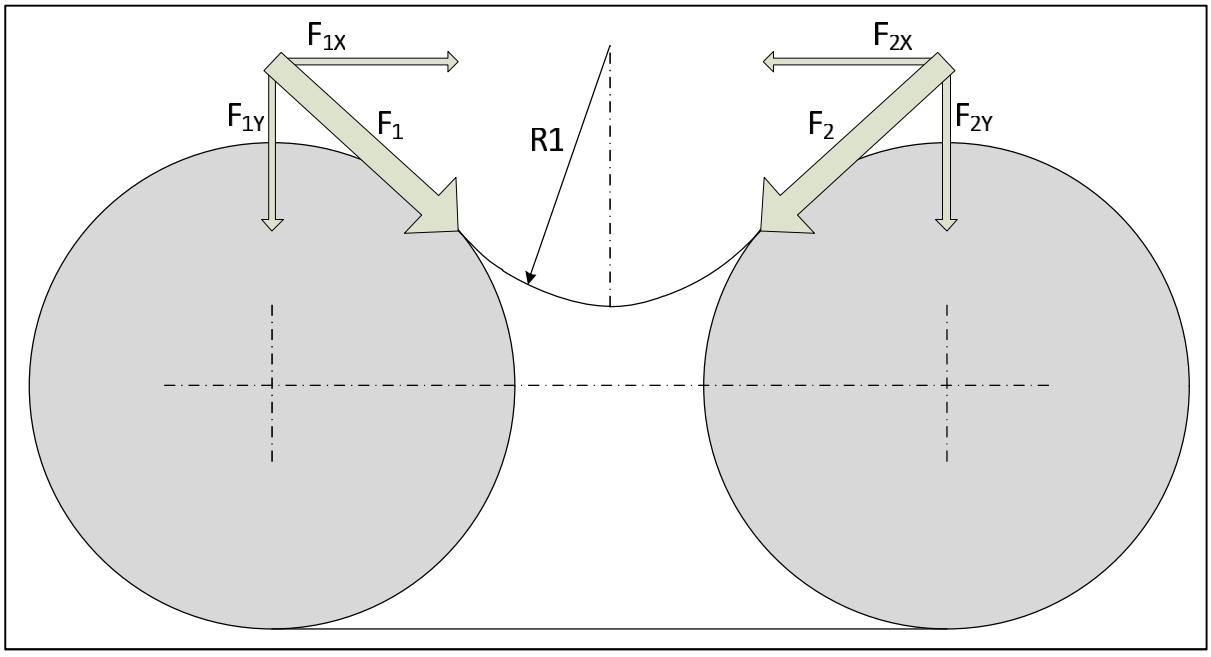

Figure 2.2 Capillary pressure in concrete pore structure (Slowik et al., 2008)

2.2.3 Air entry

The progressive evaporation of pore fluid reduces the radii of menisci and, correspondingly, increases capillary pressure. The aforementioned increase in capillary pressure is commonly referred to as capillary pressure build-up. The latter causes the network of solid particles to become progressively stiffer and, correspondingly, reduces settlement. After reaching a certain pressure, settlement reaches a maximum value as capillary pressure can no longer cause further vertical displacement of solid particles (Lura et al., 2007). This pressure is commonly referred to as the air entry value (Slowik et al., 2008). When the latter is reached, menisci reach a break-through radius causing air to locally penetrate the pore system, the system becomes unstable and a relocation of pore water takes place. Accordingly, certain pores are no longer completely filled with water although the solid particles remain interconnected by water sleeves. Research undertaken by Lura et al. (2007) found that the break-through radius of menisci, also referred to as the minimum radius, is approximately five to seven times smaller than the corresponding solid particle size.

Once air entry has occurred, PSC risk is assumed to reach a maximum. The drained pores form weak spots in the system as the contracting forces between the particles in air penetrated regions are considerably smaller than those in water filled regions. Subsequently, capillary pressure is relieved by a localisation of strain, i.e. cracking, through horisontal shrinkage (Slowik et al., 2008).

2.3 Development process of PSC

The development process of PSC can be categorised into five sequential phases starting directly after concrete is placed. The associated development phases are discussed accordingly in conjunction with Figure 2.3.

Phase I

Initially, after concrete is placed, the bleeding rate typically exceeds the evaporation rate causing the accumulation of bleed water on the concrete surface. The accumulated bleed water temporarily inhibits capillary pressure build-up as the system of interconnected pores is completely filled with water (Slowik et al., 2008). As illustrated in Figure 2.3, capillary pressure is positive in Phase I due to hydrostatic pressure within the pore fluid (Boshoff & Combrinck, 2013). At a certain point in time, the evaporation rate exceeds the bleeding rate causing a reduction of the accumulated bleed water on the surface of the bulk paste. The film of bleed water is progressively reduced to the surface although evaporation of pore water has not yet started.

Phase II

Drying time - being defined as the time when concrete pore water starts to evaporate - is reached during this phase (Boshoff & Combrinck, 2013).

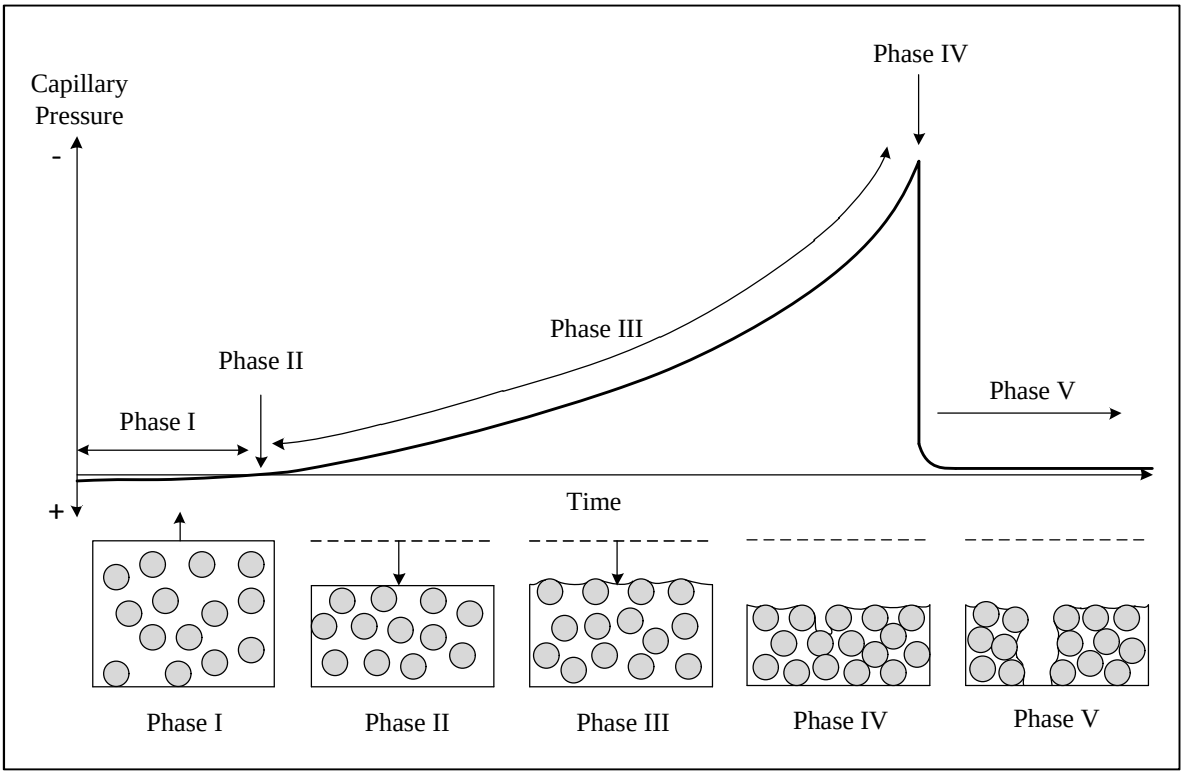

Figure 2.3 Development of PSC (Combrinck, 2012)

Phase III

After the drying time is reached, menisci start to form between adjacent solid particles on the surface of the concrete paste. The curvature of the menisci surface induces capillary tension forces in the pore water which is commonly referred to as negative capillary pressure. As discussed in Section 2.2.2, the capillary pressure acts on the solid particles both vertically and horisontally resulting in settlement and shrinkage of the still plastic concrete (Slowik et al., 2008). As particles are contracted, the pore sizes are reduced resulting in more water being forced to the concrete surface. The rate at which this water accumulates on the surface is continually exceeded by the evaporation rate and, therefore, only temporarily relieves the capillary pressure (Combrinck & Boshoff, 2013). The progressive evaporation of pore fluid reduces the radii of liquid-air menisci and, correspondingly, causes capillary pressure build-up. The latter causes the network of solid particles to become progressively stiffer and, correspondingly, reduces settlement. Maximum settlement is reached when capillary pressure can no longer cause further vertical displacement of solid particles (Lura et al., 2007). This phase continues until maximum vertical settlement is reached.

Phase IV

Air entry commonly coincides with the maximum settlement of the concrete paste. When air entry is reached, menisci reach a break-through radius causing air to locally penetrate the pore system; the system becomes unstable and a relocation of the water takes place. Accordingly, certain pores are no

longer completely filled with water although the solid particles remain interconnected by water sleeves. Once air entry is reached, PSC risk is assumed to reach a maximum as the drained pores cause weak spots in the system (Slowik et al., 2008). These weak spots locally relieve capillary pressure as the adjacent particles are able to undergo horisontal shrinkage. As illustrated in Figure 2.3, this phenomenon is locally characterised by a sudden drop in capillary pressure. From this point onwards, the horisontal component of capillary pressure will contribute to the formation of cracks; the vertical component of pressure no longer influences the cracking process as maximum settlement is already reached. It should furthermore be noted that air entry occurs at a localised position and does not occur uniformly over the surface of concrete (Slowik et al., 2008).

Phase V

Figure 2.4 illustrates the formation of a plastic shrinkage crack after air entry is reached. Particles adjacent to the location of air entry continue to experience capillary pressure build-up. The location of air entry form weak spots in the system as the contracting forces between the particles in air penetrated regions are considerably smaller than those in water-filled regions. Consequently, capillary pressure is relieved through shrinkage of the concrete paste in the water-filled regions. Shrinkage allow these particles to be drawn closer to each other until a plastic shrinkage crack is formed.

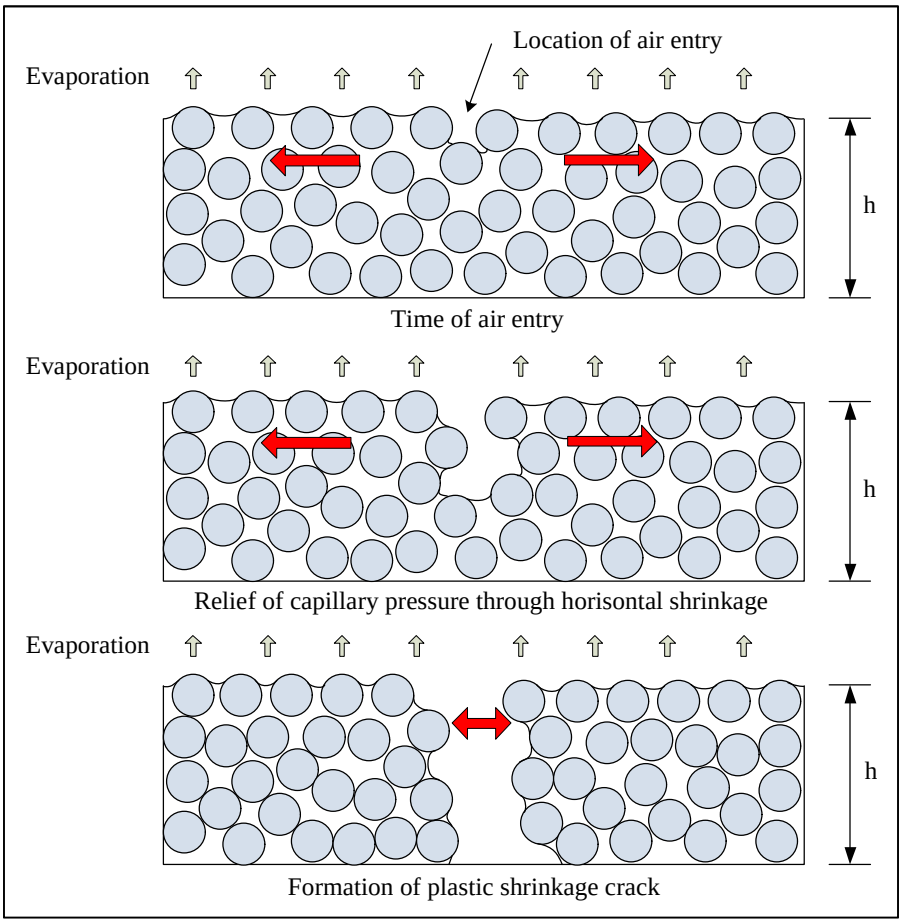

Figure 2.4 Formation of a plastic shrinkage crack

2.4 Factors influencing PSC

PSC is the result of a complicated combination of various interdependent factors that change rapidly over time (Dao et al., 2010). Plastic concrete is extremely fragile and its properties are highly time-dependent and influenced by various factors, which include:

- Restraint
- Capillary pressure
- Air entry
- Evaporation
- Bleeding
- Particle size distribution
- Surface tension
- Paste mobility
- Setting time
- Plastic settlement cracking, and
- Admixtures

The influence of restraint, capillary pressure and air entry are regarded as the mechanisms responsible for PSC and are not presented in this section as it is discussed in Section 2.2. Furthermore, the influence of admixtures is reported separately in Section 2.5 to signify the importance thereof for this study. The influences of evaporation, bleeding, particle size distribution, surface tension, paste mobility, setting time, and plastic settlement cracking on PSC are discussed accordingly.

2.4.1 Evaporation

Evaporation is defined as the process where a liquid is converted to a gas or vapour (Uno, 1998). Evaporation occurs if heat energy is absorbed into the liquid or when vapour pressure above the liquid surface is lower than that in the liquid itself, thus allowing active water molecules to escape as vapour. High evaporation rates significantly increase the risk for PSC. Evaporation rates are dependent on the ambient temperature, concrete temperature, wind speed, relative humidity, and solar radiation (Uno, 1998). In South Africa, high evaporation rates are commonly associated with high ambient temperatures, high wind speeds and a low relative humidity (Boshoff & Combrinck, 2013).

The evaporation rate from the surface of freshly-cast concrete can be estimated by using a three-component chart or its underlying formula. With reference to the equation provided below, the evaporation rate is expressed as a function of wind speed, air temperature, concrete temperature and relative humidity. The effect of solar radiation is also accounted for since the formula was derived from experiments being exposed to solar radiation for both clear and cloudy days (Uno, 1998).

$$E = 5 \cdot ([T_c + 18]^{2.5} - r \cdot [T_a + 18]^{2.5}) \cdot (V + 4) \cdot 10^{-6}$$ Equation 2.2

where E is the estimated evaporation rate [kg/m^2/h]; T_c and T_a are the concrete and air temperatures [°C]; r is the relative humidity [%]; and V is the wind speed [km/h].

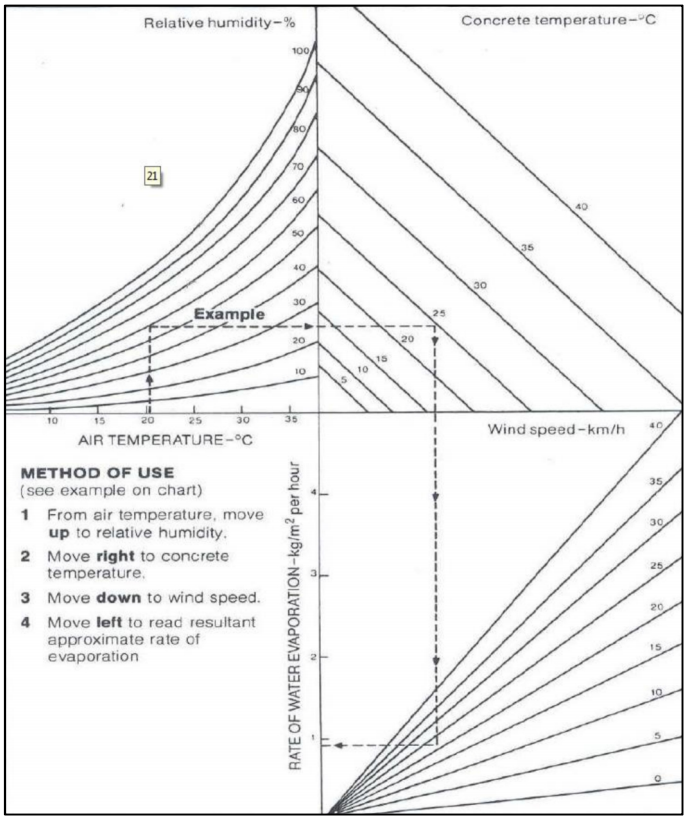

Figure 2.5 Nomograph for estimation of evaporation rates (Uno, 1998)

The nomograph and its underlying mathematical expression are used to estimate the evaporation rate from a water surface; however, when pore water starts to evaporate these measures overestimate subsequent evaporation by a factor as much as two or more. Accordingly, the estimated evaporation rate should be regarded as the potential evaporation rate until drying time is reached, after which the evaporation rate is expected to decrease (Dao et al., 2010). The interdependent factors influencing the evaporation rate are discussed accordingly.

2.4.1.1 Wind

Wind is considered to be an important factor to take into account when trying to prevent PSC. A reduction in local wind speed at the surface of freshly-placed concrete significantly reduces the evaporation rate. The presence of wind increases the evaporation rate by continually replacing saturated air with non-saturated air (Dao et al., 2010). Wind speed is measured or estimated using ventimeters, anemometers, wind socks or general observation of surrounding elements (Uno, 1998).

2.4.1.2 Relative humidity

Relative humidity is defined as the amount of moisture present in air expressed as a percentage of the amount needed for saturation at the same temperature. A reduction in local relative humidity will increase the rate of evaporation. If air is fully saturated, i.e. relative humidity equals 100 %, evaporation normally ceases, unless other factors such as wind or air temperature alter this condition. An increase in air temperature reduces relative humidity and, correspondingly, increases the evaporation rate. Relative humidity readings can be obtained by contacting the local Weather Bureau or by using a sling psychrometer (Uno, 1998).

2.4.1.3 Air temperature

Ambient air temperature influences the relative humidity and concrete temperature. An increase in air temperature increases the moisture holding capacity of air and, correspondingly, reduces the relative humidity, given no moisture is added to the air (Valsson & Bharat, 2011). A low ambient air temperature will reduce the concrete temperature, provided the air temperature is low enough to ensure a substantial thermal gradient between the concrete paste and the surrounding air. Measurement of air temperature using a thermometer should be performed away from direct sunlight to minimise direct solar radiation (Uno, 1998).

2.4.1.4 Concrete temperature

As previously mentioned, evaporation occurs when vapour pressure above the liquid surface is lower than that in the liquid itself, thus allowing active water molecules to escape as vapour. Herewith should be noted that the temperature of bleed water is required to determine the difference in the vapour pressure between the water surface and surrounding air. Since it is difficult to measure the temperature of bleed water, concrete temperature is used as a proxy, based on the assumption that concrete temperature is constant throughout the mix during the plastic state. Vapour pressure of concrete pore water is directly proportional to concrete temperature as an increase in concrete temperature causes an increase in vapour pressure. Consequently, increased concrete temperature allows active water molecules to escape the bleed water as vapour (Uno, 1998). Concrete temperature, in turn, is dependent on solar radiation and the temperature of constituent materials at the time of mixing. Reducing the temperature of constituent materials prior to mixing is regarded as an effective method to reduce concrete temperature and, more importantly, reducing evaporation.

2.4.1.5 Solar radiation

Direct solar radiation from the sun increases ambient air temperature, concrete temperature and the rate of hydration of cement. The latter correspondingly results in higher initial strength gain of concrete. Researchers have different opinions concerning the effect of direct solar radiation on the severity of PSC. Certain researchers believe that slabs cast in the shade will exhibit more cracking due

to a lower hydration rate, whilst others believe that slabs cast in the shade will exhibit less cracking due to a lower evaporation rate (Uno, 1998). However, it is speculated that an increased evaporation rate bears more concern for PSC when compared to an increased rate of hydration. The reason being is that PSC generally occurs within the first few hours after casting where an increased evaporation rate is believed to a have a more significant influence on cracking compared to an increased rate of hydration. This means an increase in solar radiation will increase the ambient evaporation rate and, correspondingly, increase the risk for PSC.

2.4.1.6 Interaction of interdependent factors

Figure 2.6 provides examples to demonstrate the interaction of the aforementioned factors that influences the evaporation rate of concrete water.

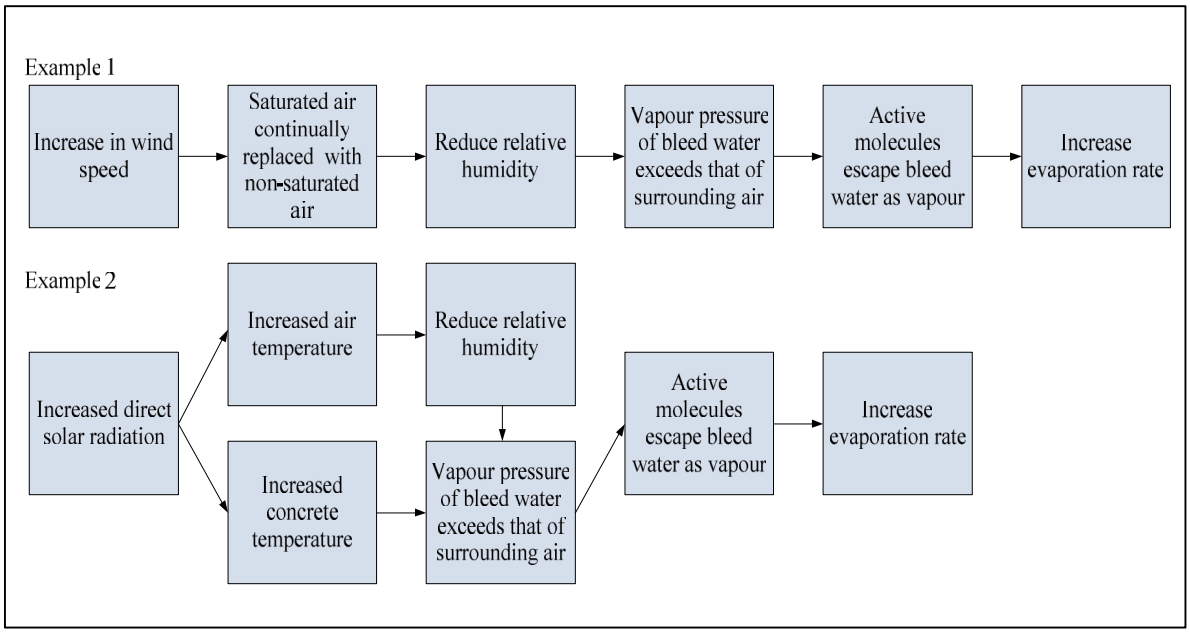

Figure 2.6 Evaporation flowchart

2.4.2 Bleeding

Bleeding is defined as a process where pore water is forced to the surface during settlement and consolidation of solid particles in the concrete paste. Concrete pore water is forced to the surface due to the inability of the solid particles to retain pore water during settlement and consolidation. In addition, water has the lowest specific gravity of all constituent materials in a concrete mix. Bleeding is attributed to two independent forces, namely, gravity and capillary pressure (Dao et al., 2010). The latter is only applicable if the drying time of concrete is reached. The time when bleeding ceases typically coincides with the initial setting time of concrete (Boshoff & Combrinck, 2013). Furthermore, bleeding ceases when the solid particles are fully consolidated or when hydration products prevent any further settlement of solid particles (Mehta & Monteiro, 2006).

Prior to 1960, the bleeding rates of concrete generally ranged between 0.5 and 1.5 kg/m^2/h. However, modern day concretes with low water-binder ratios and increased fines content commonly exhibit bleed rates significantly less than 1 kg/m^2/h (Dao et al., 2010). The corresponding reduction in bleeding capacity has significant implications concerning the limits placed on evaporation rates to minimise PSC. The extent to which bleeding occurs is governed by concrete permeability, section depth, water absorption, and vibration of concrete (Uno, 1998). The underlying factors influencing bleeding are discussed accordingly.

2.4.2.1 Permeability

Permeability has the most pronounced effect on the bleeding rate of concrete. Permeability is defined as "the rate at which a fluid is transmitted through a saturated specimen of concrete under an externally maintained hydraulic gradient" (C&CI, 1997). Correspondingly, concrete with low permeability has a reduced rate of bleeding due to a lower rate at which bleed water is transmitted through the saturated body (Mehta & Monteiro, 2006).

The permeability of concrete is dependent on the fines content of the concrete mix where a high fines content is typically associated with a low permeability. Fine constituent materials, such as cement, fine aggregate, condensed silica fumes, fly ash, and slag reduce the bleeding capacity of concrete due to the higher surface area of particles presented to the mixing water volume. Furthermore, the increased proportion of fine particles reduces the rate of settlement as these particles are subject to lower gravitational forces (Mehta & Monteiro, 2006).

2.4.2.2 Capillary pressure

With reference to Section 2.2.2, capillary tension forces act on solid particles both vertically and horisontally. The vertical component of capillary pressure causes additional settlement of solid particles and, correspondingly, results in increased bleeding (Slowik et al., 2008).

2.4.2.3 Depth of section

The depth of a concrete section influences the total bleeding capacity since a deeper section is associated with an increased bleeding volume. The increased bleeding volume is attributed to the fact that more solid particles are subject to settlement (Uno, 1998). The increased bleeding capacity will reduce the rate of water loss from the concrete paste and, more importantly, reduce the risk for PSC.

2.4.2.4 Water absorption

External and internal water absorption in concrete cause a reduction in the total amount of bleeding (Dao et al., 2010). External absorption refers to water that is absorbed through unsaturated formwork or underlying sub-grade whereas internal absorption refers to water that is absorbed by unsaturated aggregate particles in the mix.

2.4.2.5 Vibration

The application of internal vibration, using a poker vibrator amongst other methods, is used to mechanically consolidate concrete by removing entrapped air. Prolonged vibration can result in segregation of a concrete mix and, correspondingly, increase the total amount of bleeding. Overvibration is not considered to be a concern unless high-slump, improperly proportioned concrete is being used. Excessive external vibration due to nearby machinery or traffic can also cause a concrete mix to segregate, thus increasing the total bleeding volume (Suprenant, 1988). Segregation, in turn, is attributed to the excessive reduction in friction between aggregate particles which allow them to settle through the concrete paste (Owens, 2009). Conclusively, overvibration from both internal and external vibration methods increases the total amount of bleeding.

2.4.3 Particle size distribution

Particle size distribution influences the magnitude of capillary pressure in concrete. As discussed in Section 2.2.2, capillary pressure in concrete is inversely proportional to radii of pores being emptied and, therefore, a smaller radius of menisci will result in a higher capillary pressure. In addition, research undertaken by Lura et al. (2007) found that the break-through radius of menisci is approximately five to seven times smaller compared to the corresponding solid particle sizes.

In addition to particle size, particle size distribution is an important factor influencing capillary pressure build-up. A high distribution of smaller particles in a unit surface area will result in a much higher capillary pressure when compared to a distribution of larger particles in the same unit surface area (Lura et al., 2007). Variations in particle size distribution in the surface of concrete paste give rise to non-uniform capillary pressure build-up and, correspondingly, validates the occurrence of air entry at a localised position.

2.4.4 Surface tension

As discussed in Section 2.2.2, capillary pressure is directly proportional to surface tension of the pore fluid in the concrete paste and, therefore, a reduction in surface tension reduces capillary pressure and, correspondingly, lessens the risk of PSC to occur (Lura et al., 2007).

It is generally accepted that surface tension has an insignificant influence on PSC when concrete elements devoid from admixtures are compared, provided the same water source is used. The addition of admixtures, however, can significantly influence the surface tension of the pore fluid. This section provides a fundamental understanding of surface tension and together with a discussion regarding the influence of admixtures on surface tension.

2.4.4.1 Surface tension of water

Surface tension of water arises from strong attractive forces between adjacent molecules, called hydrogen bonds. Figure 2.7 illustrates the molecular basis for surface tension by considering attractive forces between water molecules. Figure 2.7 (a) illustrates a molecule within the bulk liquid whereas Figure 2.7 (b) illustrates a molecule on the surface of the liquid. The molecule in a) is attracted equally in all directions by surrounding molecules and, correspondingly, experiences a zero net force. In contrast, the molecule in b) experiences a net attractive force acting toward the interior of the bulk liquid. This net attractive force is referred to as the surface tension of water. The corresponding surface tension forces cause contraction toward the interior of the bulk liquid until repulsive colloidal forces from other water molecules prevent any further contraction. The point of maximum contraction corresponds to the minimum surface area of the liquid (He et al., 2015). In nature, water has one of the highest surface tensions, 72.8mN/m (at 20°C), only exceeded by very few liquids such as mercury. The formula for calculation of surface tension is:

$$\gamma = \frac{F}{L}$$ Equation 2.3

where γ is the surface tension [N/m]; F is the magnitude of the force exerted parallel to the surface [N]; and L is the length of the line over which the force acts [m].

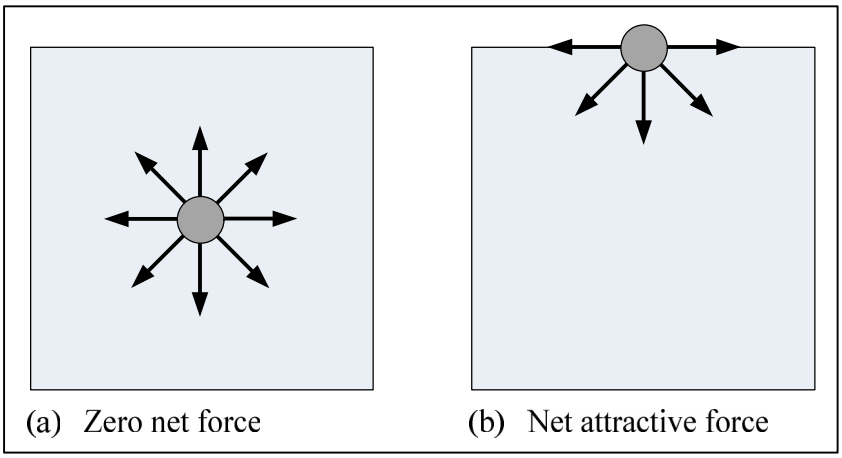

Figure 2.7 Attractive forces in liquid

2.4.4.2 Influence of surfactants on surface tension

Shrinkage reducing admixtures (SRA) belong to a class of organic chemicals known as surfactants. At molecular level, surfactants are amphiphilic, i.e. each surfactant is composed of a hydrophilic (polar) head that is covalently bonded to a hydrophobic (non-polar) tail. The polar head of each surfactant can be ionic or non-ionic and is attracted by hydrogen bonding solvents, such as water, and oppositely charged surfaces. The non-polar tail is a hydrocarbon chain that is attracted by non-polar solvents, such as oil, but is repelled from polar solvents such as water (Rajabipour et al., 2008).

Surface tension of water manifests the so-called hydrophobic effect, which is characterised as the driving force for adsorption and formation of micelles by amphiphilic molecules as illustrated in Figure 2.8. When dissolved in water, amphiphilic molecules are adsorbed to the liquid-air interface and orient so as to have their hydrophilic head with water, while projecting the hydrophobic tail into the air. Accordingly, hydrophobic tails escape from contacting water by forming a surface monolayer. Adsorption of amphiphilic molecules at the liquid-air interface reduces the interfacial energy and, correspondingly, reduces the surface tension of the pore fluid (He et al., 2015).

There is a natural saturation limit for the number of surfactant molecules adsorbed to a liquid-air interface, which is generally based on electrostatic repulsion between polar heads of adjacent surfactant molecules. Once the aforementioned limit is reached, surface tension will not be further reduced. As illustrated in Figure 2.8, excess surfactant molecules remain in bulk water as monomers or in the form of micelles. Micelles form by aggregation of approximately 20 to 100 surfactant molecules attributable to the hydrophobic effect. Hydrophobic tails are hidden inside the micelle core to reduce unfavourable contact with water molecules, while the micelle surface consists of hydrophilic heads (Rajabipour et al., 2008).

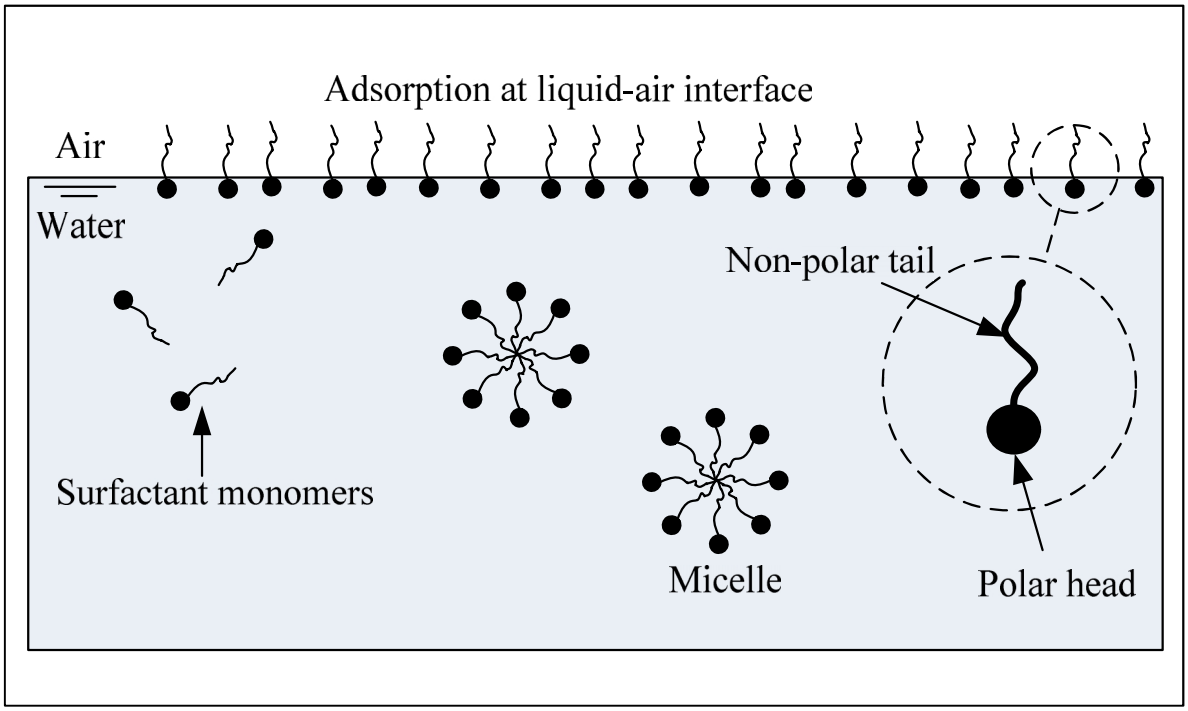

Figure 2.8 Adsorption of surfactants at liquid-air interface (Rajabipour et al., 2008)

In conclusion, the addition of surfactants reduce the surface tension of water through adsorption of amphiphilic molecules to the liquid-air interface. Surface tension is reduced until the natural saturation limit is reached after which excess surfactant molecules serve no purpose and remain in the bulk water as monomers or in the form of micelles.

2.4.4.3 Influence of admixtures on surface tension

No literature could be found regarding the influence of admixtures on surface tension. As previously discussed, water has a very high surface tension that is seldomly exceeded by other liquids (He et al., 2015). Accordingly, it is speculated that the addition of admixtures will weaken the hydrogen bonds between adjacent water molecules and, correspondingly, reduce the surface tension of the pore fluid. This is investigated further in this study.

2.4.5 Paste mobility

Paste mobility is defined as the ease by which concrete paste is able to flow or deform when subjected to a force. Concrete is considered to have a high paste mobility if the constituent particles can easily move and rotate relative to each other under an applied force. High paste mobility increases the risk of PSC to occur as the paste is more susceptible to deformations such as shrinkage. Paste mobility is mainly influenced by aggregate characteristics such as particle shape, surface texture, and average particle size (Slowik et al., 2008). The application of a load onto concrete paste forces particles to move and rotate relative to each other where the ease with which such movements can occur is influenced by the particle shape and surface texture. Smooth, rounded particles increase paste mobility as they are more mobile when compared to rough, angular particles (Owens, 2009).

In well-proportioned mixes, smaller aggregate sizes tend to improve paste mobility due to smaller gravitational forces acting on the particles. The smaller gravitational force makes the particles more susceptible to deformations caused by the horisontal component of capillary pressure (Powers, 1968; Owens, 2009). In conclusion, small aggregate sizes, smooth surface texture and rounded particle shape result in high paste mobility and, correspondingly, increase the risk for PSC.

2.4.6 Setting time

Initial and final setting time are the most important junctures with regard to setting of concrete. However, these junctures do not mark a sudden change in the physical or chemical nature of the concrete paste. Initial set defines the time limit for handling and placement of concrete whereas final set indicates the start of mechanical strength development. Setting times depend on the water-binder ratio of concrete where a lower water-binder ratio reduces initial and final setting times, provided the same cement content and aggregate grading is used (Kruml, 1990).

The reactions and resultant changes in the physical state do not proceed at a uniform rate and, therefore, it is convenient to divide the setting of concrete into three phases, being identified as stiffening, solidification and hardening (Mehta & Monteiro, 2006).

2.4.6.1 Hydration of cement

Hydration of cement refers to the chemical reaction between water and cement to form a rock-like material. The hydration process consists of various reactions which occur simultaneously at different rates. An increase in ambient or concrete temperature increases the rate of hydration reactions considering the fact that no reactions occur below -10 °C (Domone & Illston, 2010). The main components required for hydration of cement include aluminates (C_3A and C_4AF) and silicates (C_2S and C_3S).

Aluminates in cement include tricalcium aluminate (C_3A) and tetracalcium aluminoferrite (C_4AF). Aluminates are known to hydrate at a much faster rate when compared to silicates. In fact, stiffening and solidification characteristics are largely determined by hydration reactions involving aluminates (Mehta & Monteiro, 2006).

Several hydraulic calcium aluminates may occur in standard portland cement clinker including C_3A which is the principal aluminate compound. In pure form, the reaction of C_3A with water is immediate and results in an abrupt stiffening of the concrete paste, commonly referred to as a flash set. Flash setting is associated with a large heat evolution and a poor ultimate strength of concrete. In order to prevent flash setting, gypsum is added to the clinker to retard the initial hydration of C_3A. The C_4AF phase reaction, commonly referred to as the ferrite phase reaction, is similar to that of C_3A, also involving gypsum. Generally, the reactivity of the ferrite phase is somewhat slower than C_3A (Mehta & Monteiro, 2006).

Calcium silicates form the bulk of unhydrated cement paste, and include dicalcium silicate (C_2S) and tricalcium silicate (C_3S). The impure forms of C_3S and C_2S are known as alite and belite respectively (Mehta & Monteiro, 2006). The hydration products of calcium silicates are responsible for important engineering properties of concrete, such as strength and stiffness. These silicate reactions therefore dominate the properties of concrete and are extremely important (Domone & Illston, 2010).

The reaction of C_3S produces calcium silicate hydrate and calcium hydroxide, also referred to as C-S-H crystals and portlandite respectively. Although belite reacts slower than alite, it produces identical products that have a major contribution to the long-term strength of hardened concrete. C-S-H crystals constitute up to 50 to 60 % of the volume of solids in a completely hydrated cement paste. C-S-H crystals have a layer structure with a very high surface area, and are responsible for the strength of hardened concrete. Calcium hydroxide crystals constitute 20 to 25 % of the volume of solids in a completely hydrated cement paste. The latter tends to form large crystals with distinctive hexagonal-prism morphology. Compared to C-S-H, the strength contributing potential of portlandite is limited as a result of its considerably lower surface area (Mehta & Monteiro, 2006).

2.4.6.2 Phases of setting

The three phases of setting, being defined as *stiffening*, *solidification*, and *hardening* are discussed accordingly in conjunction with Figure 2.9.

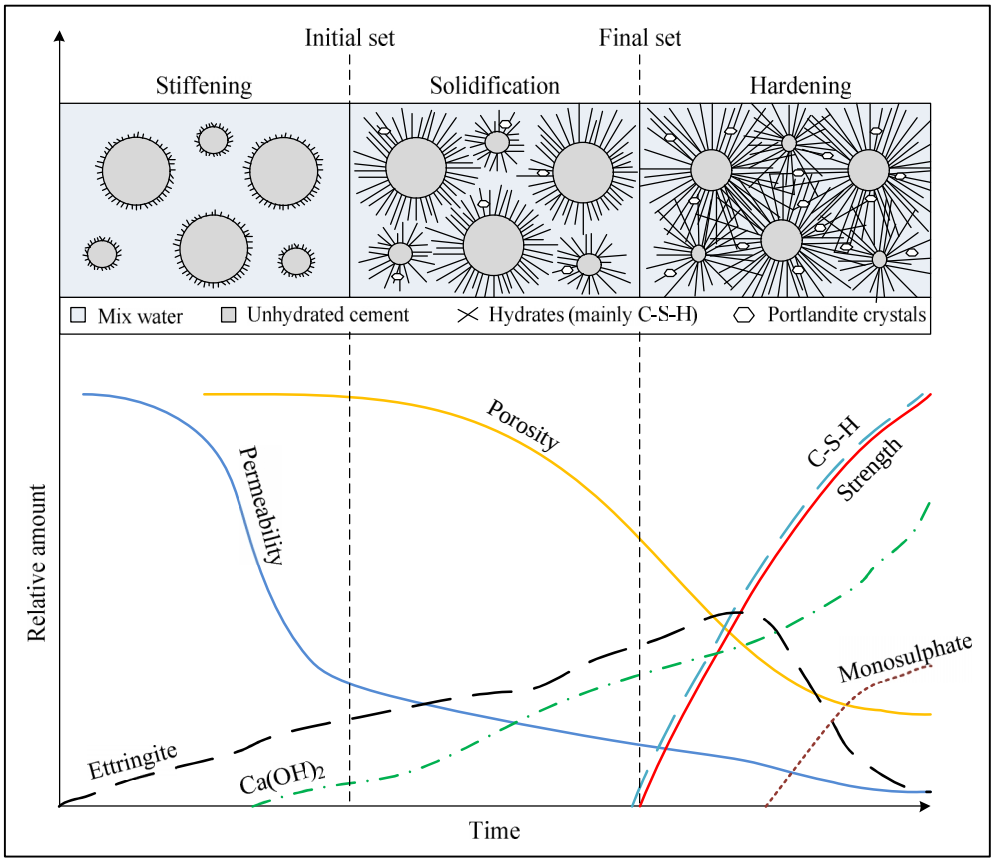

Figure 2.9 Setting of concrete (Mehta & Monteiro, 2006; Domone & Illston, 2010)

Stiffening is the first phase of concrete setting and is associated with a loss of consistency of the concrete paste which can be depicted by the slump loss phenomenon. Stiffening characteristics are largely determined by hydration reactions involving aluminates such as C_3A which reacts with gypsum to form calcium sulphoaluminate, commonly known as ettringite (Mehta & Monteiro, 2006). As shown in Figure 2.9, the production of ettringite occurs directly after concrete is mixed. As gypsum is consumed, ettringite reacts with the remaining C_3A to produce calcium monosulphoaluminate, which is one of the final products of cement hydration (Domone & Illston, 2010). This is illustrated by Figure 2.9 as the concentration of monosulphoaluminate only increases once the concentration of ettringite starts to decrease. The concrete paste has little or no strength during the stiffening phase since hardening only starts once final setting time of concrete is reached. Although a trivial amount of alite is hydrated during this phase to produce C-S-H, the amount is considered to have an insignificant influence on the strength of concrete as illustrated in Figure 2.9.

The gradual loss of free pore water during this phase causes a reduction in plasticity of the mix and, correspondingly, causes the concrete paste to stiffen. The loss of free pore water is attributed to

various factors, which include evaporation, absorption by formwork, unsaturated aggregates and sub-grade, formation of hydration products, and adsorption by poorly crystalline products such as ettringite and C-S-H. As indicated in Figure 2.9, the formation of hydration products during this phase significantly reduces the permeability of the concrete paste. The stiffening phase ends once initial setting time is reached (Mehta & Monteiro, 2006).

The *solidification* phase starts once initial setting time is reached, after which the concrete paste is unworkable as it is difficult to apply or perform tasks such as concrete placement, compaction and finishing operations. Solidification does not occur immediately as the concrete requires considerable time to become fully rigid.

A small amount of calcium hydroxide and C-S-H continue to fill the empty space formerly occupied by water and dissolving cement particles. However, as in the stiffening phase, the trivial amount of C-S-H crystals being produced is considered to have an insignificant influence on the strength of concrete. The reaction of gypsum and C_3A continues to produce ettringite during the solidification phase. Continual production of ettringite, calcium hydroxide, and C-S-H causes the concrete paste to become fully rigid and, correspondingly, reduces porosity of concrete as illustrated by Figure 2.9. The time when concrete becomes fully rigid coincides with the final setting time, and of marks the end of the solidification phase (Mehta & Monteiro, 2006).

The phenomenon of strength gain with time is called *hardening* of concrete. C-S-H, calcium sulphoaluminate hydrates and hexagonal calcium aluminate hydrates, respectively, possess enormous surface area and adhesive capability. These hydration products tend to adhere strongly not only to each other, but also to low surface-area solids, such as calcium hydroxide, unhydrated clinker grains and coarse aggregate particles. The strength of concrete, however, is mainly dependent on the production of C-S-H (Mehta & Monteiro, 2006).

Final setting time marks the beginning of significant alite hydration which is responsible for production of C-S-H and calcium hydroxide. Hydration of alite continues rapidly for several weeks and, correspondingly, causes an increase in strength as illustrated in Figure 2.9. Although belite reacts slower than alite, it produces identical products that make a significant contribution to the long-term strength of hardened concrete (Mehta & Monteiro, 2006; Domone & Illston, 2010). As illustrated in Figure 2.9, progressive filling of void spaces with hydration products causes further reduction of porosity and permeability of the concrete paste during the hardening phase.

2.4.6.3 Importance of setting on PSC

PSC is typically characterised by a rapid growth and stabilisation of cracks between initial and final setting time of concrete (Boshoff & Combrinck, 2013). Accordingly, these time measures provide an estimation of when cracking is expected to occur. The latter is especially important for application of preventative measures as discussed in Section 2.6.

The tensile strain capacity of concrete in its fresh state significantly exceeds that in its hardened state. Strain capacity refers to the maximum tensile deformation that a material can undergo before it fails, i.e. cracks. Cracking occurs when the mechanical strain induced by applied loading exceeds the strain capacity of the concrete paste. In connection herewith, research undertaken by Boshoff & Combrinck (2013) found that strain capacity of concrete reaches its lowest value around the initial setting time of concrete. In addition, Krönlof et al. (1995) found that concrete has sufficient capacity to resist capillary forces after initial set is reached. Accordingly, initial setting time provides an estimation of when PSC may occur.

2.4.7 Plastic settlement cracking

Plastic settlement cracking is a prominent form of cracking in the fresh state of concrete that influences PSC. This section provides a general discussion of plastic settlement cracking, followed by the mechanisms required for plastic settlement cracking to occur. Thereafter, the interaction between plastic settlement cracking and PSC is discussed.

2.4.7.1 General

Plastic settlement cracking occurs during the plastic state of concrete where the cracks typically form between the time of concrete placement and initial setting time. Settlement cracking ceases when maximum settlement is reached and typically coincides with the initial setting time of concrete.

Settlement cracking is caused by differential settlement, i.e. non-uniform settlement occurring in different regions of the concrete paste. A region subject to a uniform amount of settlement is commonly referred to as a settlement zone. Differential settlement induces tensile stresses between the boundaries of adjacent settlement zones and, correspondingly, encourages the formation of cracks at these locations (Combrinck & Boshoff, 2012). Differential settlement is reliant on the presence of vertical restraint which is typically provided by steel reinforcement or a change in sectional depth. In addition, settlement cracking patterns typically coincide with the reinforcement layout or locations of change in sectional depth (Kwak et al., 2010). The corresponding cracks originate at the position of vertical restraint and progressively develop towards the surface of the concrete. Accordingly, settlement cracks may be present without being visible on the surface of concrete paste (Combrinck & Boshoff, 2012).

Settlement cracks are unsightly and may reduce the durability of concrete by causing premature exposure of reinforcing steel to water and chloride ions, thus making concrete more susceptible to carbonation and corrosion of steel reinforcement. In addition, settlement can generate a pocket of water under embedded reinforcement, thereby resulting in a poor bond between concrete and steel reinforcement (Kwak et al., 2010).

2.4.7.2 Mechanisms required for plastic settlement cracking

As previously discussed, settlement cracking is attributed to differential settlement caused by steel reinforcement or changes in sectional depth.

Steel reinforcement within a concrete section provides vertical restraint that is required for differential settlement. As illustrated in Figure 2.10, a larger amount of settlement occurs at a distance farther away from the reinforcement bars. Consequently, respective settlement zones are formed which result in the development of tensile stresses above and next to the location of reinforcement as shown in Figure 2.10. The induced tensile stresses result in cracking if it exceeds the tensile strength capacity of the concrete.

Reinforcement properties such as bar diameter and cover depth further influence plastic settlement cracking. A smaller cover depth reduces the settlement of concrete above the location of reinforcement. Accordingly, a reduction in cover depth increases differential settlement and, correspondingly, increases tensile stress development above the reinforcement. Furthermore, it should be noted that a smaller bar diameter increases the stress concentration above reinforcement, thus making concrete more susceptible to plastic settlement cracking. Consequently, a reduction in cover depth and bar diameter increases the risk of plastic settlement cracking to occur (Kwak et al., 2010).

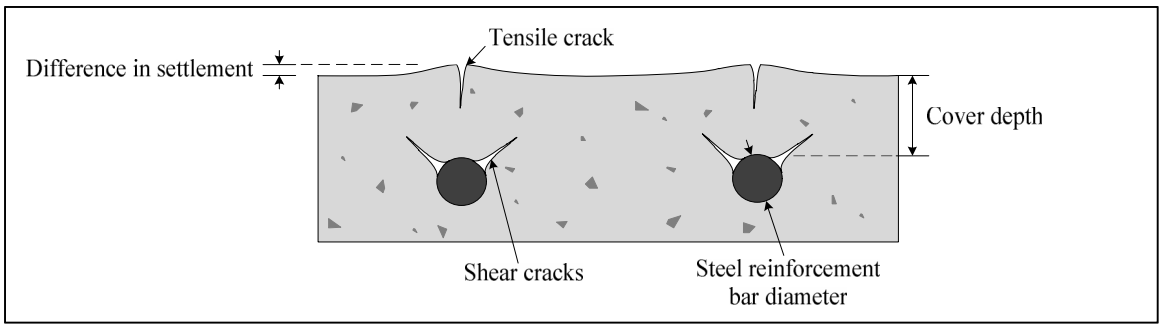

Figure 2.10 Development of plastic settlement crack above reinforcement (Combrinck & Boshoff, 2014)

The depth of a concrete section is directly related to the total amount of settlement where a deeper section is associated with increased settlement since more solid particles are subject to settlement (Uno, 1998). As illustrated in Figure 2.11, a change in sectional depth results in differential settlement as the concrete in Zone A experiences a greater amount of settlement when compared to Zone B. Consequently, tensile stresses develop at the change in sectional depth which may cause cracking. As previously mentioned, settlement cracks are formed once the induced stresses exceed the tensile strength capacity of concrete. With reference to Figure 2.11, the corresponding cracks form at the surface of the concrete paste and at the location of change in sectional depth. Settlement cracks that form at the change in sectional depth progressively develop towards the surface of the concrete paste. A greater change in sectional depth increases differential settlement between adjacent settlement zones and, correspondingly, increases the risk of plastic settlement cracking to occur.

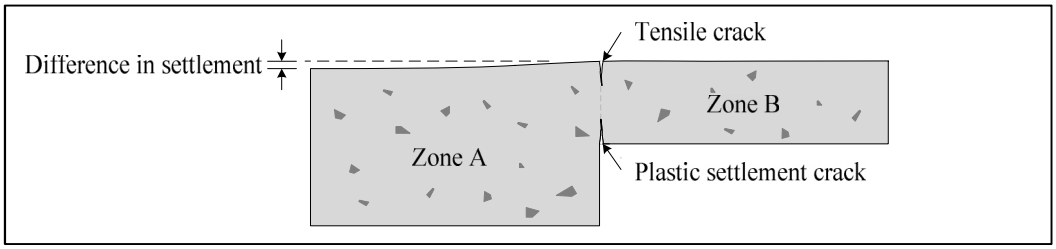

Figure 2.11 Development of plastic settlement crack at location of change in sectional depth

2.4.7.3 Interaction between plastic settlement cracking and PSC

The aforementioned forms of vertical restraint similarly provide horisontal restraint that is required for PSC to occur. As discussed in Section 2.3, particles in the concrete paste are subject to capillary pressure once drying time is reached. The presence of settlement cracks beneath the surface form weak spots in the system which locally relieve capillary pressure through air entry at the location of settlement cracks. Continued shrinkage allow these particles to be drawn closer and, correspondingly, settlement cracks are further widened by plastic shrinkage, as illustrated in Figure 2.12. Consequently, the effect of surface drying may interact with settlement at the locations of restraint which results in the formation of cracks in these regions (Kwak et al., 2010).

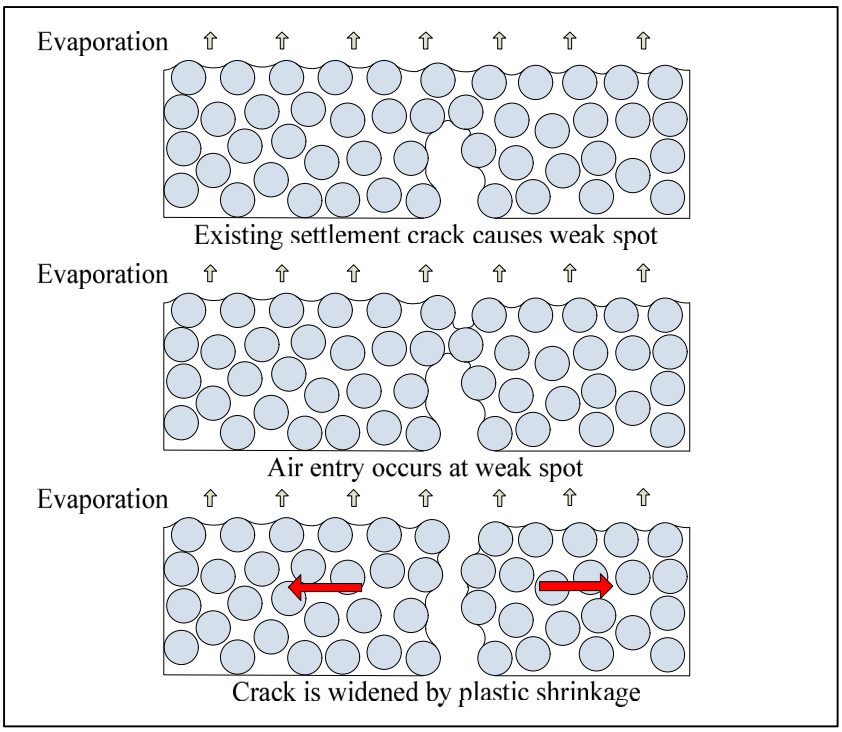

Figure 2.12 Interaction between plastic settlement cracks and plastic shrinkage

2.5 Admixtures

Admixtures refer to chemicals that are added to concrete during mixing to modify certain properties of the mix. Admixtures should not be regarded as a substitute for good construction practices and good mix design (C&CI, 1997).

Common reasons for the use of admixtures include the following:

- To increase workability without changing the water content
- To reduce water content without changing workability
- To adjust setting time
- To reduce segregation
- To reduce bleeding
- To improve pumpability
- To accelerate the rate of strength development at early ages
- To increase strength
- To improve potential durability and reduce permeability
- To compensate for poor aggregate properties

Admixtures are categorised into five main groups, namely: retarders, accelerators, air entrainers, plasticisers, and super-plasticisers (C&CI, 1997). The aforementioned admixtures as well as shrinkage reducing admixtures (SRA) are discussed in the following sections.

2.5.1 Retarders

Retarders prolong the hydration reaction of cement and, correspondingly, result in increased setting times and slower initial strength gain of concrete. Frequently used retarders include hydroxylated carboxylic acids, lignins, sugar and phosphates (Owens, 2009).

Retarders are used to prevent the formation of cold joints during extended periods of placing while similarly being used to delay setting of concrete subject to extensive transportation periods. Retarders are also used when placing concrete in hot weather, particularly when concrete is pumped (C&CI, 1997).

Experiments conducted by Louw (2014) found that the addition of glucose based retarders reduced the severity of PSC when compared to the same mix devoid from admixtures. The reduction in crack area was accompanied by an increase in shrinkage and reduction in settlement. The aforementioned results are analogous to results obtained by Combrinck & Boshoff (2013) that similarly obtained a significant reduction in crack area with addition of a retarding agent. The reduced crack area was accompanied by a delay in air entry and a reduction in bleeding. In contrast, results obtained by Löfgren & Esping (2014) found that the addition of a retarder increased the severity of PSC. The increase in crack area was attributed to the prolonged plastic period of the corresponding mix which, therefore, was exposed to prolonged evaporation of concrete pore water. Furthermore, experiments conducted by Leeman et al. (2014) found that the addition of a retarding agent did not result in formation plastic shrinkage cracks. The corresponding self-compacting concrete mix (SCC) contained both a poly carboxylate ethers based super-plasticiser and a sodium pyrophosphate based retarder.

The associated PSC results were accompanied by slightly increased settlement, increased bleeding and delayed capillary pressure build-up when compared to the reference mix containing the same dosage of poly carboxylate ethers based super-plasticiser. Consequently, further investigation is required to establish a clear influence of retarders on PSC of concrete.

2.5.2 Accelerators

Accelerators enhance the hydration rate of cement and, correspondingly, increase the rate of setting and early strength gain of concrete. Two groups of accelerating admixtures are available, namely, set accelerating admixtures and hardening accelerating admixtures. Set accelerating admixtures reduce the time for concrete to change from a plastic state to a hardened state whereas hardening accelerating admixtures increase the 24-hour strength of concrete (Chryso, 2007). Calcium chloride is regarded as the most effective accelerator and can be used in both setting and hardening applications. However, introduction of chloride ions is not permitted in steel reinforced concrete as it may reduce durability through corrosion of steel reinforcement (Owens, 2009).

Accelerators are generally used for applications where rapid setting and high early strengths are required. Common examples include shaft sinking, shotcrete and applications where rapid turnover of moulds or formwork are required. Accelerators are also used in applications where concreting takes place under very cold conditions (Owens, 2009; C&CI, 1997).

Research undertaken by Combrinck et al. (2013) found that a mix containing accelerator exhibits slightly larger plastic shrinkage cracks when compared to the same mix devoid from admixtures. The obtained crack area results was accompanied by a reduced rate of bleeding and evaporation. The aforementioned results are contradicted by Louw (2014) that found a reduction in the severity of PSC with the addition of a calcium chloride based accelerator. The reduction in the severity of cracking was accompanied by an increase in setting time which could not be explained. Results of Louw (2014) are analogous to results obtained by Löfgren & Esping (2014) that similarly obtained a reduction in crack area with addition of a sodium based accelerator. Consequently, further investigation is required to establish a clear influence of accelerators on PSC of concrete.

2.5.3 Air entrainers

Air entraining agents introduce air into concrete in the form of microscopic bubbles that are uniformly distributed through the concrete paste. The main types of air entraining agents include salts of wood resins, sulphonated hydrocarbons as well as animal and vegetable oils (Owens, 2009).

Air entraining agents are used to improve the resistance of hardened concrete to damage from freeze and thaw cycles. In addition, air entraining agents are also used to reduce the bleeding and segregation of concrete mixes (C&CI, 1997).

Research undertaken by Krönlof et al. (1995) found that a mix containing air entrainers displayed a lower rate of capillary pressure build-up which reduced the severity of PSC. Furthermore, it was found that air entry only occurred after initial setting time of the mix. The total shrinkage value remained at a relatively low level, below 1 mm/m. Similarly, Louw (2014) established a slight reduction in crack area with addition of air entrainers to a standard concrete mix. The associated reduction in crack area was supported by the results of underlying tests that were performed.

2.5.4 Plasticisers

When added to a concrete mix, plasticisers are absorbed on the surface of binder particles causing them to repel each other and deflocculate where deflocculation of particles is attributed to electrostatic and steric repulsion (Chryso, 2007). Deflocculation of particles, commonly referred to as dispersion, provides a more uniform distribution of binder particles which increases workability. The main types of plasticisers include lignosulphonic acids and hydroxylated carboxylic acids (C&CI, 1997).

Plasticisers are used to reduce the water content of concrete without changing the workability while also used to increase the workability of concrete without changing the the water content. In addition, plasticisers are generally used to enhance the pumpability of concrete (C&CI, 1997).

Research undertaken by Krönlof et al. (1995) found that a mix containing plasticiser exhibited a deviation in plastic shrinkage and capillary pressure when compared to other mixes. The mix displayed a fine net-like cracking pattern with an approximate mesh size of 30 mm. Upon investigation through optical microscopy the crack widths were found to be 5 – 10 µm with depths ranging between 2 – 5 mm. Experiments conducted by Louw (2014) found that a mix containing lignosulphate based plasticisers did not affect the severity of PSC. However, it was observed that the evaporation was reduced and setting times were delayed. Consequently, further investigation is required to establish a clear influence of plasticisers on PSC of concrete.

2.5.5 Super-plasticisers

Super-plasticisers are synthetic, water-soluble materials with very high water-reducing properties at various dosages. These admixtures function similarly to plasticisers, but they are more powerful dispersers. Super-plasticisers include chemical compounds such as sulphonated melamine formaldehyde, sulphonated naphthalene formaldehyde, modified lignosulphonates and poly carboxylate ether derivatives (Owens, 2009; C&CI, 1997).

Super-plasticisers are especially incorporated in self-compacting concrete where a self-levelling consistence facilitates placing. Furthermore, super-plasticisers are used in high-strength concrete to reduce the water-binder ratio to obtain a higher strength (C&CI, 1997).

Research conducted by Louw (2014) found that a mix containing sulphonated melamine formaldehyde based super-plasticiser displayed an extensive reduction in total crack area when compared to the same mix devoid from admixtures. Similarly, Louw (2014) found that a mix containing poly carboxylate ether based super-plasticiser slightly reduces PSC. However, the aforementioned tests results were only based on one test sample using a conventional concrete mix. Therefore, the influence of super-plasticisers on PSC remains unclear and requires further investigation.

2.5.6 Shrinkage reducing admixtures

As discussed in Section 2.4.4, shrinkage reducing admixtures (SRA) belong to a class of organic chemicals known as surfactants. At a molecular level, surfactants are amphiphilic, i.e. each surfactant is composed of a polar head and a non-polar tail (Rajabipour et al., 2008). When dissolved in water, amphiphilic molecules are attracted to liquid-air interfaces. Adsorption of surfactants at liquid-air interfaces causes a reduction in the surface tension of the pore fluid. Since capillary pressure is proportional to surface tension, as discussed in Section 2.2.2, a proportional reduction of capillary pressure build-up is expected. Furthermore, the addition of SRA's reduces the evaporation rate and sorptivity of the concrete mix, though the strength and modulus of elasticity can decrease (Lura et al., 2007).

In addition to reducing the risk of PSC, SRA are used to reduce drying shrinkage and autogenous shrinkage in high performance concretes with low water-binder ratios (Rajabipour et al., 2008).

Research undertaken by Lura et al. (2007) found a reduction in the width of plastic shrinkage cracks in concrete containing SRA's. The research suggests that the experimental results can be attributed to a reduction in surface tension of the pore fluid. The reduction in surface tension was found to be advantageous by reducing evaporation, settlement and capillary pressure build-up of the concrete samples (Lura et al., 2007). Similarly, Passuello et al. (2009) found that the addition of SRA delays the time of cracking, reducing the crack width by 40 %. According to the underlying tests performed, it was found that the mix containing SRA displayed a lower strain when compared to normal concrete. It was concluded that this strain relaxation was the consequence of the reduced total shrinkage of the mixture. Research undertaken by Mora-Raucho et al. (2009) also found a substantial reduction in PSC of concrete containing SRA. The reduction in PSC was attributed to a lower evaporation rate, delayed capillary pressure build-up and decreased settlement. Lastly, experiments conducted by Löfgren & Esping (2014) found that addition of a polymeric glycol based SRA also reduced the severity of PSC when compared to the same mix devoid from admixtures. The reduction in the PSC was accompanied by a reduction in the evaporation rate. Conclusively, previous research altogether indicate that a significant reduction in PSC is expected with addition SRA to a concrete mix.

2.6 Preventative measures for PSC

There are a number of effective measures that can be used to prevent or mitigate PSC, especially since PSC occurs in a relatively short time period. These preventative measures are often neglected or ineffective in practice due to a lack of guidance and knowledge of PSC. Preventative measures are categorised into external and internal preventative measures, and are discussed accordingly.

2.6.1 External preventative measures

External preventative measures generally focus on reducing the evaporation rate of the ambient environment. This is achieved by reducing the wind velocity, relative humidity, ambient temperature or concrete temperature. A widely used guideline is to ensure an evaporation rate of less than 1 kg/m^2/h (Uno, 1998).

External preventative measures include the following:

- Erect wind breaks to reduce air flow over the concrete surface and, correspondingly, reduce evaporation
- Erect sunshades to reduce the ambient temperature at the concrete surface
- Incorporate ice in mixing water to reduce the initial concrete temperature
- Reduce the initial concrete temperature by avoiding exposure of constituent materials to solar radiation prior to mixing
- Use a fog spray as a form of curing to increase the local relative humidity
- Reduce evaporation by applying a curing compound on the surface of the concrete
- Minimise water loss of concrete by dampening formwork and sub-grade prior to casting

2.6.2 Internal preventative measures

Internal preventative measures for PSC include the following:

- Reduce the risk of PSC with the addition of polymeric synthetic fibres such as polypropylene or polyester fibres
- Avoid excessive use of retarders that prolong the setting time of concrete
- Reduce excessive fines content in the mix to prevent an extreme reduction in bleeding of the concrete
- Avoid the use of admixtures that reduces bleeding of concrete
- Implement evaporative retarders such as aliphatic alcohols

2.7 Conclusion

The fundamental knowledge required to understand plastic shrinkage cracking (PSC) of concrete is reported in this chapter. PSC is mainly attributed to tensile stresses arising in concrete due to a combination of capillary pressure and restraints provided by the reinforcement and formwork. PSC will not occur in the absence of restraint, capillary pressure build-up or air entry. Accordingly, these components are characterised as the mechanisms required for PSC to occur. The factors influencing PSC are discussed as well as the effect of admixtures on the PSC of concrete, which remain unclear to a large extent. The experimental framework of this study is discussed in the next chapter.

CHAPTER 3

Experimental framework

The framework of the experimental tests that were performed to achieve the objectives of this study is provided in this chapter. Firstly, the experimental preparation concerning mixing and casting procedures that were used during testing are discussed. Thereafter, the setup and procedures of the various experimental tests are discussed, followed by the specification of materials used to perform the associated tests. Lastly, mix design proportions and concrete properties are discussed.

3.1 Experimental preparation

Unless otherwise stated in subsequent sections, the following mixing and casting procedures were used to perform all tests conducted in this study.

3.1.1 Mixing procedures

The constituent materials of the concrete mixes were weighed and placed in a climate controlled room at least 12 hours prior to mixing. This was done to ensure a constant temperature of constituent materials and, therefore, constant concrete temperature upon the time of mixing. The climate controlled room had a regulated temperature of 23°C and a relative humidity of 65 %.

Rotary pan mixers with capacities of 0.025 and 0.05 m^3 were used to facilitate mixing of concrete. The larger mixer was used to accommodate mixes with a maximum volume of 0.045 m^3 whereas the smaller mixer was used to accommodate mixes with a maximum volume of 0.022 m^3. The mixers were consistently cleaned and dried prior to mixing for all tests.

A consistent mixing time of 4 minutes was used for all mixes. Fine aggregates, fly ash, cement and stone were sequentially added to the mixer in the aforementioned order. Dry mixing of the constituent materials was performed during the first 20 seconds after which mixing water was added to the mix. Predefined dosages of the respective admixtures were added to the mixing water before addition to the mix.

3.1.2 Casting procedures

The respective moulds that were used to perform evaporation, bleeding, shrinkage, settlement, crack area and capillary pressure tests had a consistent sample depth of 100mm. Consequently, the same casting procedures were used to fill and consolidate the corresponding samples. Concrete samples were consolidated using the same vibrating table throughout the experimental tests.

After mixing, concrete was poured into the respective moulds to a height of 50 mm after which samples were vibrated for an approximate duration of 30 seconds. Samples were then filled to maximum capacity, i.e. 100 mm, after which vibration was applied until full compaction was achieved. Full compaction was achieved once the majority of entrapped air bubbles have been expelled. This resulted in a consistent total time of compaction of 3 minutes for all conventional concrete samples. However, for concrete samples cast from high flow mixes, as discussed in Section 3.4, the total time of compaction was only 30 seconds since these mixes were self-levelling and self-compacting to a large extent. This was done to avoid excessive vibration as this can lead to seggregation of the concrete paste.

With the exception of bleeding and setting time samples, surface finishing was applied with the use of trowels to ensure a smooth surface of samples. Care was taken to ensure that surface finishing was applied to the same extent. The respective samples were immediately placed in the climate chamber after casting. Measurements of the respective tests were recorded from the time when casting was completed, i.e. time zero.

3.2 Test setup and methods

With exception of surface tension measurements, all experimental tests were performed in the climate chamber that was used to simulate environmental conditions ideal for PSC. Relevant information regarding the climate chamber is firstly discussed followed by the setup and methods used during testing.

3.2.1 Climate chamber

The climate chamber automatically controls the evaporation rate through continuous regulation of user-specified values for wind speed, air temperature, and relative humidity. The chamber has the capacity to create extreme environmental conditions with an air temperature of up to 50 °C, relative humidity as low as 10 %, and a uniform wind speed as high as 70 km/h (Combrinck, 2012).

Figure 3.1 shows the main components of the climate chamber including a dehumidifier, heating element and axial fans. Air temperature and relative humidity are regulated using a heating element and dehumidifier respectively whereas axial fans are used to create a constant wind speed by circulating air within the climate chamber via a wind tunnel. Test samples were placed in the test compartment of the climate chamber which is easily accessible through Perspex covers. More information regarding the design and performance of the climate chamber can be found by referring to research undertaken by Combrinck (2012).

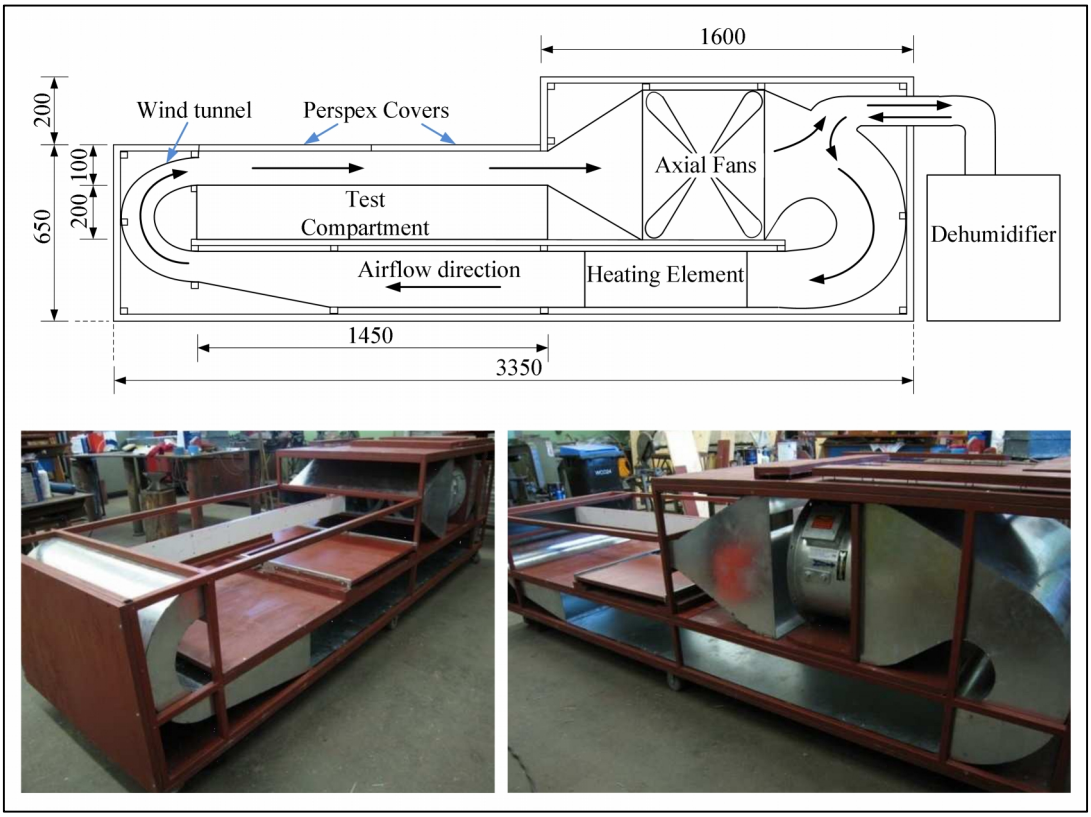

Figure 3.1 Climate chamber layout (Combrinck, 2012)

The climate chamber was set to a constant environmental condition during testing with a relative humidity of 10 %, air temperature of 40°C and a wind speed of 20.2 km/h. This simulated an extreme environmental condition ideal for PSC due to a high estimated evaporation rate of 1.05 kg/m^2/h as calculated with Equation 2.2. The climate chamber was switched on approximately one hour before mixing to ensure that the conditions stabilised once samples were placed in the chamber.

3.2.2 Crack area tests

Crack area tests were performed to determine the phenomenological influence of admixtures on the severity of PSC. The moulds that were used to measure crack area are commonly referred to as cracking or PSC moulds. These moulds are constructed of PVC with a layout based on the specifications prescribed by ASTM C1579 (2006), as illustrated in Figure 3.2. Each cracking mould contains three triangular inserts of which the largest is located in the middle of the longitudinal direction. The latter acts as a stress riser and causes a localisation of cracks in the region directly above it. A smaller triangular insert is located at each end of the mould to provide the horisontal restraint required to cause cracking above the middle triangular insert. Additional horisontal restraint is also provided by a smooth steel bar with a 10 mm diameter located at each end of the mould. These bars were added to provide additional horisontal restraint since preliminary tests without these steel bars often exhibited insignificant cracking. Four samples of each mix were tested simultaneously.

A quantitative characterisation of the cracks was facilitated by a semi-automated image analysis approach using *ImageJ* software (Rasband, 2012). The software enabled quantitative measurement of total crack area using high resolution images that were captured using a *Nikon D7000* camera. The camera was placed on a guiding rail to ensure that photos were taken at a constant height. Furthermore, markings were made on the guiding rail above each specimen to ensure that photos were consistently taken from the exact same position. A metal ruler with known dimensions was used as a scaling device by placing it on the sample when photos were taken.

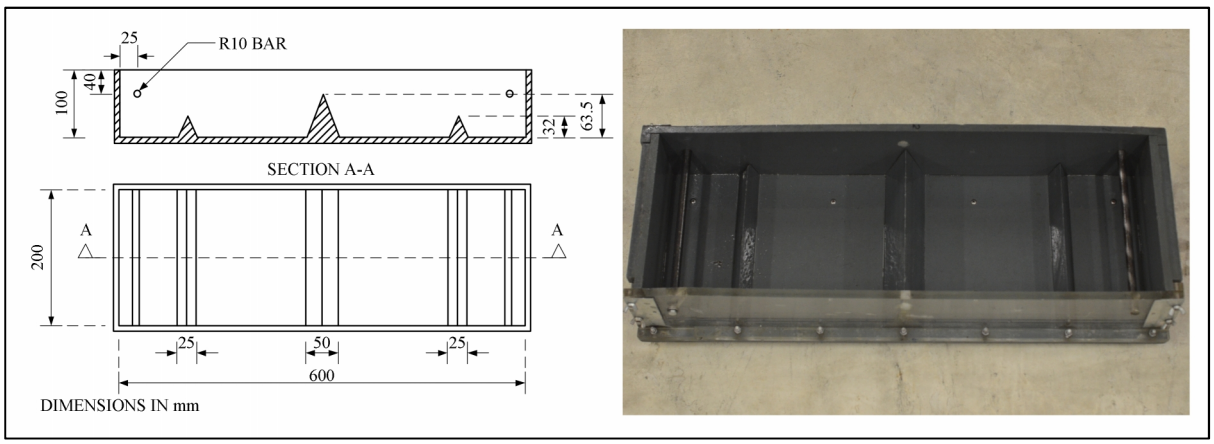

Figure 3.2 Crack area mould

The semi-automated image analysis process involves: image acquisition, image processing, and crack feature determination and measurement. Detailed information on each step is discussed accordingly in the following sections.

3.2.2.1 Image acquisition

Once the cracking moulds were placed in the climate chamber, the surface of test specimens were visually assessed for formation of plastic shrinkage cracks. Once crack onset was visually identified, image acquisition was performed by taking high resolution photos at 20 minute intervals. Image acquisition was performed on the surface of the specimen above the stress riser, i.e. at the location of the middle triangular insert. Frame size of photos was chosen to permit a resolution which could identify fine cracks while also being large enough to view the entire field in the transverse direction. The crack was not measured within the first 25 mm from the outer edges of the specimen to eliminate the influence of boundaries as prescribed by ASTM C1579 (2006) and shown in Figure 3.3.(a).

3.2.2.2 Image processing

The measured brightness of images varied depending on the severity of cracking and background grey level. A fixed brightness threshold could not be established due to minor variations in colour of images and, therefore, slight adjustments to the threshold value were made based on visual observation. This is illustrated by Figure 3.3, where (b) indicates the default brightness threshold

which was slightly adjusted to (c) in order to clearly distinguish between the crack profile and bulk matrix of the concrete paste. This is acceptable since an investigation undertaken by Qi et al. (2003) found that minor variations in brightness threshold values did not affect measurement results.

After selecting a suitable brightness threshold, images were further processed to reduce the impact of surface imperfections on the measured crack area. The unpolished concrete surface contained various small pores or craters with similar grey levels to those observed in cracks. Accordingly, these surface imperfections were falsely assigned as cracks purely based on pixel colour. This was accounted for by erasing surface imperfections to extract the crack profile as shown in Figure 3.3.(c) and (d).

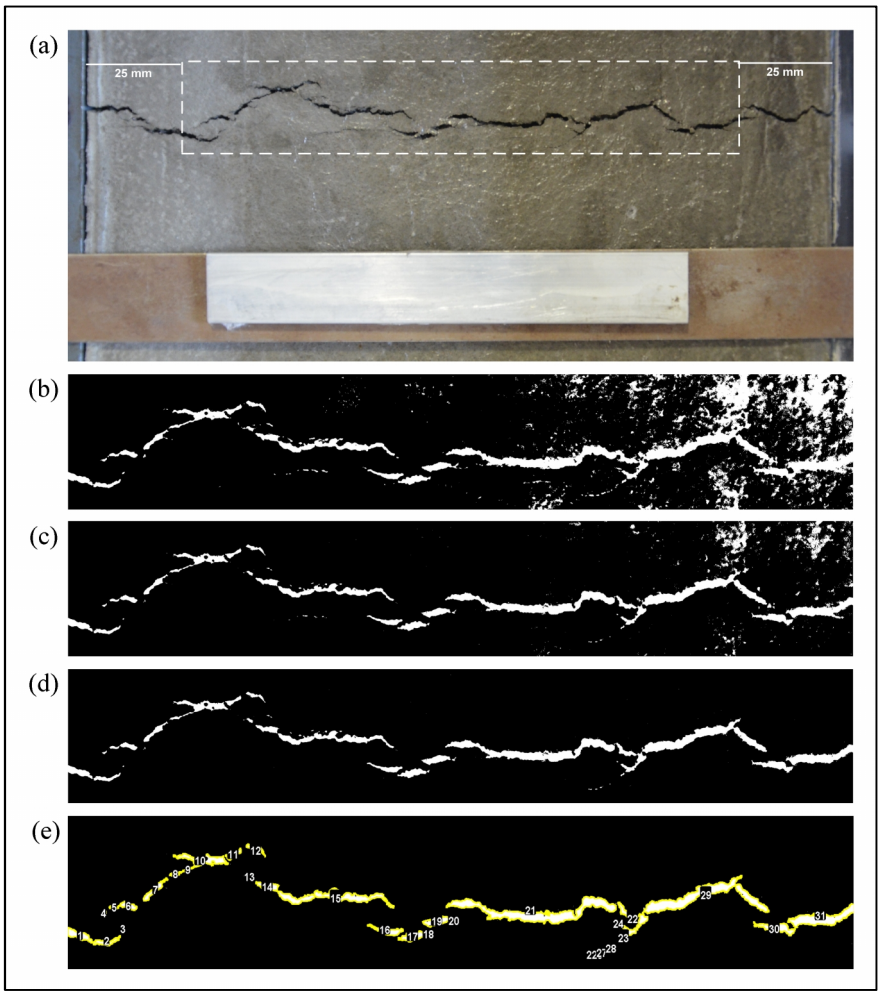

Figure 3.3 Quantification of plastic shrinkage crack area

3.2.2.3 Crack feature determination and measurement

Once the crack contour was extracted, it was possible to perform further image analysis for quantification of the total crack area. As illustrated in Figure 3.3.(e), different crack segments were identified and selected. Once selected, total crack area was automatically calculated by the *ImageJ* software as the sum of the area of all individual segments using the total amount and size of the pixels in each of the crack segments (Rasband, 2012).

3.2.3 Setting times

Setting time tests were performed using the Vicat needle apparatus in accordance with SANS 50196-3 (2006). Initial and final setting times were determined by measuring the penetration depth of needles into a concrete paste using a Vicat apparatus as shown in Figure 3.4. Three samples of each mix were tested simultaneously.

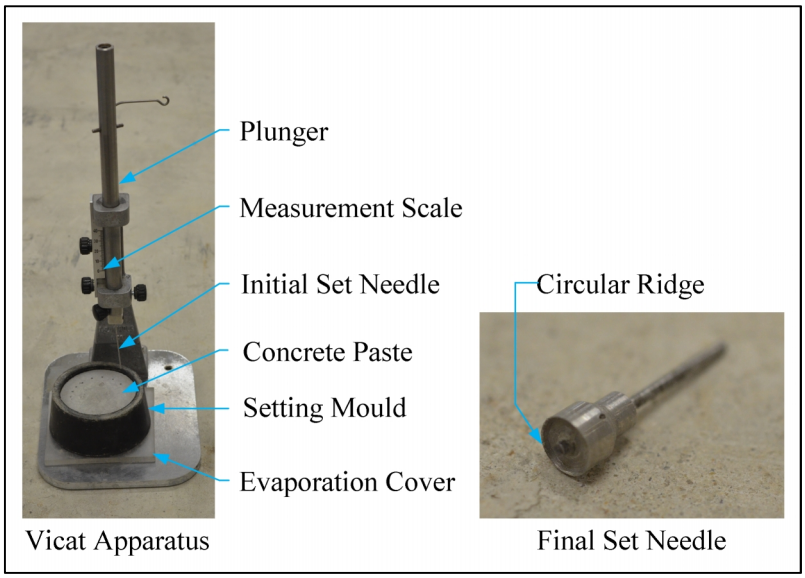

Figure 3.4 Vicat apparatus used for setting time tests

Once mixed, the concrete was sieved using a 2.36 mm sieve to obtain a paste devoid from large aggregate that is suitable for testing. The sieved concrete paste was placed in setting moulds and closed with evaporation covers to avoid water loss from the concrete paste.

Penetration readings for initial setting time were taken at 20 minute intervals. These readings were performed by positioning the samples under the plunger and gently lowering the initial set needle until in contact with the concrete paste surface. Thereafter, the plunger was released to allow vertical penetration of the needle into the concrete paste. Subsequent readings were taken approximately 30 seconds after the plunger was released. As illustrated in Figure 3.5, penetration readings were performed in a circular pattern at least 8 mm from the rim of the mould with a minimum distance of 10 mm between consecutive readings. Initial set was reached when penetration depth was measured to be 6 ± 3 mm from the bottom of the mould. Initial setting times were recorded to the nearest 20 minutes being measured from the time when casting was completed, i.e. time zero.

Once initial set was reached, the setting mould was inverted to allow final set readings to be taken on the bottom surface of the sample. Readings were taken at 20 minute intervals using similar procedures to that used for initial setting time. As illustrated in Figure 3.5, final set was reached when the circular ridge of the final set needle no longer left an imprint on the surface of specimens. Final setting time was recorded to the nearest 20 minutes being measured from the time when casting was completed.

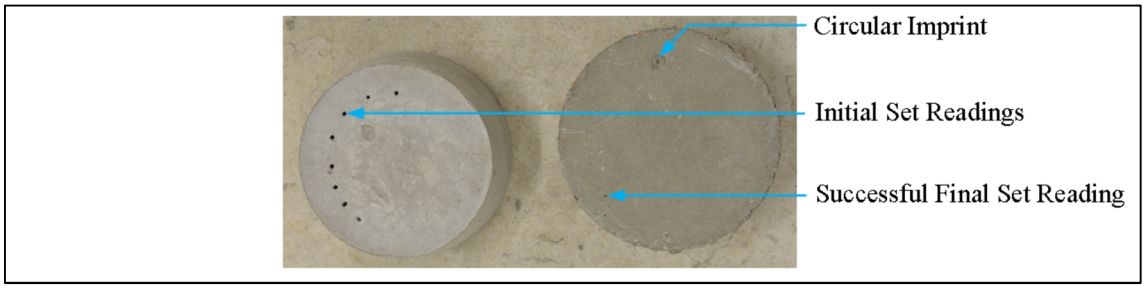

Figure 3.5 Setting time measurements

3.2.4 Bleeding

Bleeding tests were performed within the climate chamber in accordance with ASTM C232 (2010). The extraction of bleed water was facilitated by tilting the mould on the one side to a height of 50 mm as illustrated in Figure 3.6. The bleed water was withdrawn and measured using a pipet, measuring beakers and a scale. Four samples of each mix were tested simultaneously.

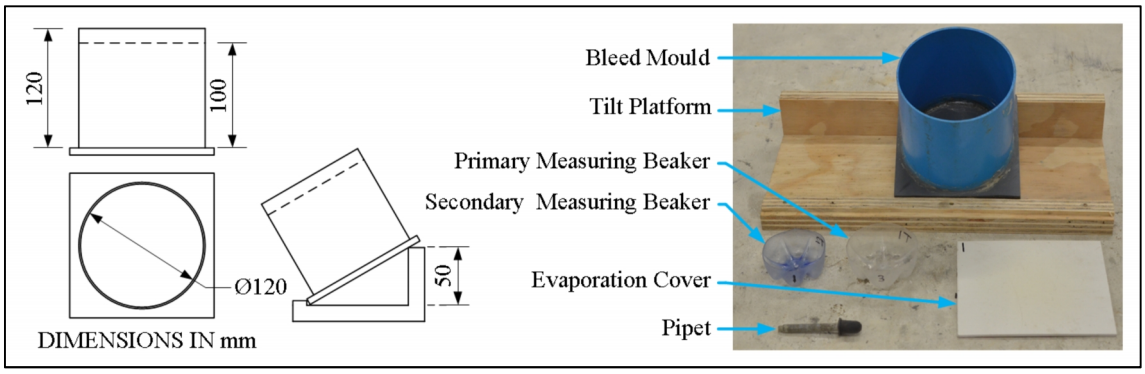

Figure 3.6 Bleeding measurement setup

Accumulated bleed water was extracted at 20 minute intervals during the first 40 minutes after casting and 30 minute intervals thereafter until bleeding ceased. Specifications prescribed by ASTM C232 (2010) state that measurements should be recorded in 10 minute intervals during the first 40 minutes, however, the cleaning process of apparatus between subsequent measurements did not permit such short intervals as four samples were tested simultaneously. Evaporation covers were placed on bleeding moulds during testing to avoid evaporation of bleed water. The evaporation covers were kept on samples throughout tests except when bleeding measurements were taken.

Once cast, the samples were placed in the climate chamber to measure the amount of bleeding at the respective time intervals. The samples were removed from the climate chamber and tilted for two minutes before extracting the bleeding water using a pipet. The aforementioned tilting procedure facilitated convenient extraction of the bleed water which accumulated at the lower part of the tilted mould. The samples were immediately returned to the climate chamber once the bleed water was extracted. Extracted bleed water was transferred to a primary measurement beaker after which the bleed water was seperated from extracted solid particles by decanting its contents into a secondary

beaker. The contents of the secondary beaker was weighed to obtain the amount of bleed water during each specific measurement. Evaporation of bleeding water was accounted for as prescribed by ASTM C232 (2010) and, therefore, the accumulated mass of bleed water per unit area available for evaporation was calculated.

3.2.5 Evaporation

The evaporation of mixing water from the bulk paste of concrete was measured by weighing concrete samples at 20 minute intervals using a scale with a resolution of 0.1 grams. Refer to Figure 3.7 for relevant dimensions of evaporation moulds. Four samples of each mix were tested simultaneously.

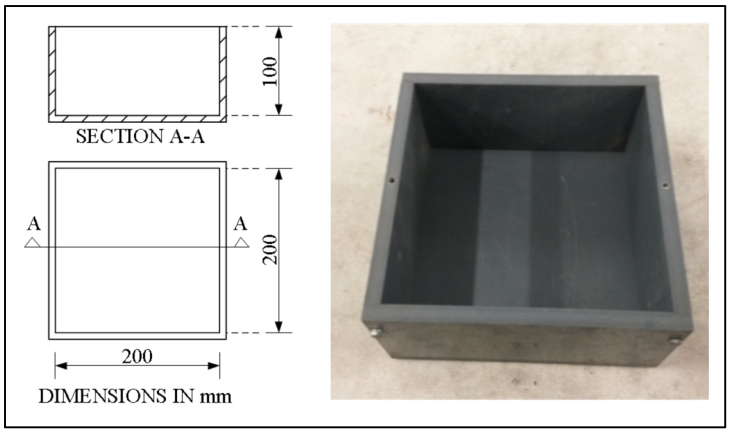

Figure 3.7 Evaporation mould

Once cast, the evaporation moulds were immediately placed in the climate chamber. Evaporation measurements were recorded at 20 minute intervals during the first 40 minutes after compaction and 30 minutes thereafter. Evaporation was calculated as the difference in mass of each concrete specimen between subsequent measurements, i.e. the mass loss between subsequent measurements represents the water loss from the concrete paste through evaporation. Corresponding measurements were recorded two hours past the final setting time of the respective mixes.

3.2.6 Capillary pressure

The method used to perform the capillary pressure tests was adopted from Slowik et al. (2008). Miniature signal conditioned pressure sensors, with a maximum capacity of 103.42 kPa, were used to measure capillary pressure. The pressure sensor was connected to a brass tube via an air tight threaded connection. The brass tube, with dimensions indicated in Figure 3.8, was carefully filled with distilled water to transmit pressure from the concrete paste to the pressure sensor. The pressure sensor fitting was inserted 50 mm from the top of the mould with its tip located in the centre of the mould. Measurement of capillary pressure was fully automated using a data acquisition system where subsequent readings were taken every second. Due to the fact that air entry is considered to be a local occurrence, only two samples of each mix were tested.

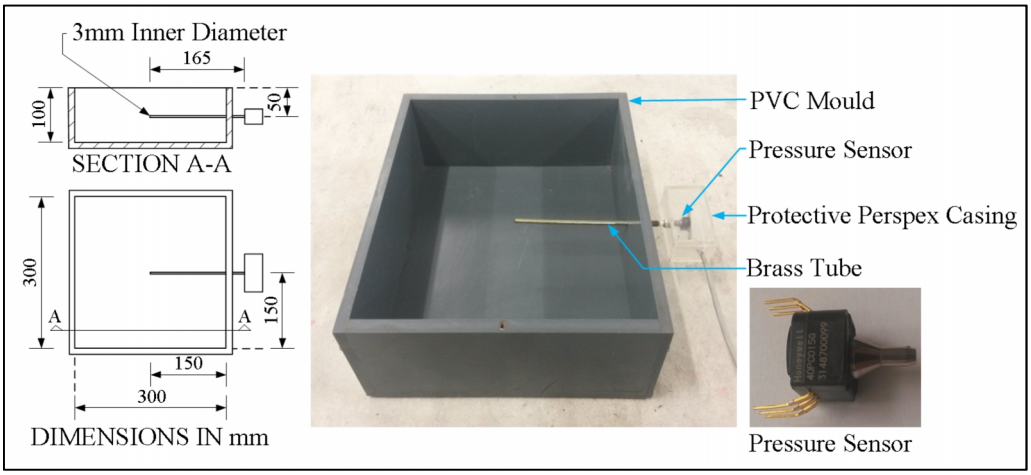

Figure 3.8 Capillary pressure measurement setup

The procedure followed to measure the capillary pressure started prior to mixing where the brass tube was carefully filled with distilled water. Air voids were removed from the pressure sensor and brass tube fitting by gently tapping the side of the tube. Once air voids were removed, a small piece of sponge was inserted to the tip of the tube to prevent the ingress of concrete after casting.

The initial casting procedures for capillary pressure tests were slightly different to that discussed in Section 3.1.2. Once mixed, the mould was filled with concrete to an approximate height of 45 mm after which the sample was compacted for 30 seconds using a vibrating table. Thereafter, the pressure sensor fitting was inserted into the mould after which the tip of the brass tube was immediately covered with concrete. From this point onwards, compaction was applied in accordance with Section 3.1.2. The corresponding measurements were recorded until final setting time of the respective mixes was reached.

3.2.7 Shrinkage

The method used to perform shrinkage tests was similar to that used by Slowik et al. (2008). Shrinkage and settlement measurements were performed simultaneously using the same mould. As indicated in Figure 3.9, shrinkage measurements were recorded on opposite sides of the mould. Shrinkage anchors were inserted 50 mm from the top of moulds with the tips embedded in the concrete paste. The guiding axis of anchors permitted horisontal displacement which allowed the embedded anchors to mimic the shrinkage of the concrete paste. The displacement of the respective shrinkage anchors were measured using a spring loaded LVDT that pressed against the guiding axis of the anchor. The force of the springs exerted onto the anchors was insignificant and had no effect on the displacement of anchors. The anchors were kept stationary during the casting process with the use of securing bolts. Total shrinkage of samples was calculated as the sum of displacement of the two shrinkage anchors. Shrinkage measurements were fully automated using a data acquisition system where subsequent readings were taken every second. Four samples of each mix were tested simultaneously.

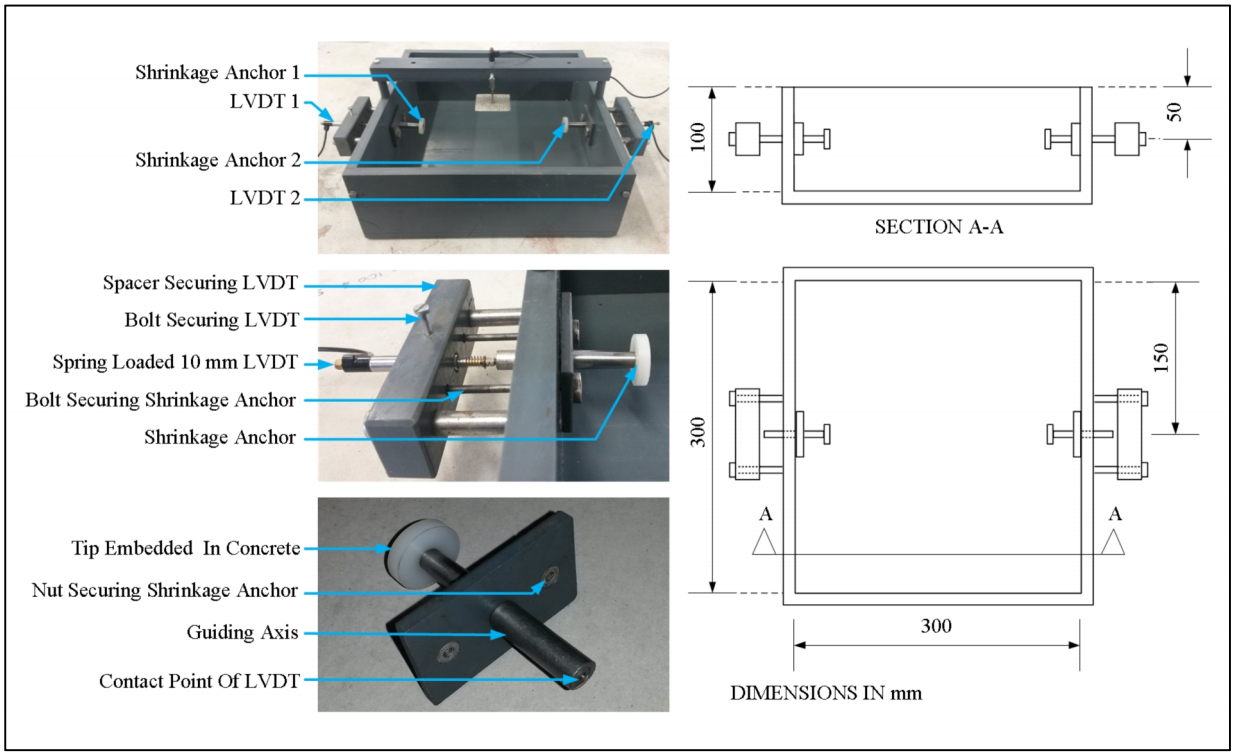

Figure 3.9 Shrinkage measurement setup

Care was taken to mitigate friction at the contact surface between the shrinkage anchors and moulds by externally applying grease to the guiding axis of anchors. As illustrated in Figure 3.9, shrinkage anchors were kept stationary during the casting process by securely fixing the anchors to the mould with the use of bolts.

Once the samples were placed in the climate chamber, each LVDT was fixed to the mould to facilitate contact with the guiding axis of the respective shrinkage anchors. After the LVDT's were fixed, the bolts securing shrinkage anchors were loosened to enable horisontal displacement of the anchors to mimic the shrinkage of the concrete paste. Shrinkage measurements were recorded until final setting time of the respective mixes was reached.

3.2.8 Settlement

The method used to perform settlement tests was similar to that used by Slowik et al. (2008). The tests were performed by placing a wire mesh centrally on the surface of the respective samples to mimic the settlement of the concrete paste. The vertical displacement of the wire mesh was measured using a LVDT that was connected to the wire mesh using a threaded connection. A wire mesh was used as this allowed the bleed water to percolate through the mesh and, therefore, prevent bleeding water from being trapped underneath. Furthermore, the mesh had a sufficient surface area to avoid penetration into the concrete paste. Settlement measurements were fully automated using a data acquisition system where subsequent readings were taken every second. Four samples of each mix were tested simultaneously.

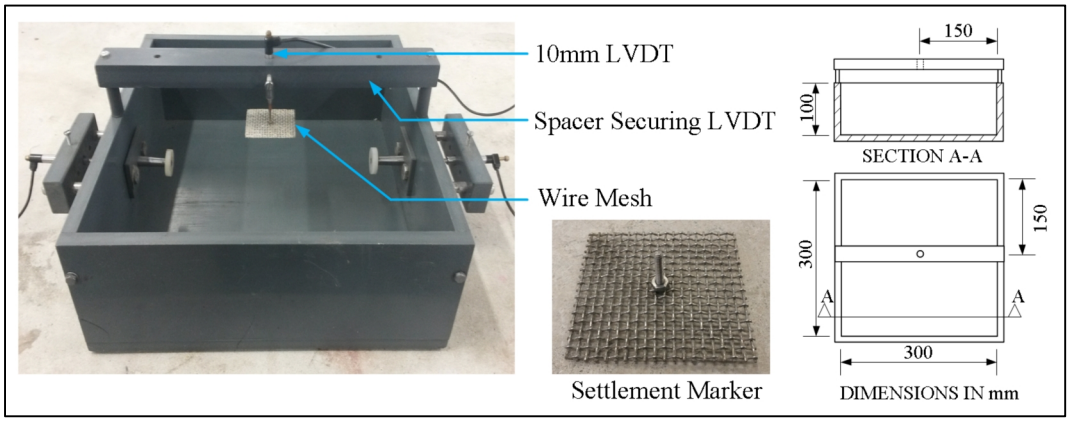

Figure 3.10 Settlement measurement setup

Once the samples were placed in the climate chamber, the respective settlement markers were connected to a LVDT and lowered onto the surface of the concrete paste. Care was taken to ensure that markers were sufficiently bonded to the concrete paste without inducing mechanical settlement. Settlement measurements were recorded using a data acquisition system until the final setting time of the respective mixes was reached.

3.2.9 Surface tension

The surface tension of the pore fluid was measured according to specifications prescribed by ASTM D971 (2004) using the *Attension Sigma 702ET* tensiometer as shown in Figure 3.11. The Du Noüy ring method was used to measure the surface tension during which a platinum ring, with a standard perimeter of 60 mm, was lifted through the liquid-air interface. The tensiometer measured the force needed to detach the ring from the surface of the liquid. The force was applied by gradual lowering of the sample platform on which the liquid was placed while the platinum ring remained stationary (Johlin, 1926). Measurements were fully automated and each measurement was obtained within 60 seconds. The *Sigma 702ET* accurately measures surface tension between 0-100mN/m. Three successive measurements of each sample were performed.

Before testing, 250ml test samples were prepared and poured into glass containers that were thoroughly rinsed using acetone, tap water and distilled water, respectively. The associated test samples contained solutions of water and the relevant admixtures at the concentrations corresponding to the ratio of admixture to concrete mixing water. Specifications regarding the solution concentrations are provided in Section 4.4 and 5.2 respectively.

The tensiometer was levelled and calibrated prior to performing the surface tension tests. Levelling of the tensiometer was facilitated by placing a bubble level device on the sample platform and adjusting the supports accordingly. The tensiometer was calibrated against known weights in accordance with procedures as prescribed by the manufacturer.

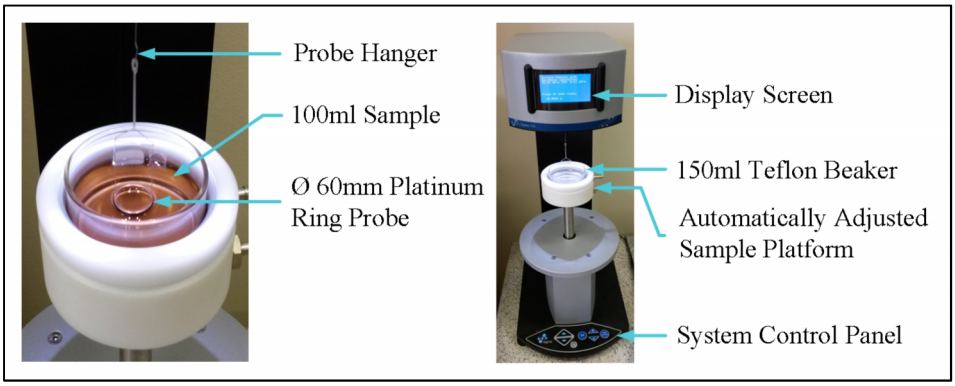

Figure 3.11 Setup of Sigma 702ET tensiometer

At the time of testing, approximately 150ml of a test sample was poured into a clean Teflon beaker. The platinum ring was cleaned by immersing it in a small container of xylene for 10 seconds while spinning the ring back and forth. The rinsing process was repeated using a container filled with acetone. Thereafter, the ring was flamed for 5 seconds using a Bunsen burner, again spinning it to obtain rapid, uniform heating. The platinum ring was used immediately after cleaning.

The test was initiated by manually raising the sample platform to a distance of 10 mm from the platinum ring while the rest of the test was fully automatic. The tensiometer raised the sample platform until the ring was immersed in the sample to a depth of 6 mm. The platform was then gradually lowered until rupture occurred. The maximum force exerted by the water surface was recorded and displayed.

3.2.10 Layout of test samples within climate chamber

Several of the aforementioned tests were performed simultaneously to ensure an efficient test schedule. However, all tests of a specific mix could not be conducted simultaneously due to the large number of samples as well as the number of experimental tests performed. This meant that the respective tests were grouped according to sample size and practicality. The layout of test samples as placed in the climate chamber for each of these test groups are discussed in subsequent paragraphs.

The crack area and setting time tests were performed simultaneously which included three setting time samples and four crack area samples of the same mix. The surface of the crack area samples was exposed direct wind whereas the setting time samples were not exposed to direct wind to avoid an increase in penetration resistance that is not related to the setting of the concrete paste. Accordingly, setting time samples were effectively only exposed to the temperature within the climate chamber. This is acceptable since temperature is the main environmental condition that influences the setting time (rate of hydration) of concrete (Mehta & Monteiro, 2006). The layout of samples in the climate chamber is illustrated in Figure 3.12. The crack area samples were undisturbed throughout tests while the setting time samples were individually removed from the climate chamber at timely intervals to conduct penetration measurements.

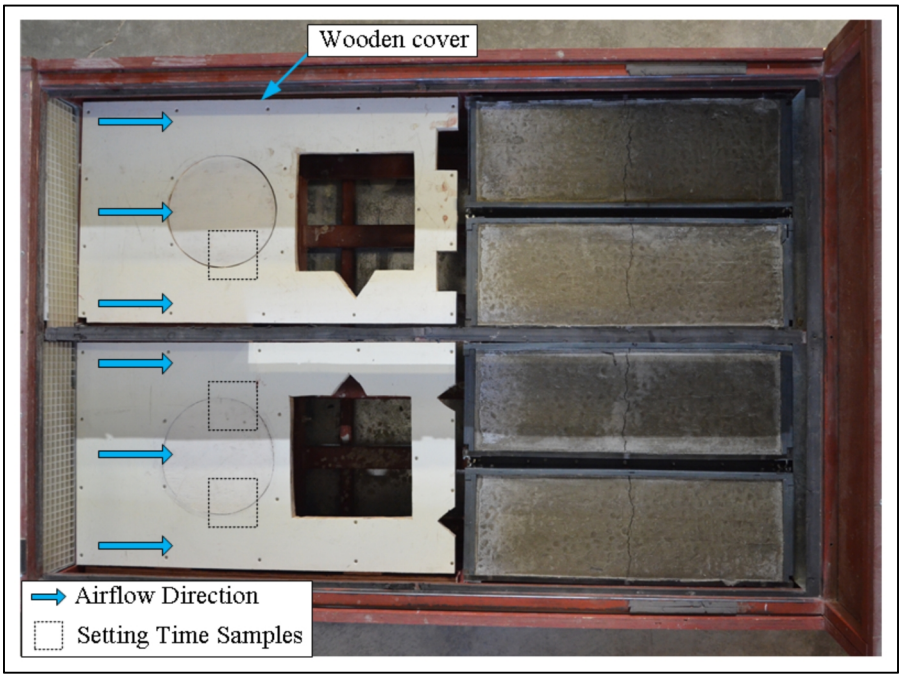

Figure 3.12 Layout of crack area and setting time samples

Bleeding and evaporation tests were performed simultaneously with four samples cast from the same mix for each test. Evaporation samples were exposed to the extreme environmental conditions while the bleeding samples were positioned similarly to setting time samples to reduce evaporation. The layout of the samples in the climate chamber is illustrated in Figure 3.13. Both bleeding and evaporation samples were individually removed from the climate chamber at timely intervals when measurements were conducted.

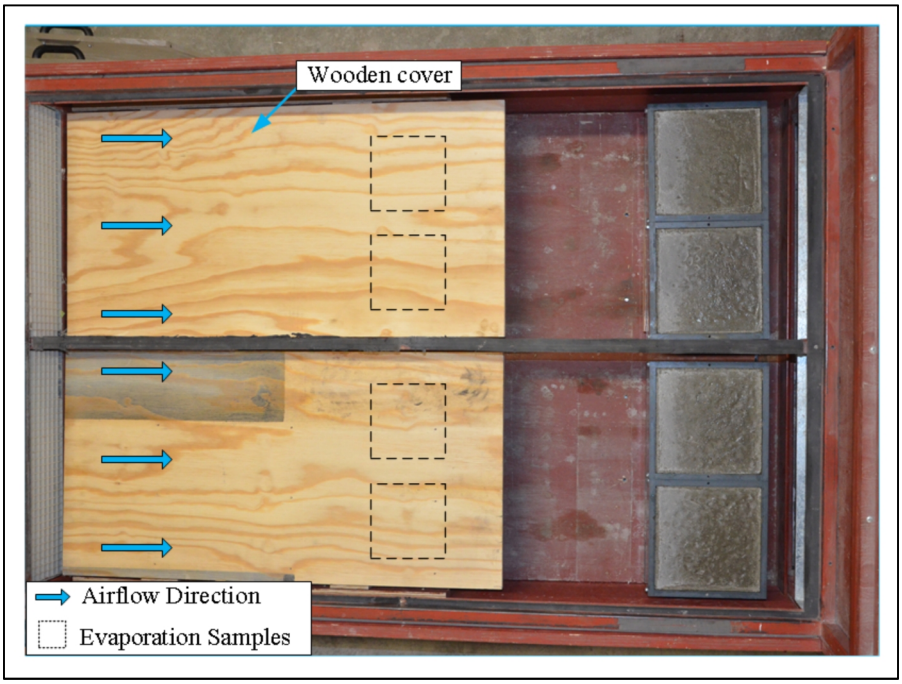

Figure 3.13 Layout of evaporation and bleeding samples

As previously discussed in Section 3.2.6, capillary pressure tests were performed using two samples of the respective concrete mixes. Accordingly, two mixes were tested simultaneously although being cast separately due to variations in the mix design. The layout of the moulds in the climate chamber is illustrated in Figure 3.14. The surface of the capillary pressure samples were exposed to direct wind once placed in the climate chamber while being undisturbed throughout testing.

Figure 3.14 Layout of capillary pressure samples

Shrinkage and settlement tests were performed simultaneously using the same mould. As previously discussed, four samples of each mix were tested. The layout of samples in the climate chamber is illustrated in Figure 3.15. The surface of the shrinkage and settlement samples samples were exposed to direct wind once placed in the climate chamber while respective test samples were undisturbed throughout testing.

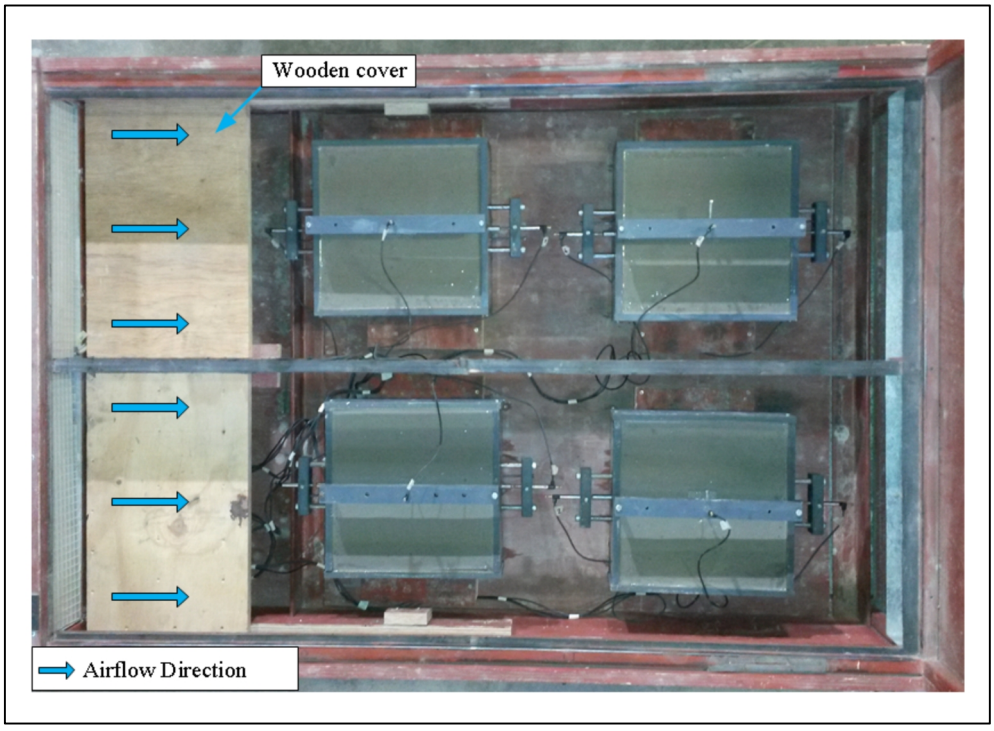

Figure 3.15 Layout of shrinkage and settlement samples

3.3 Material specifications

The materials used in the concrete mixes to perform the aforementioned tests are discussed in this section. This includes the specification of admixtures and constituent materials of the respective concrete mixes.

3.3.1 Admixtures

As previously mentioned, retarders, accelerators, air entraining agents, plasticisers, super-plasticisers, and shrinkage reducing admixtures, respectively, were used to perform the experimental tests. These admixtures were supplied by Chryso SA (Pty) Ltd. The specifications and recommended dosages of these admixtures are provided in Table 3.1.

Both a minimum and maximum dosage of the respective admixtures were used to perform the experimental tests. The minimum dosages correspond to the minimum recommended dosage as prescribed by the supplier whereas the maximum dosages correspond to the maximum dosage permitted by the respective concrete mixes without segregation. The specification of admixture dosages of is provided in Section 3.4.

Table 3.1 Specification of admixtures

Admixture	Description	Commercial name	Specific Gravity	Recommended dosage****
Retarder	Glucose based retarder	Tard CHR	1.06	0.2 – 1.0
Accelerator	Calcium chloride based accelerator	Xel A639	1.35	1.6 – 3.0
Air entrainer	Chloride free synthetic air entrainer	Air 7	1.01	0.15 – 0.3
Plasticiser	Lignosulphonate based plasticiser	Plast 900	1.18	0.2 – 0.5
SRA*	Glycol ether based SRA	Serenis	0.95	0.5 – 3.0
SP**	SMF*** based SP	Fluid Optima 207	1.15	0.6 – 5.0
SP**	Poly carboxylate ethers based SP	Fluid GT	1.06	0.3 – 3.0

Notes:

**SRA*	*Shrinkage reducing admixture*
***SP*	*Super-plasticiser*
****SMF*	*Sulphonated melamine formaldehyde*
*****Dosage units*	*[litre / 100 kg of cementitious material]*

3.3.2 Water

Municipal tap water was used as mixing water for the respective concrete mixes. The same source of water was used throughout the experimental work.

3.3.3 Cement

All mixes contained CEM II/A-L 52.5N Portland-limestone cement supplied by PPC (Pretoria Portland Cement Co.). The main constituent materials of the cement included clinker and limestone containing between 6 and 20 % limestone by mass. The cement has a 52.5 MPa strength class with an ordinary rate of hardening (SANS 50197-1, 2013).

3.3.4 Fly ash

Fly ash refers to a powdery residue that was extracted from flue gases of furnaces fired with pulverised coal (Owens, 2009). Siliceous fly ash was incorporated in the high flow concrete mix, as discussed in Section 3.4, to increase flowability of the mix. Furthermore, siliceous fly ash has pozzolanic properties with a reactive proportion of calcium oxide of less than 10 % by mass.

3.3.5 Fine aggregates

Fine aggregates, or sand, refer to aggregates of which more than 90 % of particles by mass pass a 4.75 mm sieve (SANS 201, 2008). Respective sands, locally known as Malmesbury sand and Greywacke crusher dust, were incorporated in the concrete mixes. Malmesbury sand was formed by natural disintegration of rock while Greywacke crusher dust was formed as a by-product of the mechanical crushing of Malmesbury shale. In addition, the Greywacke crusher dust was sieved using a 2.36 mm sieve to obtain a grading with a higher distribution of fine particles. This increased the amount of fine particles and, therefore, also increased the risk for PSC as discussed in Section 2.4.3. The grading of the respective fine aggregates shown in Figure 3.16 was determined in accordance with SANS 201 (2008). The relevant fine aggregate properties are provided in Table 3.2.

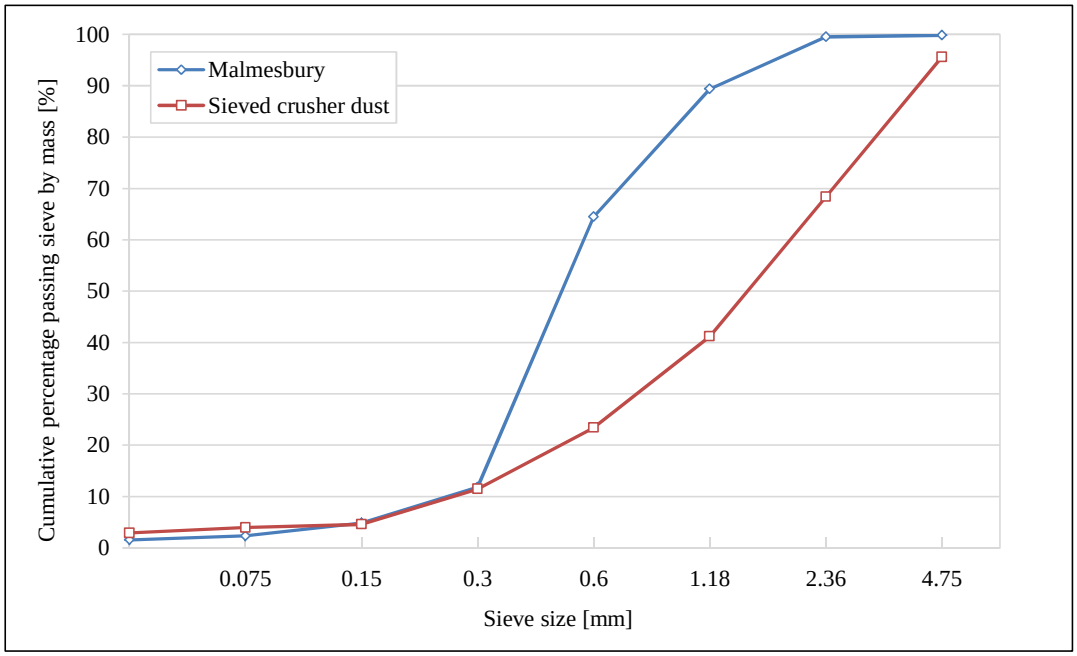

Figure 3.16 Grading of sand

3.3.6 Coarse aggregates

Coarse aggregates, or stone, refer to aggregates of which more than 90 % of the particles by mass are retained on a 4.75 mm sieve. Coarse aggregates that were used included 6 and 13 mm Greywacke stone respectively which was produced by mechanical crushing of Malmesbury shale and graded according to SANS 201 (2008). The relevant coarse aggregate properties are provided in Table 3.2.

Table 3.2 Aggregate properties

Material	Fineness modulus	Relative density [kg/m^3]	Aggregate crushing value [%]	Particle shape
Malmesbury sand	2.33	2.57	-	Round
Greywacke Crusher dust	3.55	2.69	-	Angular
6 mm Greywacke stone	-	2.73	11.2	Angular
13 mm Greywacke stone	-	2.73	10.3	Angular

3.4 Mix specification

Two different concrete mixes were used to accommodate the aforementioned admixtures. A conventional concrete mix was used to accommodate the addition of retarders, accelerators, air entrainers, plasticisers, and shrinkage reducing admixtures, respectively, whereas a high flow concrete mix was used to accommodate the addition of super-plasticisers. The mix specifications of the conventional and high flow concrete mixes are discussed in the following sections.

3.4.1 Conventional concrete mix

The conventional concrete mix was similar to mixes frequently used by local ready-mix companies for industrial floor slabs being comprised of standard municipal supplied water, CEM II 52.5N Portland-limestone cement, 13 mm Greywacke stone, and blended fine aggregate of Malmesbury sand and Greywacke crusher dust. The blended fine aggregate comprised of 70 % Malmesbury sand and 30 % Greywacke crusher dust by mass. The mix had a corresponding water-cement ratio of 0.6.

The conventional concrete mix accommodated the prescribed maximum dosages of the associated admixtures without segregation. Accordingly, the minimum and maximum dosages of admixtures in the respective conventional concrete mixes correspond to the values provided in Table 3.1. A total of eleven conventional concrete mixes were used during testing. The relevant notations, descriptions and dosages of the mixes are provided in Table 3.3 while mix design proportions are provided in Table 3.4.

The average densities, slump values and 28 day compressive strengths of the respective conventional concrete mixes are provided in Table 3.4. The compressive strengths and densities were determined

using four samples of each mix. The corresponding slump values and compression strengths were determined in accordance with SANS 5862-1 (2006) and SANS 5863 (2006) respectively.

Table 3.3 Description of conventional concrete mixes

Notation	Description	Dosage**
REF	Conventional concrete reference mix	-
RET_Max	Conventional concrete mix containing maximum dosage retarder	1.0
RET_Min	Conventional concrete mix containing minimum dosage retarder	0.2
AC_Max	Conventional concrete mix containing maximum dosage accelerator	3.0
AC_Min	Conventional concrete mix containing minimum dosage accelerator	1.6
AIR_Max	Conventional concrete mix containing maximum dosage air entrainer	0.3
AIR_Min	Conventional concrete mix containing minimum dosage air entrainer	0.15
PL_Max	Conventional concrete mix containing maximum dosage plasticiser	0.5
PL_Min	Conventional concrete mix containing minimum dosage plasticiser	0.2
S_Max	Conventional concrete mix containing maximum dosage SRA*	3.0
S_Min	Conventional concrete mix containing minimum dosage SRA*	0.5

Notes

**SRA* *Shrinkage reducing admixture*

***Dosage units* *[litre / 100 kg of cementitious material]*

Table 3.4 Conventional concrete mix design proportions

		REF	RET_Min	RET_Max	AC_Min	AC_Max	AIR_Min	AIR_Max	PL_Min	PL_Max	S_Min	S_Max
Slump value	mm	92	88	128	98	97	89	98	91	128	92	94
Compressive strength	MPa	40.1	41.5	41.1	41.4	39.5	38.8	33.9	43.3	41.3	34.9	33.8
Average density	kg/m^3	2442	2434	2478	2430	2406	2397	2388	2438	2457	2377	2387
Mix design proportions												
Water	kg/m^3	205	205	205	205	205	205	205	205	205	205	205
Cement CEMII 52.5N	kg/m^3	341.7	341.7	341.7	341.7	341.7	341.7	341.7	341.7	341.7	341.7	341.7
Malmesbury sand	kg/m^3	569.2	569.2	569.2	569.2	569.2	569.2	569.2	569.2	569.2	569.2	569.2
Crusher dust	kg/m^3	244.0	244.0	244.0	244.0	244.0	244.0	244.0	244.0	244.0	244.0	244.0
13mm Greywacke stone	kg/m^3	1036.2	1036.2	1036.2	1036.2	1036.2	1036.2	1036.2	1036.2	1036.2	1036.2	1036.2
Retarder	kg/m^3	-	0.72	3.62	-	-	-	-	-	-	-	-
Accelerator	kg/m^3	-	-	-	7.38	13.84	-	-	-	-	-	-
Air entrainer	kg/m^3	-	-	-	-	-	0.52	1.04	-	-	-	-
Plasticiser	kg/m^3	-	-	-	-	-	-	-	0.81	2.02	-	-
SRA	kg/m^3	-	-	-	-	-	-	-	-	-	1.71	10.25
Total content	kg/m^3	2396.1	2396.8	2399.7	2403.5	2409.9	2396.6	2397.1	2396.9	2398.1	2397.8	2406.4

3.4.2 High flow concrete mix

Due to segregation, the conventional concrete mix could not accommodate a significant dosage of the respective super-plasticisers and, therefore, a high flow concrete was used to accommodate a more substantial dosage of the respective super-plasticisers. The concrete properties and mix design proportions of high flow concrete mix are discussed accordingly.

The corresponding mix design proportions were determined in accordance with specifications provided by European guidelines for self-compacting concrete (European Federation for Precast Concrete, 2005). The high flow reference mix, devoid of super-plasticiser, governed the specification of the associated mix design proportions. The reference mix had to be classified as a high flow concrete mix to ensure similar compaction requirements considering that the mixes containing super-plasticisers are self-compacting to a large extent. The mix had to obtain a slump value greater than 180 mm to be characterised as a high flow mix. In order to meet this criterion, the high flow concrete reference mix had a relatively high water content of 222.22 kg/m^2. The mix was comprised of standard municipal supplied water, CEM II 52.5 N Portland-limestone cement, fly ash, Malmesbury sand, and 6 mm Greywacke stone. The mix had a corresponding water-binder ratio of 0.5 which was high enough to avoid the effect of autogenous and drying shrinkage of the concrete paste. A maximum prescribed stone content of 30 % by volume was used in the mix. Siliceous fly ash was used to replace 35 % of cement by mass to increase flowability of the mix.

Optimal dosages were determined by visual assessment of the concrete paste where maximum dosages of the respective mixes correspond to the limit just before segregation occurred. A total of five high flow concrete mixes were used to perform tests. The relevant notations, descriptions and dosages of these mixes are provided in Table 3.5 while the mix design proportions are provided in Table 3.6.

Table 3.5 Description of high flow concrete mixes

Notation	Description	Dosage
REF2	High flow concrete reference mix	-
PCE_Max	High flow concrete containing maximum dosage PCE* based super-plasticiser	1.25
PCE_Min	High flow concrete containing minimum dosage PCE* based super-plasticiser	0.3
SMF_Max	High flow concrete containing maximum dosage SMF** based super-plasticiser	1.0
SMF_Min	High flow concrete containing minimum dosage SMF** based super-plasticiser	0.6

Notes

**PCE* *Poly carboxylate ethers*

***SMF* *Sulphonated melamine formaldehyde*

Dosage units

[litre / 100 kg of cementitious material]

Table 3.6 High flow concrete mix proportions

High flow concrete mix	REF	PCE_Max	PCE_Min	SMF_Max	SMF_Min
			kg/m^3		
Water	222.2	222.2	222.2	222.2	222.2
Cement CEM II 52.5	288.9	288.9	288.9	288.9	288.9
Fly ash	155.6	155.6	155.6	155.6	155.6
Malmesbury sand	865.2	865.2	865.2	865.2	865.2
6 mm Greywacke stone	840.0	840.0	840.0	840.0	840.0
PCE super-plasticiser	-	5.83	1.40	-	-
SMF super-plasticiser	-	-	-	5.11	3.07
Total content	2371.9	2377.7	2373.3	2377.0	2375.0

The average densities and 28 day compressive strengths of the respective high flow mixes are provided in Table 3.7. Compressive strengths and densities were determined using four samples of each mix. Compression strengths were determined in accordance with SANS 5863 (2006).

Table 3.7 Concrete properties of high flow concrete mixes

Test		REF2	PCE_Min	PCE_Max	SMF_Min	SMF_Max
Average density	[kg/m^3]	2320	2209	2251	2263	2250
Compressive strength	[MPa]	35.7	33.2	31.8	39.4	39.2
Fresh properties						
Slump flow	[mm]	335	455	670	615	740
Filling ability classification		Fails	Fails	SF2	SF1	SF2
Passing ability	[%]	Fails	42.9	81.1	65.8	88.6
Passing ability classification		Fails	Fails	PA2	Fails	PA2
T_{500}	[s]	Fails	Fails	< 2	< 2	< 2
Viscosity classification		Fails	Fails	VS1	VS1	VS1
Segregation resistance	[%]	0.1	1.9	9.8	3.8	12.0
Segregation resistance classification		SR1	SR1	SR1	SR1	SR1

Various tests were performed to measure the fresh properties of the respective high flow mixes such as filling ability, passing ability, viscosity, and segregation resistance. The corresponding tests were

performed in accordance with the European guidelines for self-compacting concrete (SCC) since most of these mixes fulfil the requirements of a SCC. The fresh properties of the respective high flow mixes are provided in Table 3.7. A brief discussion of the corresponding tests is provided in the following paragraphs while further information regarding the setup and procedures of subsequent tests can be found in European guidelines for SCC (European Federation for Precast Concrete, 2005).

Slump flow tests were performed to measure the filling ability of the respective mixes. Filling ability refers to the ability of fresh concrete to flow into, and fill, all spaces within the formwork under its own weight. The classification of filling ability is provided in Table 3.8 while the results of slump flow tests are provided in Table 3.7.

Table 3.8 Classification of filling ability

Class	Slump flow [mm]
SF1	550 to 650
SF2	660 to 750
SF3	760 to 850

L-Box tests were performed to measure the passing ability of the respective mixes. Passing ability refers to the ability of fresh concrete to flow through tight openings, such as spaces between steel reinforcing bars, without segregation or blocking. The classification of passing ability is provided in Table 3.9 while the results of L-Box tests are provided in Table 3.7.

Table 3.9 Classification of passing ability

Class	Passing ability [%]
PA1	> 80 (2 rebars)
PA2	> 80 (3 rebars)

T_{500} tests were used to measure the viscosity of the respective mixes. Viscosity refers to the resistance to flow of fresh concrete once flow has started. The classification of viscosity is provided in Table 3.10 while the results of T_{500} tests are provided in Table 3.7.

Table 3.10 Classification of viscosity

Class	T_{500} [s]
VS1	≤ 2
VS2	> 2

Sieve segregation tests were used to measure the segregation resistance of the respective mixes. Segregation resistance refers to the ability of concrete to remain homogenous in composition while in its fresh state. The classification of segregation resistance is provided in Table 3.11 while the results of sieve segregation tests are provided in Table 3.7.

Table 3.11 Classification of segregation resistance

Class	Segregation resistance [%]
SR1	≤ 20
SR2	≤ 15

With reference to Table 3.7, the mixes containing a maximum dosage of PCE-based super-plasticiser and SMF-based super-plasticiser conformed to all classifications of fresh property tests for SCC whereas the reference mix failed to comply with the majority of tests. Accordingly, the high flow reference mix was not characterised as a SCC mix, although the corresponding specifications were used to obtain a mix that was able to accommodate a more substantial dosage of the respective super-plasticisers.

3.5 Conclusion

This chapter provides the details of the experimental tests that were performed to investigate the phenomenological and fundamental influences of a wide range of admixtures on the PSC of concrete. Crack area tests were performed to determine the phenomenological influence of admixtures while tests for measurement of surface tension, capillary pressure, bleeding, setting time, evaporation, shrinkage, and settlement of concrete were performed to investigate the fundamental influences of admixtures. The test setup and procedures of the aforementioned tests are discussed accordingly. The material and mix specifications of both the conventional and high flow concrete mixes are also provided. The test results of the respective conventional concrete mixes are provided and discussed in the next chapter.

CHAPTER 4

Results and discussions of conventional concrete

Experimental results of the conventional concrete mixes are presented and discussed accordingly in this chapter. Firstly, a general discussion is provided that comprehends different procedures that were used to analyse results as well as preliminary conclusions that were drawn with respect to certain test results. In relation to the research objectives, phenomenological and fundamental results are discussed seperately in Section 4.5 and Section 4.6. Lastly, a concluding summary is provided with regard to the results and discussions presented in this chapter.

4.1 Data processing and presentation methodology

This section provides a discussion of the data processing methodology followed to present certain experimental results. This includes: representative capillary pressure and the rapid crack growth period. It should further be noted that the results presented in this chapter are the calculated average of at least three samples, unless stated otherwise. The results of the individual samples together with the calculated averages are provided in Appendix A.

4.1.1 Calculation of representative capillary pressure

Capillary pressure is dependent on the rate of water loss, surface tension and particle size distribution of the concrete paste. Correspondingly, the capillary pressure results were primarily used to determine the rate of pressure build-up since it can be correlated to the aforementioned factors. Although air entry is required for PSC to occur, it is not considered to be the governing aspect since measurements were performed at a specific location. Therefore, due to variability of particle size distribution at the concrete surface, air entry could have occurred sooner at a different location in the concrete sample.

Corresponding capillary pressure samples were cast from the same mix and exposed to the same environmental conditions. Therefore, the surface tension of the pore fluid and the associated rates of evaporation are expected to be the same. This is validated by the fact that the corresponding samples displayed similar rates of capillary pressure build-up. However, as expected, samples exhibited variations in the time of air entry.

Capillary pressure results of two samples per mix were combined to provide a representative capillary pressure build-up. As shown in Figure 4.1, the results of the mix containing a minimum dosage of SRA (Shrinkage reducing admixture) are used to illustrate the related calculation procedures. The

aforementioned results are merely used based on the fact that it provides a clear example for explanation purposes.

The representative capillary pressure build-up was calculated as the average of the corresponding samples up to the first occurrence of air entry, as indicated by Peak 1 in Figure 4.1. Thereafter, linear interpolation was performed between the respective values of air entry to determine a representative air entry value. A straight line was used to connect the representative air entry value and the average capillary pressure. The part of the graph calculated as the average of samples is indicated by a solid line whereas the interpolated part of the graph is indicated by a dashed line.

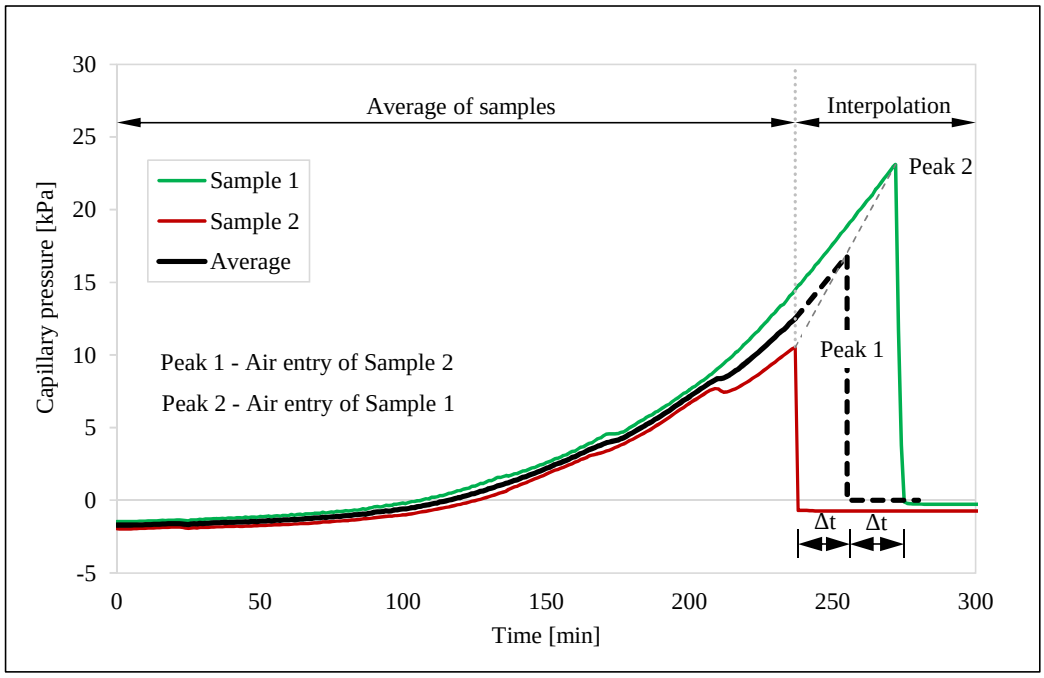

Figure 4.1 Calculation of representative capillary pressure build-up of S_Min

This calculation method served to fulfil the primary objective of the capillary pressure results, namely, to determine the rate of capillary pressure build-up of the respective mixes. The rate of pressure build-up is partly used to elucidate the fundamental influences of admixtures on the PSC of concrete. Air entry is not directly correlated to crack onset since measurements were performed at a localised position. The calculation of representative capillary pressure for the respective mixes is presented in Appendix A.6.

4.1.2 Rapid crack growth period

The rapid crack growth period is defined as the time interval during which the majority of plastic shrinkage cracks are formed. The time after casting during which rapid crack growth is expected to occur is especially important in construction practices for application of external preventative measures, as discussed in Section 2.6. External preventative measures need to be applied in advance of the rapid crack growth to mitigate or possibly inhibit PSC.

The rapid crack growth period was determined by identifying crack onset and crack stabilisation respectively. Crack onset is defined as the first crack measurement of which the measured crack area is greater than zero, whereas crack stabilisation is defined as the time when the rate of crack growth is insignificant. The rate of crack growth was calculated as the average rate of growth during the 20 minute measurement intervals. Due to differences in relative magnitudes between the total crack area and the rate of crack growth, the latter was displayed on a secondary axis to provide a comprehensible presentation of the rate of development. Furthermore, the major and minor units of the secondary axis were kept constant for all mixes to ensure consistent identification of crack onset and crack stabilisation.

The crack area results of the conventional concrete reference mix, as shown in Figure 4.2, is used to illustrate the rate of crack growth, and identification of crack onset and crack stabilisation respectively. The grey columns in the figure illustrate the average rate of crack growth during the respective 20 minute measuring intervals which was used to identify the time of crack onset and crack stabilisation.

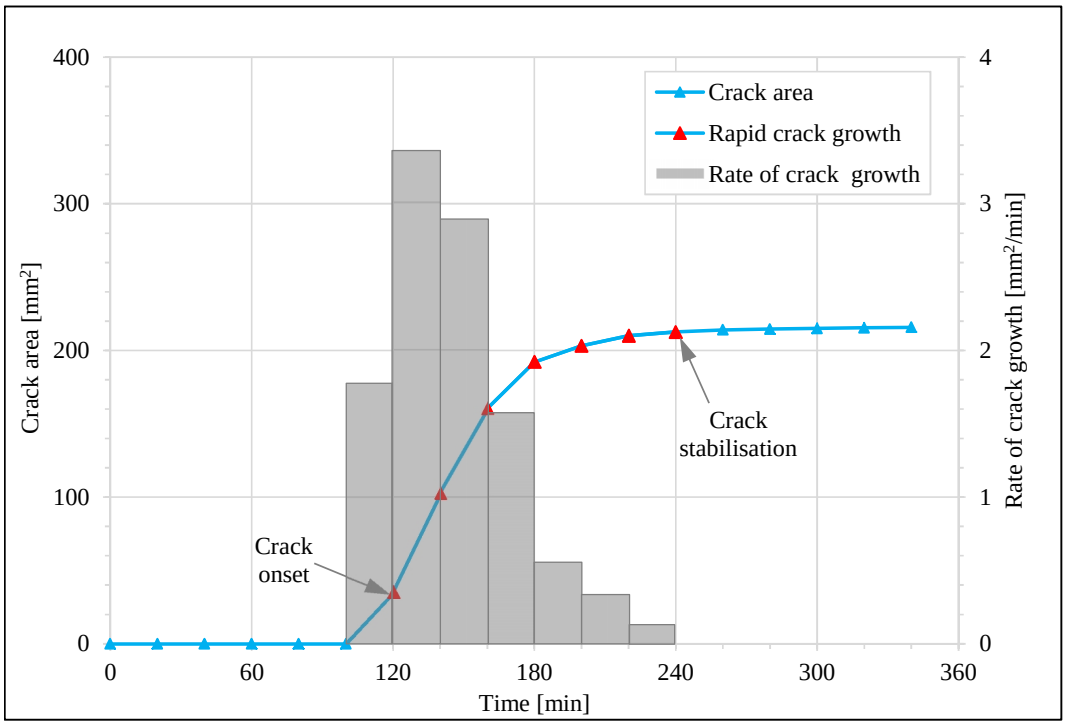

Figure 4.2 Rate of crack growth of the conventional concrete reference mix

As shown in Figure 4.2 and Figure 4.3, crack onset corresponds to the first measured crack area greater than zero at 120 minutes while the time after which the rate of crack growth became insignificant was graphically identified as 240 minutes and, therefore, also designates the time of crack stabilisation. The rapid crack growth period of the respective mixes, starting with crack onset and ending with crack stabilisation, is graphically illustrated with the use of red markers as shown in Figure 4.2 and Figure 4.3 respectively.

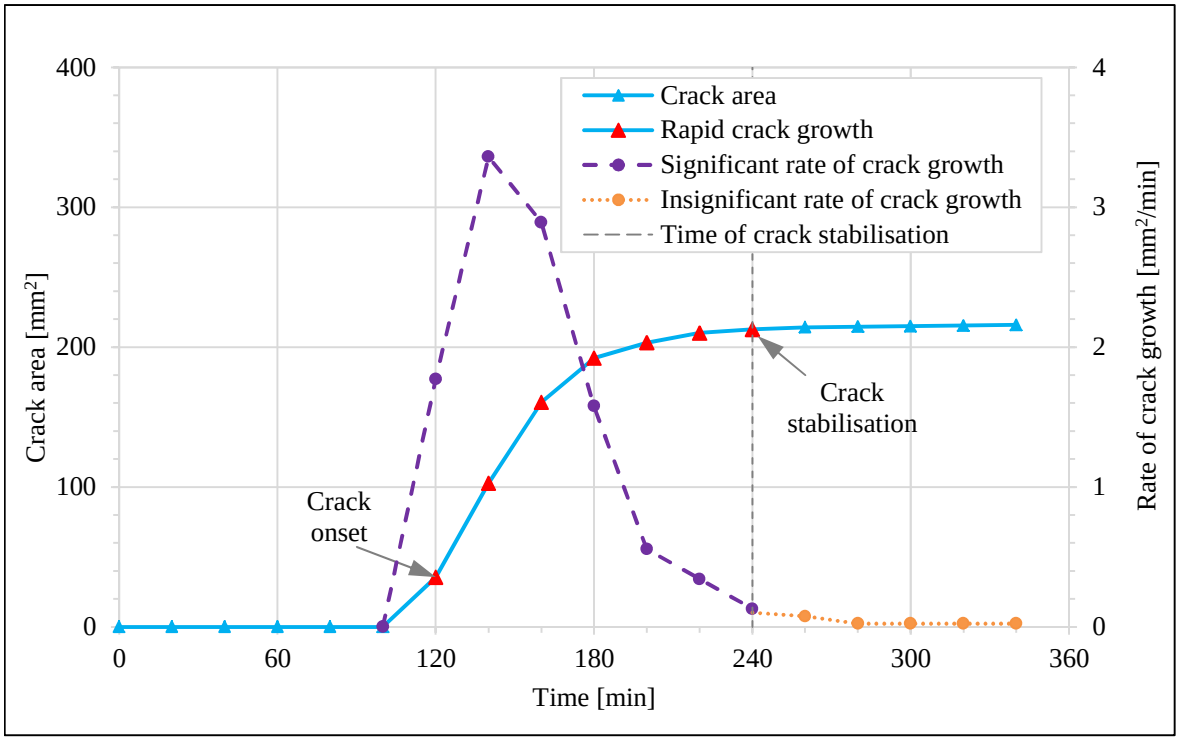

Figure 4.3 Rapid crack growth of the conventional concrete reference mix

The rapid crack growth period of the respective mixes was determined in a similar manner to the conventional concrete reference mix as discussed in this section. This method serves to provide a consistent procedure to identify the time period during which rapid crack growth occurs. The rapid crack growth and crack area results of the respective concrete mixes are provided in Appendix A.2 and Appendix A.1 respectively.

4.2 Correlation between setting times and rapid crack growth

Research undertaken by Combrinck (2012) found that PSC is typically characterised by a rapid growth and stabilisation of cracks between the initial and final setting time of concrete. However, the related tests conducted by Combrinck were performed using conventional concrete mixes containing insignificant dosages of accelerators, plasticisers, and retarders, respectively. Hence, the results of the respective conventional concrete mixes, which contains both a high and low dosage of the respective admixtures, are analysed to determine the correlation between setting times and rapid crack growth. The results of rapid crack growth and setting times are provided by Figure 4.4 and Table 4.1.

The conventional concrete reference mix (REF) reached initial set at approximately 160 minutes after casting whereas final set was reached at approximately 210 minutes. Furthermore, crack onset and crack stabilisation occurred 120 and 240 minutes after casting respectively. Therefore, it is apparent that the setting times of REF were reached during the rapid crack growth period where crack onset occurred approximately 40 minutes prior to initial set while crack stabilisation was reached approximately 30 minutes after final set.

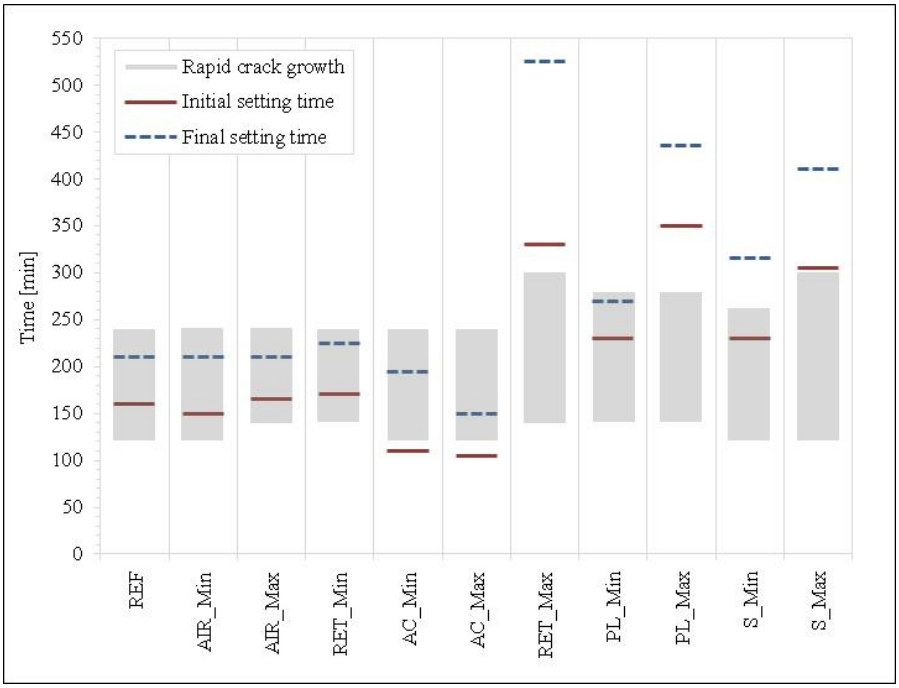

Figure 4.4 Correlation between setting times and rapid crack growth of conventional concrete mixes

Table 4.1 Setting time and rapid crack growth results of conventional concrete mixes

	Initial set [min]	Crack onset [min]	Final set [min]	Crack stabilisation [min]
REF	160	120	210	240
RET_Min	170	140	225	240
RET_Max	330	140	525	300
AC_Min	110	120	195	240
AC_Max	105	120	150	240
AIR_Min	150	120	210	240
AIR_Max	165	140	210	240
PL_Min	230	140	270	280
PL_Max	350	140	435	280
S_Min	230	120	315	260
S_Max	305	120	410	300

Mixes containing air entrainer (AIR_Min & AIR_Max) and a minimum dosage of glucose based retarder (RET_Min) exhibited similar setting times than REF. Therefore, the respective dosages of air entrainer and a minimum dosage of retarder do not have a profound influence on setting times of concrete. Although the addition of glucose based retarder is expected to delay the initial and final set of concrete, the minor delay in setting times of RET_Min is attributed to the insignificant dosage

added to the mix. The respective initial setting times of the mentioned mixes were reached in the course of 150 to 170 minutes after casting whereas the respective final setting times were reached in the course of 210 to 225 minutes. Therefore, similar to REF, the setting times of these mixes were reached during the rapid crack growth period. Crack onset of the respective mixes occurred at least 20 minutes before initial set whereas final set occurred at least 15 minutes before crack stabilisation.

Mixes containing calcium chloride based accelerator (AC_Min & AC_Max) display accelerated setting times. The initial set of AC_Min and AC_Max was respectively reached approximately 110 and 105 minutes after casting whereas the respective final setting times were reached at approximately 195 and 150 minutes. Therefore, similar to REF, the associated setting times coincided with rapid crack growth, however, initial set of the aforementioned mixes closely corresponds to crack onset.

Mixes containing minimum dosages of lignosulphonate based plasticiser (PL_Min) and SRA (S_Min) display moderately retarded setting times. Initial set of PL_Min and S_Min was correspondingly reached 230 minutes after casting whereas final set was reached at approximately 270 and 315 minutes respectively. Therefore, similar to REF, setting times of PL_Min were reached during the rapid crack growth period, however, final set closely corresponds to crack stabilisation. Although initial set of S_Min was reached during rapid crack growth, final set was reached approximately 55 minutes after crack stabilisation.

Mixes containing maximum dosages of glucose based retarder (RET_Max), lignosulphonate based plasticiser (PL_Max), and SRA (S_Max) display extensively delayed setting times compared to REF. The respective initial setting times were reached in the course of 305 to 350 minutes after casting whereas the respective final setting times were reached in the course of 410 to 525 minutes. Therefore, setting times of the aforementioned mixes were reached long after crack stabilisation.

In conclusion, the cracking behaviour of mixes containing no admixtures, mixes containing low dosages of the accelerator, air entrainer, plasticiser and retarder as well as mixes containing high dosages of the accelerator and air entrainer, respectively, resembles a correlation between the setting times and rapid crack growth since the respective setting times were reached during the rapid crack growth period. However, mixes containing high dosages of the retarder, plasticiser and SRA as well as low dosages of the SRA do not resemble a correlation between the setting times and rapid crack growth. In general, it can also be concluded that the more substantial the delay in setting times the less significant the correlation between the rapid crack growth and setting times. Finally, the characterisation of typical PSC by Combrinck (2012) between the initial and final setting times seems to have merrit for conventional concrete mixes with various dosages of admixtures that do not significantly delay setting times while this is not valid for mixes containing dosages of admixtures that cause a significant delay in setting times.

4.3 Rapid crack growth period

Crack onset of the respective mixes occurred in the course of 120 to 140 minutes after casting. Therefore, the addition of the respective admixtures did not have a profound influence on the time of crack onset. Furthermore, different dosages of the respective admixtures also did not have a profound influence on the time of crack onset. In fact, with exception of AIR_Min and AIR_Max, mixes containing the same admixture at different dosages displayed similar times of crack onset.

Crack stabilisation of the respective mixes occurred in the course of 240 to 300 minutes after casting. The mixes subject to normal and accelerated setting times displayed similar times of crack stabilisation whereas crack stabilisation of mixes with retarded setting times was identified within a range of 20 minutes. It is therefore reasoned that crack stabilisation corresponds to the setting time characteristics of the respective concrete mixes.

With regard to mixes containing the same admixture, mixes containing plasticiser, air entrainer, and accelerator displayed a similar time of crack stabilisation. Consequently, the dosage limits of the associated admixtures did not have a profound influence on the time of crack stablisation. With regard to mixes containing SRA's and retarders, crack stabilisation of S_Max occurred 40 minutes after that of S_Min whereas crack stabilisation of RET_Max occurred 60 minutes after that of RET_Min.

In conclusion, crack onset of the respective mixes occurred in close proximity regardless of the admixture and corresponding dosage limits. Furthermore, crack stabilisation corresponds to the setting time characteristics of the respective concrete mixes. Rapid crack growth of mixes containing both low and high dosages of accelerator, air entrainer and plasticiser, respectively, occurred during the same time interval. Consequently, the corresponding dosage limits of the associated admixtures do not have a profound influence on the rapid crack growth period. Lastly, with regard to crack onset of the respective mixes, external preventative measures need to be applied approximately at the same time for all mixes to mitigate or possibly inhibit PSC.

4.4 Surface tension results

The surface tension results of the respective conventional concrete mixes are shown in Table 4.2 and Figure 4.5 respectively. Three successive measurements of each sample were recorded.

The addition of air entrainer, retarder and SRA progressively influenced the surface tension of the pore fluid since a higher dosage of the aforementioned admixtures resulted in a more substantial reduction in surface tension. The addition of a minimum dosage of plasticiser resulted in a significant reduction in surface tension when compared to REF although the reduction in surface tension between PL_Min and PL_Max is less profound. Therefore, various dosages of plasticiser, ranging between the minimum and maximum prescribed dosage limits, are expected to display a similar reduction in the surface tension of the pore fluid. Lastly, the addition of accelerator has an insignificant influence on

the surface tension of the pore fluid with the surface tension of both AC_Min and AC_Max only slightly lower than that of REF. The significance of surface tension and the influence it has on the PSC of concrete is further discussed in Section 4.5 and 4.6.

Table 4.2 Surface tension results of respective conventional concrete mixes

Mix	Admixture	Solution concentration of admixtures [g/L of solution]	Average surface tension [mN/m]	Standard deviation
REF	-	-	70.55	0.12
RET_Min	Retarder	0.72	66.43	0.70
RET_Max	Retarder	3.62	62.52	0.47
AC_Min	Accelerator	7.38	70.23	0.51
AC_Max	Accelerator	13.84	70.09	0.19
AIR_Min	Air entrainer	0.52	58.3	0.84
AIR_Max	Air entrainer	1.04	45.67	0.46
PL_Min	Plasticiser	0.81	61.05	0.27
PL_Max	Plasticiser	2.02	58.31	0.14
S_Min	SRA	1.71	68.25	0.08
S_Max	SRA	10.25	61.05	0.02

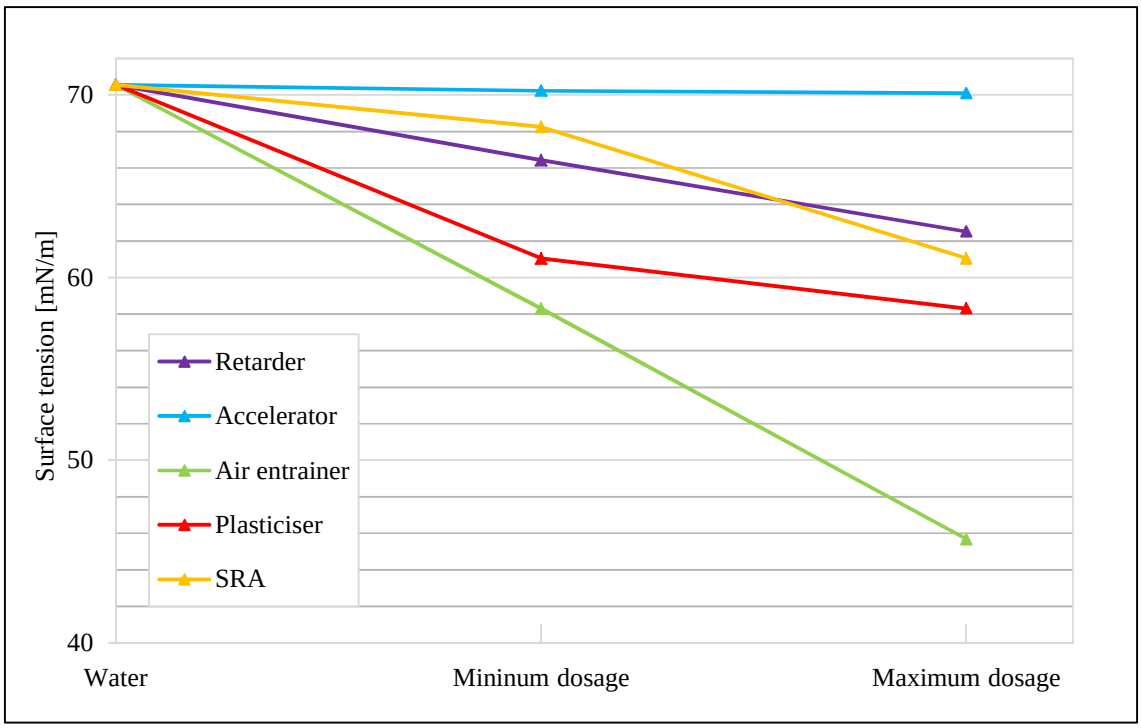

Figure 4.5 Surface tension results of respective conventional concrete mixes

4.5 Phenomenological behaviour

The crack area results of the respective conventional concrete mixes are used to determine the phenomenological influence of admixtures on the severity of PSC. Total crack area of mixes containing various admixtures were measured and compared to that of a reference mix devoid from admixtures to determine the physical increase or reduction in the severity of cracking. The crack area results of the respective mixes are shown in Figure 4.6 and Table 4.3 respectively.

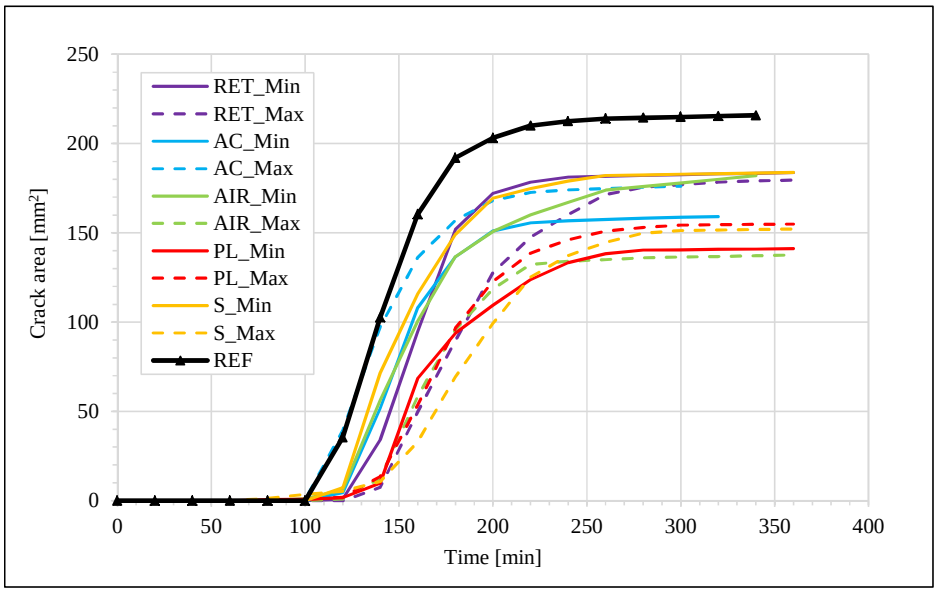

Figure 4.6 Crack area comparison of respective conventional concrete mixes

Table 4.3 Crack area results of respective conventional concrete mixes

	Crack onset [min]	Crack stabilisation [min]	Crack area at stabilisation [mm^2]	% Reduction in crack area at stabilisation	Time of final measurement [min]	Final crack area [mm^2]
REF	120	240	213	-	340	216
RET_Min	140	240	181	15.0	360	184
RET_Max	140	300	177	16.9	580	184
AC_Min	120	240	157	26.3	320	159
AC_Max	120	240	174	18.3	300	176
AIR_Min	120	240	167	21.6	340	182
AIR_Max	140	240	134	37.1	360	138
PL_Min	140	280	140	34.3	420	142
PL_Max	140	280	153	28.2	480	156
S_Min	120	260	182	14.6	440	185
S_Max	140	300	151	29.1	520	155

Average crack area measurements were conducted at 20 minute intervals, however, measurement markers are only displayed for REF in Figure 4.6 to avoid overly congested results. Furthermore, with reference to Figure 4.6 and Table 4.3, the mixes containing admixtures altogether display a reduction in the severity of PSC. Correspondingly, the total crack area of mixes are scaled with respect to the crack area of REF, as shown in Figure 4.7, to illustrate the relative reductions in the severity of cracking.

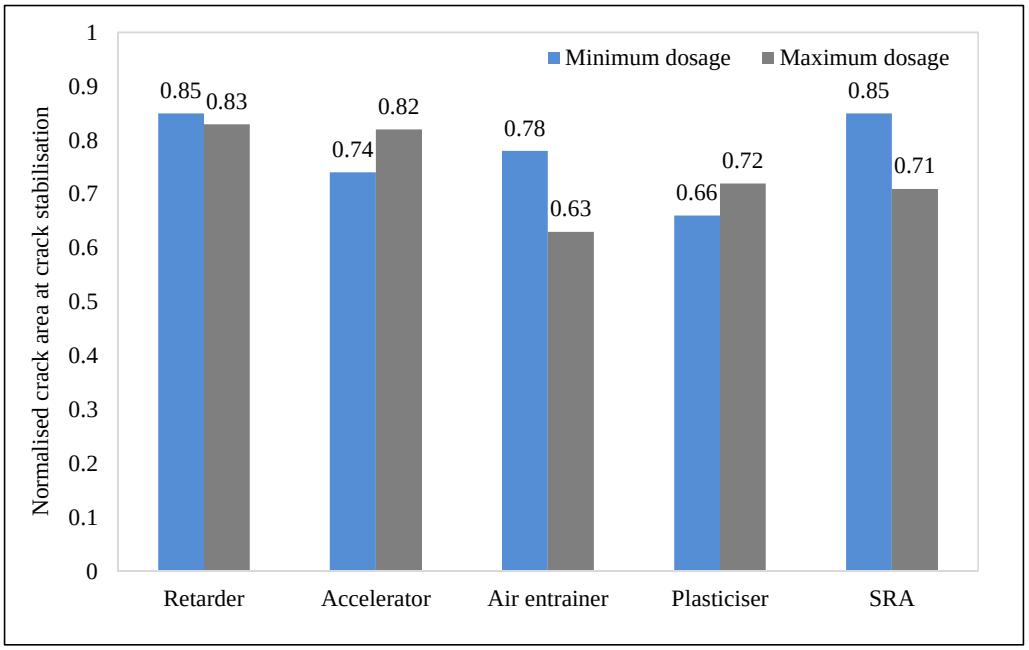

Figure 4.7 Normalised crack area of respective conventional concrete mixes

The conventional concrete reference mix (REF) displayed the most severe cracking with a measured crack area of 213 mm^2 at crack stabilisation. Furthermore, REF displayed an insignificant rate of crack growth beyond crack stabilisation since the associated rate corresponds to a growth of only 3 mm^2 in the course of 100 minutes.

Mixes containing glucose based retarder, i.e. RET_Min and RET_Max, displayed a total crack area of 181 and 177 mm^2 respectively which corresponds to a reduction of 15 and 16.9 % in the total crack area when compared to REF. Therefore, the associated dosage limits caused a similar reduction in the severity of cracking. Furthermore, similar to REF, the respective mixes displayed an insignificant rate of crack growth after crack stabilisation. The rate of growth after crack stabilisation of RET_Min corresponds to a growth of 3 mm^2 in the course of 120 minutes whereas that of RET_Max corresponds to a growth of 7 mm^2 in the course of 280 minutes.

Mixes containing calcium chloride based accelerator, i.e. AC_Min and AC_Max, displayed a total crack area of 157 and 174 mm^2 respectively. Correspondingly, AC_Min and AC_Max respectively displayed a reduction of 26.3 and 18.3 % in the total crack area when compared to REF. Therefore, the mix containing a minimum dosage of calcium chloride based accelerator displayed a more

substantial reduction in the severity of PSC compared to the mix containing a maximum dosage. AC_Min and AC_Max also displayed an insignificant rate of crack growth after crack stabilisation. The associated rate of growth after crack stabilisation of AC_Min and AC_Max corresponds to a growth of 2 mm^2 in the course of 80 and 60 minutes respectively.

Mixes containing chloride free air entrainer, i.e. AIR_Min & AIR_Max, progressively influenced the severity of PSC since a higher dosage of air entrainer corresponds to a more substantial reduction in cracking. AIR_Min and AIR_Max displayed a total crack area of 167 and 134 mm^2 respectively which correspond to a reduction of 21.6 and 37.1 % in total crack area when compared to REF. AIR_Min displayed the highest rate of crack growth beyond crack stabilisation being associated with a growth of 15 mm^2 in the course of 100 minutes. However, compared to the corresponding crack area at stabilisation, the associated rate of growth after crack stabilisation is considered to be insignificant. AIR_Max also displayed an insignificant rate of crack growth beyond crack stabilisation being associated with a growth of 4 mm^2 in the course of 120 minutes.

Mixes containing lignosulphonate based plasticiser, i.e. PL_Min and PL_Max, displayed a total crack area of 140 and 153 mm^2 respectively which corresponds to a reduction of 34.3 and 28.2 % in total crack area at crack stabilisation. Therefore, similar to mixes containing accelerator, PL_Min displayed a more substantial reduction in PSC compared to PL_Max. Furthermore, PL_Min and PL_Max also displayed an insignificant rate of crack growth beyond crack stabilisation. The associated rate of growth after crack stabilisation of PL_Min corresponds to a growth of 2 mm^2 in the course of 140 minutes whereas that of PL_Max corresponds to a growth of 3 mm^2 in the course of 200 minutes.

Similar to mixes containing air entrainer, S_Min and S_Max progressively influenced the severity of PSC since a higher dosage of air entrainer corresponds to a more substantial reduction in cracking. S_Min and S_Max displayed a total crack area of 182 and 151 mm^2 respectively which correspond to a reduction of 14.6 and 29.1 % in total crack area when compared to REF. Furthermore, S_Min and S_Max also displayed an insignificant rate of crack growth beyond crack stabilisation. The associated rate of growth after crack stabilisation of S_Min corresponds to a growth of 3 mm^2 in the course of 180 minutes whereas that of S_Max corresponds to a growth of 4 mm^2 in the course of 220 minutes.

In conclusion, the respective conventional concrete mixes altogether display an insignificant rate of crack growth beyond crack stabilisation. Therefore, the comparison of total crack area at the time of crack stabilisation can be justified since the majority of cracking occurred during the rapid crack growth period.

The addition of the associated admixtures altogether displayed a reduction in the severity of PSC compared to a reference mix devoid from admixtures. The mix containing a maximum dosage of air entrainer displayed the most substantial reduction in the severity of PSC whereas mixes containing a minimum dosage of retarder and SRA displayed the least significant reduction in cracking.

Mixes containing both high and low dosages of glucose based retarder displayed a similar reduction in the severity of cracking. Furthermore, mixes containing the respective dosages of air entrainer and SRA progressively influenced the severity of cracking since a higher dosage of the associated admixtures corresponds to a more substantial reduction in PSC. Contrarily, mixes containing a minimum dosage of calcium chloride based accelerator and lignosulphonate based plasticiser respectively displayed a more substantial reduction in the severity of PSC when compared to mixes containing a maximum dosage.

4.6 Fundamental behaviour

The fundamental influences of admixtures on the severity of cracking are discussed in this section. The methodology that was used to elucidate the fundamental influences of the respective admixtures are as follows:

- Firstly, a comprehensive discussion regarding the behaviour of the conventional concrete reference mix is provided.
- Secondly, the fundamental results of mixes containing the same admixture are interpreted to determine whether the addition of the respective admixtures resulted in similar PSC behaviour than the reference mix.
- Finally, once the PSC behaviour of the respective mixes is determined, the magnitudes of the fundamental results are interpreted to elucidate the differences in the severity of cracking. The fundamental results of mixes containing the same admixture are compared to each other and to the reference mix to establish progressive influences on the PSC of concrete.

4.6.1 Behaviour of the conventional concrete reference mix

Initially, after concrete was cast, the concrete displayed a rapid increase in settlement as shown in Figure 4.8. The associated settlement can be attributed to gravitational forces being accountable for consolidation of the solid particles in the concrete paste.

Upon casting, the capillary pressure is positive due to hydrostatic pressure within the pore fluid. However, soon after casting the capillary pressure started to decrease as shown in Figure 4.9. The associated reduction in capillary pressure can be attributed to the formation of water menisci on the surface of the concrete paste. The curvature of the water menisci surface induces capillary tension forces which draws the solid particles closer together, causing a negative pressure within the pore fluid. The formation of water menisci, in turn, was caused by the evaporation of pore water from the concrete paste. The concrete was exposed to an extreme evaporation rate which exceeded the bleeding rate since the onset of the tests as shown in Figure 4.9.

The capillary pressure remained positive until the capillary tension forces exceeded the internal water pressure of the pore fluid. In connection herewith, the onset of negative capillary pressure build-up

designated the time after which the concrete paste was subjected to resultant capillary tension forces. With reference to Figure 4.9, the onset of negative capillary pressure build-up was reached approximately 70 minutes after casting. The time interval during which the capillary pressure was positive is indicated by the shaded area in Figure 4.8. Progressive evaporation of pore water from the concrete paste caused negative capillary pressure build-up. The rate of build-up is directly related to the rate of evaporation, the rate of bleeding, surface tension of the pore fluid and particle distribution of the concrete paste (Slowik et al., 2008).

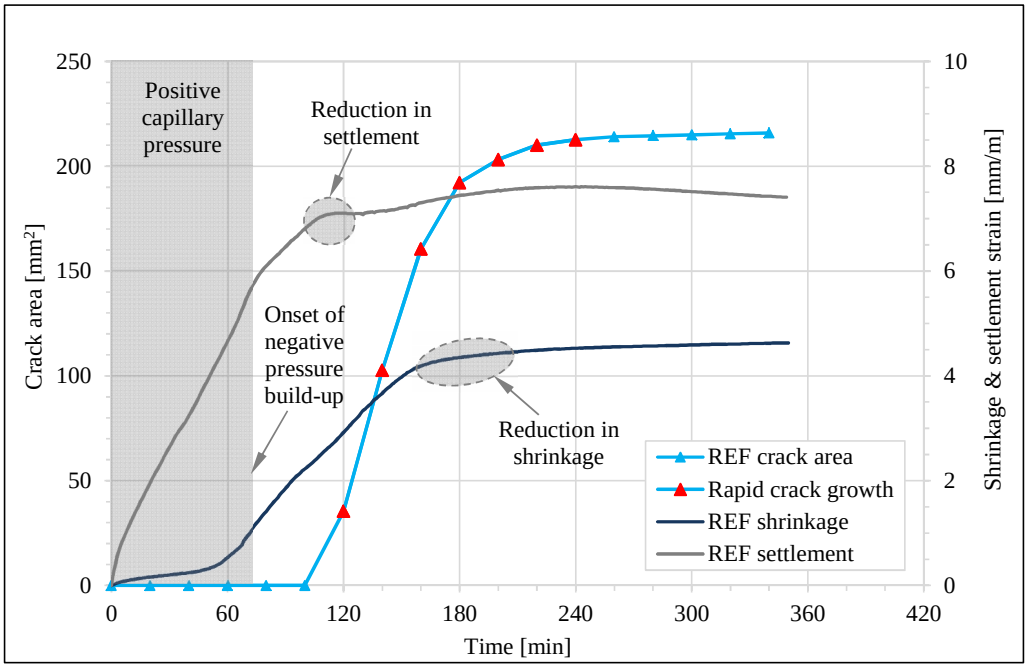

Figure 4.8 Correlation between crack area, shrinkage and settlement of REF

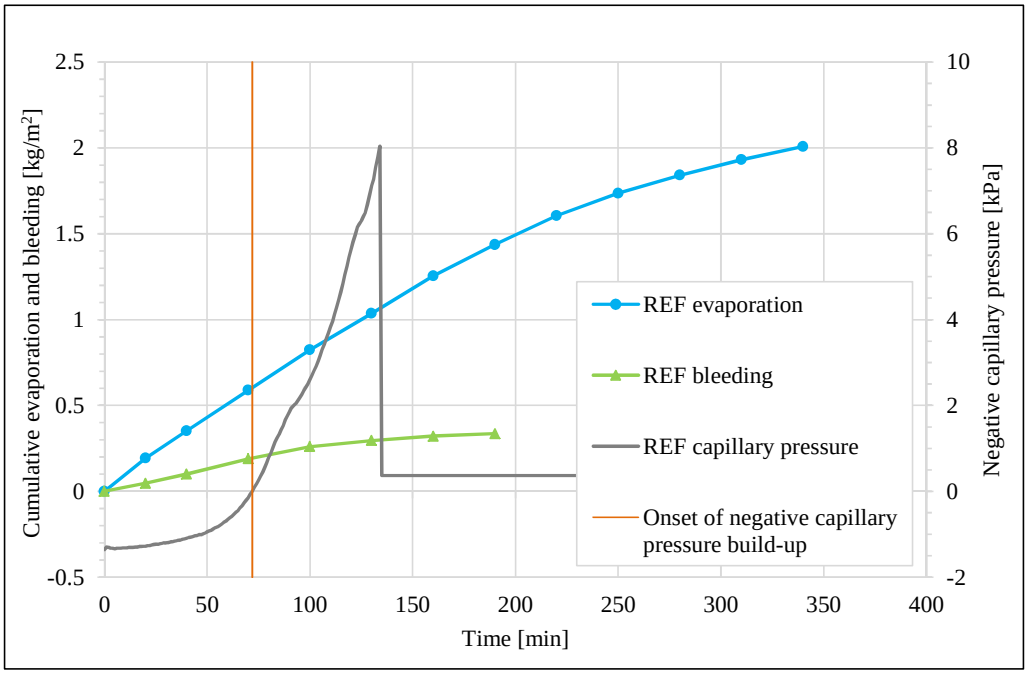

Figure 4.9 Correlation between evaporation, bleeding and capillary pressure of REF

As result of the negative capillary pressure build-up, the capillary tension forces acted on the solid particles both vertically and horisontally which resulted in settlement and shrinkage of the still plastic concrete. Subsequently, once the negative capillary pressure build-up is reached, settlement can be attributed to a combination of gravitational and capillary tension forces. Furthermore, the onset of the negative capillary pressure build-up closely corresponds to a significant increase in shrinkage of the concrete paste as shown in Figure 4.8.

The negative capillary pressure build-up caused the network of solid particles to become progressively stiffer and, correspondingly, caused a reduction in settlement in the course of 100 to 120 minutes after casting. As shown in Figure 4.8, the significant reduction in settlement closely corresponds to crack onset at approximately 120 minutes after casting. From this point onwards, the vertical component of the capillary tension forces no longer have a pronounced influence on the cracking process since settlement has stabilised to a large extent. With reference to Figure 4.9, air entry occurred at an approximate time of 135 minutes. However, the time of air entry is not correlated to crack onset and the associated reduction in settlement since measurements were performed at a localised position. Therefore, due to variability of particle size distribution at the surface of the concrete paste, air entry could have occurred sooner at a different location. Also, capillary pressure measurements were not conducted at the crack location. If so, it is believed that air entry would have occurred just before crack onset.

As previously mentioned, the onset of negative capillary pressure build-up corresponds to a rapid increase in shrinkage results which is mainly attributed to the horisontal component of the capillary tension forces. After crack onset, the particles adjacent to the air penetrated regions continue to experience capillary pressure build-up as discussed in Section 2.3. The air penetrated regions form weak spots in the system as the contracting forces between these particles are considerably smaller than those in water-filled regions. Consequently, capillary pressure in the water filled regions of the concrete paste can possibly be relieved by horisontal shrinkage or a combination of horisontal shrinkage and settlement of the concrete paste after crack onset is reached. Therefore, considering that settlement has stabilised to a large extent at crack onset, horisontal shrinkage is mainly responsible for the formation of plastic shrinkage cracks after crack onset is reached. Furthermore, the significant reduction in shrinkage in the course of 150 to 200 minutes after casting corresponds to a reduction in the rate of crack growth as shown in Figure 4.8.

In summary, the settlement of the concrete paste is attributed to gravitational forces until commencement of the negative capillary pressure build-up approximately 70 minutes after casting. Thereafter, settlement is attributed to a combination of gravitational and capillary tension forces. The onset of negative capillary pressure build-up corresponds to a significant increase in shrinkage. The significant increase in shrinkage is attributed to the horisontal component of capillary tension forces. Shrinkage and settlement induced by capillary tension forces caused the network of solid particles to

become progressively stiffer and, correspondingly, caused a reduction in settlement. The associated reduction in settlement corresponds to crack onset at an approximate time of 120 minutes after casting. From this point onwards, the vertical component of capillary tension forces no longer has a pronounced influence on the cracking process and, therefore, horisontal shrinkage is mainly responsible for the formation of plastic shrinkage cracks.

4.6.2 Glucose based retarder

Mixes containing glucose based retarder, i.e. RET_Min and RET_Max respectively, displayed a reduction of 15 and 16.9 % in total crack area when compared to REF. Therefore, various dosages of the aforementioned retarder are expected to display a similar reduction in the severity of PSC.

Fundamental behaviour

With reference to Table 4.4, the onset of negative capillary pressure build-up of RET_Min and RET_Max occurred approximately 80 and 100 minutes after casting respectively. In addition, RET_Min and RET_Max respectively showed a significant increase in shrinkage at approximately 80 and 90 minutes after casting. Therefore, similar to REF, mixes containing the respective dosages of retarder display a close correlation between the onset of negative capillary pressure build-up and a significant increase in shrinkage. Furthermore, crack onset of RET_Min and RET_Max respectively occurred during the interval when a significant reduction in settlement was observed. Lastly, with reference to Figure 4.10, the reduction in shrinkage of the respective mixes corresponds to a reduction in the rate of crack growth. In conclusion, mixes containing the respective dosages of retarder displays similar behaviour than the reference mix.

Table 4.4 Fundamental results of REF, RET_Min and RET_Max

		REF	RET_Min	RET_Max
Onset of negative capillary pressure build-up	[min]	70	80	100
Approximation of significant increase in shrinkage	[min]	60	80	90
Approximation of significant reduction in settlement	[min]	100 to 120	90 to 120	110 to 160
Crack onset	[min]	120	140	140
Settlement at crack onset	[mm/m]	7.1	6.7	7.0
Approximation of significant reduction in shrinkage	[min]	150 to 180	170 to 210	200 to 250
Crack stabilisation	[min]	240	240	300
Shrinkage at crack stabilisation	[mm/m]	4.53	3.15	2.99
Surface tension of pore fluid	[mN/m]	70.55	66.43	62.52

Fundamental influences

Shrinkage and settlement results are shown in Table 4.4 and Figure 4.10. RET_Min and RET_Max exhibited an approximate shrinkage of 3.15 and 2.99 mm/m respectively at crack stabilisation and, therefore, display a significant reduction in shrinkage compared to that of REF which was measured as 4.53 mm/m. Therefore, the associated shrinkage results validate the overall reduction in the severity of PSC since the addition of retarder corresponds to a significant reduction in shrinkage. Furthermore, as shown in Figure 4.10, RET_Min and RET_Max displayed a similar amount of shrinkage at crack stabilisation with the shrinkage of RET_Min only slightly exceeding that of RET_Max. Correspondingly, the shrinkage results of RET_Min and RET_Max further validate the associated phenomenological behaviour since the minor difference in the severity of cracking is validated by the similar extent of shrinkage at crack stabilisation. In addition, an increased content of the glucose based retarder resulted in a progressive reduction in the rate of shrinkage after 60 minutes which corresponds to the progressively delayed increase in the rate of crack growth as shown in Figure 4.10.

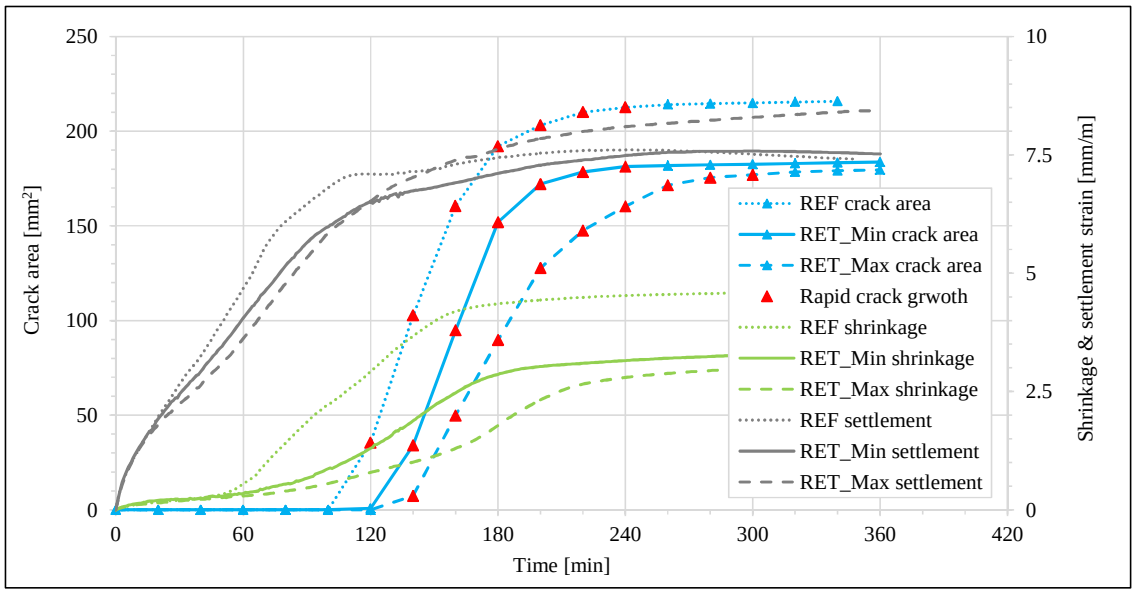

Figure 4.10 Crack area, shrinkage and settlement of REF, RET_Min and RET_Max

Using crack onset as a point of reference, RET_Min and RET_Max exhibited settlement of 6.7 and 7.0 mm/m respectively whereas that of REF was measured as 7.1 mm/m. Therefore, RET_Min and RET_Max mutually displayed a slight reduction in settlement at crack onset compared to REF. Furthermore, with reference to Figure 4.10, the settlement of RET_Max exceeded that of RET_Min after crack onset was reached. RET_Max maintained a steady increase in settlement after crack onset until approximately 220 minutes after casting. Therefore, after crack onset was reached, it is believed that the capillary pressure in the water-filled regions of RET_Max was relieved through a combination shrinkage and settlement which partly validates the reduced initial rate of shrinkage of RET_Max compared to RET_Min.

The associated reduction in shrinkage and settlement of RET_Min and RET_Max is attributed to lower rates of capillary pressure build-up. With reference to Figure 4.11, the addition of retarder progressively influenced the rate of capillary pressure build-up since a higher dosage of retarder corresponds to a more substantial reduction in the rate of pressure build-up. The reduced rate of capillary pressure build-up of RET_Max further validates the gradual increase in shrinkage of RET_Max compared to RET_Min.

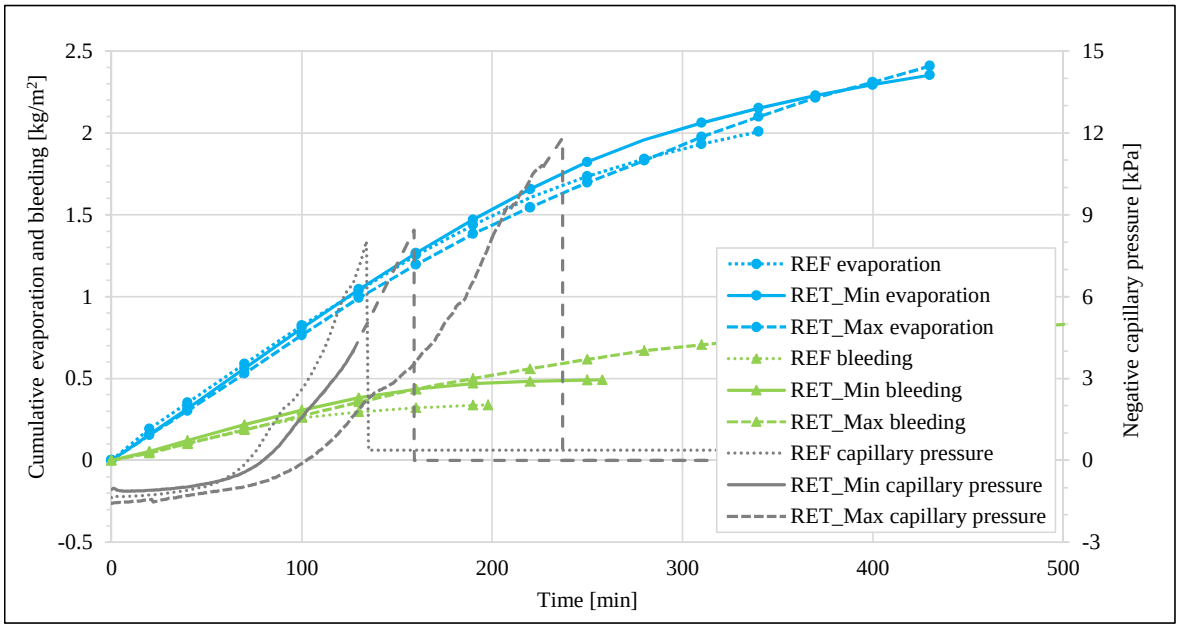

Figure 4.11 Capillary pressure, evaporation and bleeding of REF, RET_Min and RET_Max

With reference to the bleeding results in Figure 4.11, the addition of retarder progressively influenced the duration of bleeding since a higher dosage of retarder resulted in prolonged bleeding of the concrete paste. Furthermore, RET_Max displayed a slightly decreased rate of evaporation compared to REF and RET_Min while the difference in the initial rate of evaporation between REF and RET_Min is considered to be insignificant. Therefore, with consideration to prolonged bleeding and similar evaporation rates, the addition of retarder results in a slight progressive reduction in the effective water loss from the concrete paste. However, the associated reduction in effective water loss is not considered to be the governing reason for the reduction in the rate of capillary pressure build-up due to the minor difference in the bleeding and evaporation results. With reference to Table 4.4, the addition of retarder progressively influenced the surface tension of the pore fluid since a higher dosage of retarder corresponds to a more substantial reduction in surface tension. Consequently, the progressive reduction in the rate of capillary build-up is mainly attributed to the reduction in surface tension with increasing content of glucose based retarder.

In conclusion, mixes containing the respective dosages of retarder mutually displayed a significant reduction in shrinkage compared to REF which validates the overall reduction in the severity of PSC. Furthermore, the difference in the severity of cracking between RET_Min and RET_Max is validated

by the similar extent of shrinkage at crack stabilisation. The comparatively gradual increase in shrinkage of RET_Max compared to RET_Min is mainly attributed to the progressive reduction in the rate of capillary pressure build-up with increasing content of retarder. The gradual increase in shrinkage is further validated since it is believed for RET_Max that the capillary pressure in the water-filled regions of the concrete paste is relieved through a combination of shrinkage and settlement after crack onset was reached. Lastly, the progressive reduction in the rate of capillary pressure build-up is mainly attributed to the reduction in surface tension of the pore fluid with increasing content of glucose based retarder.

4.6.3 Lignosulphonate based plasticiser

Mixes containing lignosulphonate based plasticiser, i.e. PL_Min and PL_Max respectively, displayed a reduction of 34.3 and 28.2 % in total crack area compared to the reference mix. Correspondingly, the mix containing a minimum dosage of plasticiser exhibited a more substantial reduction in the severity of PSC when compared to the mix containing a maximum dosage.

Fundamental behaviour

With reference to Table 4.5, the onset of negative capillary pressure build-up of both PL_Min and PL_Max occurred approximately 80 minutes after casting. In addition, a significant increase in shrinkage was mutually observed approximately 20 minutes before the commencement of negative capillary pressure build-up. Therefore, mixes containing the respective dosages of plasticiser also display a correlation between the onset of negative capillary pressure build-up and an increase in shrinkage although the correlation is slightly less prominent than for REF. Similar to REF, crack onset of both PL_Min and PL_Max occurred during the interval when a reduction in settlement was observed. However, PL_Max maintained a steady increase in settlement after crack onset was reached until approximately 170 minutes after casting, as shown in Figure 4.12. Therefore, after crack onset was reached, it is believed that capillary tension forces in the water-filled regions of PL_Max were relieved by both settlement and shrinkage of the concrete paste. Although the significant reduction in shrinkage of PL_Min and PL_Max is observed at least 80 minutes before crack stabilisation, the associated reductions in shrinkage correspond to moderate reductions in the rate of crack growth as shown in Figure 4.12. In conclusion, mixes containing the respective dosages of plasticiser display similar behaviour than the reference mix.

Table 4.5 Fundamental results of RET, PL_Min and PL_Max

		REF	PL_Min	PL_Max
Onset of negative capillary pressure build-up	[min]	70	80	80
Approximation of significant increase in shrinkage	[min]	60	60	60
Approximation of significant reduction in settlement	[min]	100 to 120	90 to 130	90 to 160
Crack onset	[min]	120	140	140
Settlement at crack onset	[mm/m]	7.1	7.1	7.6
Approximation of significant reduction in shrinkage	[min]	150 to 180	160 to 200	160 to 200
Crack stabilisation	[min]	240	280	280
Shrinkage at crack stabilisation	[mm/m]	4.53	3.72	2.53
Surface tension of pore fluid	[mN/m]	70.55	61.05	58.31

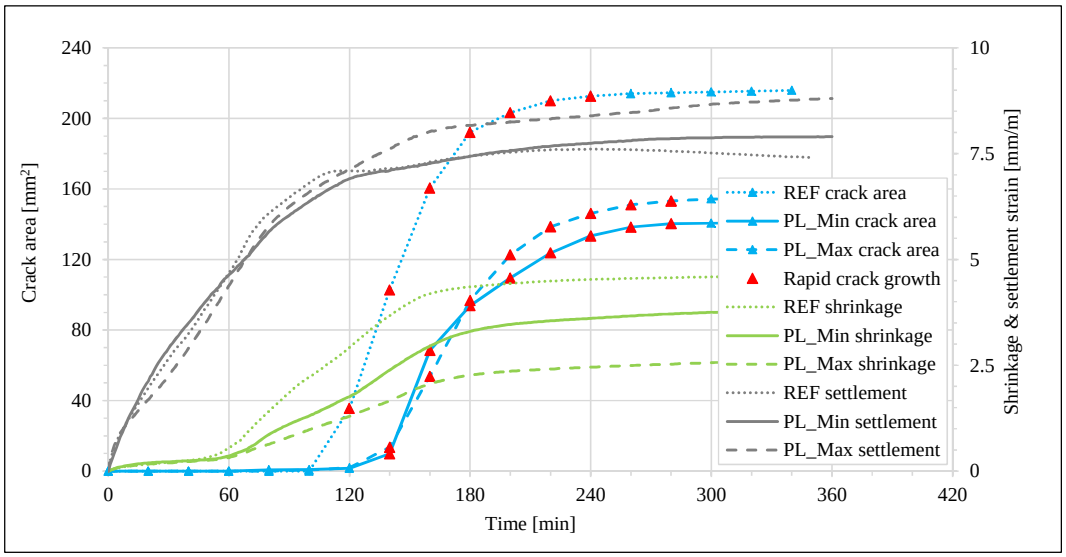

Figure 4.12 Crack area, shrinkage and settlement of REF, PL_Min and PL_Max

Fundamental influences

Shrinkage and settlement results are shown in Table 4.5 and Figure 4.12. PL_Min and PL_Max exhibited an approximate shrinkage of 3.72 and 2.53 mm/m respectively at crack stabilisation and, therefore, displayed a significant reduction in shrinkage compared to that of REF which was measured as 4.53 mm/m. Correspondingly, the overall reduction in the severity of cracking is validated by the associated shrinkage results since mixes containing plasticiser mutually displayed a significant reduction in shrinkage compared to REF. However, PL_Max displayed reduced shrinkage at crack stabilisation compared to PL_Min which does not correspond to the associated phenomenological behaviour. PL_Max displays an increased severity of cracking and can, therefore, be expected to display increased shrinkage compared to PL_Min. The associated discrepancy is explained in the following paragraphs.

Using crack onset as a point of reference, PL_Min and PL_Max displayed settlement of 7.1 and 7.6 mm/m respectively whereas that of REF was measured as 7.1 mm/m. Therefore, the respective mixes displayed similar settlement at crack onset and, with reference to Figure 4.12, the respective mixes also displayed a similar rate of settlement until crack onset was reached. However, as previously mentioned, PL_Max maintained a steady increase in settlement after crack onset until approximately 170 minutes after casting. Therefore, due to the prolonged settlement of PL_Max after crack onset, the concrete is more susceptible to plastic settlement cracking since settlement cracking only ceases when maximum settlement is reached, as discussed in Section 2.4.7. Therefore, it is speculated that the prolonged settlement of PL_Max resulted in increased interaction between plastic settlement cracking and PSC and, correspondingly, PL_Max displayed an increased severity of cracking compared to PL_Min despite the reduced rate of shrinkage. However, the aforementioned speculation requires further investigation since no tests were performed to determine the influence of plastic settlement cracks on the PSC of concrete.

With reference to Figure 4.13, the addition of plasticiser progressively influenced the rate of capillary pressure build-up since a higher dosage of plasticiser corresponds to a reduction in the rate of capillary pressure build-up. Therefore, the associated shrinkage results are validated since a lower rate of capillary pressure build-up corresponds to a reduction in shrinkage. Furthermore, due to the prolonged settlement of PL_Max after crack onset, the capillary pressure in the water-filled regions of PL_Max was relieved through both shrinkage and settlement of the concrete paste whereas that of PL_Min was mainly relieved by horisontal shrinkage. This further validates the reduced shrinkage of PL_Max compared to that of PL_Min.

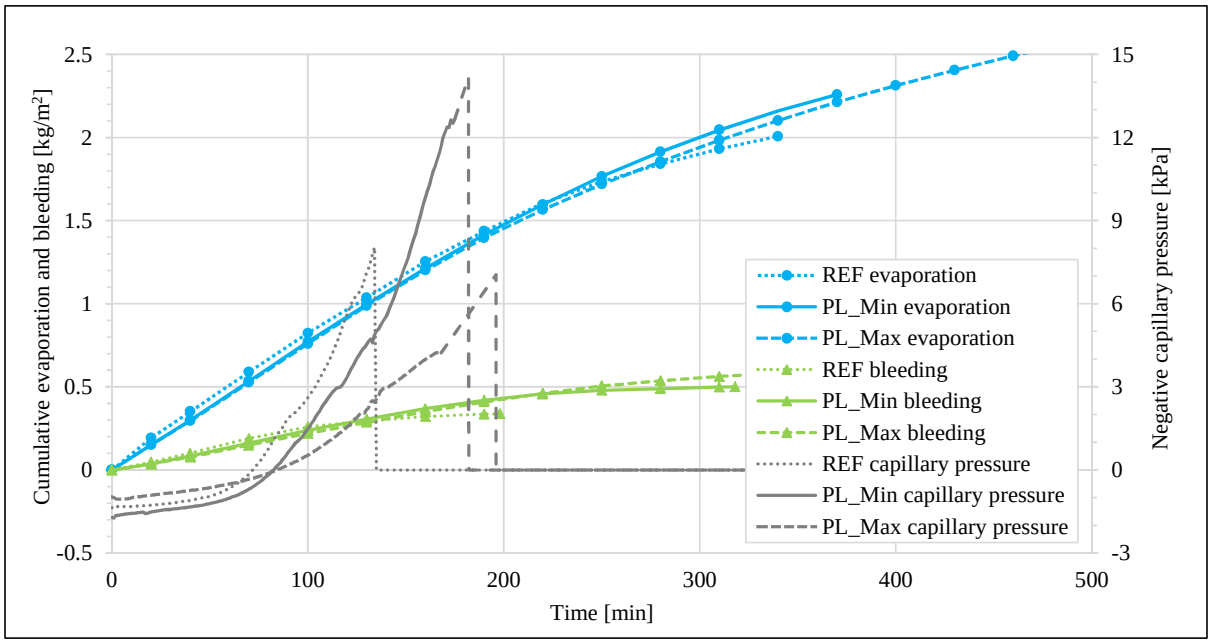

Figure 4.13 Capillary pressure, evaporation and bleeding of REF, PL_Min and PL_Max

With reference to Figure 4.13, the addition of plasticiser progressively influenced the duration of bleeding since a higher dosage of plasticiser resulted in prolonged bleeding of the concrete paste. Therefore, the prolonged settlement of PL_Max is supported by the corresponding bleeding results. Nonetheless, the respective mixes displayed a similar initial rate of bleeding. Although REF initially displayed a slightly increased evaporation rate, the difference in the evaporation rates of the respective mixes is considered to be insignificant. Therefore, with reference to Figure 4.13, the differences in bleeding and evaporation results of the respective mixes are too small to draw definitive conclusions. However, it is believed that the respective mixes were subjected to a similar rate of effective water loss from the concrete paste during the plastic state of the concrete. With reference to Table 4.5, PL_Min displayed a significant reduction in the surface tension of the pore fluid compared to REF while the reduction in surface tension between PL_Min and PL_Max is less profound. Furthermore, considering that PL_Max contains an increased content of plasticiser compared to PL_Min, it is speculated that the corresponding solid particles are subjected to improved dispersion and are, therefore, more evenly distributed. Even distribution of solid particles, in turn, causes a reduction in the rate of capillary pressure build-up compared to unevenly distributed particles. Therefore, the progressive reduction in the rate of capillary pressure build-up is mainly attributed to the improved particle distribution and reduction in surface tension with increasing plasticiser content.

In conclusion, the overall reduction in the severity of cracking is validated by the associated shrinkage results since a higher dosage of plasticiser corresponds to a more substantial reduction in shrinkage. The progressive reduction in the rate of shrinkage is mainly attributed to the reduction in the rate of capillary pressure build-up with increasing content of retarder. The reduced shrinkage of PL_Max compared to PL_Min is further validated since it is believed that the capillary pressure in the water-filled regions of PL_Max was relieved through a combination of shrinkage and settlement after crack onset was reached. The progressive reduction in the rate of capillary pressure build-up is mainly attributed to the improved particle distribution and the reduction in surface tension with increasing plasticiser content. Lastly, it is speculated that the increased cracking of PL_Max compared to PL_Min is attributed to increased interaction of plastic settlement cracking and PSC due to prolonged settlement of PL_Max after crack onset. Consequently, due to the increased interaction of plastic settlement cracking and PSC, PL_Max displayed an increased severity of cracking despite the reduced rate of both shrinkage and capillary pressure build-up. However, the aforementioned speculation requires further investigation since no tests were performed to determine the influence of plastic settlement cracks on PSC of concrete.

4.6.4 Calcium chloride based accelerator

Mixes containing calcium chloride based accelerator, i.e. AC_Min and AC_Max respectively, displayed a reduction of 26.3 and 18.3 % in total crack area compared to REF. Therefore, the mix containing a minimum dosage of accelerator exhibited a more substantial reduction in the severity of cracking compared to the mix containing a maximum dosage.

Fundamental behaviour

With reference to Table 4.6, the onset of negative capillary pressure build-up of both AC_Min and AC_Max occurred approximately 80 minutes after casting. Furthermore, AC_Min and AC_Max mutually displayed a significant increase in shrinkage at approximately 70 minutes after casting. Therefore, similar to REF, mixes containing the respective dosages of accelerator display a close correlation between the onset of negative capillary pressure build-up and a significant increase in shrinkage. Crack onset of AC_Min and AC_Max respectively occurred during the interval when a significant reduction in settlement was observed as shown in Figure 4.14. Therefore, it is believed that for both AC_Min and AC_Max the vertical component of the capillary tension forces does not have a profound influence on the cracking process after crack onset is reached since settlement has stabilised to a large extent. Although AC_Min and AC_Max displayed a significant reduction in shrinkage at least 60 minutes before crack stabilisation, the associated reduction in shrinkage corresponds to a reduction in the rate of crack growth. In conclusion, mixes containing the respective dosages of accelerator display similar fundamental behaviour than REF.

Table 4.6 Fundamental results of REF, AC_Min and AC_Max

		REF	AC_Min	AC_Max
Onset of negative capillary pressure build-up	[min]	70	80	80
Approximation of significant increase in shrinkage	[min]	60	70	70
Approximation of significant reduction in settlement	[min]	100 to 120	90 to 130	100 to 130
Crack onset	[min]	120	120	120
Settlement at crack onset	[mm/m]	7.1	5.7	6.6
Approximation of significant reduction in shrinkage	[min]	150 to 180	160 to 190	200 to 240
Crack stabilisation	[min]	240	240	240
Shrinkage at crack stabilisation	[mm/m]	4.53	3.38	3.49
Surface tension of pore fluid	[mN/m]	70.55	70.23	70.09

Fundamental influences

Shrinkage and settlement results are shown in Table 4.6 and Figure 4.14. AC_Min and AC_Max exhibited approximate shrinkage of 3.38 and 3.49 mm/m respectively at crack stabilisation and, therefore, display a significant reduction in shrinkage compared to REF which was measured as

4.53 mm/m. The associated shrinkage results validate the overall reduction in the severity of cracking since the addition of accelerator corresponds to a reduction in shrinkage. With reference to Figure 4.14, the phenomenological behaviour of AC_Min and AC_Max is partly attributed to the slightly reduced shrinkage of AC_Min compared to AC_Max. However, considering the difference in the severity of cracking, a more substantial difference in shrinkage between AC_Min and AC_Max can be expected. This is discussed in the following paragraphs.

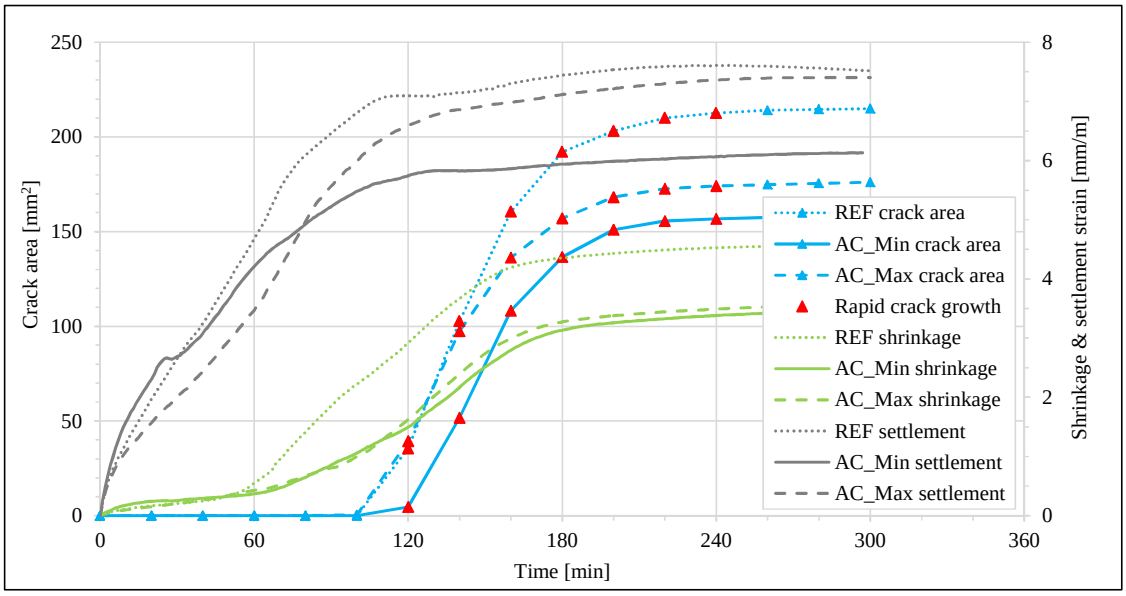

Figure 4.14 Crack area, shrinkage and settlement of REF, AC_Min and AC_Max

Using crack onset as a point of reference, AC_Min and AC_Max exhibited settlement of 5.7 and 6.6 mm/m respectively whereas that of REF was measured as 7.1 mm/m. Furthermore, with reference to Figure 4.14, the settlement rate of REF and AC_Max exceeded that of AC_Min at approximately 30 and 80 minutes after casting respectively. Therefore, AC_Min displayed reduced settlement at crack onset as well as a reduced rate of settlement before crack onset was reached. Due to the associated reduction in settlement of AC_Max, the concrete is less susceptible to the formation of plastic settlement cracks. As previously discussed in Section 2.4.7, the presence of settlement cracks beneath the surface form weak spots in the system that locally relieve capillary pressure through air entry at the location of settlement cracks. Therefore, it is speculated that the increased settlement of REF and AC_Max resulted in an increased severity of plastic settlement cracks beneath the concrete surface and, therefore, resulted in earlier air entry at the location of the settlement cracks compared to AC_Min. The crack area results of the respective mixes support the associated speculation since the increase in the rate of crack growth of both AC_Max and REF occurred before that of AC_Min as shown in Figure 4.14. Furthermore, considering that initial setting time of AC_Min and AC_Max occurred at 110 and 105 minutes respectively, it is believed that AC_Min had increased capacity to resist the capillary tension forces due to the delayed air entry. This is supported by findings of Krönlof et al. (1995) stating that concrete has increased capacity to resist capillary forces after initial

set is reached. Therefore, due to the increased capacity of AC_Min to resist capillary tension forces after crack onset, the reduced cracking of AC_Min compared to AC_Max is validated despite the similar rate of shrinkage as shown in Figure 4.14. However, as for the mixes containing plasticiser, the aforementioned speculation requires further investigation since no tests were performed to determine the influence of plastic settlement cracks on the PSC of concrete.

With reference to Figure 4.15, REF and AC_Min displayed a similar rate of capillary pressure build-up although the commencement of negative capillary pressure build-up of REF occurred approximately 10 minutes before that of AC_Min. Consequently, REF was subjected to higher initial capillary tension forces which validate the associated early increase in shrinkage compared to AC_Min and AC_Max since shrinkage is mainly attributed to the horisontal component of capillary tension forces. Furthermore, AC_Min displayed a slightly increased rate of capillary pressure build-up compared to AC_Max which does not correlate to the associated shrinkage results since AC_Min displayed a slightly reduced shrinkage compared to AC_Max. However, with reference to Figure 4.14 and Figure 4.15, AC_Min and AC_Max displayed similar shrinkage as well as a similar rate of capillary pressure build-up. Therefore, the differences in the results are too small to draw definitive conclusions and further investigation is required. The minor variations in the shrinkage and capillary pressure results can possibly be attributed to the fact that the respective tests were performed independently.

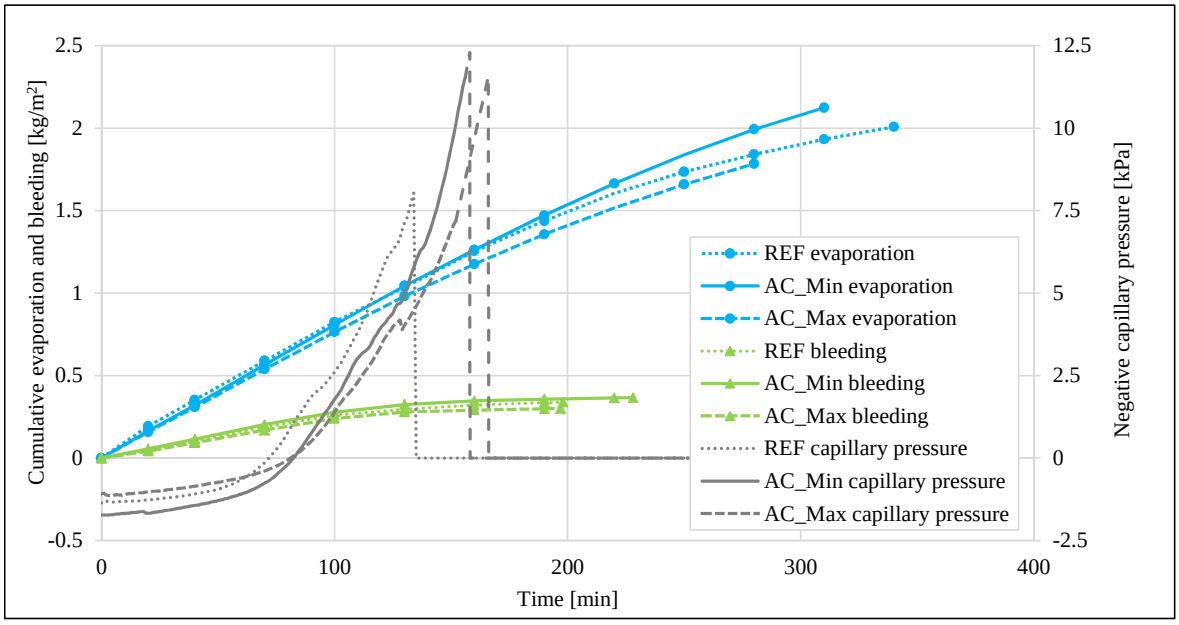

Figure 4.15 Capillary pressure, evaporation and bleeding of REF, AC_Min and AC_Max

With reference to Figure 4.15, REF, AC_Min and AC_Max displayed similar rates of bleeding with the bleeding of AC_Max only marginally lower than REF while the bleeding of AC_Min is only marginally higher than REF. Furthermore, AC_Max displayed a slightly reduced evaporation rate compared to REF and AC_Min whereas the difference in the initial rate of evaporation between

AC_Min and REF are considered to be insignificant. Therefore, with reference to Figure 4.15, the differences in bleeding and evaporation results of the respective mixes are too small to draw definitive conclusions. However, it is believed that AC_Max was exposed to a slightly reduced rate of effective water loss from the concrete paste whereas differences between effective water loss between REF and AC_Min are considered to be insignificant. The addition of accelerator did not significantly influence the surface tension of the pore fluid with the surface tension of AC_Min only slightly higher than that of AC_Max, as shown in Table 4.6. Both the slightly reduced surface tension and effective water loss of AC_Max partly explains the slightly reduced rate of capillary pressure build-up compared to AC_Min. However, the differences between the effective water loss and the surface tension of these mixes are also too small to make definitive conclusions and further investigation is required.

In conclusion, AC_Min and AC_Max displayed a significant reduction in shrinkage compared to REF which validates the overall reduction in the severity of PSC. AC_Min displayed reduced cracking compared to AC_Max which is partly attributed to the slightly reduced shrinkage of AC_Min compared to AC_Max. However, it is further speculated that the reduced cracking of AC_Min is also attributed to increased capacity to resist capillary tension forces after crack onset due to a delayed time of air entry. The delayed time of air entry, in turn, is attributed to differences in the severity of plastic settlement cracking. Differences between effective water loss, surface tension and capillary pressure results are also too small to make definitive conclusions and further investigation is required.

4.6.5 Chloride free air entrainer

Mixes containing air entrainer, i.e. AIR_Min and AIR_Max respectively, displayed a reduction of 21.6 and 37.1 % in total crack area compared to REF. Correspondingly, the addition of air entrainer progressively influenced the severity of cracking with a higher dosage of air entrainer corresponding to a more substantial reduction in cracking.

Fundamental behaviour

With reference to Table 4.7, the onset of negative capillary pressure build-up of AIR_Min and AIR_Max occurred approximately 80 and 90 minutes after casting respectively. Furthermore, a significant increase in shrinkage for both AIR_Min and AIR_Max was observed approximately 20 minutes prior to the commencement of negative capillary pressure build-up. Therefore, AIR_Min and AIR_Max also display a correlation between the onset of negative capillary pressure build-up and an increase in shrinkage although the correlation is slightly less prominent than for REF. Similar to REF, crack onset for both AIR_Min and AIR_Max occurred during the interval when a significant reduction in settlement was observed. However, AIR_Min maintained a steady increase in settlement after crack onset until approximately 240 minutes after casting as shown in Figure 4.16. Therefore, after crack onset was reached, it is believed that capillary tension forces in the water-filled regions of AIR_Min were relieved by both settlement and shrinkage of the concrete paste. Lastly, it can be

graphically seen that AIR_Min and AIR_Max displayed a more profound correlation between the reduction in shrinkage and crack stabilisation than REF. In conclusion, mixes containing the respective dosages of air entrainer display similar behaviour than REF.

Table 4.7 Fundamental results of REF, AIR_Min and AIR_Max

		REF	AIR_Min	AIR_Max
Onset of negative capillary pressure build-up	[min]	70	80	90
Approximation of significant increase in shrinkage	[min]	60	60	70
Approximation of significant reduction in settlement	[min]	100 to 120	90 to 130	80 to 120
Crack onset	[min]	120	120	140
Settlement at crack onset	[mm/m]	7.1	7.2	4.4
Approximation of significant reduction in shrinkage	[min]	150 to 180	160 to 210	180 to 240
Crack stabilisation	[min]	240	240	240
Shrinkage at crack stabilisation	[mm/m]	4.53	3.19	3.77
Surface tension of pore fluid	[mN/m]	70.55	58.30	45.67

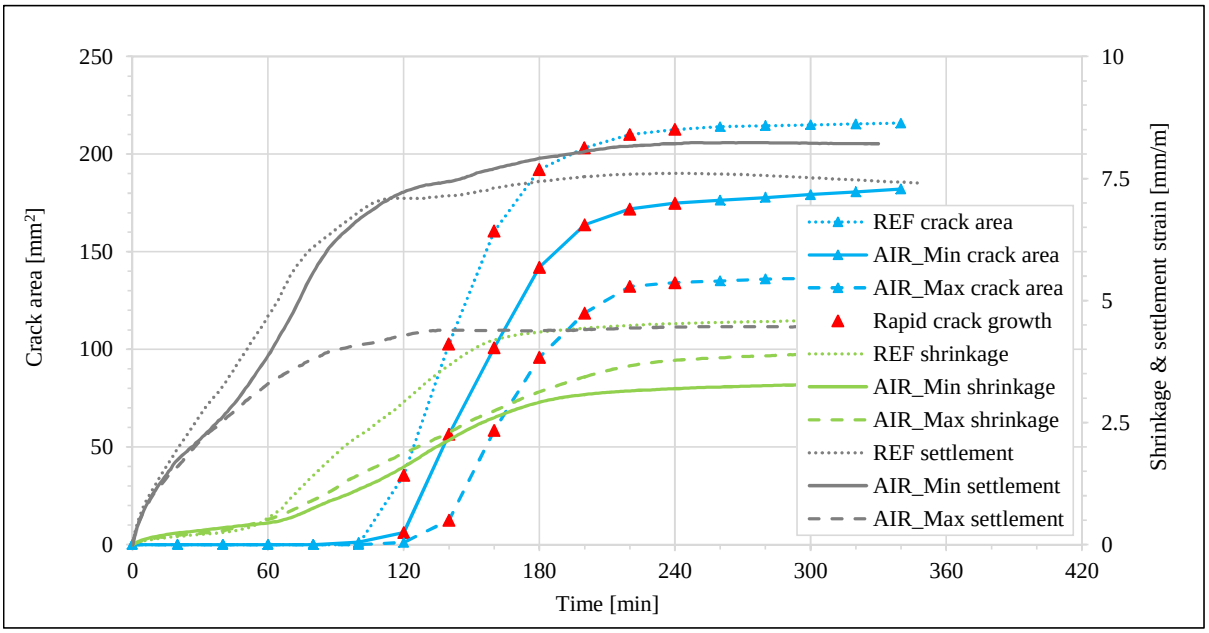

Figure 4.16 Crack area, shrinkage and settlement of REF, AIR_Min and AIR_Max

Fundamental influences

Shrinkage and settlement results are shown in Table 4.7 and Figure 4.16. AIR_Min and AIR_Max exhibited an approximate shrinkage of 3.19 and 3.77 mm/m respectively at crack stabilisation and, therefore, display a reduction in shrinkage compared to REF which was measured as 4.53 mm/m. Therefore, the associated shrinkage results validate the overall reduction in the severity of cracking.

Furthermore, with reference to Figure 4.16, the shrinkage rate of AIR_Max exceeded that of AIR_Min from approximately 60 minutes after casting. Therefore, AIR_Max displayed an increased shrinkage rate and an increased total shrinkage at crack stabilisation compared to AIR_Min which does not correlate to the corresponding phenomenological behaviour since AIR_Max displayed reduced cracking compared to AIR_Min. The associated discrepancy is explained in the following paragraphs.

Using the crack onset as a point of reference, AIR_Min and AIR_Max exhibited settlement of 7.2 and 4.4 mm/m respectively whereas that of REF was measured as 7.1 mm/m. Therefore, AIR_Min and REF displayed similar settlement at crack onset whereas AIR_Max displayed a significant reduction in total settlement. Due to the significantly reduced settlement of AIR_Max, the concrete is less susceptible to the formation of settlement cracks. Therefore, it is speculated that the increased settlement of REF and AIR_Min resulted in the increased interaction between plastic settlement cracking and PSC. The corresponding crack area results validate the associated speculation since crack onset of REF and AIR_Min occurred sooner than that of AIR_Max as shown in Figure 4.16. This can be attributed to the earlier occurrence of air entry due to the increased interaction of plastic settlement cracks and PSC. Therefore, similar to mixes containing accelerator, it is believed that AIR_Max had increased capacity to resist the capillary tension forces due to the delayed air entry. This validates the reduced severity of cracking of AC_Max despite the higher shrinkage of AC_Max compared to AC_Min. However, the aforementioned speculation requires further investigation since no tests were performed to determine the influence of plastic settlement cracks on the PSC of concrete.

With reference to Figure 4.17, REF displayed the highest rate of capillary pressure build-up which corresponds to the shrinkage results since REF displayed the highest shrinkage. AIR_Min and AIR_Max displayed a similar rate of capillary pressure build-up although the commencement of negative capillary pressure build-up of AIR_Min occurred approximately 10 minutes prior to that of AIR_Max. Therefore, AIR_Min was subjected to a higher initial capillary pressure compared to AIR_Max. As previously mentioned, AIR_Min maintained a steady increase in settlement after crack onset until approximately 240 minutes after casting. Therefore, after crack onset, it is believed that capillary pressure in the water-filled regions of AIR_Min was relieved through both shrinkage and settlement of the concrete paste whereas that of AIR_Max was mainly relieved by horisontal shrinkage. Thus, although AIR_Min was subjected to a higher initial capillary pressure, the reduced shrinkage of AIR_Min compared to that of AIR_Max is validated since the capillary pressure of AIR_Min was relieved through a combination of shrinkage and settlement after crack onset was reached.

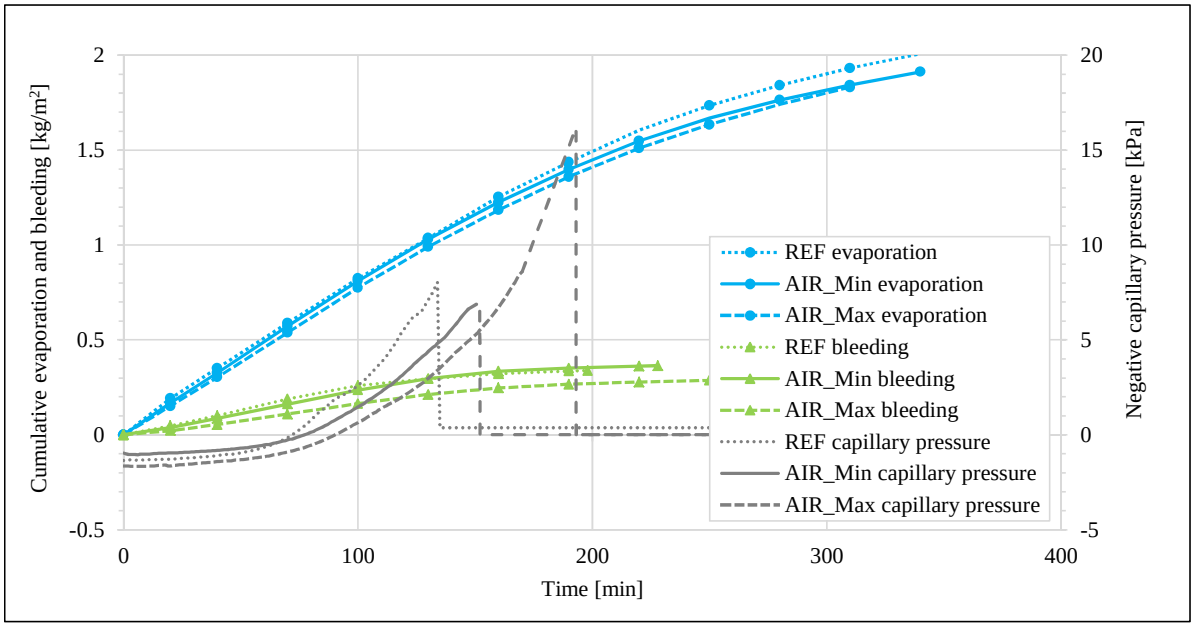

Figure 4.17 Capillary pressure, evaporation and bleeding of REF, AIR_Min and AIR_Max

With reference to Figure 4.17, AIR_Max displayed a slightly reduced rate of evaporation compared to REF and AIR_Min while the difference in the initial rate of evaporation between AIR_Min and REF are considered to be insignificant. Furthermore, the significant reduction in settlement of AIR_Max is validated by the corresponding bleeding results since AIR_Max displayed reduced bleeding compared to REF and AIR_Min. The reduced bleeding of AIR_Max can be attributed to the increased content of entrained air which hinders the upward movement of bleeding water to the surface and, therefore, reduces settlement of the concrete paste. AIR_Max displayed a reduced rate of both bleeding and evaporation and is, therefore, effectively exposed to the same water loss than AIR_Min and REF. With reference to Table 4.7, the addition of air entrainer showed a significant progressive influence on the surface tension of the pore fluid since a higher dosage of air entrainer corresponds to a more substantial reduction in surface tension. Therefore, differences in the rate of capillary pressure build-up are mainly attributed to the progressive reduction in surface tension with increasing content of air entrainer.

In conclusion, the overall reduction in the severity of cracking is validated since both mixes containing air entrainer displayed a significant reduction in shrinkage compared to REF. The reduced shrinkage of AIR_Min compared to AIR_Max is validated since the capillary pressure of AIR_Min is relieved through a combination of shrinkage and settlement after crack onset was reached. Differences in the rate of capillary pressure build-up are mainly attributed to the reduction in surface tension with increasing content of air entrainer. It is speculated that the increased cracking of AIR_Min compared to AIR_Max is attributed to increased capacity to resist capillary tension forces after crack onset due to a delayed time of air entry. The delayed time of air entry, in turn, is attributed to differences in the extent of plastic settlement cracking. AIR_Max displayed a significant reduction in settlement

compared to AIR_Min and is, therefore, less susceptible to plastic settlement cracking. The significant reduction in settlement of AIR_Max is validated by the corresponding bleeding results since AIR_Max displayed reduced bleeding compared to REF and AIR_Min. The reduced amount of bleeding is attributed to the increased content of entrained air which hinders the upward movement of bleeding water to the surface of the concrete paste.

4.6.6 Shrinkage reducing admixture (SRA)

Mixes containing SRA, i.e. S_Min and S_Max respectively, displayed a reduction of 14.6 and 29.1 % in total crack area when compared to the reference mix. Therefore, the addition of SRA progressively influenced the severity of cracking since a higher dosage of SRA corresponds to a more substantial reduction in PSC.

Fundamental behaviour

With reference to Table 4.8, the onset of negative capillary pressure build-up of S_Min and S_Max occurred approximately 90 and 100 minutes after casting respectively. In addition, similar to mixes containing air entrainer and plasticiser, S_Min and S_Max both displayed a significant increase in shrinkage approximately 20 minutes before the commencement of negative capillary pressure build-up. Therefore, mixes containing the respective dosages of SRA also display a correlation between the onset of negative capillary pressure build-up and an increase in shrinkage. Furthermore, crack onset of S_Min occurred just before the significant reduction in settlement was observed while crack onset of S_Max occurred during the initial stages of the significant reduction in settlement. Although the significant reduction in shrinkage of S_Min and S_Max was observed at least 50 minutes in advance of crack stabilisation, the associated reduction in shrinkage of the respective mixes corresponds to a reduction in the rate of crack growth as shown in Figure 4.18. Conclusively, mixes containing the respective dosages of SRA displayed similar behaviour than the reference mix.

Fundamental influences

Shrinkage and settlement results are shown in Table 4.8 and Figure 4.18. S_Min and S_Max exhibited approximate shrinkage of 4.05 and 4.02 mm/m respectively at crack stabilisation and, therefore, display a reduction in shrinkage compared to that of REF which was measured as 4.53 mm/m. Correspondingly, the overall reduction in the severity of cracking is validated by the associated shrinkage results. Although S_Min and S_Max displayed similar shrinkage at crack stabilisation, S_Max displayed a slightly reduced shrinkage rate compared to S_Min between approximately 70 to 220 minutes after casting as shown in Figure 4.18. The reduction in the severity of PSC of S_Max compared to S_Min can possibly be attributed the reduced shrinkage rate of S_Max. However, the differences between shrinkage results of S_Min and S_Max are too small to draw definitive conclusions and further investigation is required.

Table 4.8 Fundamental results of REF, S_Min and S_Max

		REF	S_Min	S_Max
Onset of negative capillary pressure build-up	[min]	70	90	100
Approximation of significant increase in shrinkage	[min]	60	70	80
Approximation of significant reduction in settlement	[min]	100 to 120	90 to 110	120 to 170
Crack onset	[min]	120	120	120
Settlement at crack onset	[mm/m]	7.1	5.9	10.0
Approximation of significant reduction in shrinkage	[min]	150 to 180	160 to 190	200 to 250
Crack stabilisation	[min]	240	260	300
Shrinkage at crack stabilisation	[mm/m]	4.53	4.05	4.02
Surface tension of pore fluid	[mN/m]	70.55	68.25	61.05

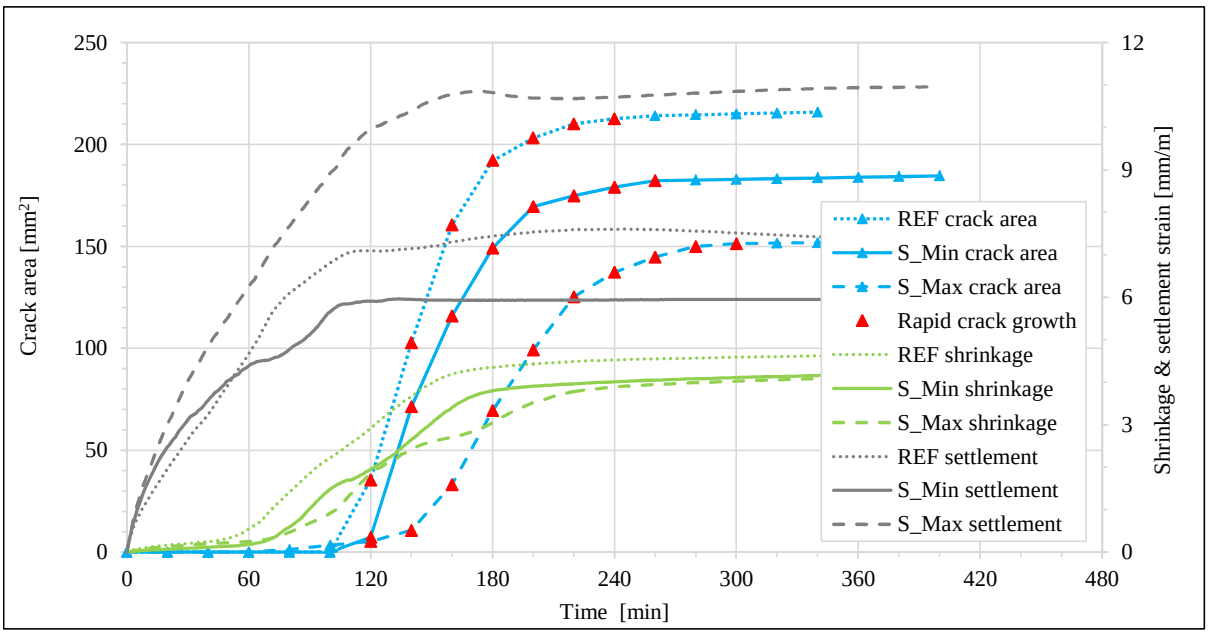

Figure 4.18 Crack area, shrinkage and settlement of REF, S_Min and S_Max

Using crack onset as a point of reference, S_Min and S_Max was subjected to settlement of 5.9 and 10.0 mm/m respectively whereas that of REF was measured as 7.1 mm/m. Therefore, S_Max displayed significantly increased settlement at crack onset compared to REF. In addition, S_Max displayed the highest rate of settlement from the onset of tests and also displayed prolonged settlement compared to S_Min and REF as shown in Figure 4.18. Contrarily, S_Min displayed reduced settlement at crack onset compared to REF although the initial settlement rate during the first 60 minutes after casting corresponds to that of REF. With regard to mixes containing plasticiser, accelerator and air entrainer, it is speculated that an increased amount of settlement resulted in an increased severity of cracking due to the interaction of plastic settlement cracking and PSC. However,

with reference to the phenomenological behaviour of the mixes containing SRA, this is not the case since S_Max displayed the most substantial reduction in the severity of PSC despite its significantly increased settlement. Therefore, the associated discrepancy remains unclear and requires further investigation.

With reference to Figure 4.19, the addition of SRA progressively influenced the rate of capillary pressure build-up since a higher dosage of SRA corresponds to a reduction in the rate of capillary pressure build-up. Therefore, the overall reduction in shrinkage of S_Min and S_Max is validated since mixes containing SRA displayed a reduced rate of capillary pressure build-up compared to REF. With consideration to the prolonged settlement of S_Max, it is believed that the associated capillary pressure in the water-filled regions of the concrete paste was relieved through a combination of shrinkage and settlement after crack onset was reached. Therefore, considering that S_Max displayed a reduced rate of capillary pressure build-up compared to S_Min together with the associated relief of capillary pressure through a combination of shrinkage and settlement, the reduced shrinkage rate of S_Max compared to S_Min is validated. However, with reference to Figure 4.18, it can be expected that S_Max should display a more profound reduction in the rate of shrinkage compared to S_Min. Therefore, the slightly reduced shrinkage rate of S_Max compared to S_Min requires further investigation.

With reference to the bleeding results in Figure 4.19, the addition of SRA progressively influenced the duration of bleeding since a higher dosage of SRA corresponds to prolonged bleeding of the concrete paste. The respective mixes display a similar rate of bleeding during the first 130 minutes after which the bleeding of REF decreased while S_Min and S_Max displayed a similar rate of bleeding throughout the tests. Furthermore, with reference to the evaporation results in Figure 4.19, REF displayed an increased rate of evaporation from the onset of the tests compared to S_Min and S_Max. In addition, S_Min and S_Max displayed a similar rate of evaporation during the first 130 minutes after which the evaporation rate of S_Min exceeded that of S_Max. Therefore, considering that S_Min and S_Max displayed prolonged bleeding and reduced evaporation compared to REF, the respective mixes were effectively exposed to a reduced rate of effective water loss from the concrete paste. With reference to Table 4.8, the addition of SRA progressively influenced the surface tension of the pore fluid since a higher dosage of SRA corresponds to a reduction in surface tension. Therefore, the reduction in both surface tension and effective water loss with increasing content of SRA validates the progressive reduction in the rate of capillary pressure build-up.

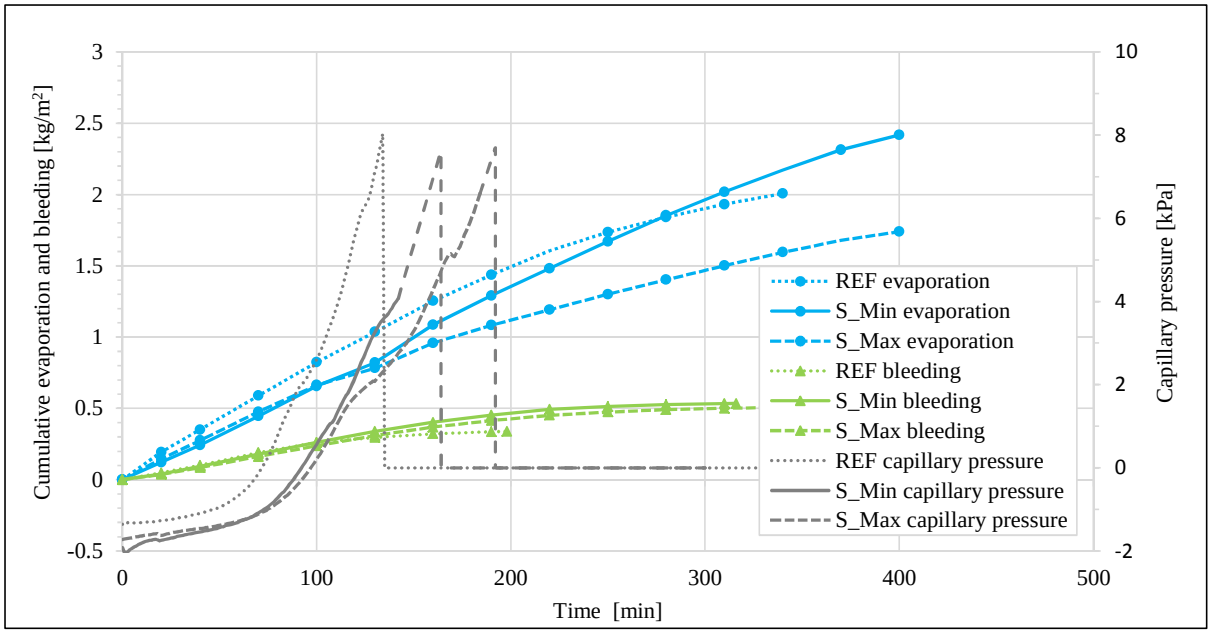

Figure 4.19 Capillary pressure, evaporation and bleeding of REF, S_Min and S_Max

In conclusion, the overall reduction in the severity of PSC is validated by the associated shrinkage results since mixes containing SRA displayed a reduction in shrinkage compared to REF. Furthermore, S_Max displayed a slightly reduced shrinkage rate compared to S_Min which possibly validates the associated reduction in the severity of PSC of S_Max compared to S_Min. The reduction in the rate of shrinkage with increasing content of SRA is supported by the underlying capillary pressure results since a higher dosage of SRA corresponds to a reduction in the rate of capillary pressure build-up. Therefore, S_Max displayed a reduced rate of capillary pressure build-up compared to S_Min and, furthermore, it is believed that the reduced capillary pressure of S_Max was relieved through a combination of shrinkage and settlement due to prolonged settlement after crack onset. Therefore, it can be expected that S_Max should display a more substantial reduction in the shrinkage rate compared to S_Min which requires further investigation. The progressive reduction in the rate of capillary pressure build-up is attributed to the reduction in both surface tension and effective water loss with increasing content of SRA. Lastly, S_Max displayed significantly increased settlement at crack onset compared to REF and S_Min. Therefore, it can be expected that S_Max had to display an increased severity of cracking compared to S_Min due to the interaction of plastic settlement cracking and PSC. However, this is not the case since S_Max displayed the most substantial reduction in the severity of PSC. Therefore, the associated discrepancy between settlement and the phenomenological behaviour remains unclear and requires further investigation.

4.7 Concluding summary

Experimental results of the respective conventional concrete mixes are presented and discussed in this chapter. Firstly, the methodology used to analyse results are discussed, followed by preliminary conclusions concerning the correlations between setting times and rapid crack growth as well as the rapid crack growth periods of the respective mixes. Thereafter, the phenomenological influence of the associated admixtures is investigated by comparing the total crack area of mixes containing admixtures to that of a reference mix deviod from admixtures. Lastly, the fundamental influences of the respective admixtures are investigated to elucidate differences in the severity of PSC. The experimental results of the respective high flow concrete mixes are presented and discussed in the next chapter.

CHAPTER 5

Results and discussions of high flow concrete

Experimental results of the respective high flow concrete mixes are presented and discussed accordingly in this chapter. The layout of this chapter corresponds to that of Chapter 4. Similarly, a general discussion is provided that comprehends different procedures that were used to analyse results, followed by preliminary conclusions that were drawn with respect to certain test results. In relation to the research objectives, phenomenological and fundamental results are discussed seperately in Section 5.5 and Section 5.6 respectively. Lastly, a concluding summary is provided with regard to results and discussions of the respective high flow concrete mixes.

5.1 General

Related discussions regarding the calculation of representative capillary pressure and the calculation of rapid crack growth of the respective mixes correspond to that of the conventional concrete mixes and are, therefore, not discussed in this section. Individual sample results of the respective tests together with calculated averages are provided in Appendix B. Furthermore, calculated results of representative capillary pressure are provided in Appendix B.6 whereas rapid crack growth and crack area results are provided in Appendix B.2 and Appendix B.1 respectively.

5.1.1 Bleeding results

Bleeding tests were successfully performed for the high flow reference mix (REF) and the mix containing a minimum dosage of poly carboxylate ethers based super-plasticiser (PCE_Min). However, as result of self-levelling properties, bleeding results could not be obtained for mixes containing sulphonated melamine formaldehyde based super-plasticiser (SMF_Max & SMF_Min) and a maximum dosage of PCE-based super-plasticiser (PCE_Max).

As discussed in Section 3.2.4, bleeding tests were performed by placing moulds on a tilt platform to facilitate the accumulation of bleed water. In connection herewith, Figure 5.1 illustrates the behaviour of the respective high flow mixes when bleeding measurements were conducted. As illustrated by (a), REF and PCE_Min facilitated convenient extraction of bleed water since the concrete paste was not subjected to self-levelling upon placement on the tilt stand. Contrarily, as illustrated by (b), the self-levelling properties of SMF_Min, SMF_Max and PCE_Max did not permit extraction of bleed

water. Therefore, only bleeding results of REF and PCE_Min are used to partly elucidate the fundamental influences of the respective admixtures on the PSC of concrete.

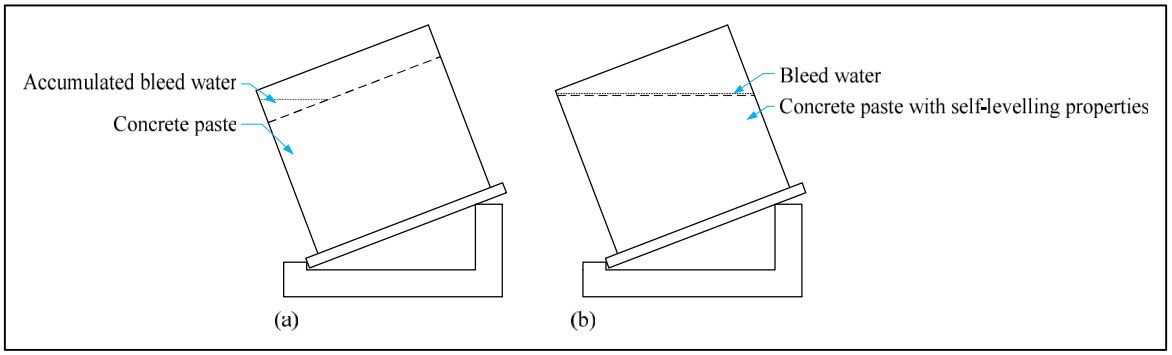

Figure 5.1 Extraction of bleed water for high flow concrete mixes

5.2 Surface tension results

Surface tension results of the respective high flow concrete mixes are provided in Table 5.1 and Figure 5.2. Solution concentrations, average surface tension, and standard deviation of the respective mixes are provided accordingly.

Table 5.1 Surface tension results of high flow concrete mixes

Mix	Admixture	Solution concentration of admixtures [g/L of solution]	Average surface tension [mN/m]	Standard deviation [mN/m]
REF	-	-	70.55	0.12
PCE_Min	PCE based SP	1.40	61.28	0.07
PCE_Max	PCE based SP	5.83	60.59	0.08
SMF_Min	SMF based SP	3.07	70.17	0.05
SMF_Max	SMF based SP	5.10	65.57	0.15

**Notes*

PCE *Poly carboxylate ethers*

SMF *Sulphonated melamine formaldehyde*

SP *Super-plasticiser*

The addition of a minimum dosage of PCE-based super-plasticiser caused a significant reduction in surface tension while the reduction in surface tension between PCE_Min and PCE_Max is less profound. Therefore, various dosages of PCE-based super-plasticiser, ranging between the high and low dosage limits, are expected to display a similar reduction in the surface tension of the pore fluid. The addition of a minimum dosage SMF-based super-plasticiser caused an insignificant reduction in surface tension while the maximum dosage caused a substantial reduction in surface tension. Therefore, the addition of SMF-based super-plasticiser has a progressive influence on the reduction of

surface tension, ranging from an insignificant reduction with the addition of a low dosage to a substantial reduction with the addition of a high dosage. References to surface tension results in Section 5.6 should be used in conjunction with this section.

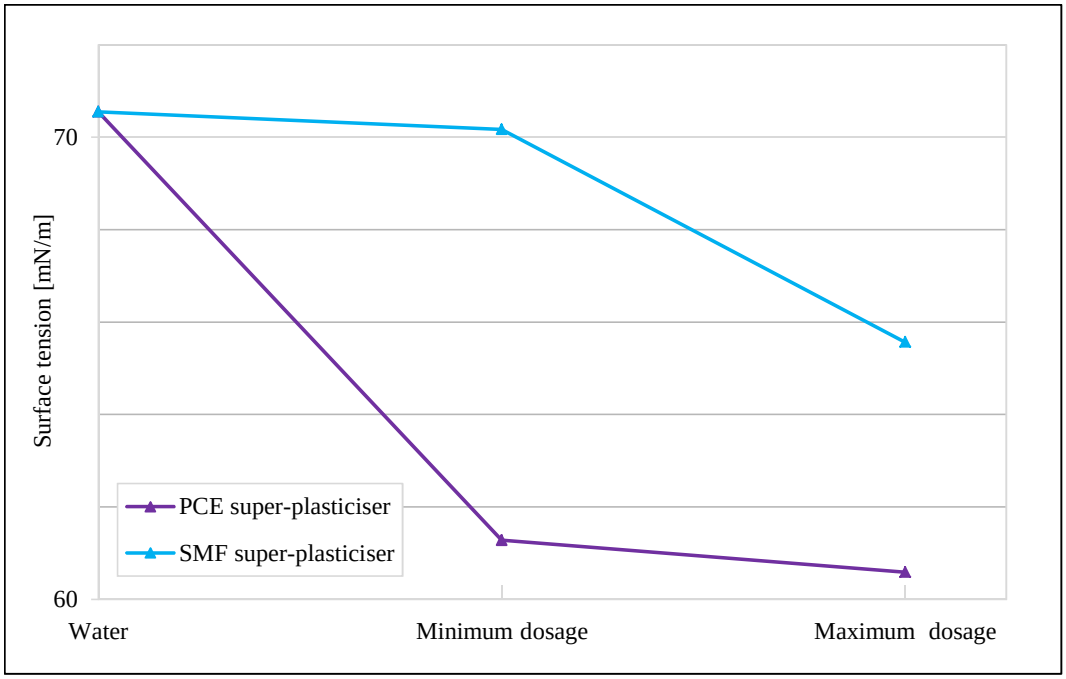

Figure 5.2 Surface tension results of high flow concrete mixes

5.3 Correlation between setting times and rapid crack growth

The rapid crack growth and setting time results are provided in Table 5.2 and Figure 5.3. The initial set of REF occurred approximately 335 minutes after casting whereas final set occurred at an approximate time of 375 minutes. Furthermore, crack onset and crack stabilisation respectively occurred 160 and 320 minutes after casting. Therefore, initial set closely corresponds to crack stabilisation. The prolonged initial setting time of REF is mainly attributed to the reduced cement content considering that 35 % of cement by mass is replaced with siliceous fly ash.

Table 5.2 Setting time and rapid crack growth results of respective high flow mixes

	Initial set [min]	Crack onset [min]	Final set [min]	Crack stabilisation [min]
REF	335	160	375	320
PCE_Min	480	200	540	320
PCE_Max	1180	200	1260	340
SMF_Min	550	180	615	300
SMF_Max	900	200	1005	360

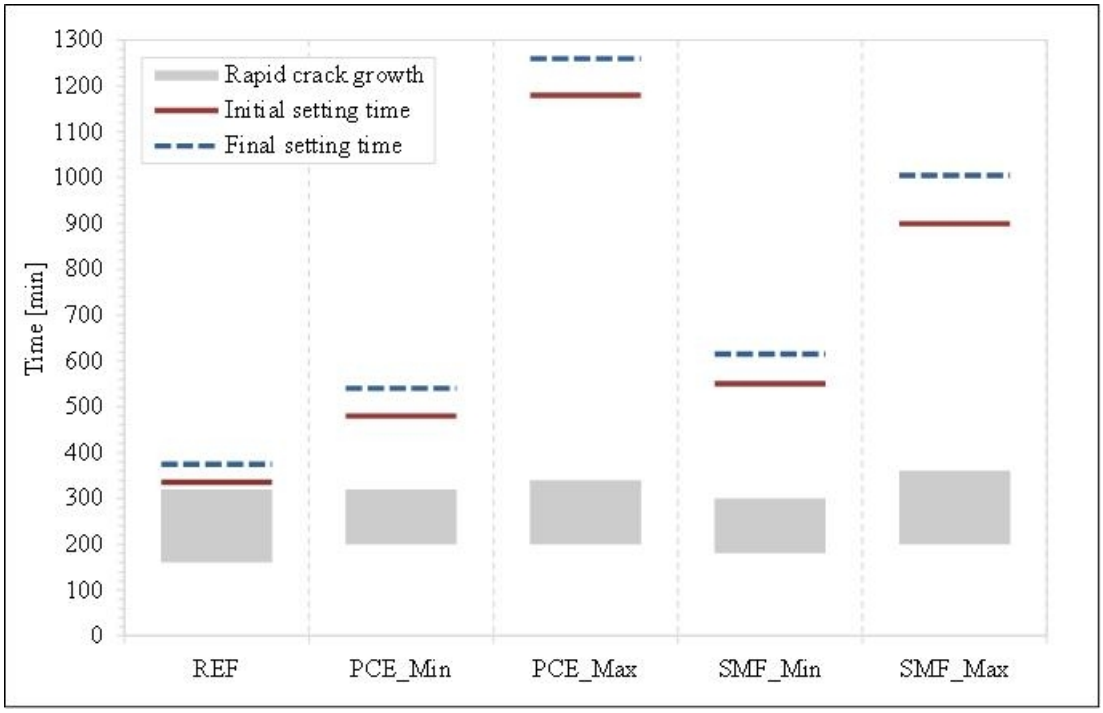

Figure 5.3 Setting time and rapid crack growth results of respective high flow mixes

PCE_Min and SMF_Min displayed moderately retarded setting times compared to REF. The initial set of PCE_Min and SMF_Min respectively occurred 480 and 550 minutes after casting whereas final set occurred at an approximate time of 540 and 615 minutes respectively. Therefore, similar to REF, the initial set of the aforementioned mixes is reached after crack stabilisation. Initial set of PCE_Min is reached approximately 160 minutes after crack stabilisation whereas that of SMF_Min is reached approximately 250 minutes after crack stabilisation.

PCE_Max and SMF_Max displayed extensively retarded setting times compared to REF. The initial set of PCE_Max and SMF_Max respectively occurred 1180 and 900 minutes after casting whereas final set occurred at an approximate time of 1260 and 1005 minutes respectively. Once again, initial set of the aforementioned mixes is reached after crack stabilisation. Initial set of PCE_Max is reached approximately 840 minutes after crack stabilisation whereas that of SMF_Min is reached approximately 540 minutes after crack stabilisation.

In summary, the initial setting time of REF and the mixes containing both high and low dosages of the related super-plasticisers is reached after crack stabilisation. Therefore, the respective high flow concrete mixes do not display a correlation between setting times and rapid crack growth. Similar to the findings of the conventional concrete mixes as discussed in Section 4.2, a more substantial delay in setting times results in a less significant correlation between rapid crack growth and setting times. Lastly, the high flow reference mix displayed prolonged setting times compared to the conventional concrete reference mix. The associated delay in setting times is attributed to the reduced cement content considering that 35 % of cement by mass is replaced with siliceous fly ash.

5.4 Rapid crack growth period

The crack onset of the respective mixes occurred in the course of 160 to 200 minutes after casting. Crack onset of REF occurred 160 minutes after casting whereas that of PCE_Min and PCE_Max correspondingly occurred at approximately 200 minutes. Furthermore, crack onset of SMF_Min and SMF_Max occurred at an approximate time of 180 and 200 minutes respectively. Subsequently, crack onset of the mixes containing the related super-plasticisers occurred within a range of 20 minutes regardless of the corresponding dosage limits.

Crack stabilisation of the respective high flow mixes occurred in the course of 300 to 360 minutes after casting with that of REF identified at approximately 320 minutes after casting. Furthermore, crack stabilisation of PCE_Min and SMF_Min respectively occurred 320 and 300 minutes after casting whereas that of PCE_Max and SMF_Max occurred at an approximate time of 340 and 360 minutes respectively. Therefore, crack stabilisation of mixes subject to moderately retarded setting times (PCE_Min & SMF_Min) occurred within a range of 20 minutes. Similarly, crack stabilisation of mixes subject to extensively retarded setting times (PCE_Max & SMF_Max) also occurred within a range of 20 minutes. Furthermore, crack stabilisation of REF coincided with that of PCE_Min and SMF_Min.

With regard to mixes containing the same admixture, crack stabilisation of SMF_Max occurred 60 minutes after that of SMF_Min whereas crack stabilisation of PCE_Max only occurred 20 minutes after that of PCE_Min. Therefore, the respective dosages of PCE-based super-plasticiser do not have a profound influence on the time of crack stabilisation.

In conclusion, crack onset of the mixes containing the related super-plasticisers approximately occurred during the same time interval regardless of the corresponding dosage limits. Furthermore, similar to the findings of the conventional concrete mixes as discussed in Section 4.3, crack stabilisation corresponds to the setting time characteristics of the respective mixes. With regard to mixes containing the same admixture, the respective dosage limits of PCE-based super-plasticiser do not have a profound influence on the rapid crack growth period.

5.5 Phenomenological behaviour

The crack area results of the respective high flow concrete mixes are used to determine the phenomenological influence of admixtures on the severity of PSC. Similar to the conventional concrete mixes, total crack area of the mixes were measured at crack stabilisation and compared to that of a reference mix devoid from admixtures to determine the physical increase or reduction in the severity of cracking. Admixtures that are used included a poly carboxylate ethers based super-plasticiser and a sulphonated melamine formaldehyde based super-plasticiser. Crack area results of the respective mixes are provided in Figure 5.4 and Table 5.3.

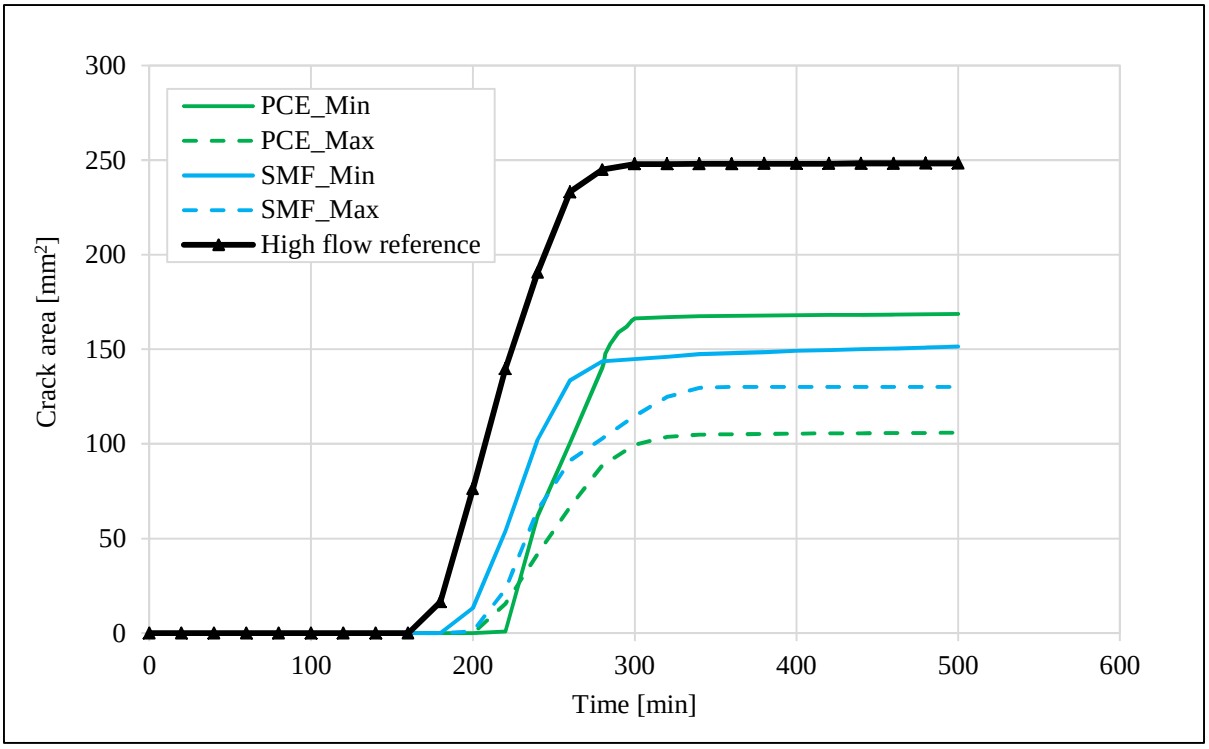

Figure 5.4 Crack area comparison of respective high flow mixes

Table 5.3 Crack area results of respective high flow mixes

	Crack onset [min]	Crack stabilisation [min]	Crack area at stabilisation [mm^2]	% Reduction in crack area at stabilisation	Time of final measurement [min]	Final crack area [mm^2]
REF	160	320	248	-	500	249
PCE_Min	200	320	168	32.3	520	169
PCE_Max	200	340	100	59.7	1280	109
SMF_Min	180	300	145	41.5	580	153
SMF_Max	200	360	130	47.6	1120	131

With reference to Figure 5.4 and Table 5.3, the addition of the associated super-plasticisers altogether displayed a substantial reduction in the severity of PSC. Subsequently, total crack area of the respective mixes is scaled with respect to the corresponding crack area of the reference mix, as shown in Figure 5.5, to illustrate the related reductions in the severity of cracking.

The high flow reference mix (REF) displayed the most severe cracking with a measured crack area of 248 mm^2 at crack stabilisation. Furthermore, REF displayed an insignificant rate of crack growth beyond crack stabilisation since the associated rate corresponded to a growth of only 1 mm^2 in the course of 180 minutes.

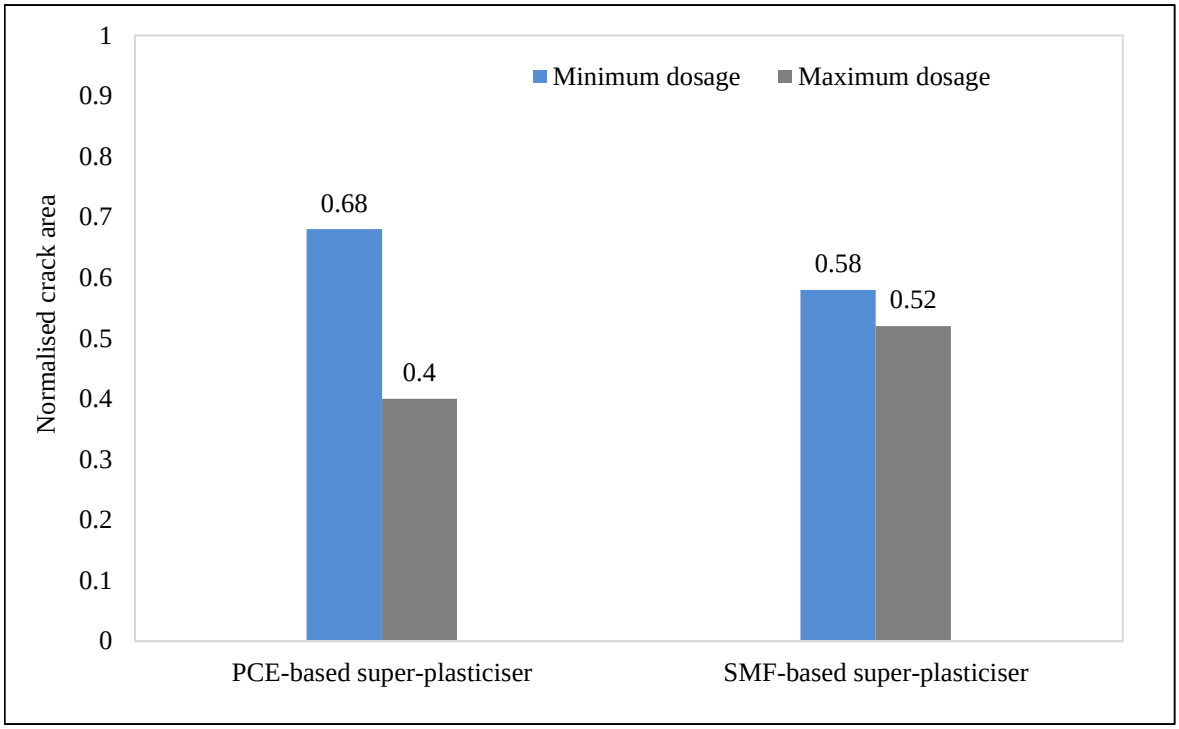

Figure 5.5 Normalised crack area of respective high flow mixes

Mixes containing PCE-based super-plasticiser, i.e. PCE_Min and PCE_Max, displayed a progressive reduction in PSC since a higher dosage of PCE-based super-plasticiser corresponds to a more substantial reduction in the severity of cracking. PCE_Min and PCE_Max displayed a total crack area of 168 and 100 mm^2 respectively which correspond to a reduction of 32.3 and 59.7 % in total crack area compared to REF. Furthermore, similar to the reference mix, PCE_Min and PCE_Max display an insignificant rate of crack growth beyond crack stabilisation. The associated rate of growth after crack stabilisation of PCE_Min corresponds to a growth of only 1 mm^2 in the course of 200 minutes whereas that of PCE_Max corresponds to a growth of 9 mm^2 in the course of 940 minutes.

Mixes containing SMF-based super-plasticiser, i.e. SMF_Min and SMF_Max, displayed a total crack area of 140 and 130 mm^2 respectively which correspond to a reduction of 41.5 and 47.6 % in total crack area. Therefore, SMF_Min and SMF_Max display a similar reduction in the severity of cracking. Furthermore, similar to the aforementioned mixes, SMF_Min and SMF_Max also display an insignificant rate of crack growth beyond crack stabilisation. The associated rate of growth after crack stabilisation of SMF_Min corresponds to a growth of 8 mm^2 in the course of 250 minutes whereas that of SMF_Max corresponds to a growth of 1 mm^2 in the course of 760 minutes.

In conclusion, similar to the conventional concrete mixes, the respective high flow mixes altogether display an insignificant rate of crack growth beyond crack stabilisation. Therefore, comparison of total crack area of the respective mixes at the time of crack stabilisation is also justified since the majority of cracking occurred prior to this time.

With regard to the phenomenological influence of admixtures on PSC, mixes containing the associated super-plasticisers altogether display a substantial reduction in the severity of PSC when compared to REF. In addition, PCE_Max exhibited the most substantial reduction in the severity of PSC whereas PCE_Min displayed the least significant reduction in the severity of cracking. SMF_Min and SMF_Max displayed a similar reduction in the severity of cracking whereas PCE_Min and PCE_Max displayed a progressive reduction in cracking with increasing content of PCE-based super-plasticiser.

5.6 Fundamental behaviour

The fundamental influences of the respective admixtures are discussed in this section to elucidate differences in the severity of PSC. The methodology that is used to elucidate the fundamental influences of the respective admixtures corresponds to that of the conventional concrete mixes as discussed in Section 4.6 and is, therefore, not discussed in this section. It should be noted that a more concise discussion regarding the behaviour of the high flow reference mix is provided compared to that of the conventional concrete reference mix since the majority of the concepts are already discussed in Section 4.6.1.

5.6.1 Behaviour of the high flow reference mix

Similar to the conventional concrete reference mix, REF displayed a rapid increase in settlement as shown in Figure 5.6. The associated settlement can be attributed to gravitational forces being accountable for consolidation of solid particles in the concrete paste.

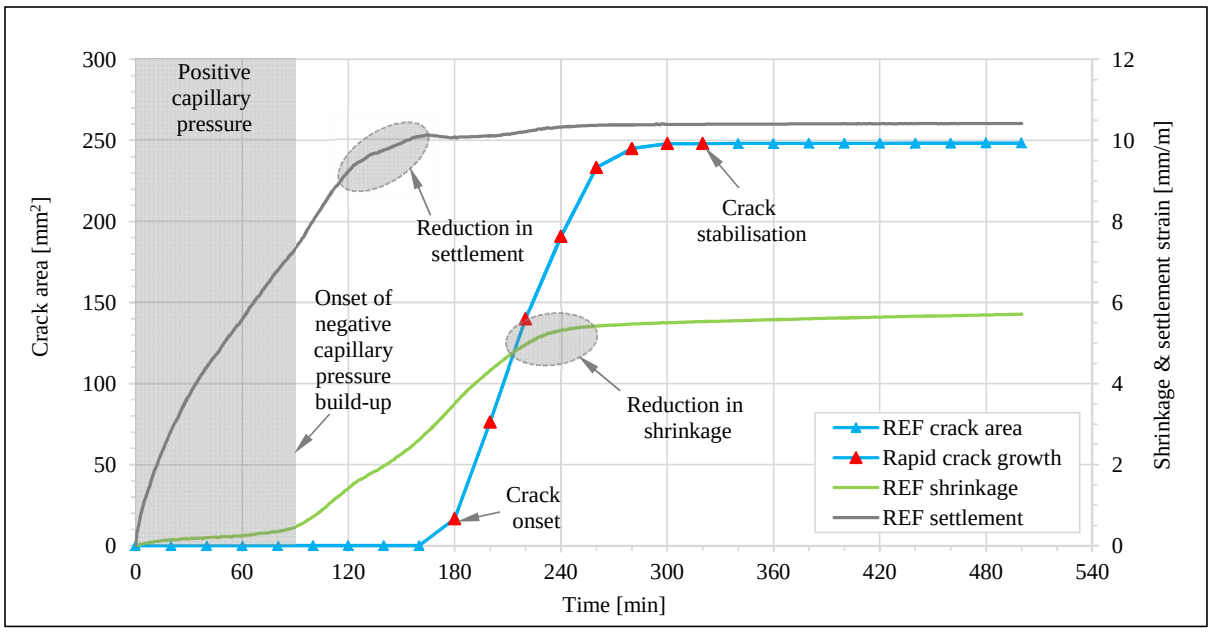

Figure 5.6 Crack area, shrinkage and settlement results of REF

The onset of negative capillary pressure build-up occurred approximately 100 minutes after casting as shown in Figure 5.7. The corresponding time interval during which capillary pressure is in compression is indicated by the shaded area in Figure 5.6. The progressive evaporation of pore water from the concrete paste caused negative capillary pressure build-up. The rate of negative capillary pressure build-up is directly related to the rate of evaporation, the rate of bleeding, surface tension of the pore fluid and particle distribution in the surface of the concrete paste.

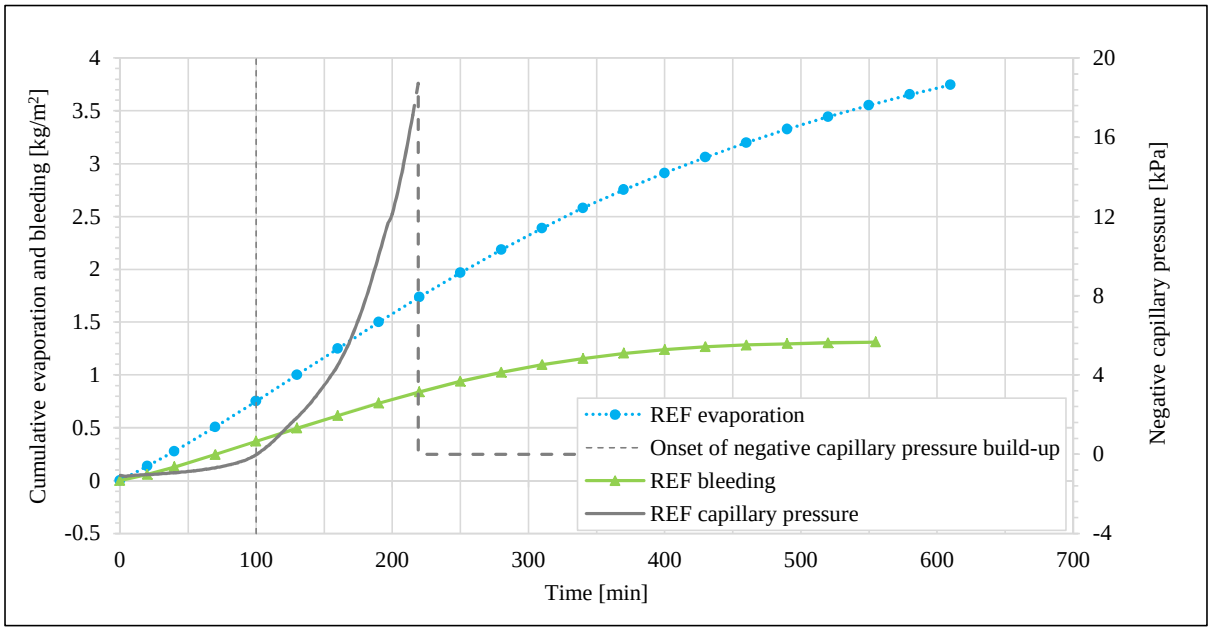

Figure 5.7 Capillary pressure, evaporation and bleeding of REF

As result of the negative capillary pressure build-up, the capillary tension forces acted on the solid particles both vertically and horisontally which resulted in settlement and shrinkage of the still plastic concrete. Subsequently, once the negative capillary pressure build-up is reached, settlement can be attributed to a combination of gravitational forces and capillary tension forces. Furthermore, the onset of negative capillary pressure build-up closely corresponds to a significant increase in shrinkage of the concrete paste as shown in Figure 5.6.

The negative capillary pressure build-up caused the network of solid particles to become progressively stiffer and, correspondingly, caused a reduction in settlement in the course of 120 to 170 minutes after casting. As shown in Figure 5.6, the significant reduction in settlement occurred just before the time of crack onset at approximately 180 minutes after casting. From this point onwards, the vertical component of the capillary tension forces no longer had a pronounced influence on the cracking process since settlement has stabilised to a large extent. With reference to Figure 5.7, air entry occurred at an approximate time of 220 minutes. However, the time of air entry is not correlated to crack onset and the associated reduction in settlement since measurements were performed at a localised position. Also, capillary pressure measurements were not conducted at the crack location. If so, it is believed that air entry would have occurred just before crack onset.

As previously mentioned, the onset of negative capillary pressure build-up corresponds to a rapid increase in shrinkage results which is mainly attributed to the horisontal component of the capillary tension forces. After crack onset, the particles adjacent to the air penetrated regions continue to experience capillary pressure build-up as discussed in Section 2.3. The air penetrated regions form weak spots in the system as the contracting forces between these particles are considerably smaller than those in the water-filled regions. Consequently, capillary pressure in the water-filled regions of the concrete paste can possibly be relieved by horisontal shrinkage or a combination of horisontal shrinkage and settlement after crack onset is reached. Therefore, considering that settlement has stabilised to a large extent at crack onset, horisontal shrinkage is mainly responsible for the formation of plastic shrinkage cracks after crack onset is reached. Furthermore, the significant reduction in shrinkage in the course of 210 to 260 minutes after casting closely corresponds to a reduction in the rate of crack growth as shown in Figure 5.6.

In summary, the behaviour of the high flow reference mix closely corresponds to that of the conventional concrete reference mix. The settlement of the concrete paste is attributed to gravitational forces until commencement of the negative capillary pressure build-up approximately 100 minutes after casting. Thereafter, settlement is attributed to a combination of gravitational and capillary tension forces. Similar to the convetional concrete reference mix, the onset of negative capillary pressure build-up corresponds to a significant increase in shrinkage. The significant increase in shrinkage is attributed to the horisontal component of the capillary tension forces. Shrinkage and settlement induced by the capillary tension forces caused the network of solid particles to become progressively stiffer and, correspondingly, caused a reduction in settlement. The associated reduction in settlement occurred just before the time of crack onset at approximately 180 minutes after casting. From this point onwards, the vertical component of capillary tension forces no longer has a pronounced influence on the cracking process and, therefore, horisontal shrinkage is mainly responsible for the formation of plastic shrinkage cracks.

5.6.2 Poly carboxylate ethers based super-plasticiser (PCE)

Mixes containing PCE-based super-plasticiser, i.e. PCE_Min and PCE_Max respectively, displayed a reduction of 32.3 and 59.7 % in total crack area compared to REF. Therefore, the addition of PCE-based super-plasticiser progressively reduced the severity of PSC since a higher dosage corresponds to a more substantial reduction in the severity of cracking.

Fundamental behaviour

With reference to Table 5.4, the onset of negative capillary pressure build-up of PCE_Min and PCE_Max occurred approximately 115 and 120 minutes after casting respectively. In addition, PCE_Min and PCE_Max mutually displayed a significant increase in shrinkage approximately 20 minutes before the commencement of negative capillary pressure build-up. Therefore, mixes

containing the respective dosages of PCE-based super-plasticiser also display a correlation between the onset of negative capillary pressure build-up and an increase in shrinkage. Furthermore, crack onset of PCE_Min and PCE_Max occurred during the interval when a reduction in settlement was observed as shown in Figure 5.8. Therefore, it is believed that for both PCE_Min and PCE_Max the vertical component of the capillary tension forces does not have a profound influence on the cracking process after crack onset is reached since settlement has stabilised to a large extent. Lastly, the significant reduction in shrinkage of both PCE_Min and PCE_Max closely corresponds to crack stabilisation. In conclusion, mixes containing the respective dosages of PCE-based super-plasticiser display similar behaviour than the reference mix.

Table 5.4 Fundamental results of REF, PCE_Min and PCE_Max

		REF	PCE_Min	PCE_Max
Onset of negative capillary pressure build-up	[min]	100	115	120
Approximation of significant increase in shrinkage	[min]	100	100	110
Approximation of significant reduction in settlement	[min]	120 to 170	120 to 200	130 to 220
Crack onset	[min]	180	220	220
Settlement at crack onset	[mm]	10.1	17.1	16.7
Approximation of significant reduction in shrinkage	[min]	220 to 260	260 to 320	280 to 320
Crack stabilisation	[min]	260	320	340
Shrinkage at crack stabilisation	[mm/m]	5.41	4.60	4.40
Surface tension of pore fluid	[mN/m]	70.55	61.28	60.59

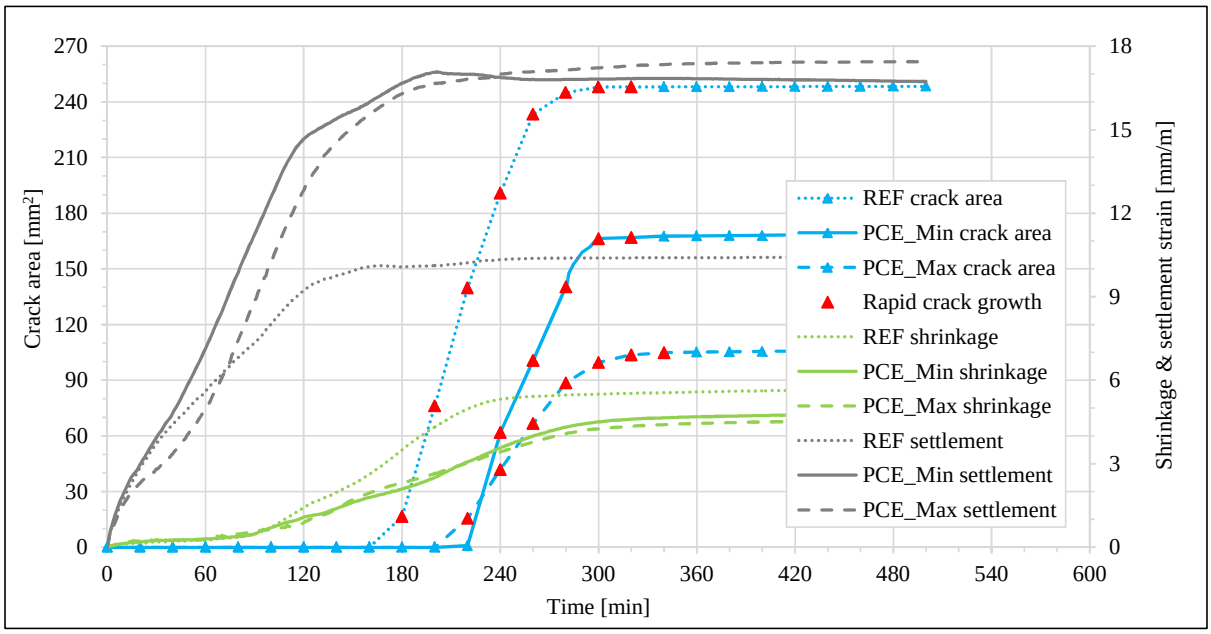

Figure 5.8 Crack area, shrinkage and settlement of REF, PCE_Min and PCE_Max

Fundamental influences

The shrinkage and settlement results are shown Table 5.4 and Figure 5.8. PCE_Min and PCE_Max exhibited approximate shrinkage of 4.60 and 4.40 mm/m respectively at crack stabilisation and, therefore, altogether display a significant reduction in shrinkage compared to that of REF which was measured as 5.41 mm/m. Therefore, the overall reduction in the severity of cracking is validated by the associated shrinkage results since mixes containing PCE-based super-plasticiser mutually display a significant reduction in shrinkage compared to the reference mix. PCE_Min and PCE_Max display a similar rate of shrinkage from the onset of tests as shown in Figure 5.8. Furthermore, both PCE_Min and PCE_Max display a significantly lower shrinkage rate compared to REF beyond approximately 100 minutes after casting. With reference to Table 5.4 and Figure 5.8, the onset of the significant reduction in shrinkage of REF occurred at least 40 minutes before that of PCE_Min and PCE_Max. The associated reduction in shrinkage corresponds to the phenomenological behaviour since crack onset of PCE_Min and PCE_Max respectively occurred approximately 40 and 60 minutes after that of the reference mix. Lastly, PCE_Max displays a slightly reduced shrinkage rate from 230 minutes after casting compared to PCE_Min which can possibly validate the progressive reduction in the severity of cracking. However, considering the difference in the severity of cracking, a more substantial difference in shrinkage between PCE_Min and PCE_Max can be expected and further investigation is required.

Using crack onset as a point of reference, PCE_Min and PCE_Max displayed settlement of 17.1 and 16.7 mm/m respectively whereas that of REF was measured as 10.1 mm/m. Therefore, the mixes containing PCE-based super-plasticiser altogether display significantly increased settlement at crack onset compared to REF. In addition, with reference to Figure 5.8, PCE_Min and PCE_Max also display prolonged settlement compared to REF. The prolonged settlement is attributed to the delayed setting times considering that the initial set of REF, PCE_Min and PCE_Max respectively occurred approximately 335, 480 and 1180 minutes after casting. The increased settlement of both PCE_Min and PCE_Max is attributed to the improved particle distribution in the concrete paste due to the dispersion properties of the PCE-based super-plasticiser. The improved dispersion of solid particles provides more room for unhindered settlement and, therefore, results in increased settlement.

As previously discussed in Section 5.6.1, capillary tension forces in the concrete paste can be relieved through a combination of shrinkage and settlement. Therefore, if two identical mixes are compared with the only difference being that the one mix displays prolonged settlement compared to the other, i.e. mixes display an identical rate of both capillary pressure build-up and shrinkage, the mix with the prolonged settlement will exhibit a delayed time of air entry, provided the particle distribution is theoretically the same. The reason being is that prolonged settlement results in increased relief of capillary tension forces in the concrete paste and, therefore, the time for menisci to reach a break-through radius is delayed. Therefore, considering that both PCE_Min and PCE_Max displayed

prolonged settlement compared to REF, it is speculated that the prolonged settlement resulted in a more substantial relief of capillary pressure in the concrete paste despite the reduced shrinkage rate compared to REF and, therefore, resulted in a delayed time of air entry. As shown in Figure 5.8, the associated speculation serves to provide a viable explanation since the prolonged settlement of both PCE_Min and PCE_Max corresponds to a delayed time of crack onset compared to REF. In addition, it is believed for REF, PCE_Min and PCE_Max that the vertical component of the capillary tension forces does not have a profound influence on the formation of PSC after crack onset is reached since settlement of the respective mixes has stabilised to a large extent. Lastly, the interaction of plastic settlement cracking and PSC does not have a profound influence on the severity of cracking since PCE_Min and PCE_Max displayed progressively reduced cracking despite the significantly increased settlement compared to REF. Therefore, the interaction between plastic settlement cracking and PSC also requires further investigation.

With reference to Figure 5.9, PCE_Min and PCE_Max displayed a reduced rate of capillary pressure build-up compared to REF. The associated reduction in the rate of capillary pressure build-up further validates the delay in crack onset of mixes containing PCE-based super-plasticiser. However, PCE_Max displayed a slightly higher rate of capillary pressure build-up compared to PCE_Min which does not correspond to crack onset of the respective mixes since crack onset of PCE_Min occurred approximately 20 minutes before that of PCE_Max. However, considering the significant crack area of PCE_Min at crack onset, it can be expected that crack onset of PCE_Min possibly occurred sooner or at a similar time than PCE_Max which requires further investigation.

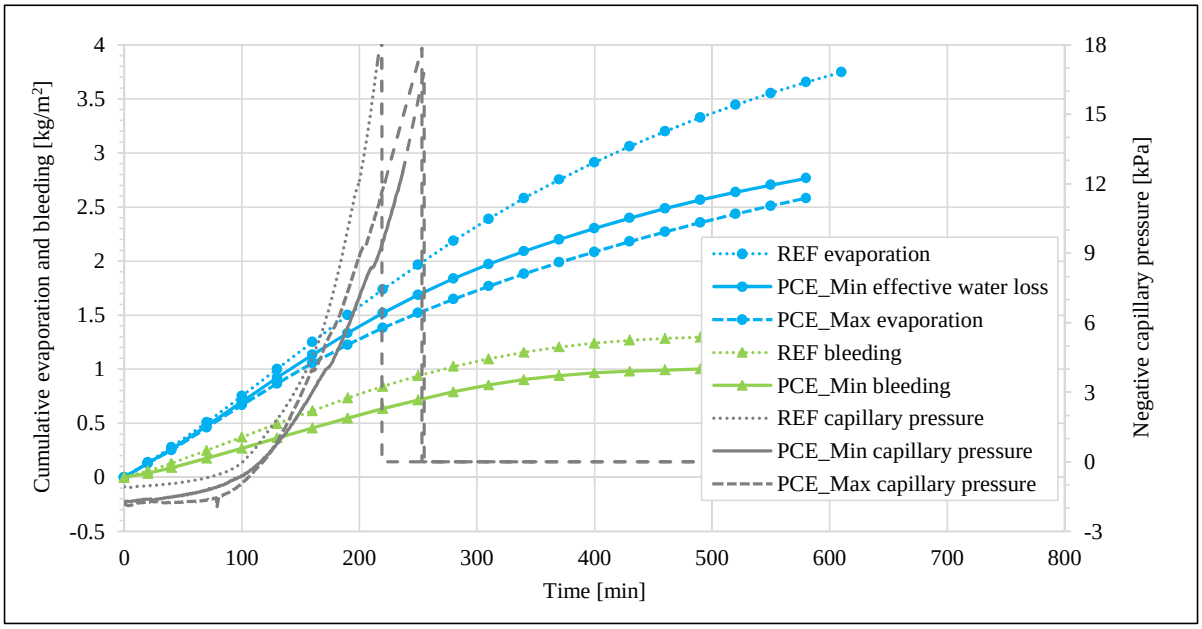

Figure 5.9 Capillary pressure, evaporation and bleeding of REF, PCE_Min and PCE_Max

With reference to Figure 5.9, the addition of PCE-based super-plasticiser progressively influenced evaporation since a higher dosage of super-plasticiser corresponds to a more substantial reduction in

the rate of evaporation. PCE_Min displayed reduced bleeding compared to the reference mix despite the significantly increased settlement of PCE_Min. As discussed in Section 2.4.2, bleeding results from concrete pore water being forced to the surface due to the inability of solid particles to retain the pore water during settlement and consolidation. Consequently, concrete with increased resistance to segregation is less susceptible to bleeding. Therefore, it is believed that the reduced bleeding of PCE_Min is attributed to improved particle distribution which results in increased resistance to segregation. With reference to Table 5.4, the addition of a minimum dosage of PCE-based super-plasticiser resulted in a significant reduction in surface tension compared to REF although the reduction in surface tension between PCE_Min and PCE_Max is less profound. Therefore, the overall reduction in the rate of capillary pressure of mixes containing PCE-based super-plasticiser is mainly attributed to the progressively reduced evaporation and reduced surface tension with increasing content of PCE-based super-plasticiser. Furthermore, it is believed that the improved particle distribution with the addition of PCE-based super-plasticiser contributed to the reduced rate of capillary pressure build-up. Lastly, PCE_Max displayed reduced evaporation and slightly reduced surface tension compared to PCE_Min and is, therefore, expected to display a reduced rate of capillary pressure build-up. However, since bleeding results could not be obtained for PCE_Max, definitive conclusions could not be drawn.

In conclusion, the overall reduction in the severity of PSC is validated by the associated shrinkage results since mixes containing PCE-based super-plasticiser mutually displayed a significant reduction in shrinkage compared to the reference mix. PCE_Max displayed a reduced severity of cracking compared to PCE_Min which can possibly be attributed to the slightly reduced shrinkage rate of PCE_Max compared to PCE_Min. However, a more substantial difference in shrinkage between PCE_Min and PCE_Max can be expected and further investigation is required. The delayed crack onset of PCE_Min and PCE_Max is attributed to prolonged settlement of the concrete paste. PCE_Min and PCE_Max altogether displayed a reduced rate of capillary pressure build-up compared to REF which further validates the delay in crack onset of mixes containing PCE-based super-plasticiser. The reduction in the rate of capillary pressure build-up of mixes containing PCE-based super-plasticiser is mainly attributed to the reduction in evaporation and surface tension as well as improved particle distribution with increasing content of PCE-based super-plasticiser. PCE_Min displayed reduced bleeding compared to REF despite the significantly increased settlement. Lastly, since bleeding results could not be obtained for PCE_Max, definitive conclusions could not be drawn with regard to differences in the rate of capillary pressure build-up between PCE_Min and PCE_Max.

5.6.3 Sulphonated melamine formaldehyde (SMF) based super-plasticiser

Mixes containing SMF-based super-plasticiser, i.e. SMF_Min and SMF_Max respectively, displayed a reduction of 41.5 and 47.6 % in total crack area. Therefore, the respective dosages of SMF-based super-plasticiser displayed a similar reduction in the severity of cracking.

Fundamental behaviour

With reference to Table 5.5, the onset of negative capillary pressure build-up of SMF_Min and SMF_Max occurred approximately 125 and 140 minutes after casting respectively. In addition, a significant increase in shrinkage mutually occurred approximately 120 minutes after casting. Therefore, shrinkage results of SMF_Min display a strong correlation between the onset of negative capillary pressure build-up and an increase in shrinkage although the correlation of SMF_Max is slightly less prominent. Furthermore, crack onset of SMF_Min and SMF_Max occurred during the interval when a reduction in settlement is observed. With reference to Figure 5.10, SMF_Min displays a strong correlation between the significant reduction in shrinkage and crack stabilisation. Although the significant reduction in shrinkage of SMF_Max occurred at least 20 minutes before crack stabilisation, the associated reduction in shrinkage corresponds to a reduction in the rate of crack growth. In conclusion, mixes containing the respective dosages of SMF-based super-plasticiser display similar behaviour than the reference mix.

Table 5.5 Fundamental results of REF, SMF_Min and SMF_Max

		REF	SMF_Min	SMF_Max
Onset of negative capillary pressure build-up	[min]	100	125	140
Approximation of significant increase in shrinkage	[min]	100	120	120
Approximation of significant reduction in settlement	[min]	120 to 170	120 to 200	160 to 240
Crack onset	[min]	180	200	220
Settlement at crack onset	[mm]	10.1	20.5	24.0
Approximation of significant reduction in shrinkage	[min]	220 to 260	260 to 360	280 to 320
Crack stabilisation	[min]	260	320	340
Shrinkage at crack stabilisation	[mm/m]	5.41	4.87	4.55
Surface tension of pore fluid	[mN/m]	70.55	70.17	65.57

Fundamental influences

The shrinkage and settlement results are shown in Table 5.5 and Figure 5.10. SMF_Min and SMF_Max exhibited approximate shrinkage of 4.87 and 4.55 mm/m respectively at crack stabilisation and, therefore, display a reduction in shrinkage compared to that of REF which was measured as 5.41 mm/m. Therefore, the overall reduction in the severity of cracking is validated by the associated

shrinkage results since mixes containing SMF-based super-plasticiser mutually display a reduction in shrinkage compared to REF. With reference to Figure 5.10, both SMF_Min and SMF_Max display a reduced shrinkage rate compared to REF beyond approximately 100 minutes after casting. In addition, the onset of the significant reduction in shrinkage of REF occurred at least 40 minutes before that of SMF_Min and SMF_Max. The associated reduction in shrinkage correlates to the phenomenological behaviour since crack onset of SMF_Min and SMF_Max respectively occurred approximately 20 and 60 minutes after that of the reference mix. Furthermore, SMF_Min and SMF_Max displayed a similar rate of shrinkage for the first 300 minutes after casting. Thereafter, shrinkage of SMF_Max stabilised to a large extent whereas SMF_Min displayed prolonged shrinkage as shown in Figure 5.10. The prolonged shrinkage of SMF_Min beyond 300 minutes does not validate the reduced cracking of SMF_Max compared to SMF_Min since crack growth of SMF_Min has stabilised to a large extent at 300 minutes after casting as shown in Figure 5.10. Therefore, the shrinkage results do not provide a clear explanation for the difference in the severity of PSC between SMF_Min and SMF_Max and further investigation is required.

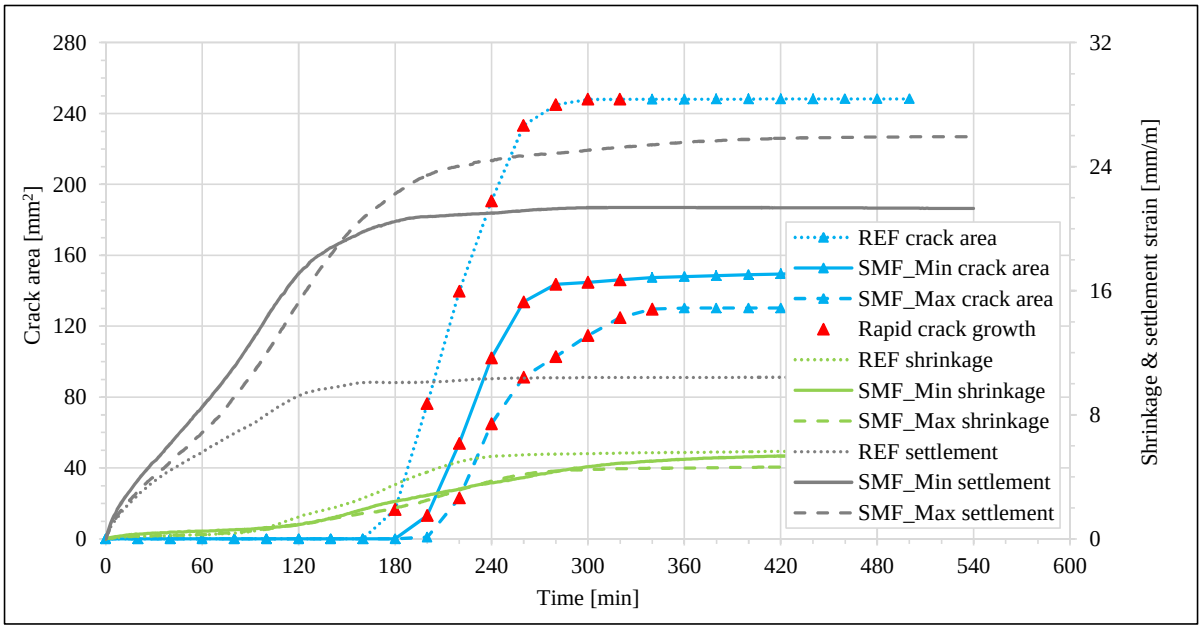

Figure 5.10 Crack area, shrinkage and settlement of REF, SMF_Min and SMF_Max

Using crack onset as a point of reference, SMF_Min and SMF_Max exhibited settlement of 20.5 and 24.0 mm/m respectively whereas that of REF was measured as 10.1 mm/m. Therefore, the addition of SMF-based super-plasticiser resulted in progressively increased settlement compared to REF. In addition, with reference to Figure 5.10, a higher dosage SMF-based super-plasticiser also results in prolonged settlement of the concrete paste. Similar to the mixes containing PCE-based super-plasticiser, the prolonged settlement is attributed to the delayed setting times considering that the initial set of REF, SMF_Min and SMF_Max respectively occurred approximately 335, 500 and 900 minutes after casting. The increased settlement of SMF_Min and SMF_Max is attributed to the

improved particle distribution in the concrete paste due to the dispersion properties of SMF-based super-plasticiser. The improved dispersion of solid particles provides more room for unhindered settlement and, therefore, results in increased settlement. In connection herewith, considering that SMF_Max contains an increased content of super-plasticiser compared to SMF_Min, the increased settlement at crack onset of SMF_Max compared to SMF_Min is validated.

Similar to mixes containing PCE-based super-plasticiser, the progressive delay in crack onset of REF, SMF_Min and SMF_Max is attributed to the prolonged settlement with increasing content of SMF-based super-plasticiser. Furthermore, it is believed that the capillary pressure in the water-filled regions of the respective mixes is mainly relieved through shrinkage after crack onset since settlement has stabilised to a large extent. Lastly, similar to mixes containing PCE-based super-plasticiser, the interaction of plastic settlement cracking and PSC does not have a profound influence on the severity of cracking since SMF_Min and SMF_Max displayed progressively reduced cracking despite the significantly increased settlement compared to REF. Therefore, the interaction of plastic settlement cracking and PSC requires further investigation.

With reference to Figure 5.11, SMF_Min and SMF_Max altogether displayed a significant reduction in the rate of capillary pressure build-up compared to REF. The reduced rate of capillary pressure build-up of mixes containing SMF-based super-plasticiser further validates the progressive delay in crack onset of REF, SMF_Min and SMF_Max. Furthermore, SMF_Min and SMF_Max displayed a similar rate of capillary pressure build-up which validates the similar shrinkage rate of SMF_Min and SMF_Max. However, differences in both shrinkage results and capillary pressure results of SMF_Min and SMF_Max requires further investigation to elucidate differences in the severity of PSC.

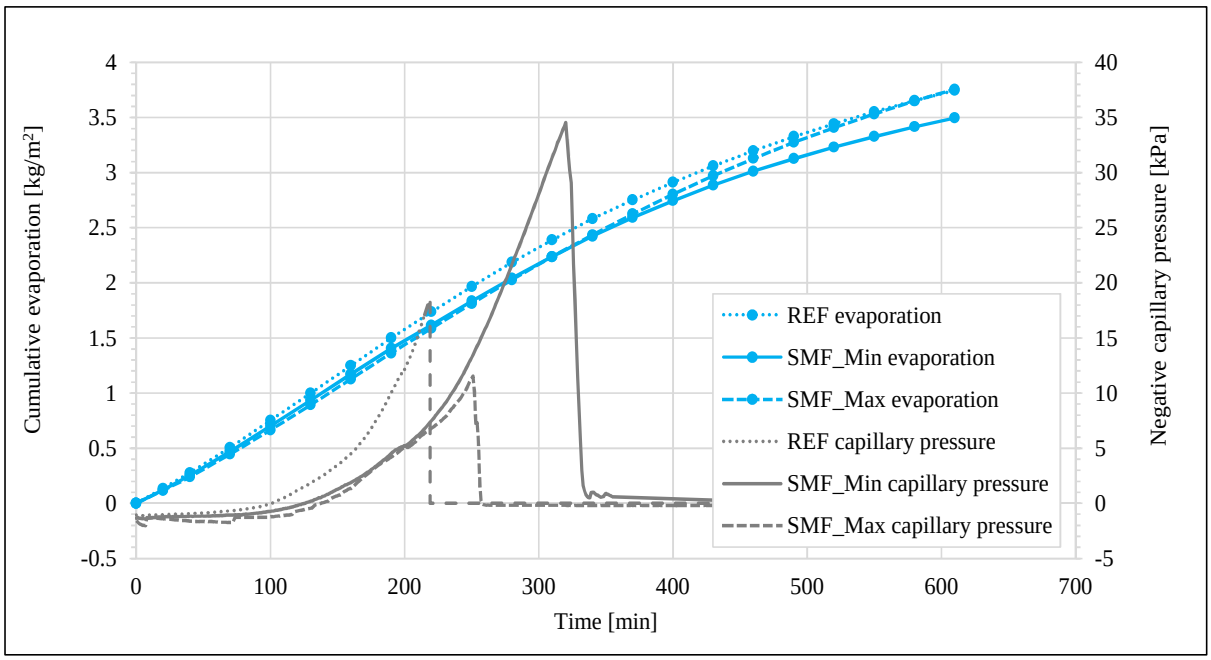

Figure 5.11 Capillary pressure and evaporation of REF, SMF_Min and SMF_Max

With reference to Figure 5.11, REF displayed a slightly increased evaporation rate from the onset of tests. SMF_Min and SMF_Max displayed a similar evaporation rate during the first 380 minutes after which the evaporation rate of SMF_Max exceeded that of SMF_Min. However, the increased evaporation rate of SMF_Max after 380 minutes is not considered to influence PSC since crack stabilisation of the respective mixes is already reached. With reference to Table 5.5, the addition of the low dosage of SMF-based super-plasticiser insignificantly influenced the surface tension compared to REF although the addition of the high dosage caused a significant reduction in surface tension. Therefore, the reduced rate of capillary pressure build-up of SMF_Max and SMF_Min compared to REF is attributed to slightly reduced evaporation and reduced surface tension with increasing content of SMF-based super-plasticiser. In addition, it is believed that the improved particle distribution with increasing content of SMF-based super-plasticiser contributed to the reduced rate of capillary pressure build-up. Bleeding results of SMF_Min and SMF_Max could not be obtained which requires further investigation.

In conclusion, the overall reduction in the severity of cracking is validated by the associated shrinkage results since mixes containing SMF-based super-plasticiser mutually display a significant reduction in shrinkage compared to the reference mix. The similar shrinkage rate of SMF_Min and SMF_Max do not provide a clear explanation for the difference in the severity of PSC between SMF_Min and SMF_Max and further investigation is required. The progressively delayed times of crack onset of REF, PCE_Min and PCE_Max is attributed to prolonged settlement of the concrete paste. The prolonged settlement, in turn, is attributed to the progressively delayed setting times with increasing content of SMF-based super-plasticiser. Furthermore, the increase in settlement is attributed to improved dispersion of solid particles which resulted in more room for unhindered settlement. SMF_Min and SMF_Max altogether displayed a reduced rate of capillary pressure build-up compared to REF which further validates the overall delay in crack onset of mixes containing SMF-based super-plasticiser. The reduced rate of capillary pressure build-up of SMF_Max and SMF_Min compared to REF is mainly attributed to slightly reduced evaporation, reduced surface tension and improved particle distribution with addition of SMF-based super-plasticiser.

5.7 Concluding summary

The experimental results of the respective high flow concrete mixes are presented and discussed accordingly in this chapter. Firstly, the methodology used to analyse results are discussed, followed by preliminary conclusions concerning the correlations between setting times and rapid crack growth as well as the rapid crack growth periods of the respective mixes. Thereafter, the phenomenological influence of the respective admixtures is investigated by comparing the total crack area of the respective mixes to that of a reference mix deviod from admixtures. Lastly, the fundamental influences of the respective admixtures are investigated to elucidate differences in the severity of PSC. Phenomenological and fundamental behaviour of the respective admixtures used in both high flow and conventional concrete mixes are summarised in the next chapter.

CHAPTER 6

Conclusions and recommendations

The main objectives of this study are to determine both the phenomenological and fundamental influences of a wide range of admixtures at different dosages on the plastic shrinkage cracking (PSC) of concrete.

The following conclusions can be drawn from this study with regard to the phenomenological influence of admixtures on the PSC of concrete:

- The addition of the glucose based retarder, calcium chloride based accelerator, chloride free air entraining agent, lignosulphonate plasticiser, shrinkage reducing admixture (SRA), poly carboxylate ethers based super-plasticiser, and a sulphonated melamine formaldehyde based super-plasticiser, respectively, at different dosages altogether results in a reduced severity of PSC compared to reference mixes devoid from admixtures.

- The different dosage limits of the retarder (RET_Min & RET_Max) and SMF-based super-plasticiser (SMF_Min & SMF_Max) resulted in a similar reduction in the severity of PSC. The addition of air entrainer (AIR_Min & AIR_Max), SRA (S_Min & S_Max) and PCE-based super-plasticiser (PCE_Min & PCE_Max) progressively reduced the severity of PSC since a higher dosage corresponds to a more profound reduction in cracking. Lastly, the minimum dosage of plasticiser (PL_Min) and accelerator (AC_Min) respectively exhibited a more substantial reduction in the severity of PSC compared to the maximum dosage (PL_Max & AC_Max).

The following conclusions can be drawn from this study with regard to the fundamental behaviour of admixtures on the PSC of concrete:

- The addition of the associated admixtures at different dosages resulted in similar PSC behaviour compared to the reference mixes. The onset of negative capillary pressure build-up corresponds to a significant increase in shrinkage which is attributed to the horisontal component of the capillary tension forces. After the commencement of the negative capillary pressure build-up, settlement is attributed to a combination of gravitational and capillary

tension forces. The significant reduction in settlement predominantly corresponds to crack onset, although AIR_Min, PL_Max and S_Max displayed prolonged settlement after crack onset. Lastly, the significant reduction in shrinkage corresponds to a reduction in the rate of crack growth.

- A more substantial delay in setting times corresponds to a less significant correlation between the rapid crack growth and setting times. PSC can only be characterised as the rapid growth and stabilisation of cracks between initial and final set for AC_Min, AC_Max, AIR_Min, AIR_Max, PL_Min and RET_Min.

- The crack onset of both the conventional and high flow concrete mixes respectively occurred in close proximity regardless of the admixture and corresponding dosage limits, while crack stabilisation corresponds to the setting time characteristics of the respective concrete mixes. The rapid crack growth periods of mixes containing high and low dosages of accelerator, air entrainer, plasticiser and PCE-based super-plasticiser, respectively, occurred during the same time interval.

The following conclusions can be drawn from this study with regard to the fundamental influences of admixtures on the PSC of concrete:

- The addition of retarder, accelerator, air entrainer, plasticiser, SRA and PCE-based super-plasticiser progressively reduced the rate of capillary pressure build-up while the different dosages of SMF-based super-plasticiser displayed a similar reduction in the rate of build-up.

- The addition of air entrainer, retarder, SRA and SMF-based super-plasticiser progressively reduced the surface tension while the different dosages of plasticiser and PCE-based super-plasticiser displayed a similar reduction in surface tension. Furthermore, the addition of accelerator insignificantly influenced the surface tension of the pore fluid.

- The addition of SRA and PCE-based super-plasticiser progressively reduced the evaporation rate while air entrainer and plasticiser did not significantly influence evaporation. Furthermore, the addition of SMF-based super-plasticiser and a maximum dosage of both accelerator and retarder caused a slightly reduced evaporation rate.

- The addition of retarder, SRA and plasticiser resulted in prolonged bleeding while the addition of accelerator did not influence bleeding. Furthermore, a maximum dosage of air entrainer and a minimum dosage of PCE-based super-plasticiser resulted in reduced bleeding.

- The addition of the associated admixtures resulted in an overall reduction in shrinkage. The addition of retarder and plasticiser progressively reduced shrinkage while the different dosages of accelerator, PCE-based super-plasticiser and SMF-based super-plasticiser displayed a similar reduction in shrinkage. Furthermore, the minimum dosage of air entrainer displayed slightly reduced shrinkage compared to the maximum dosage whereas the maximum dosage of SRA displayed slightly reduced shrinkage compared to the minimum dosage.

- The addition of SMF-based super-plasticiser, PCE-based super-plasticiser and a maximum dosage of SRA resulted in both increased and prolonged settlement while the addition of retarder did not influence the amount of settlement. The maximum dosage of plasticiser displayed prolonged settlement whereas the addition of accelerator, a minimum dosage of SRA and a maximum dosage air entrainer resulted in reduced settlement.

The following conclusions can be drawn from this study with regard to the explanations of the phenomenological behaviour:

- The minor difference in the severity of cracking between RET_Min and RET_Max is mainly attributed to the similar extent of shrinkage at crack stabilisation.

- The increased cracking of PL_Max compared to PL_Min is mainly attributed to the increased interaction of plastic settlement cracking and PSC due to prolonged settlement of PL_Max after crack onset.

- The reduced cracking of AC_Min compared to AC_Max is mainly attributed to the slightly reduced shrinkage of AC_Min compared to AC_Max and the increased capacity to resist capillary tension forces after crack onset due to a delayed time of air entry.

- The increased cracking of AIR_Min compared to AIR_Max is mainly attributed to the increased capacity to resist capillary tension forces after crack onset due to a delayed time of air entry. The delayed time of air entry, in turn, is attributed to differences in the severity of plastic settlement cracking.

- The reduction in the severity of PSC of S_Max compared to S_Min is mainly attributed to the slightly reduced shrinkage rate of S_Max compared to S_Min.

- PCE_Max displayed a reduced severity of cracking compared to PCE_Min which is attributed to the slightly reduced shrinkage rate of PCE_Max compared to PCE_Min. However, a more

substantial difference in shrinkage between PCE_Min and PCE_Max can be expected and further investigation is required.

- The similar shrinkage rate of SMF_Min and SMF_Max do not provide a clear explanation for the difference in the severity of PSC between SMF_Min and SMF_Max and further investigation is required. The progressively delayed times of crack onset of REF, PCE_Min and PCE_Max is attributed to prolonged settlement of the concrete paste.

From the knowledge gained during this study, the following recommendations are considered to be important for future investigation:

- Develop a test setup to determine the interaction between plastic settlement cracking and PSC or, alternatively, design a suitable mould which results in pure PSC cracking, i.e. eliminate differential settlement of the concrete paste.
- Perform optical microscopy at the concrete surface during the plastic state to investigate the distribution of solid particles. These results can be used to compare the dispersion properties of the respective admixtures such as plasticisers and super-plasticisers.
- Perform capillary pressure measurements and crack area tests using the same mould to possibly correlate crack onset and the time of air entry.
- Lastly, measure the bleeding of mixes subject to high self-levelling properties using appropriate guidelines.

References

ASTM C1579, 2006. *Standard Test Method for Evaluating Plastic Shrinkage Cracking of Restrained Fiber Reinforced Concrete*, West Conshohocken, Philadelphia: American Society for Testing and Materials.

ASTM C232 / C232M-09, 2010. *Standard Test Methods for Bleeding of Concrete*, West Conshohocken, Philadelphia: American Society for Testing and Materials.

ASTM D971, 2004. *Standard test method for interfacial tension of oil against water by the Ring Method*, West Conshohocken, Philadelphia: American Society for Testing and Materials.

Boshoff, W.P., 2012. Plastic Shrinkage Cracking of Concrete, Part 1: Guideline. *Institute of Structural Engineering*, pp.89–97, Stellenbosch. Report Number: ISI2012–17.

Boshoff, W.P. & Combrinck, R., 2013. Modelling the severity of plastic shrinkage cracking in concrete. *Cement and Concrete Research*, 48, pp.34–39.

Cement and Concrete Institute, 1997. Admixtures for Concrete. *Cement & Concrete Institute*, 23, pp.466–472.

Chryso, 2007. *General Catalogue. Chemical solutions for the construction site* First ed., Boksburg, South Africa: Chryso South Africa (Pty) Ltd.

Combrinck, R., 2012. *Investigation of plastic shrinkage cracking in conventional and low volume fibre reinforced concrete*. MSC thesis. Stellenbosch University.

Combrinck, R. & Boshoff, W.P., 2014. Fundamentals of Plastic Settlement Cracking in Concrete. *Concrete Materials CONMAT'15 conference*, 4, pp.65–73.

Combrinck, R. & Boshoff, W.P., 2012. Theory for the early age plastic cracking behaviour of concrete. In *fib International PhD Symposium in Civil Engineering*. Karlsruhe, Germany, pp. 124–129.

Combrinck, R. & Boshoff, W.P., 2013. Typical plastic shrinkage cracking behaviour of concrete. *Magazine of Concrete Research*, 65(8), pp.486–493.

Dao, V.T.N. et al., 2010. Plastic shrinkage cracking of concrete. *Australian Journal of Structural Engineering*, 10(3), pp.207 – 214.

Dao, V.T.N., Dux, P.F. & Morris, P.H., 2011. Plastic shrinkage cracking of concrete - roles of osmotic suction. *Magazine of Concrete Research*, 63(10), pp.743–750.

Domone, P.L.J. & Illston, J.M., 2010. *Construction materials : their nature and behaviour*, London; New York: Spon Press.

European Federation for Precast Concrete, 2005. *European guidelines for self-compacting concrete: specification, production and use* J. Brussels, ed., BIBM.

He, Y. et al., 2015. Adsorption–desorption kinetics of surfactants at liquid surfaces. *Advances in Colloid and Interface Science*, 222, pp.377–384.

Johlin, J.M., 1926. The Ring Method for Surface Tension Measurement. *American Association for the Advancement of Science*, 64(1647), pp.93–94.

Krönlof, A., Leivo, M. & Sipari, P., 1995. Experimental study on the basic phenomena of shrinkage and cracking of fresh mortar. *Cement and Concrete Research*, 25(8), pp.1747–1754.

Kruml, F., 1990. Setting process of concrete. In H.-J. Wierig, ed. *Properties of fresh concrete: Proceedings of the RILEM Colloquim*. Hanover, Germany: Chapman and Hall, pp. 10–16.

Kwak, H. et al., 2010. Experimental and Numerical Quantification of Plastic Settlement in Fresh Cementitious Systems. *Journal of materials in Civil Engineering*, 22, pp.951–966.

Leeman, A., Nygaard, P. & Lura, P., 2014. Impact of admixtures on the plastic shrinkage cracking of self-compacting concrete. *Cement and Concrete Composites*, 46, pp.1–7.

Löfgren, I. & Esping, O., 2014. Early age cracking of self-compacting concrete. In *International RILEM conference on volume changes of hardening concrete: testing and mitigation*. Lyngby, Denmark: Rilem publications, pp. 26–34.

Louw, J.P., 2014. *Influence of admixtures on the early age plastic cracking of concrete*. University of Stellenbosch.

Lura, P. et al., 2007. Influence of shrinkage-reducing admixtures on development of plastic shrinkage cracks. *ACI Materials Journal*, 104, pp.187–194.

Mehta, P.K. & Monteiro, P.J.M., 2006. *Concrete: microstructure, properties, and materials* 3rd ed. McGraw-Hill, ed., New York, USA.

Owens, G. ed., 2009. *Fulton's concrete technology.* Ninth ed., Midrand, South Africa: Cement & Concrete Institute.

Passuello, A., Moriconi, G. & Shah, S.P., 2009. Cracking behavior of concrete with shrinkage reducing admixtures and PVA fibers. *Cement and Concrete Composites*, 31, pp.699–704.

Powers, T.C., 1968. *The properties of fresh concrete*, New York, USA: John Wiley & Sons, Inc.

Qi, C., Weiss, J. & Olek, J., 2003. Characterization of plastic shrinkage cracking in fiber reinforced concrete using image analysis and a modified Weibull function. *Materials and Structures*, 36(6), pp.386–395.

Rajabipour, F., Sant, G. & Weiss, J., 2008. Interactions between shrinkage reducing admixtures (SRA) and cement paste's pore solution. *Cement and Concrete Research*, 38(5), pp.606–615.

Rasband, W.S., 2012. ImageJ. Available at: imagej.nih.gov/ij/.

SANS 201, 2008. *Sieve analysis, fines content and dust content of aggregates*, Pretoria, South Africa: South African Bureau of Standards.

SANS 50196-3, 2006. *Methods of testing cement. Part 3: Determination of setting times and soundness*, Pretoria, South Africa: South African Bureau of Standards.

SANS 50197-1, 2013. *Cement - Part 1: Composition , specifications and conformity criteria for common cements*, Pretoria, South Africa: South African Bureau of Standards.

SANS 5862-1, 2006. *Concrete tests Part 1: Consistence of freshly mixed concrete - Slump test*, Pretoria, South Africa: South African Bureau of Standards.

SANS 5863, 2006. *Concrete tests - Compressive strength of hardened concrete*, Pretoria, South Africa: South African Bureau of Standards.

Slowik, V., Schmidt, M. & Fritzsch, R., 2008. Capillary pressure in fresh cement-based materials and identification of the air entry value. *Cement and Concrete Composites*, 30(7), pp.557–565.

Suprenant, B.A., 1988. *Concrete vibration*. Tampa, Florida: University of South Florida.

Uno, P.J., 1998. Plastic Shrinkage Cracking and Evaporation Formulas. *ACI Materials Journal*, 95(4), pp.365 – 375.

Valsson, S. & Bharat, A., 2011. Impact of Air Temperature on Relative Humidity. *Architecture - Time Space & People*, (February), pp.38–41.

Appendices

List of Appendices

APPENDIX A:

Conventional concrete results

A.1. Crack area

The crack area results of the respective conventional concrete mixes are provided in this section. Four samples of each mix were tested simultaneously. Crack area measurements were conducted at 20 minute intervals. Average crack areas of the respective mixes are provided accordingly.

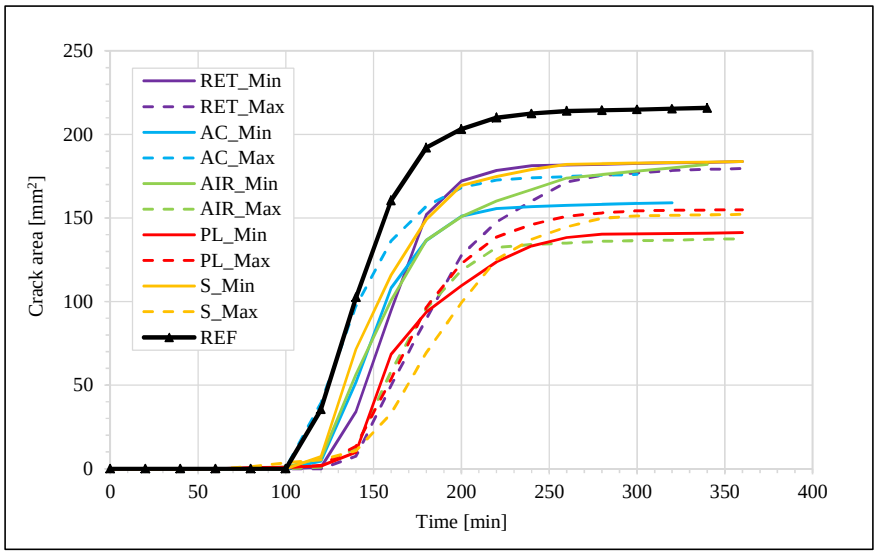

Figure 0.1 Crack area comparison of conventional concrete mixes

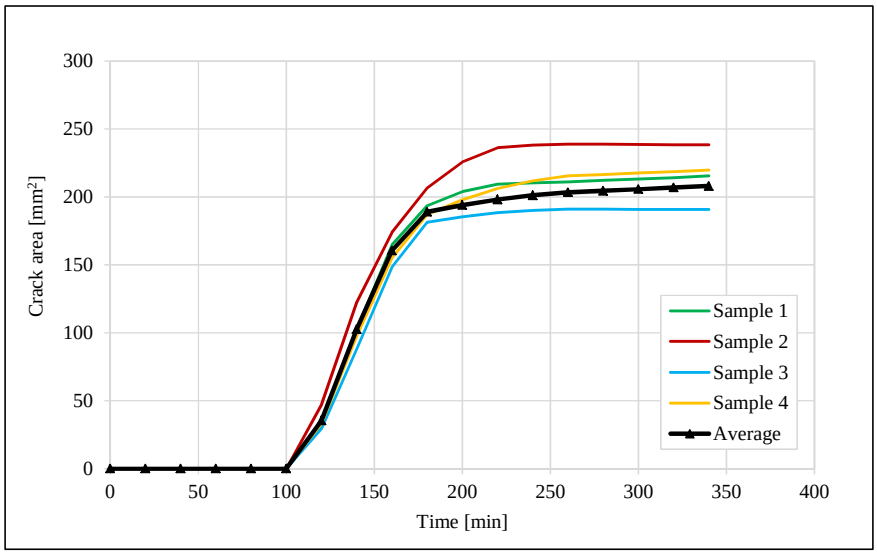

Figure 0.2 Conventional concrete REF crack area results

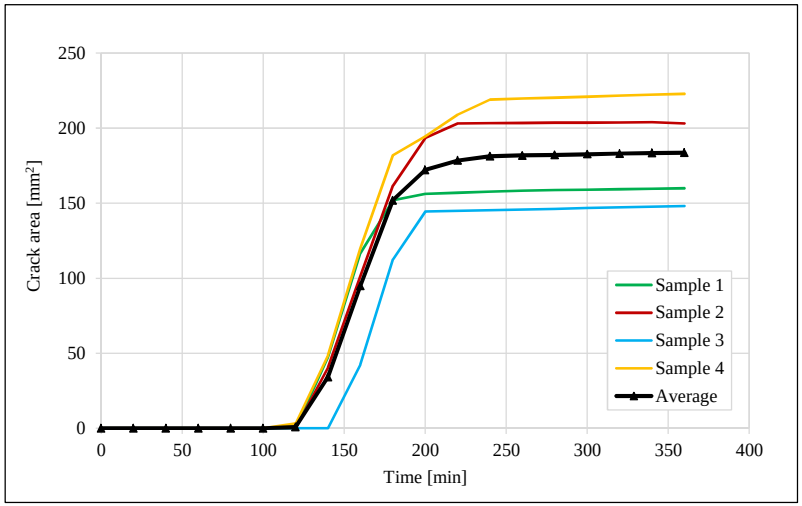

Figure 0.3 RET_Min crack area results

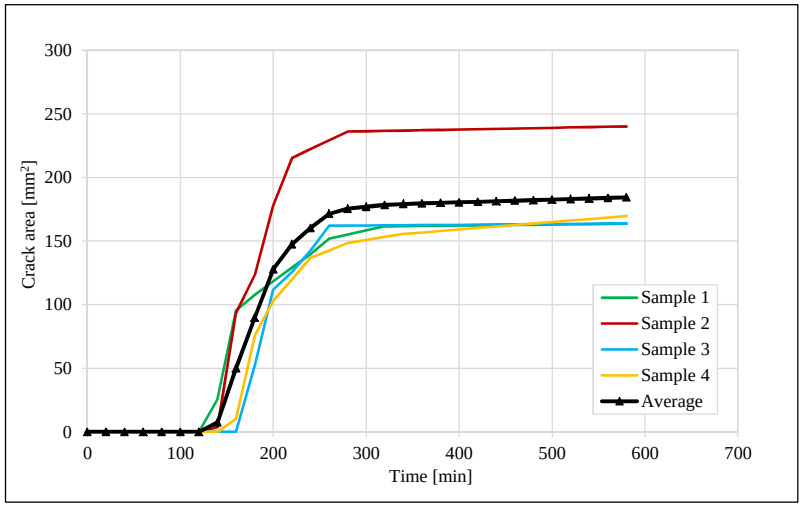

Figure 0.4 RET_Max crack area results

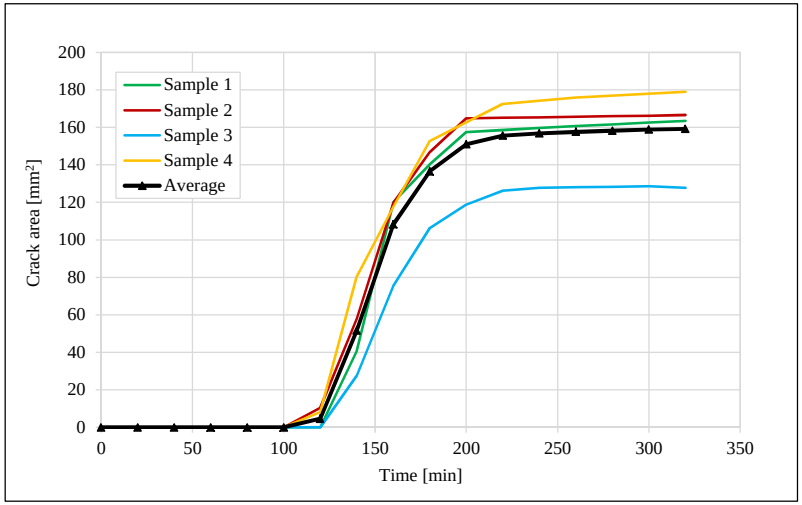

Figure 0.5 AC_Min crack area results

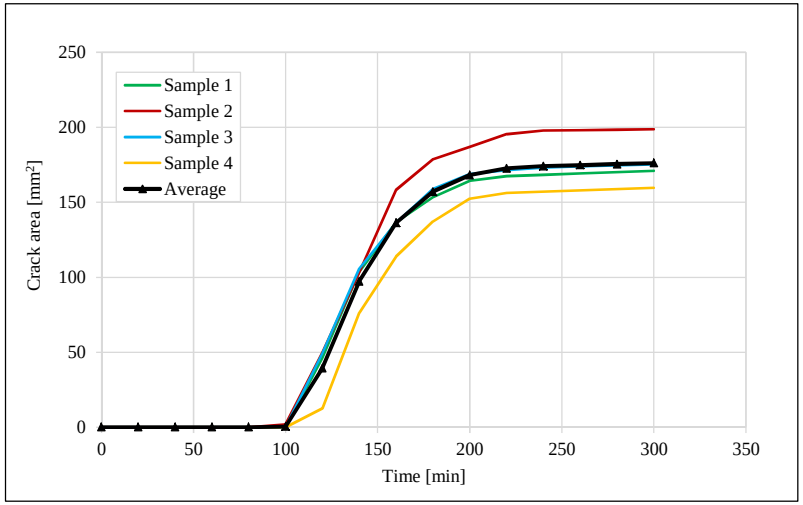

Figure 0.6 AC_Max crack area results

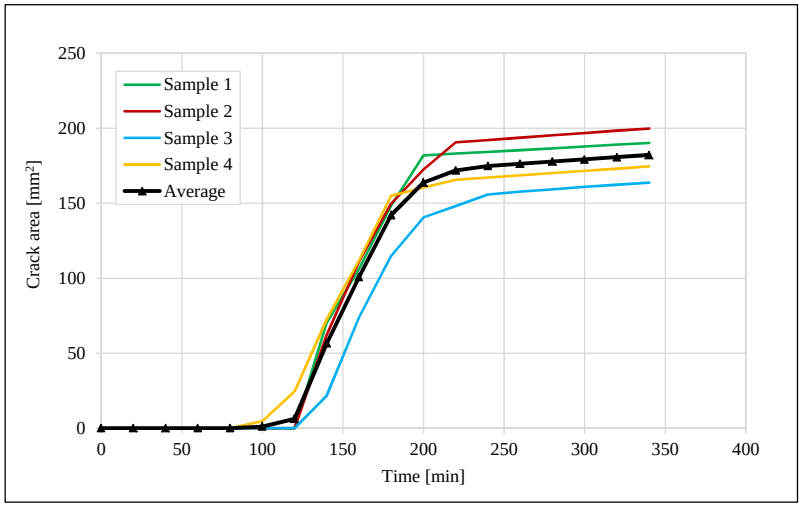

Figure 0.7 AIR_Min crack area results

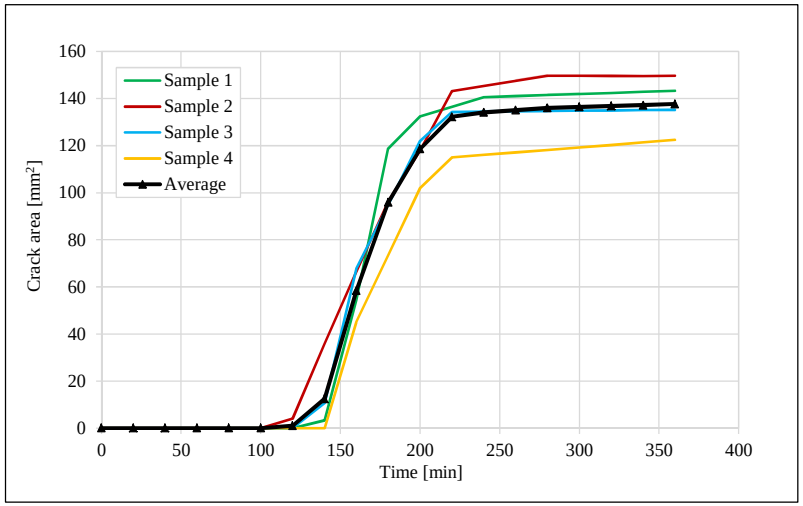

Figure 0.8 AIR_Max crack area results

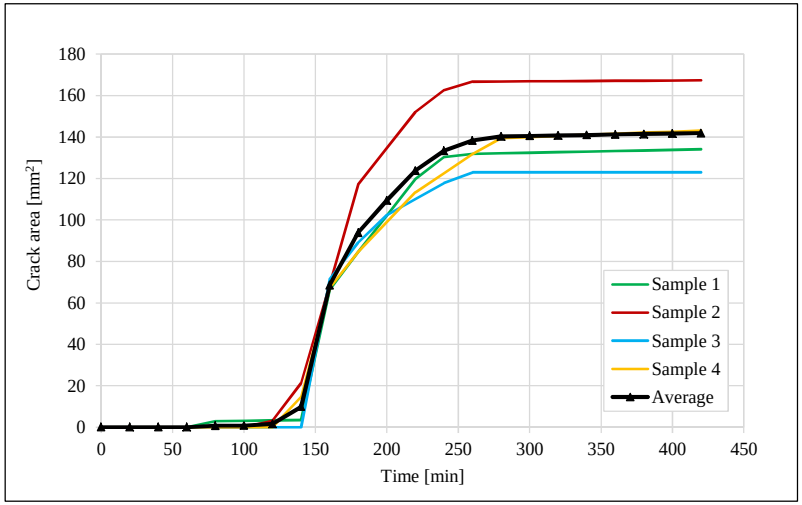

Figure 0.9 PL_Min crack area results

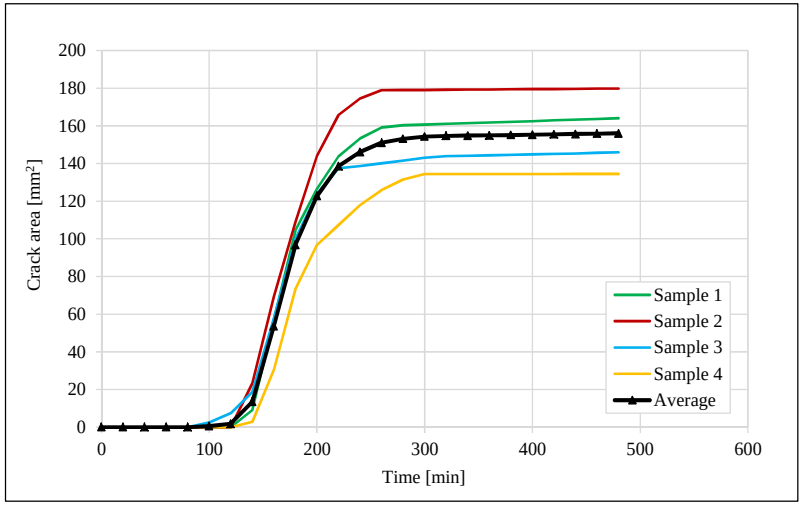

Figure 0.10 PL_Max crack area results

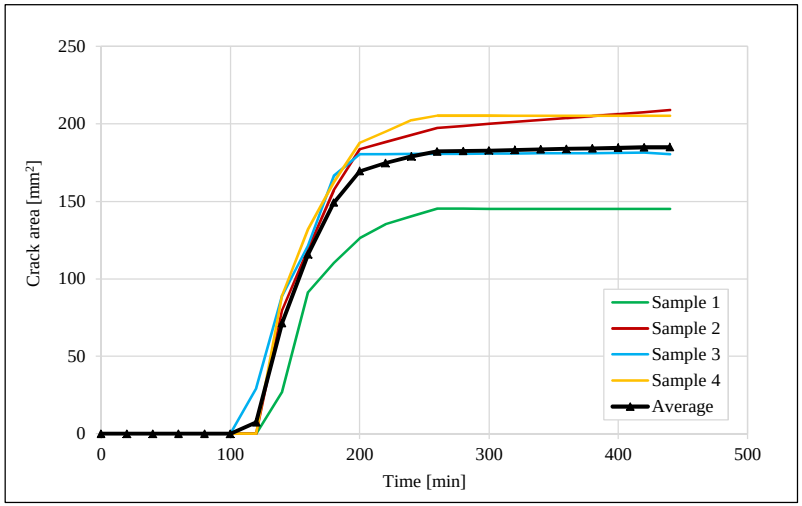

Figure 0.11 S_Min crack area results

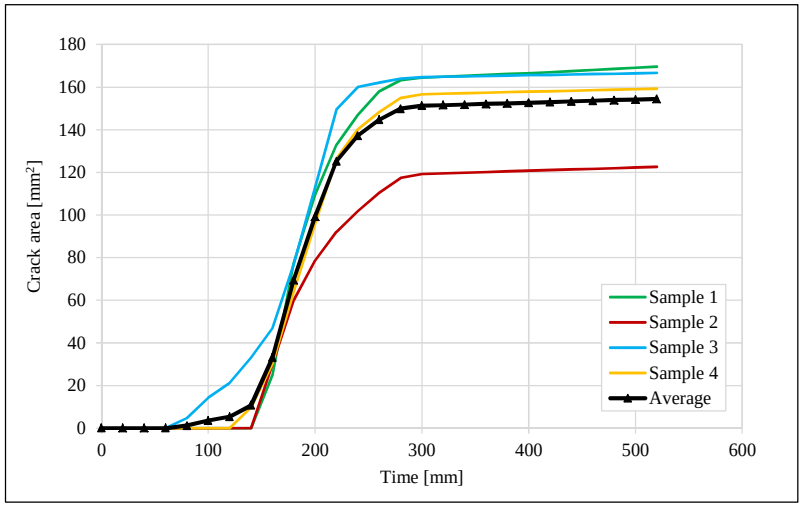

Figure 0.12 S_Max crack area results

A.2. Rapid crack growth

The calculated rapid crack growth period of the respective conventional concrete mixes are provided in this section. The rate of crack growth is calculated as average growth during the 20 minute measurement intervals. Crack onset is defined as the first crack area measurement of which the measured crack area is greater than zero whereas crack stabilisation is defined as the time when the rate of crack growth became insignificant.

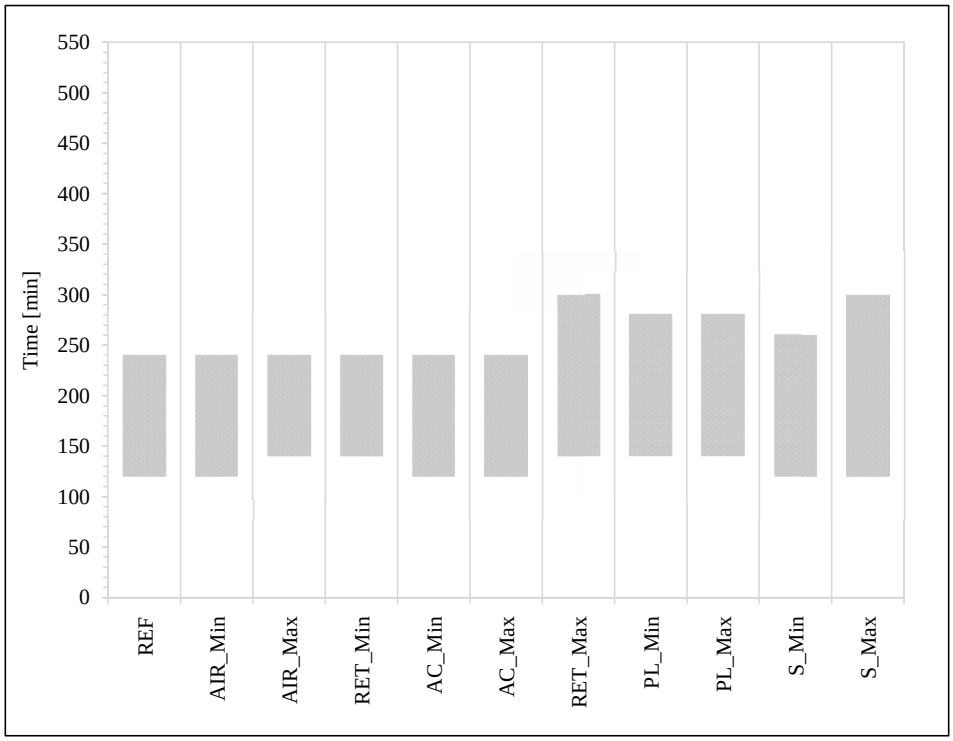

Figure 0.13 Rapid crack growth comparison

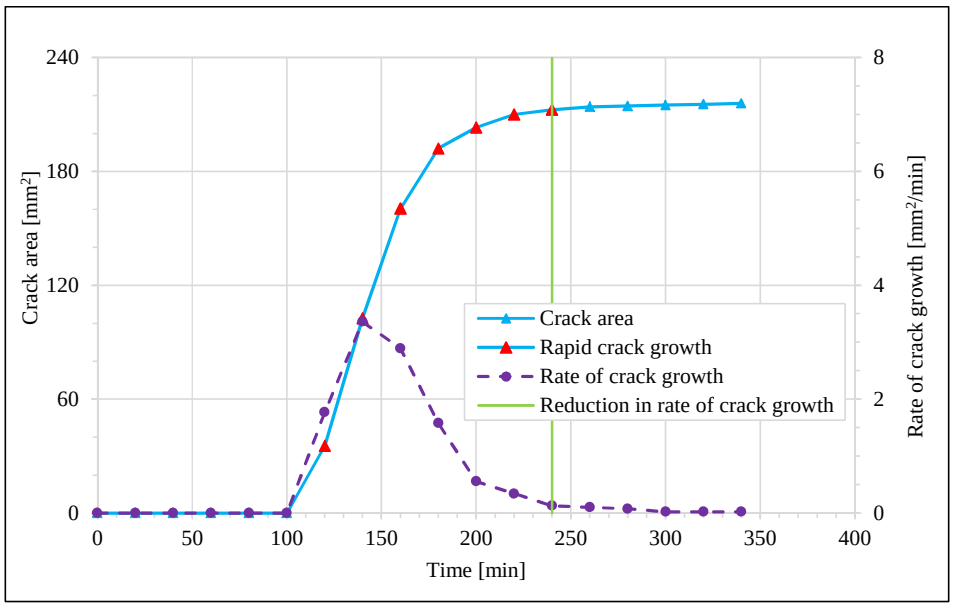

Figure 0.14 Rapid crack growth of REF

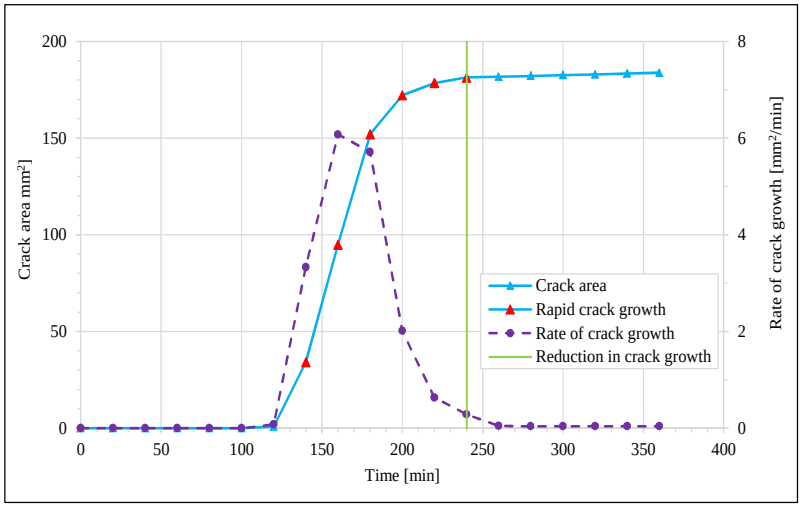

Figure 0.15 RET_Min rapid crack growth

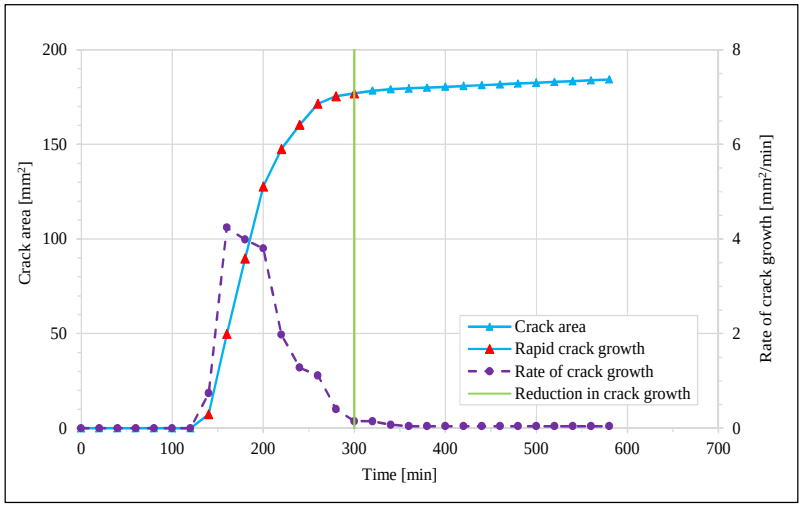

Figure 0.16 RET_Max rapid crack growth

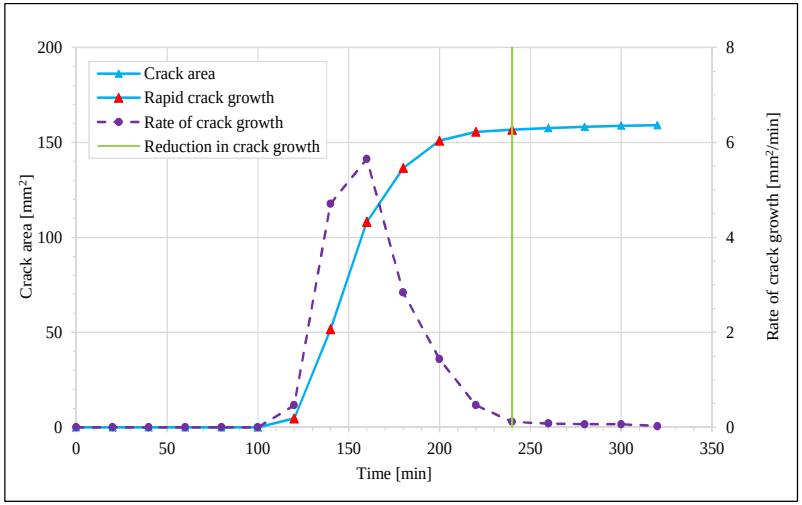

Figure 0.17 AC_Min rapid crack growth

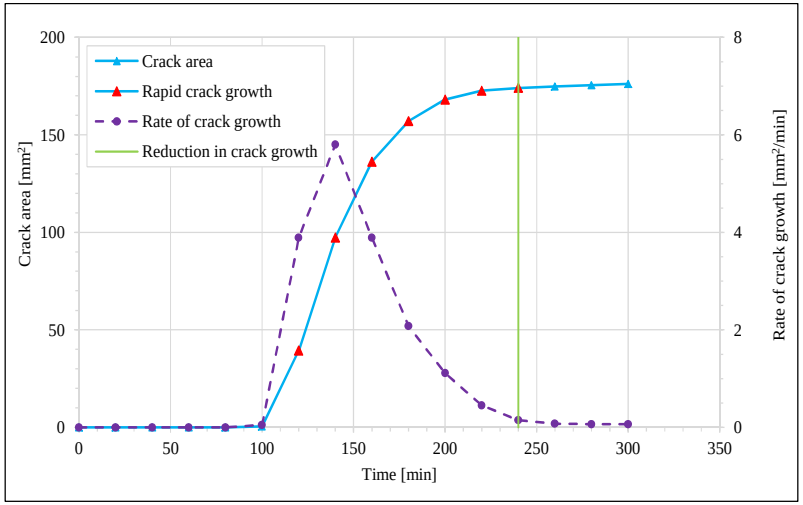

Figure 0.18 AC_Max rapid crack growth

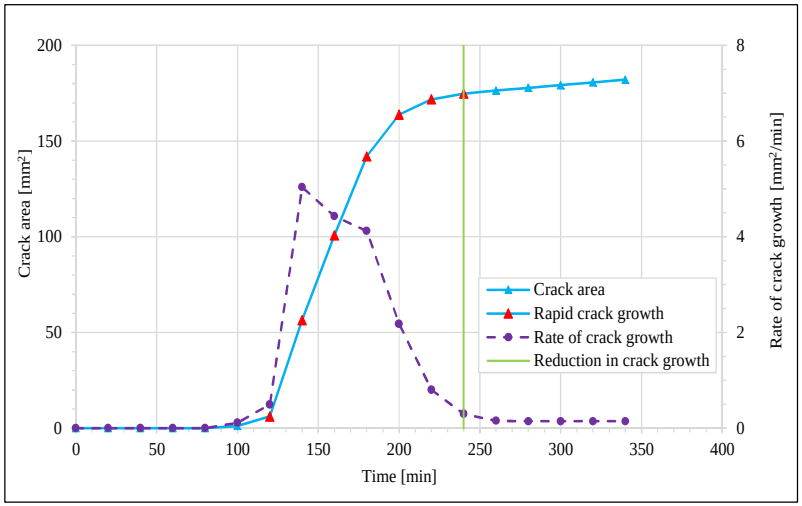

Figure 0.19 AIR_Min rapid crack growth

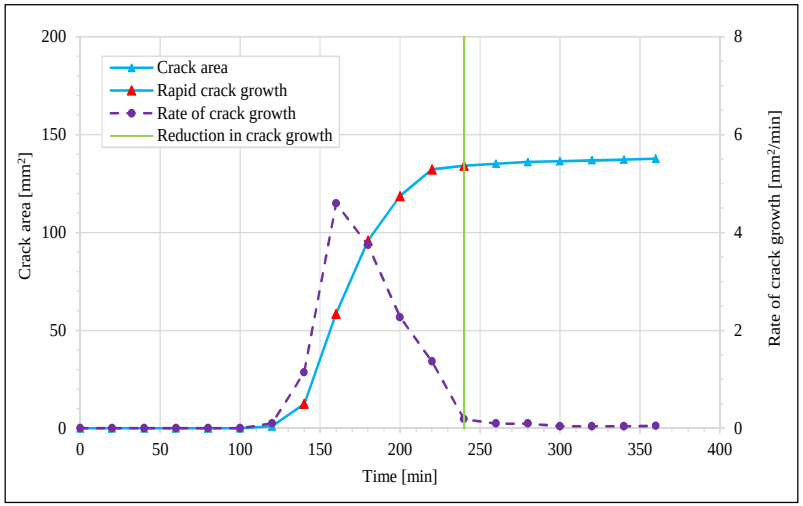

Figure 0.20 AIR_Max rapid crack growth

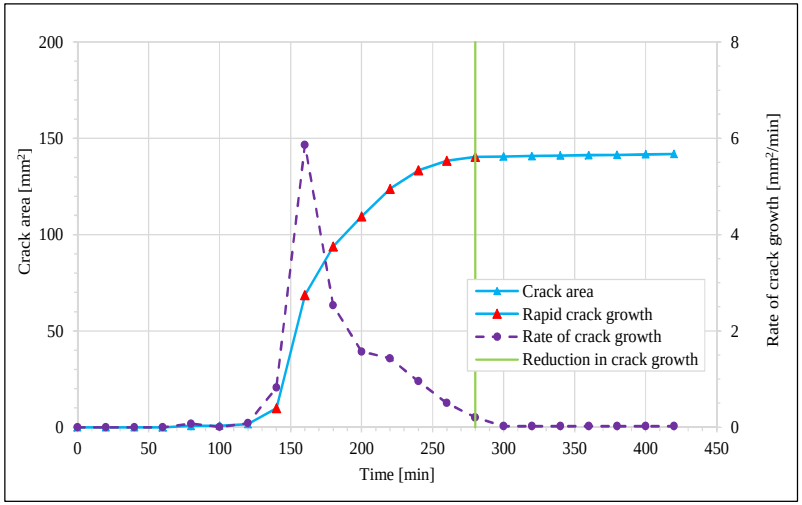

Figure 0.21 PL_Min rapid crack growth

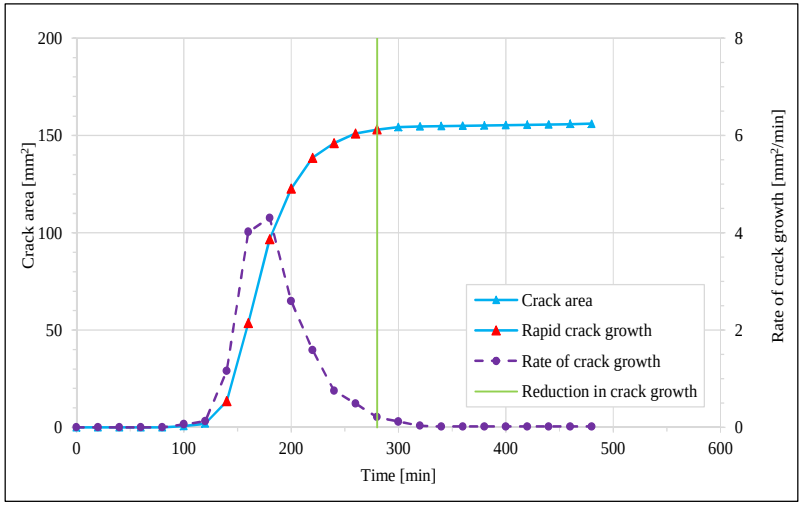

Figure 0.22 PL_Max rapid crack growth

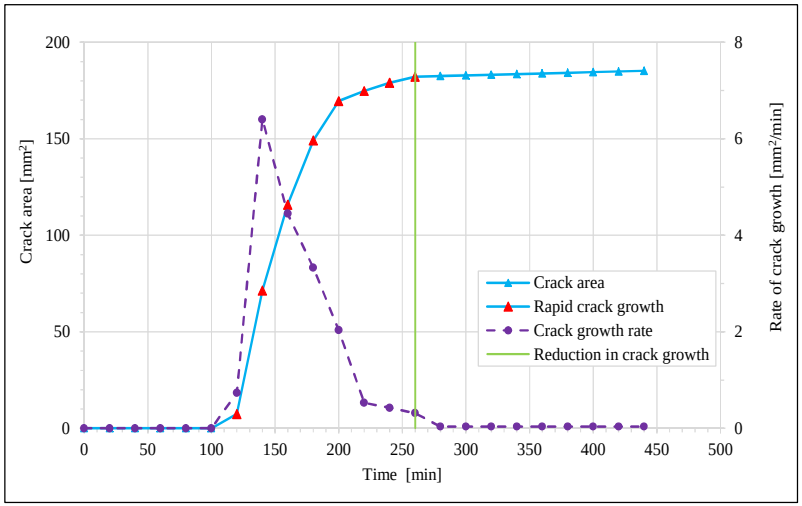

Figure 0.23 S_Min rapid crack growth

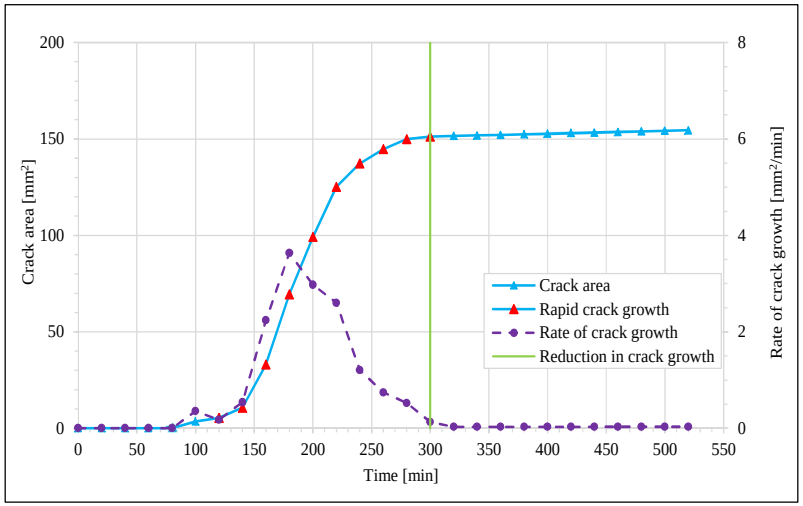

Figure 0.24 S_Max rapid crack growth

A.3. Setting time

The initial and final setting times of the respective conventional concrete mixes are provided in this section. Three samples of each mix were tested simultaneously and calculated averages are provided accordingly.

Table 0.1 Initial and final setting time results

Mix	Initial setting time [min]	Final setting time [min]
REF	160	210
RET_Min	170	225
RET_Max	330	525
AC_Min	110	195
AC_Max	105	150
AIR_Min	150	210
AIR_Max	165	210
PL_Min	230	270
PL_Max	350	435
S_Min	230	315
S_Max	305	410

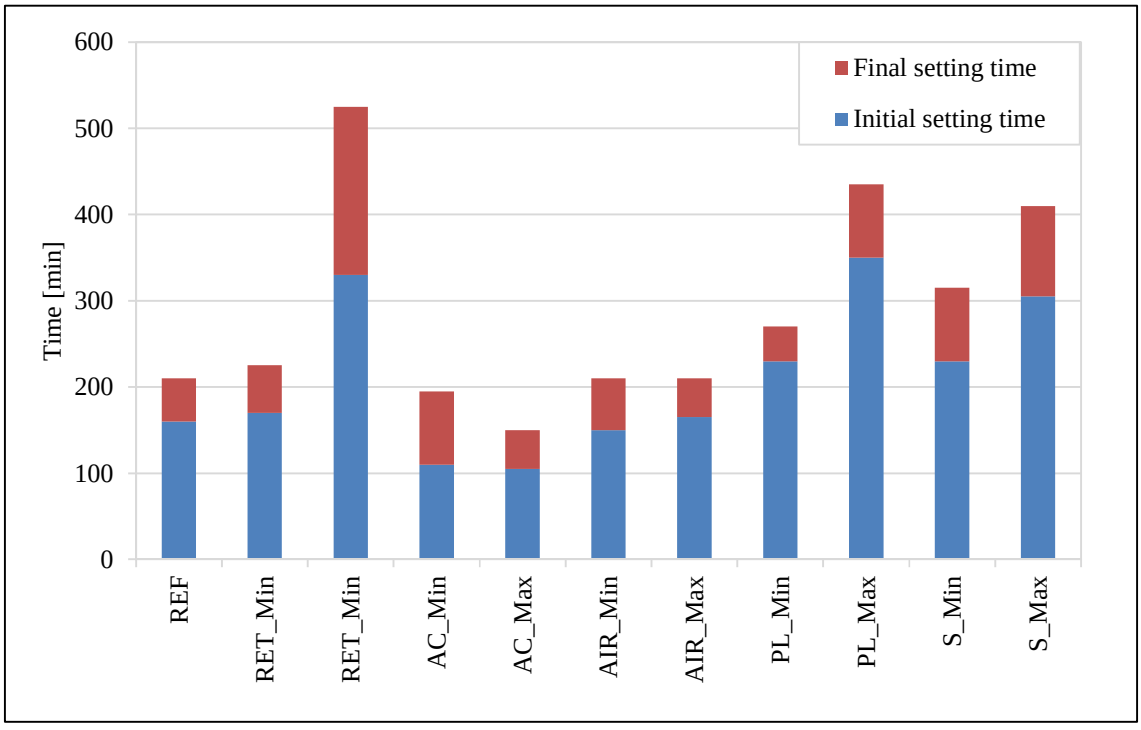

Figure 0.25 Setting time results of conventional concrete mixes

A.4. Bleeding

The bleeding results of the respective conventional concrete mixes are provided in this section. Four samples of each mix were tested simultaneously and calculated averages are provided accordingly. Accumulated bleed water was extracted at 20 minute intervals during the first 40 minutes after casting and 30 minute intervals thereafter until bleeding ceased. Measurement markers are only displayed once to avoid overly congested results.

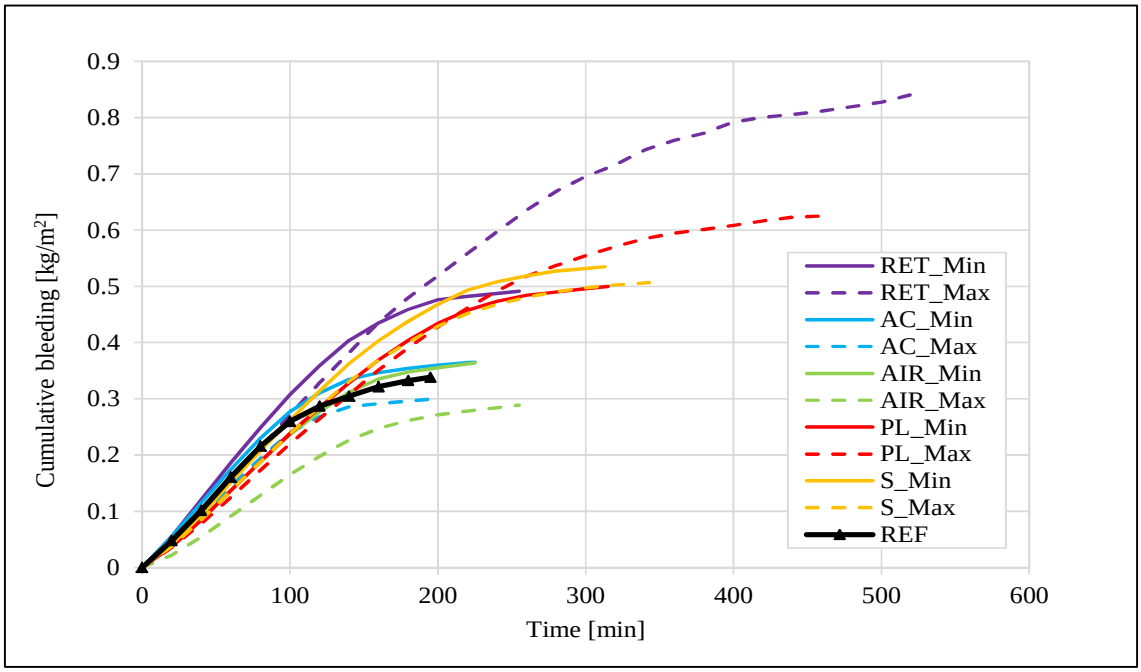

Figure 0.26 Bleeding comparison of conventional concrete mixes

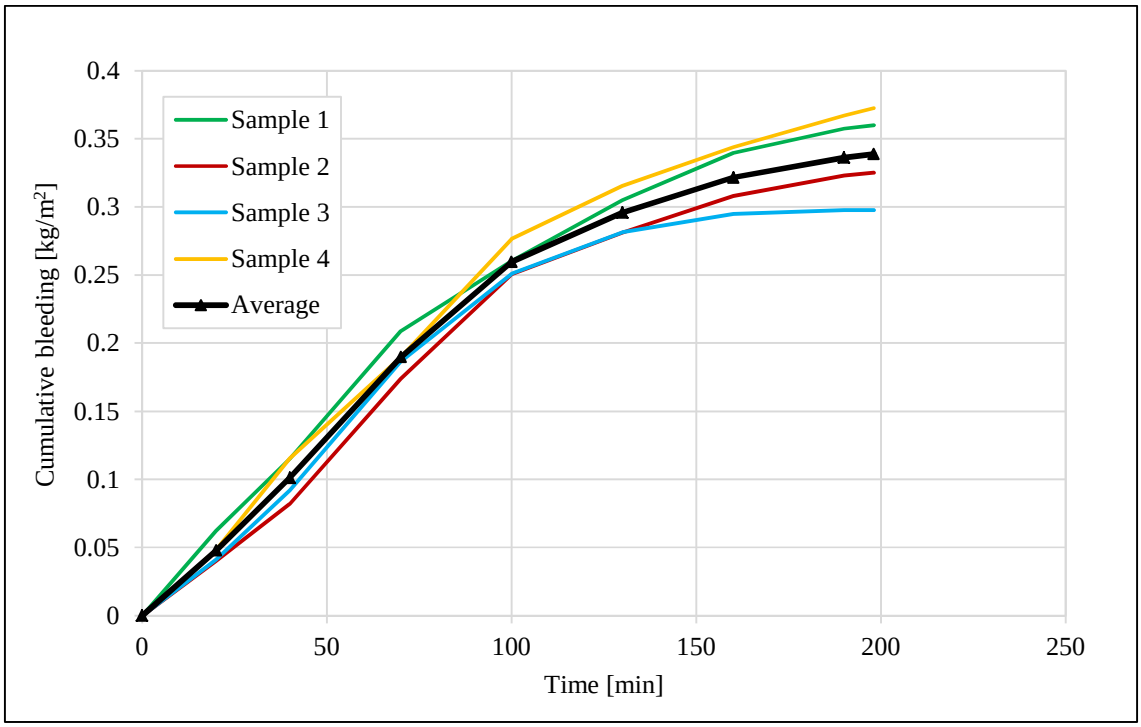

Figure 0.27 Conventional concrete REF bleeding results

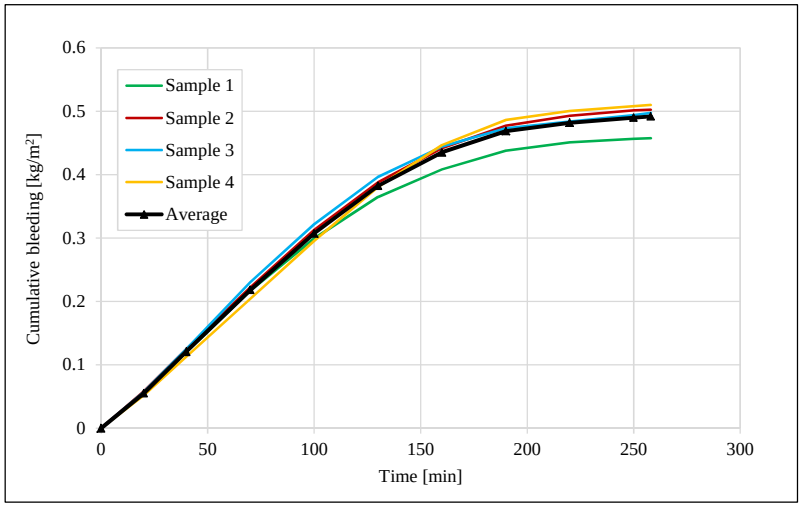

Figure 0.28 RET_Min bleeding results

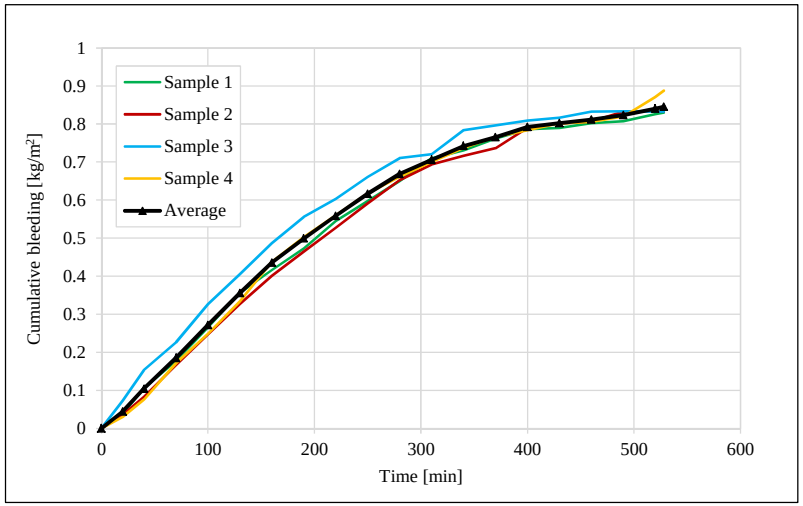

Figure 0.29 RET_Max bleeding results

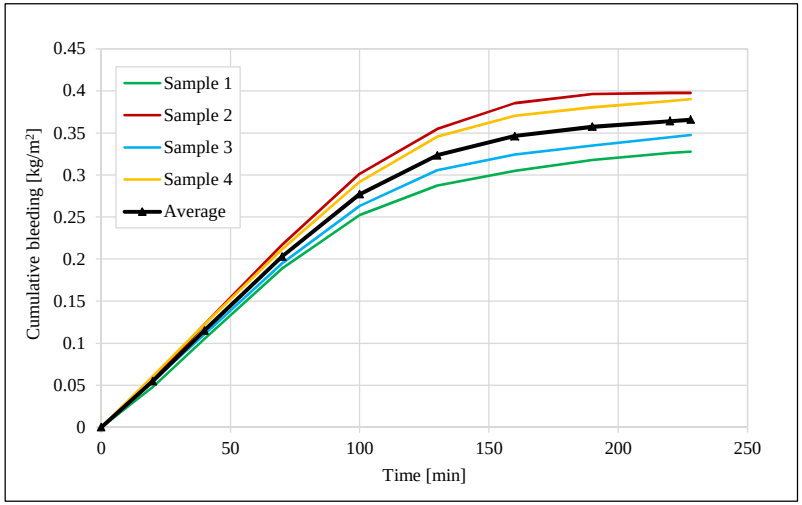

Figure 0.30 AC_Min bleeding results

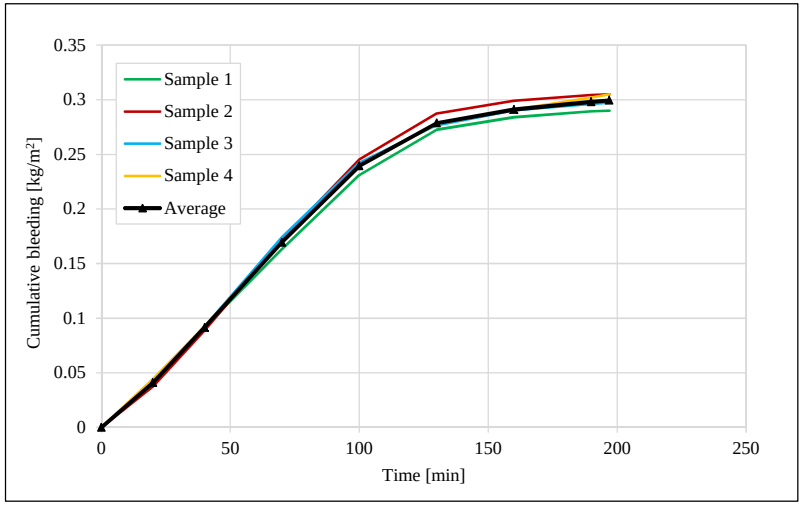

Figure 0.31 AC_Max bleeding results

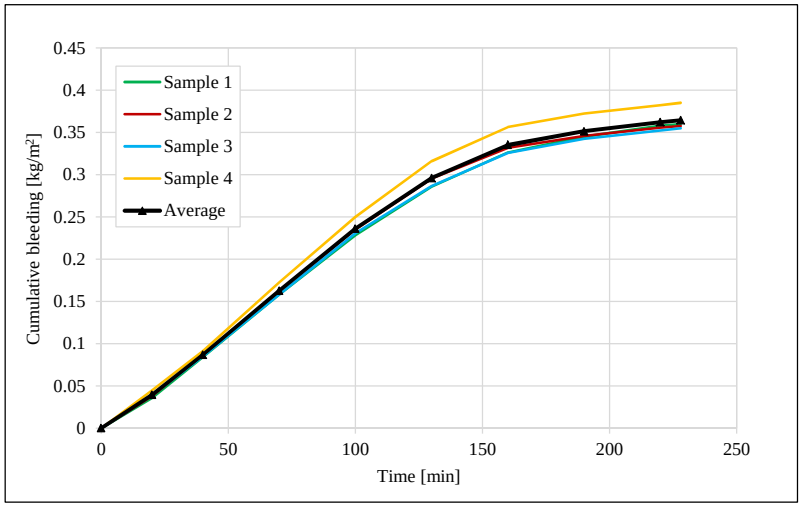

Figure 0.32 AIR_Min bleeding results

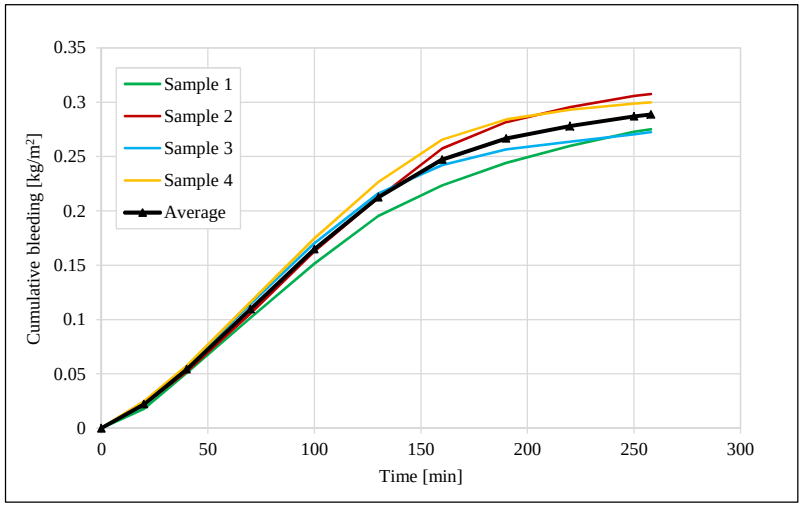

Figure 0.33 AIR_Max bleeding results

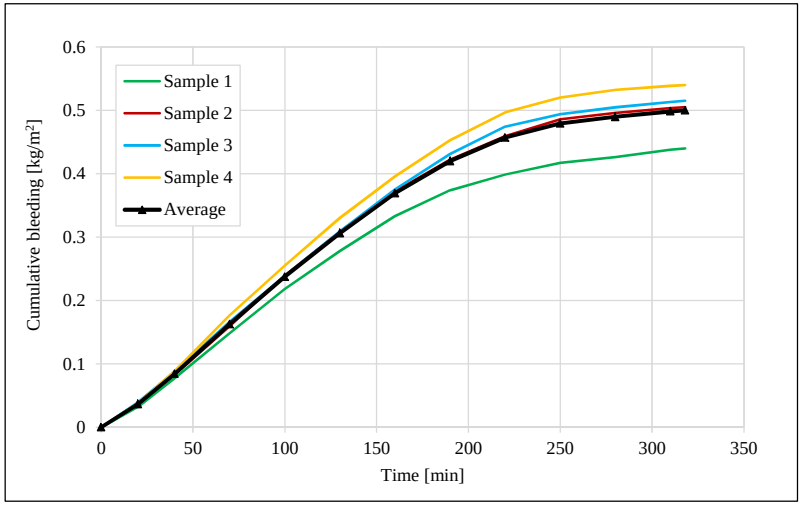

Figure 0.34 PL_Min bleeding results

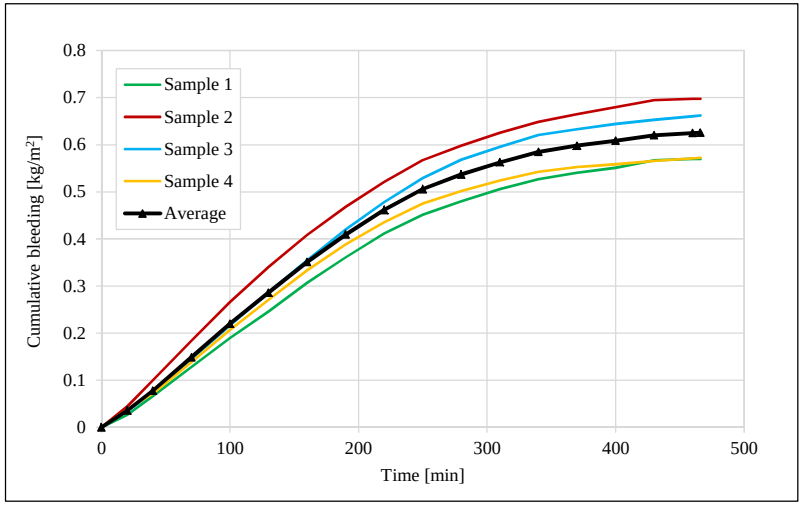

Figure 0.35 PL_Max bleeding results

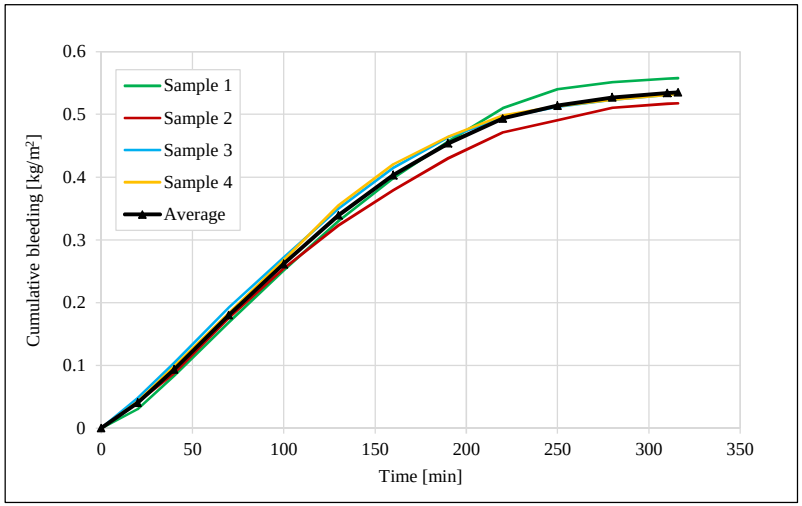

Figure 0.36 S_Min bleeding results

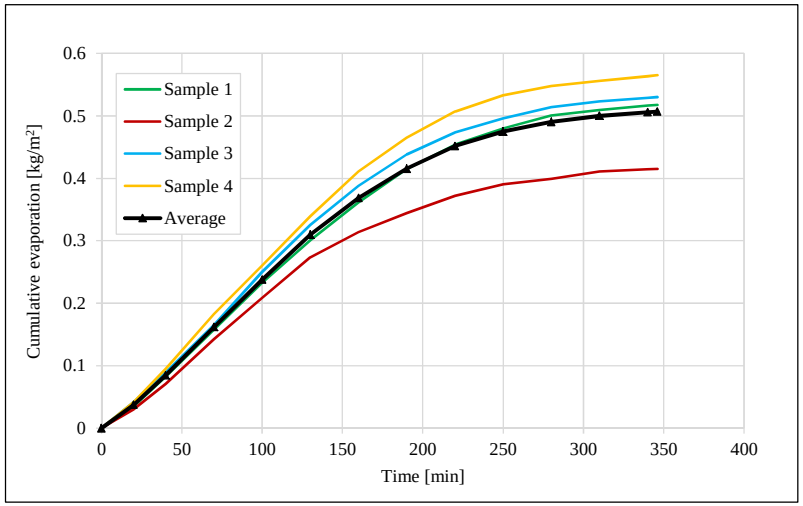

Figure 0.37 S_Max bleeding results

A.5. Evaporation

The evaporation results of the respective conventional concrete mixes are provided in this section. Four samples of each mix were tested and calculated averages are provided accordingly. Evaporation readings were conducted at 20 minute intervals during the first 40 minutes after casting and 30 minute intervals thereafter. Measurement markers are only displayed once to avoid overly congested results.

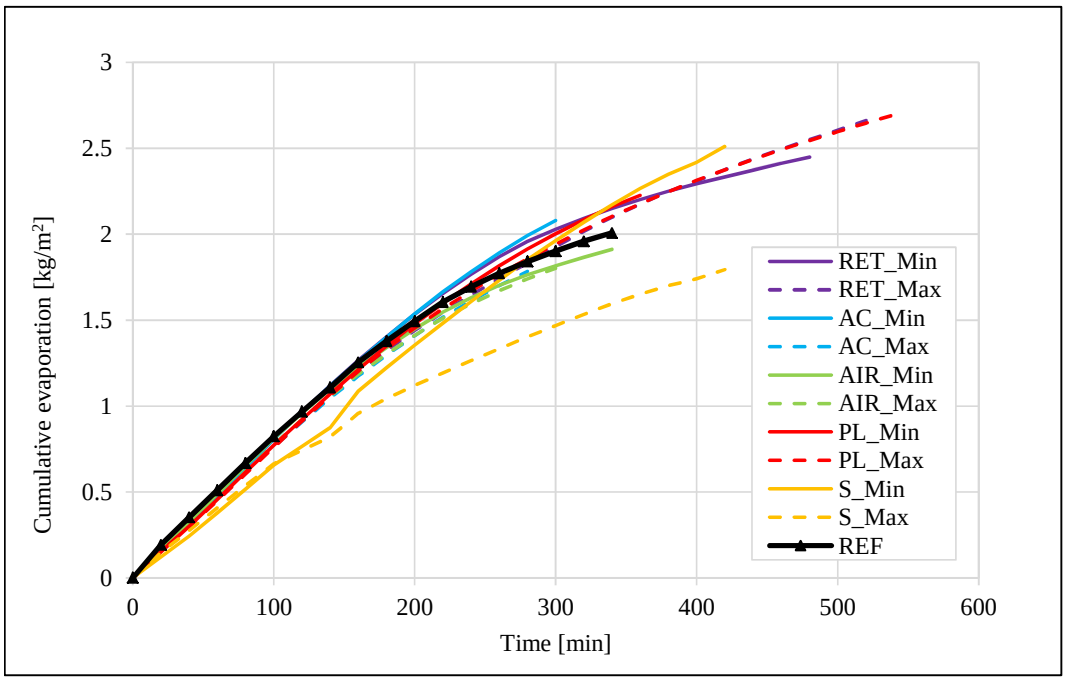

Figure 0.38 Evaporation comparison of conventional concrete mixes

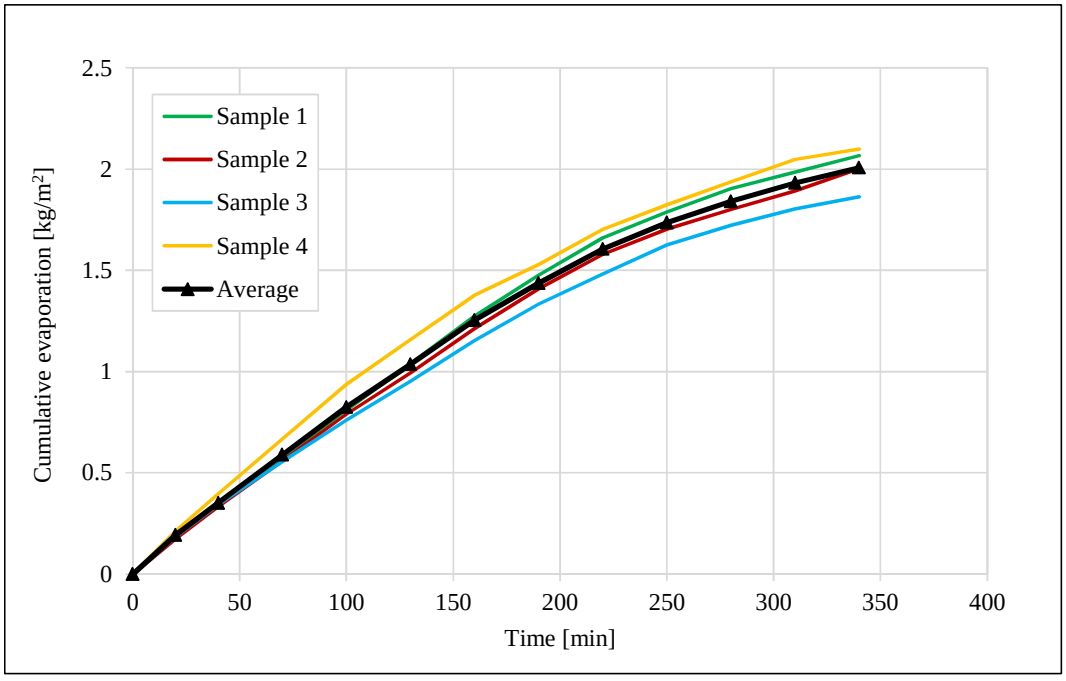

Figure 0.39 Conventional concrete REF evaporation results

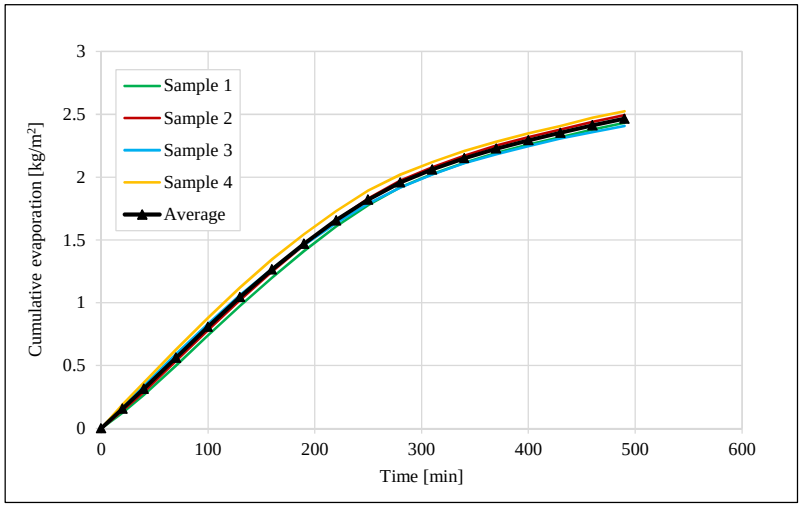

Figure 0.40 RET_Min evaporation results

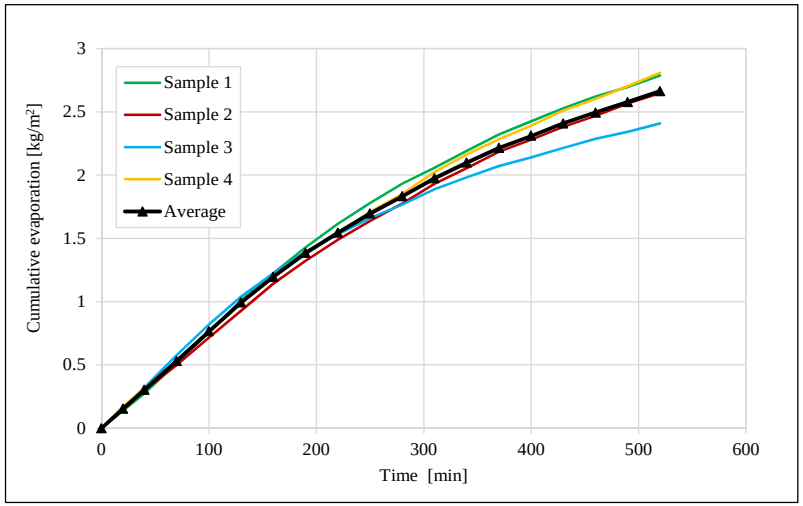

Figure 0.41 RET_Max evaporation results

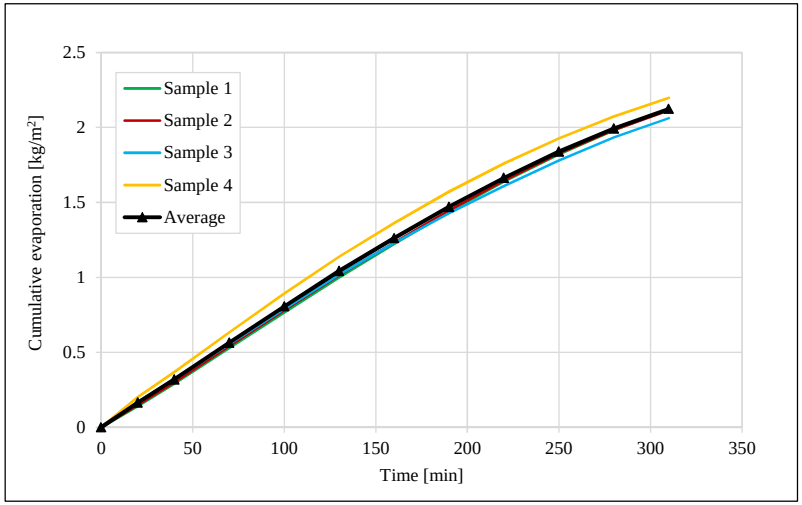

Figure 0.42 AC_Min evaporation results

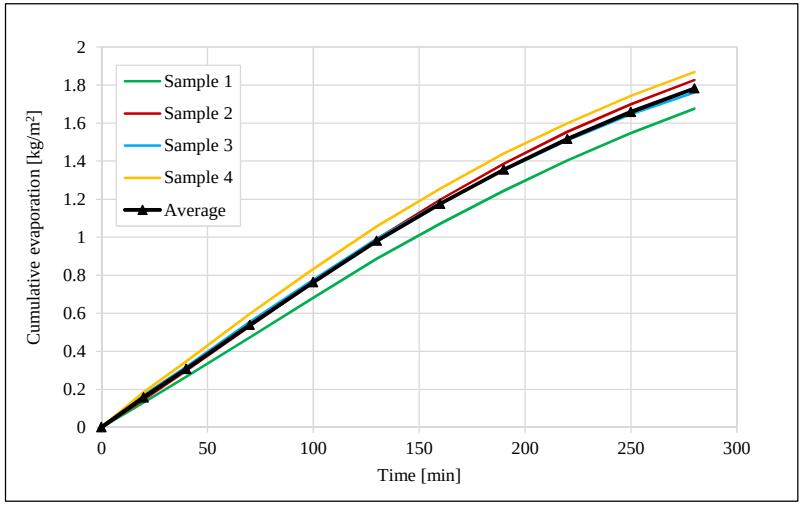

Figure 0.43 AC_Max evaporation results

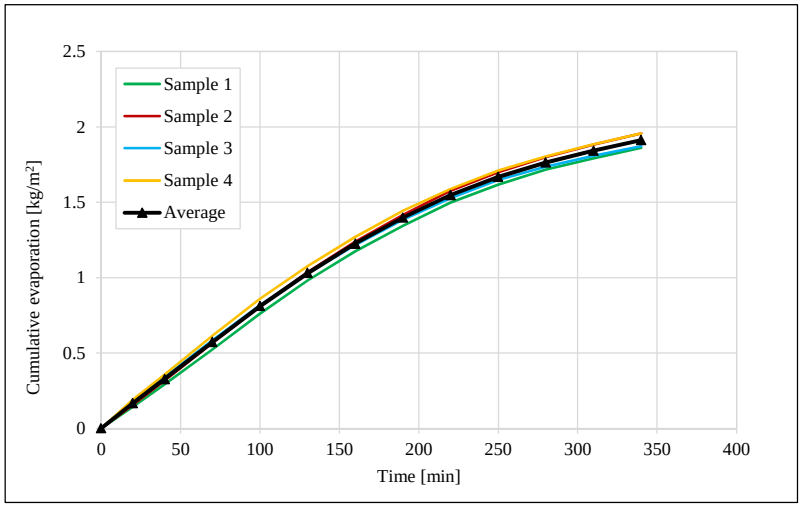

Figure 0.44 AIR_Min evaporation results

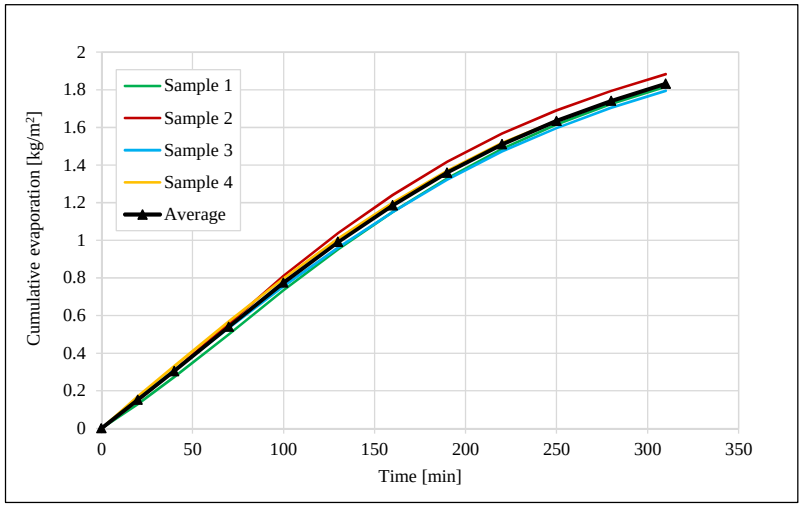

Figure 0.45 AIR_Max evaporation results

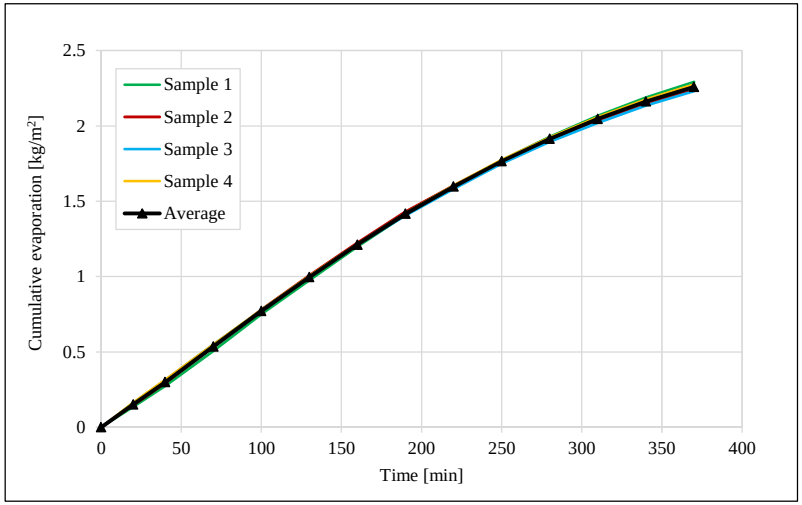

Figure 0.46 PL_Min evaporation results

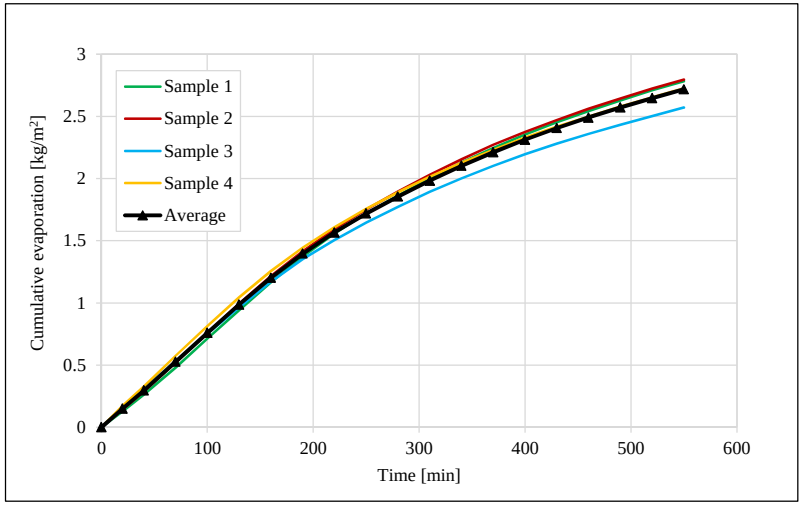

Figure 0.47 PL_Max evaporation results

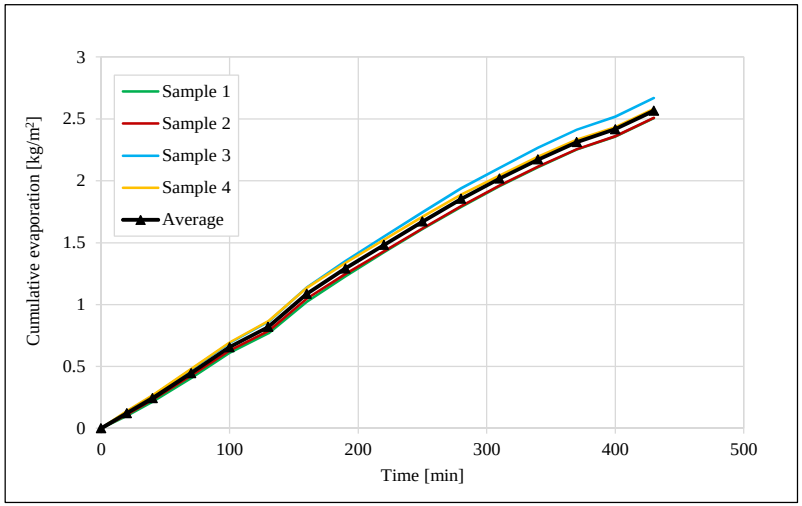

Figure 0.48 S_Min evaporation results

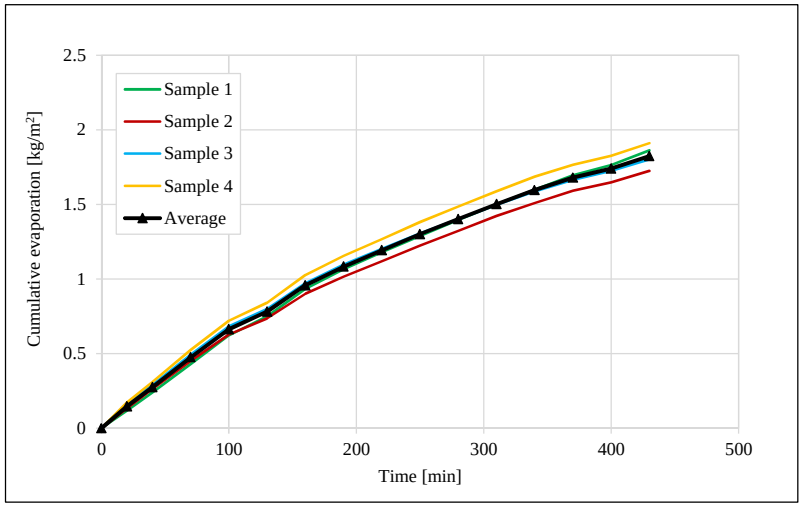

Figure 0.49 S_Max evaporation results

A.6. Capillary pressure

The capillary pressure results of the respective conventional concrete mixes are provided in this section. Capillary pressure tests were fully automated and subsequent readings were taken every second. Due to the fact that air entry is considered to be arbitrary for different samples, only two samples of each mix were tested. Calculated results of the representative capillary pressure build-up are provided accordingly.

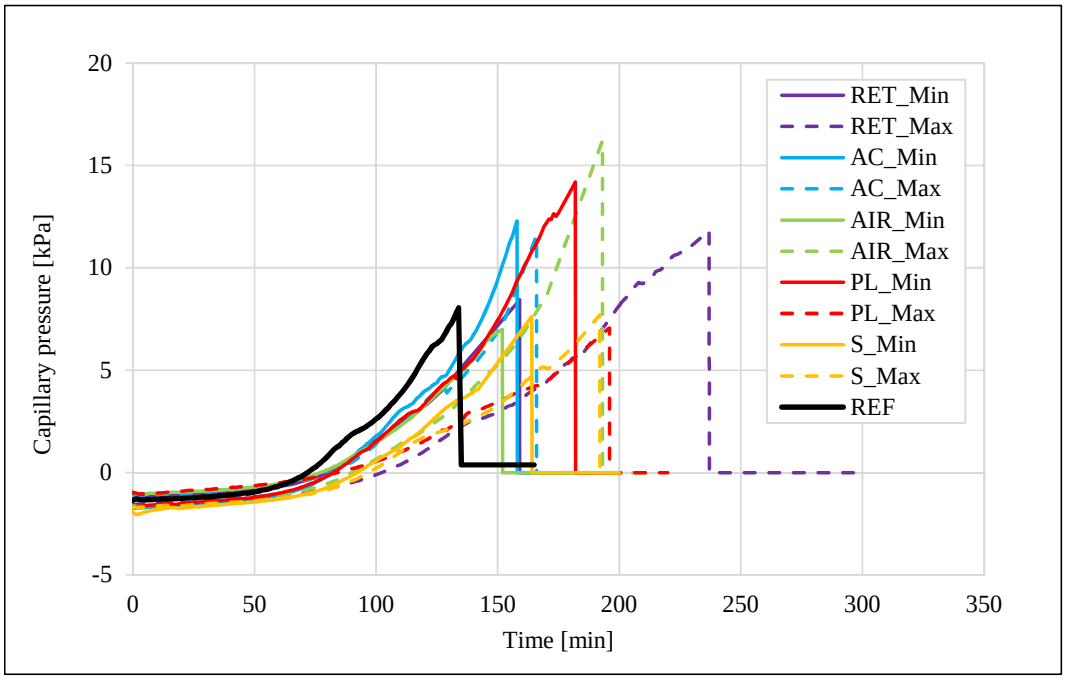

Figure 0.50 Capillary pressure comparison of conventional concrete mixes

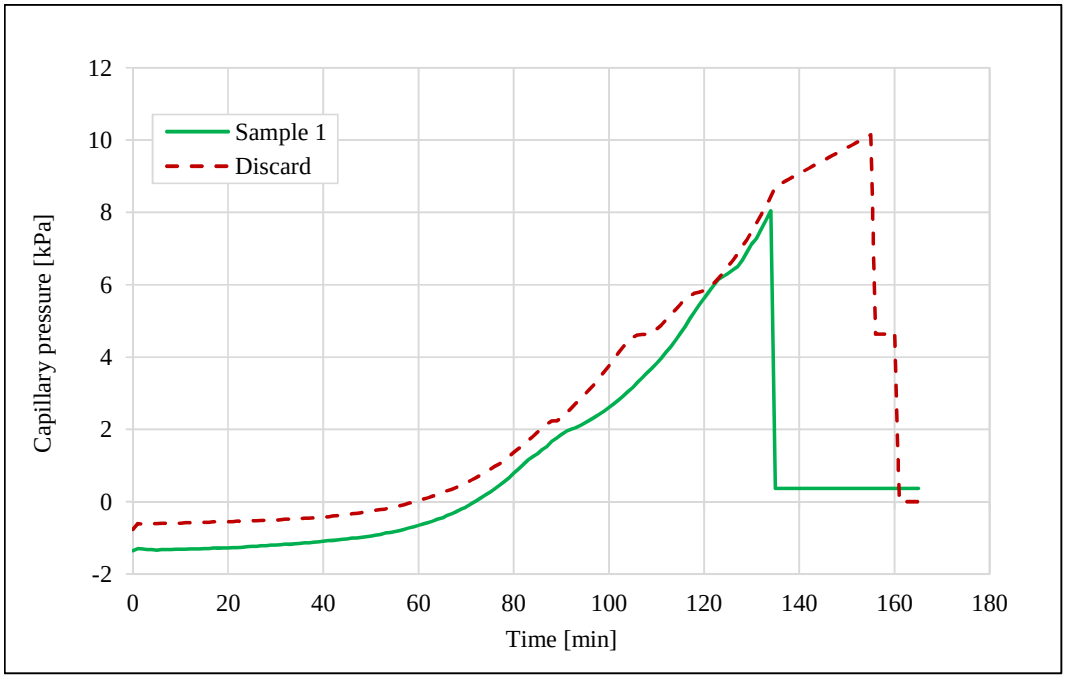

Figure 0.51 Conventional concrete REF capillary pressure results

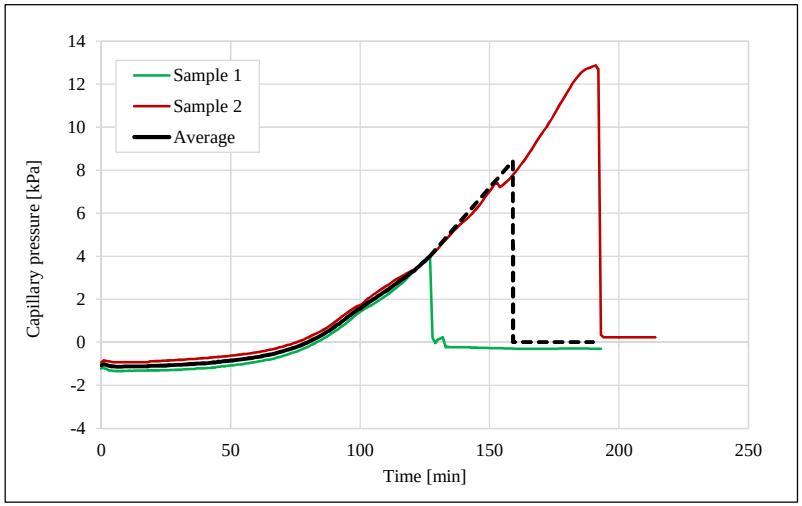

Figure 0.52 RET_Min capillary pressure results

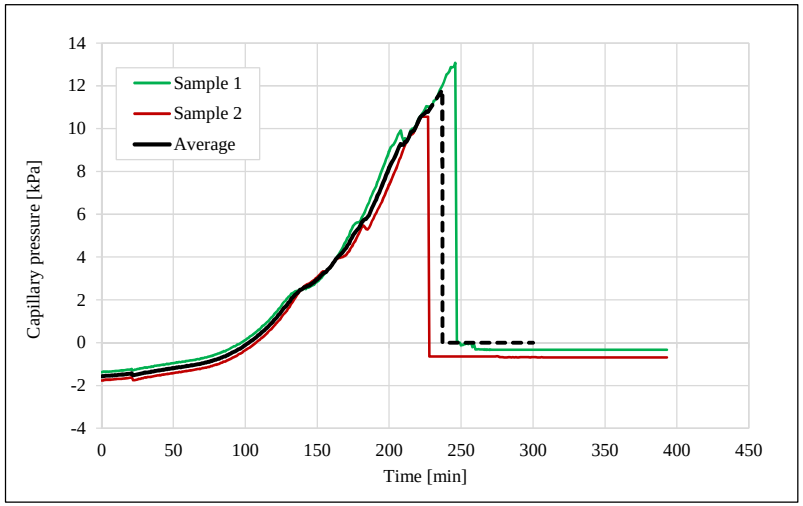

Figure 0.53 RET_Max capillary pressure results

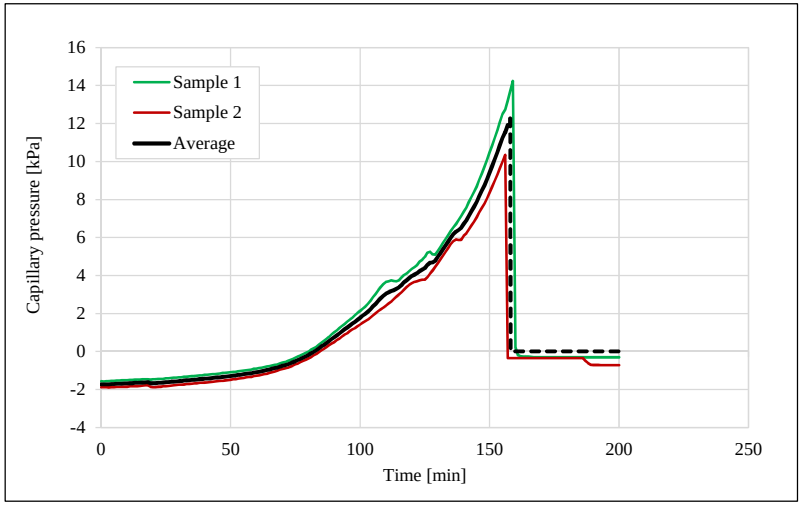

Figure 0.54 AC_Min capillary pressure results

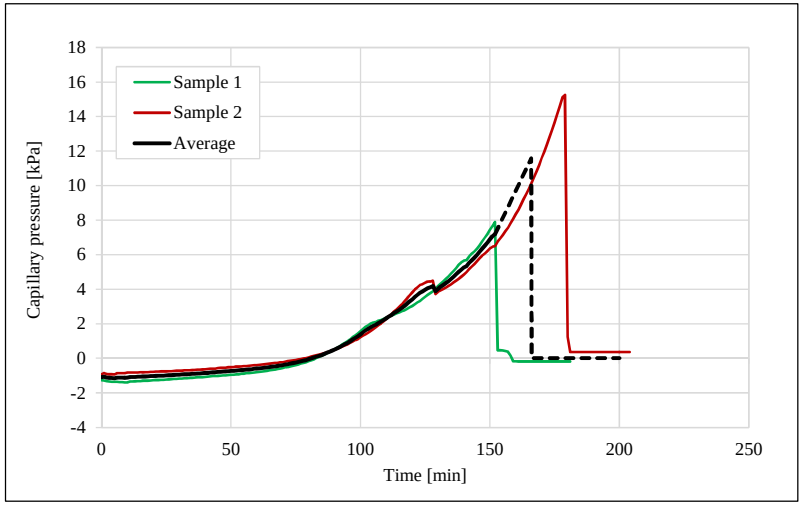

Figure 0.55 AC_Max capillary pressure results

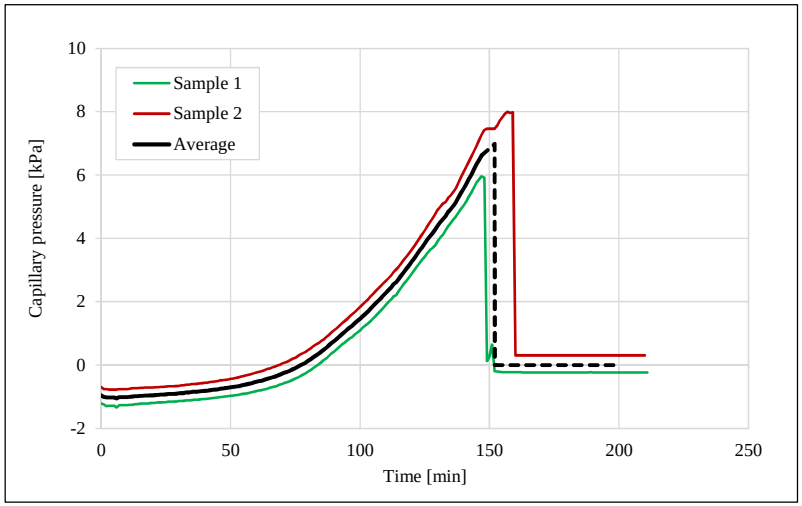

Figure 0.56 AIR_Min capillary pressure results

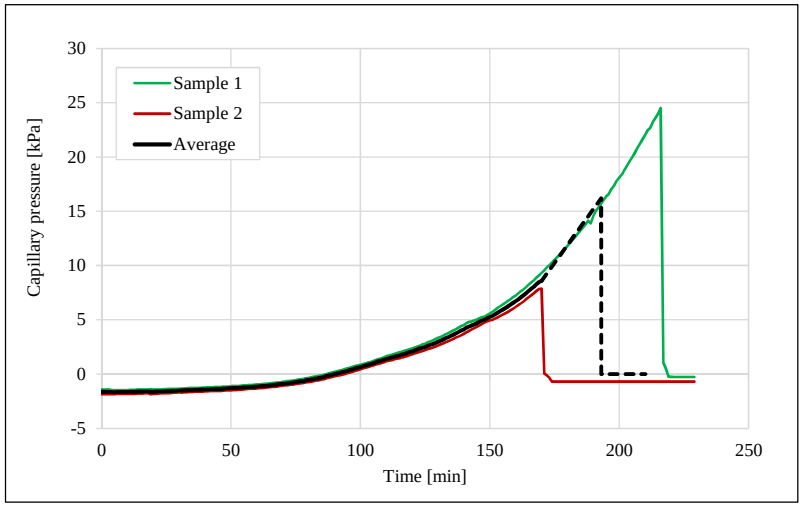

Figure 0.57 AIR_Max capillary pressure results

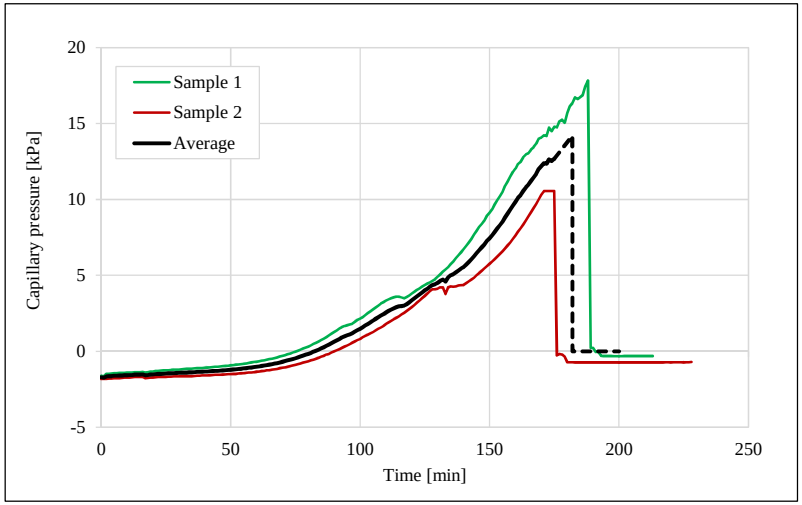

Figure 0.58 PL_Min capillary pressure results

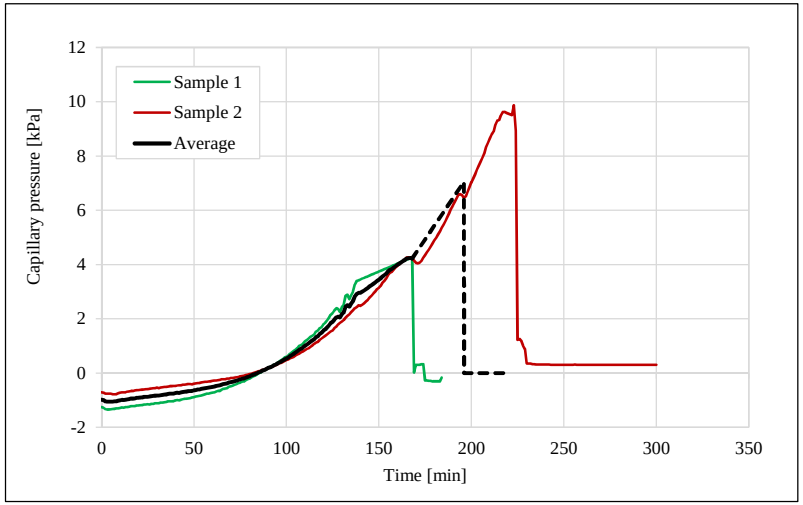

Figure 0.59 PL_Max capillary pressure results

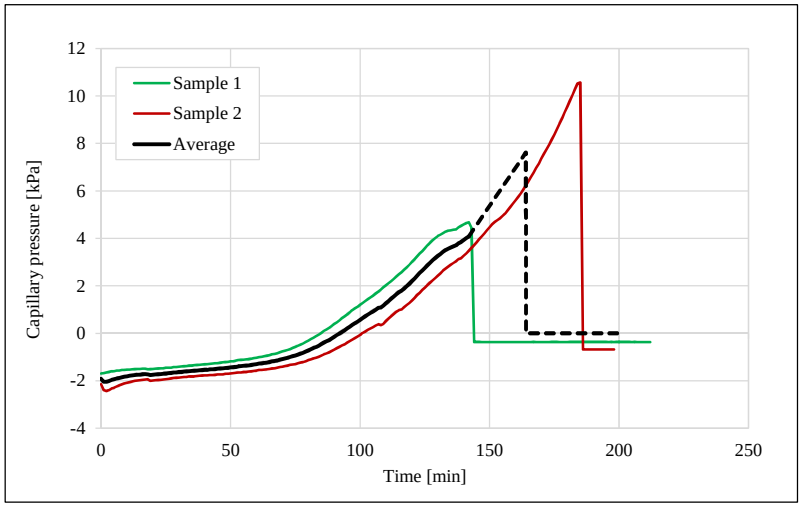

Figure 0.60 S_Min capillary pressure results

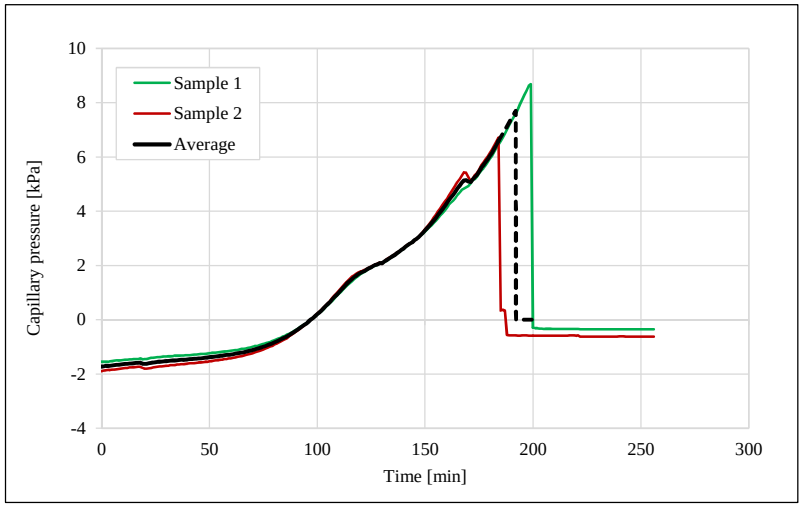

Figure 0.61 S_Max capillary pressure results

A.7. Shrinkage

The shrinkage results of the respective conventional concrete mixes are provided in this section. Shrinkage tests were fully automated and subsequent readings were taken every second. Four samples of each mix were tested simultaneously and calculated averages are provided accordingly.

Friction at the contact surface between the shrinkage anchors and moulds were reduced by externally applying grease to the guiding axis of anchors. In addition, grease was also applied to the embedded perimeter of shrinkage anchors to avoid ingress of concrete that could obstruct movement of anchors. However, certain samples displayed significantly reduced shrinkage when compared to corresponding samples of the same mix. This is attributed to increased friction at the contact surface due to an insufficient amount of grease applied to the guiding axis or ingress of concrete which obstructed displacement of shrinkage anchors. Shrinkage results of these samples are discarded, and include individual samples of AC_Min, S_Min, and S_Max, respectively.

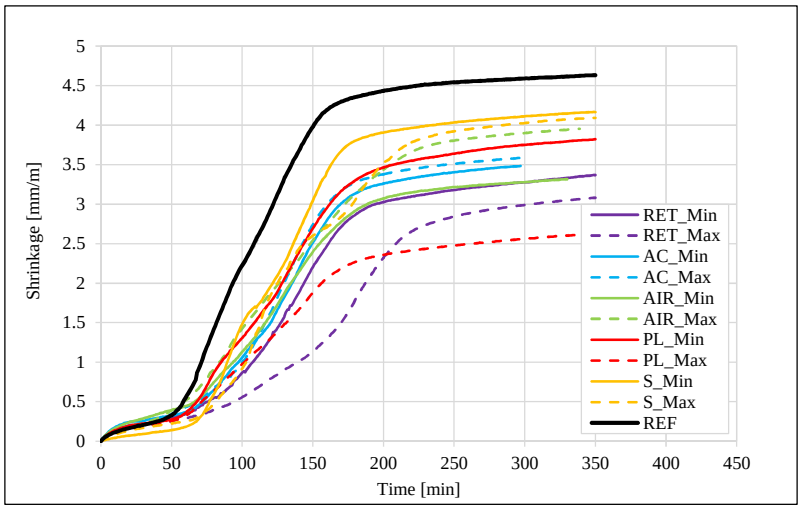

Figure 0.62 Shrinkage comparison of conventional concrete mixes

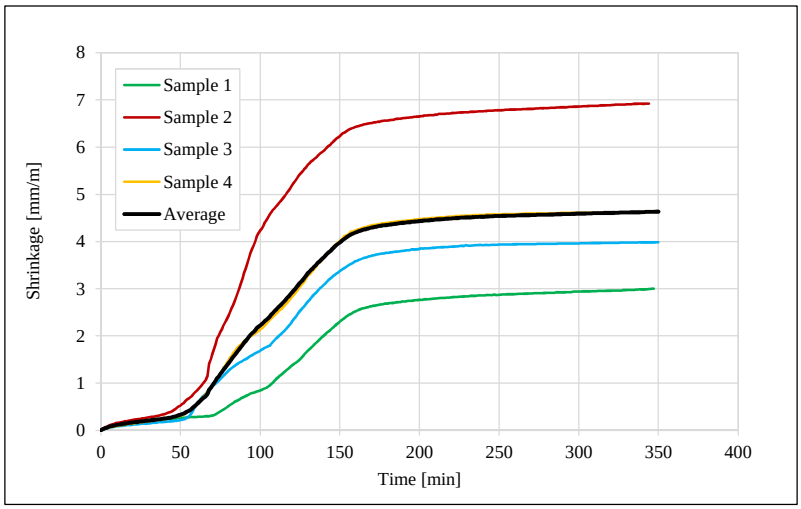

Figure 0.63 Conventional concrete REF shrinkage results

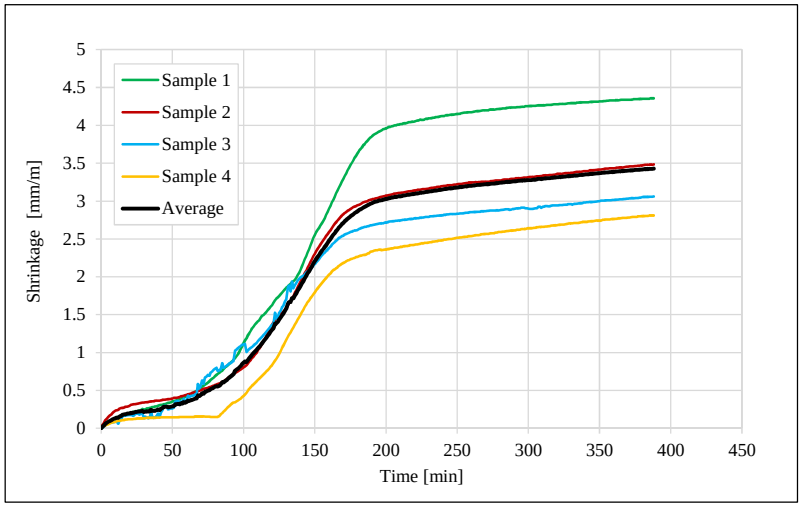

Figure 0.64 RET_Min shrinkage results

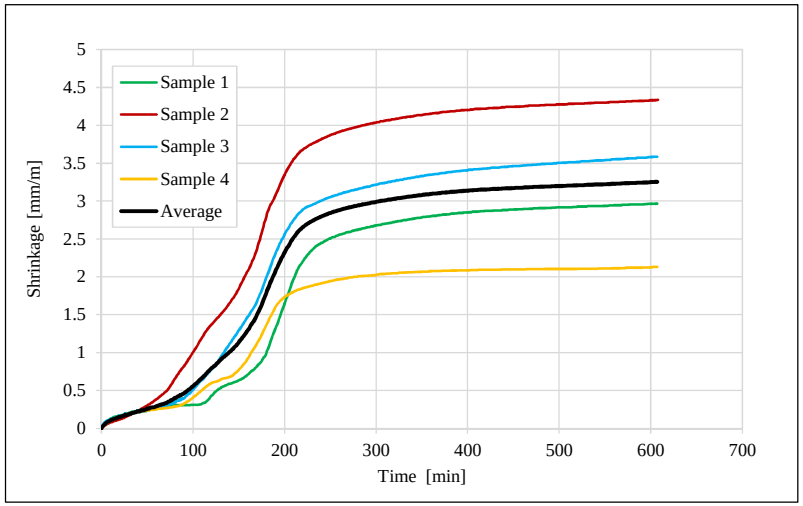

Figure 0.65 RET_Max shrinkage results

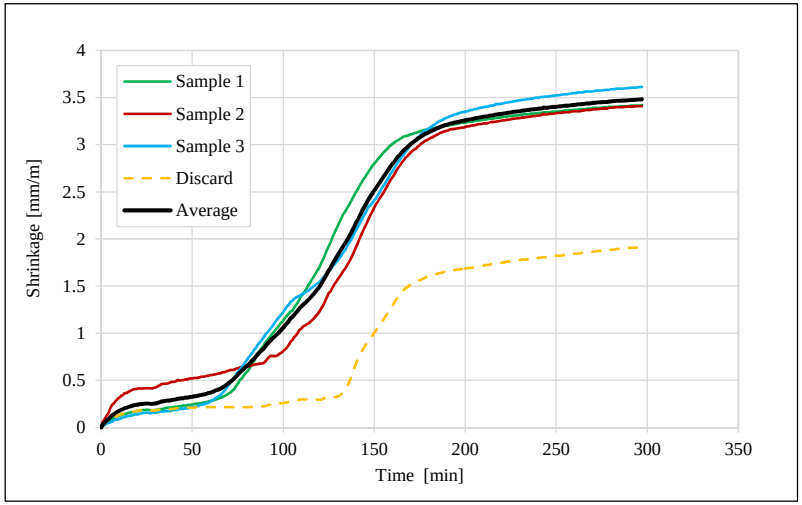

Figure 0.66 AC_Min shrinkage results

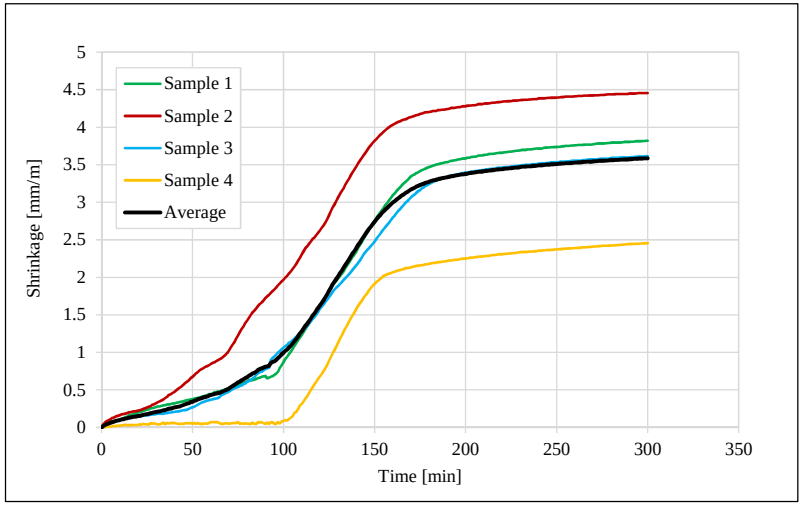

Figure 0.67 AC_Max shrinkage results

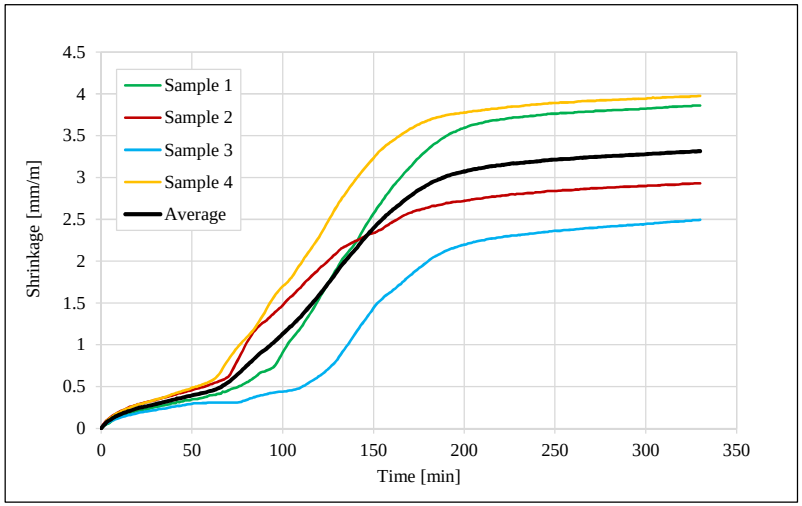

Figure 0.68 AIR_Min shrinkage results

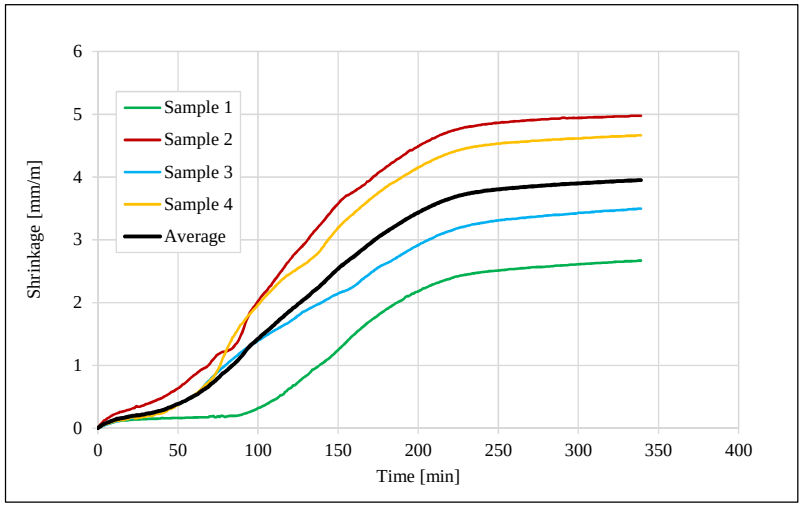

Figure 0.69 AIR_Max shrinkage results

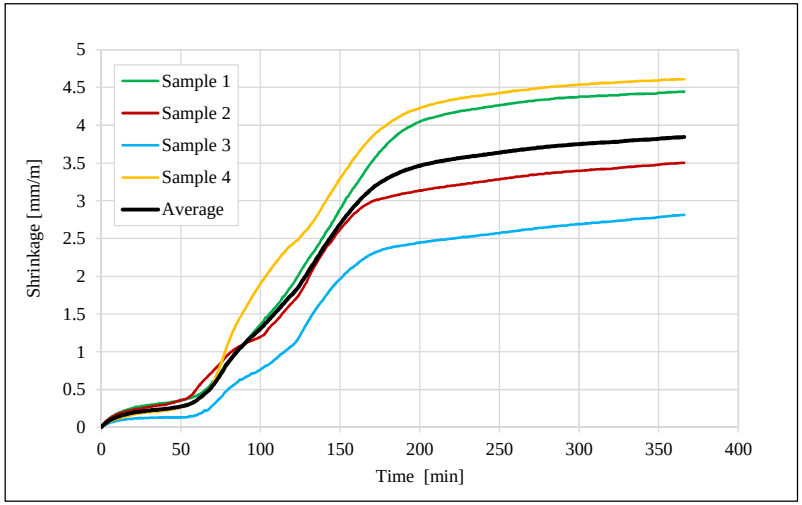

Figure 0.70 PL_Min shrinkage results

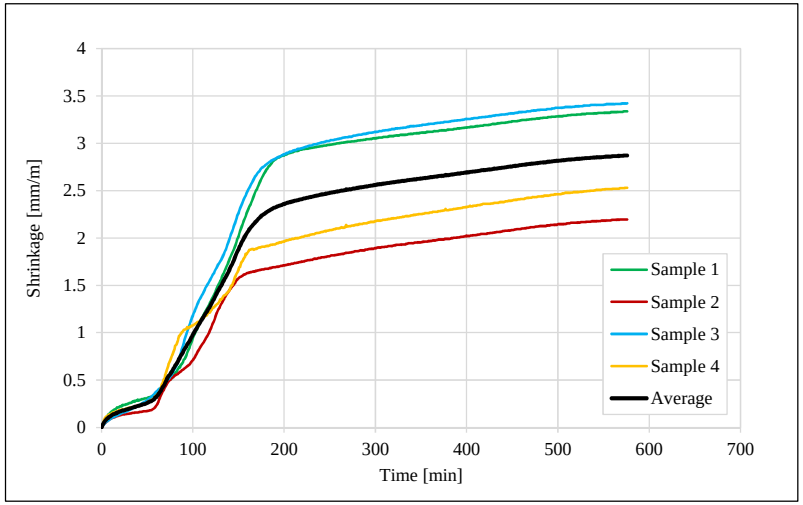

Figure 0.71 PL_Max shrinkage results

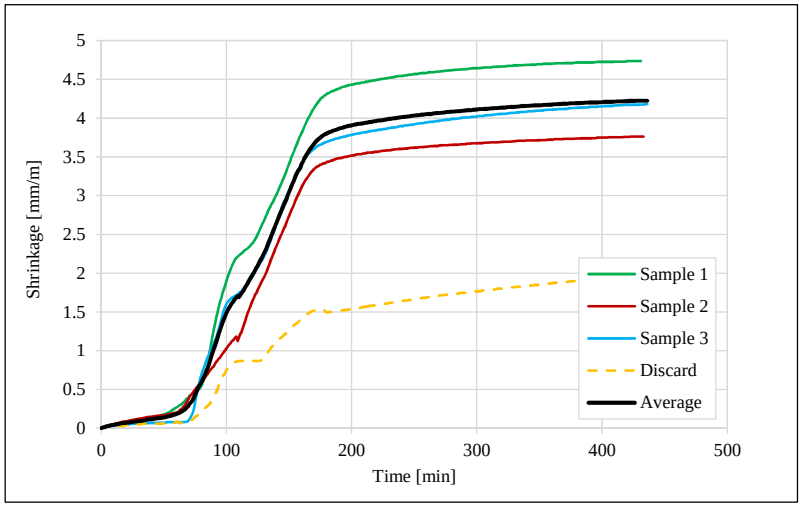

Figure 0.72 S_Min shrinkage results

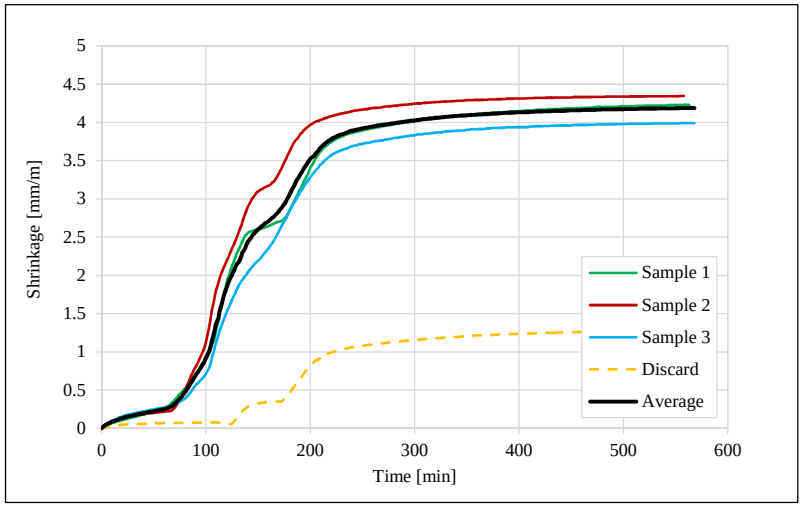

Figure 0.73 S_Max shrinkage results

A.8. Settlement

The settlement results of the respective conventional concrete mixes are provided in this section. Settlement tests were fully automated and subsequent readings were taken every second. Four samples of each mix were tested simultaneously and calculated averages are provided accordingly.

As previously discussed, LVDT's were used to measure settlement of the respective samples. The LVDT's were connected to settlement markers in such a way as to accommodate movement to adapt to an uneven surface caused by coarse aggregate beneath the concrete surface. A sufficient bond between settlement markers and concrete paste is required to facilitate uniform settlement measurement. However, settlement markers of certain samples were insufficiently bonded resulting in unrepresentative measurement of settlement. Settlement results of these samples are discarded, and include individual samples of RET_Min, RET_Max, AIR_Min, PL_Min, PL_Max, and S_Min. The figure below provides a visual illustration of unrepresentative settlement measurement due to insufficiently bonded markers.

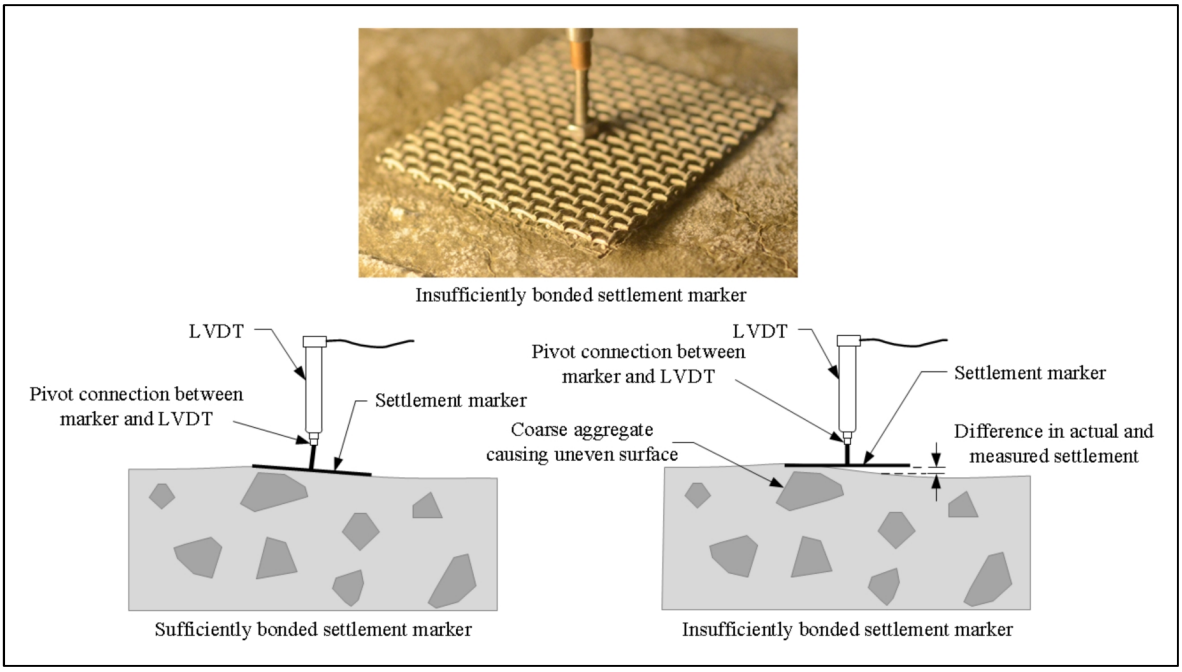

Figure 0.74 Insufficiently bonded settlement markers

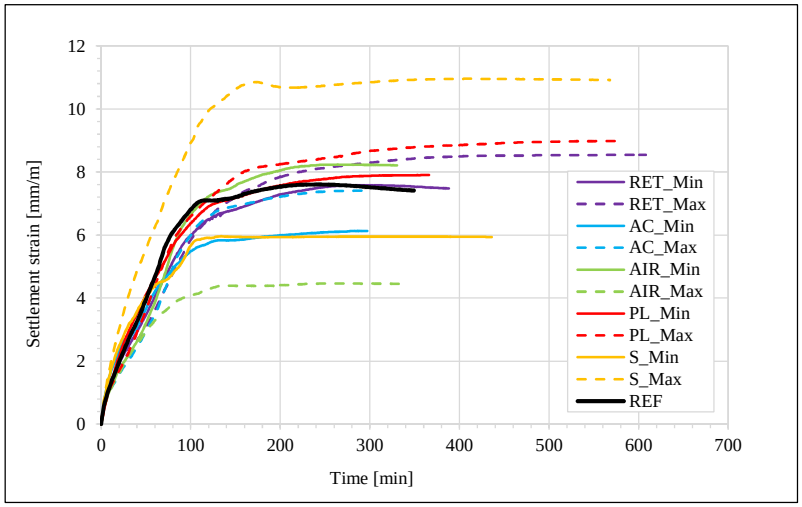

Figure 0.75 Settlement comparison of conventional concrete mixes

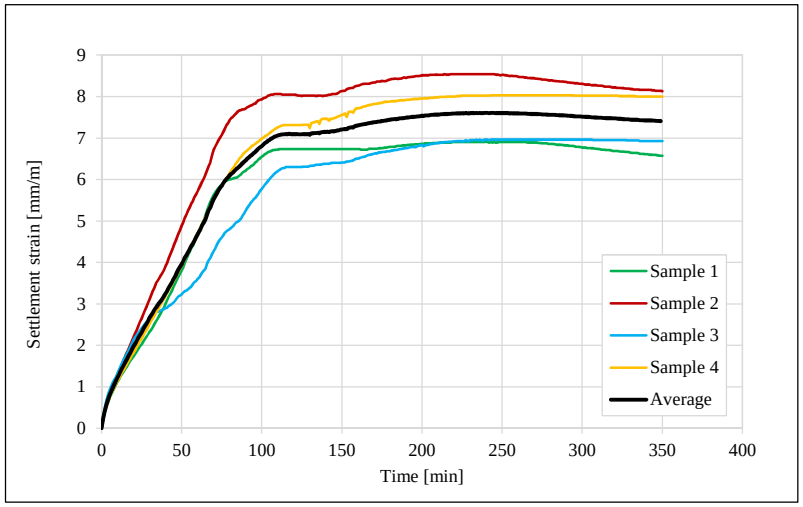

Figure 0.76 Conventional concrete REF settlement results

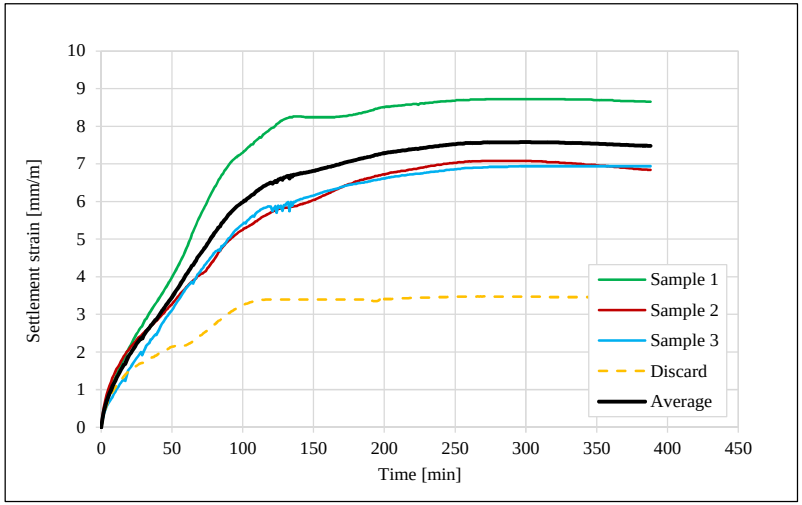

Figure 0.77 RET_Min settlement results

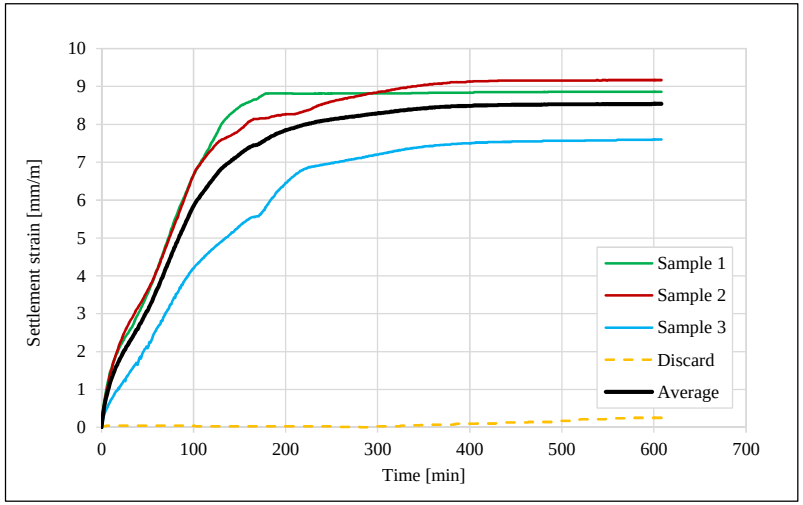

Figure 0.78 RET_Max settlement results

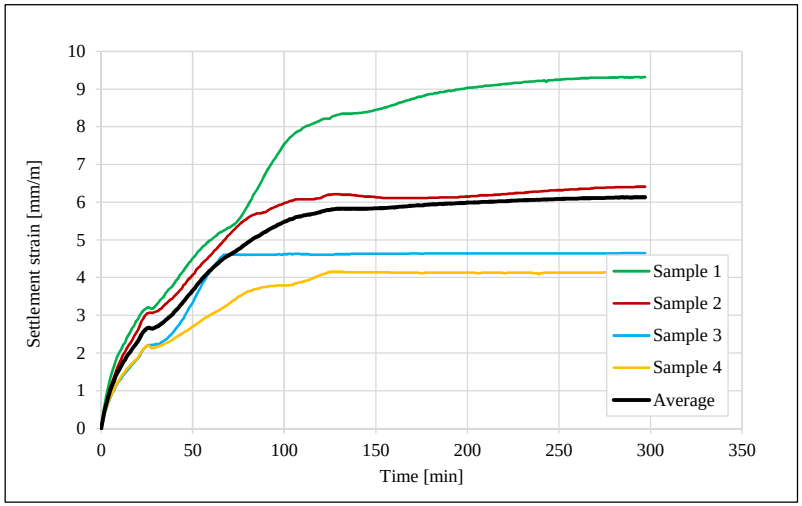

Figure 0.79 AC_Min settlement results

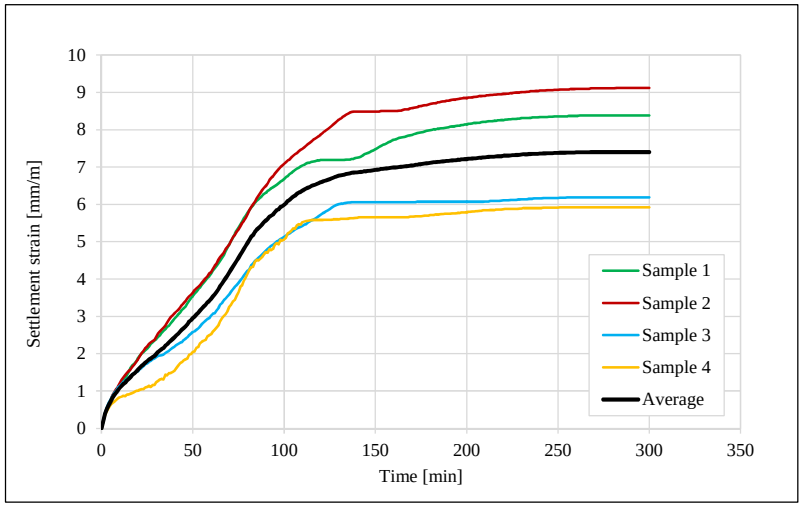

Figure 0.80 AC_Max settlement results

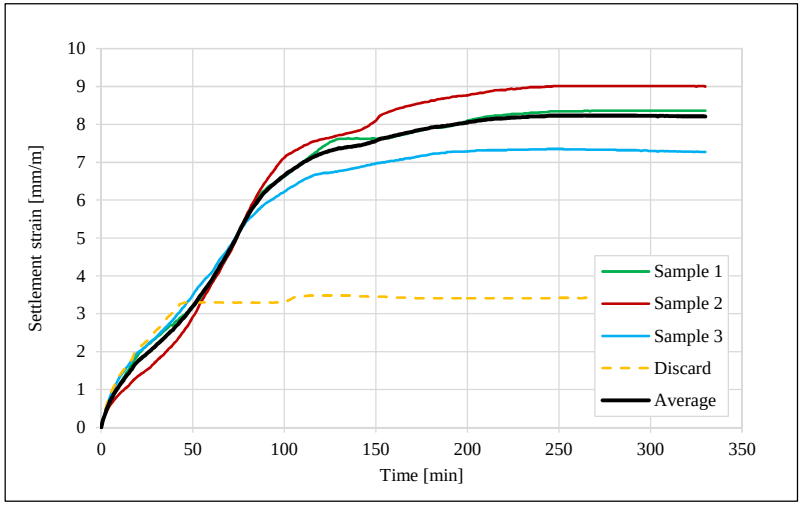

Figure 0.81 AIR_Min settlement results

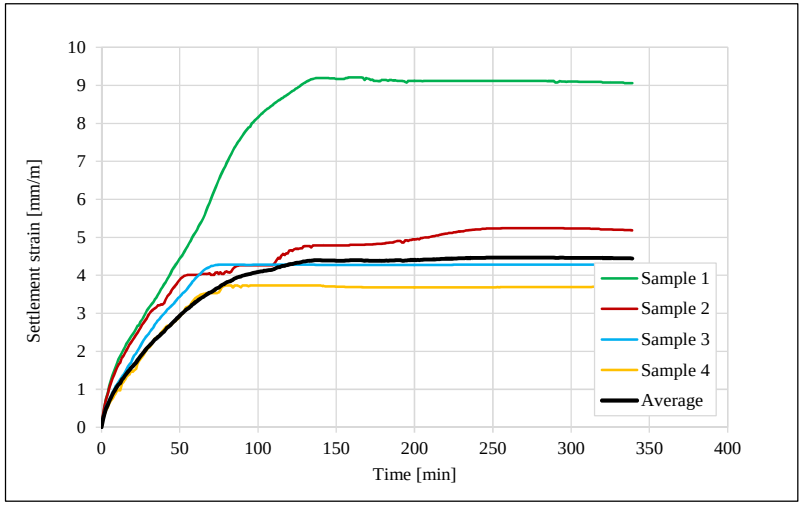

Figure 0.82 AIR_Max settlement results

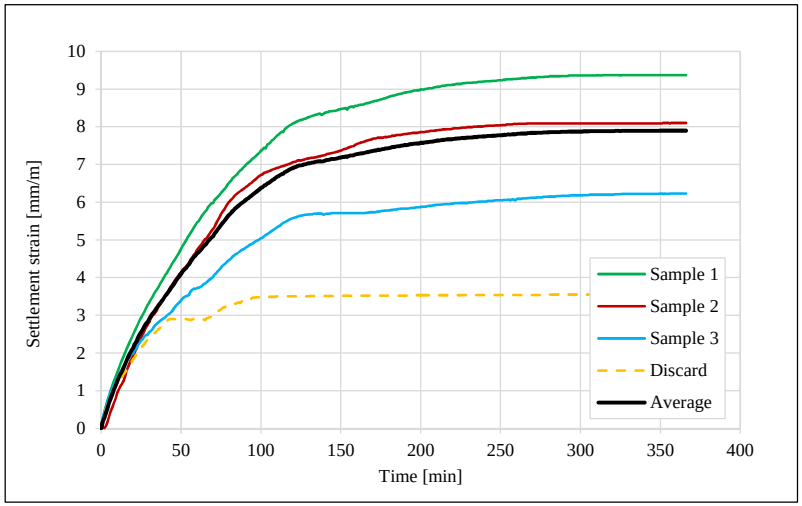

Figure 0.83 PL_Min settlement results

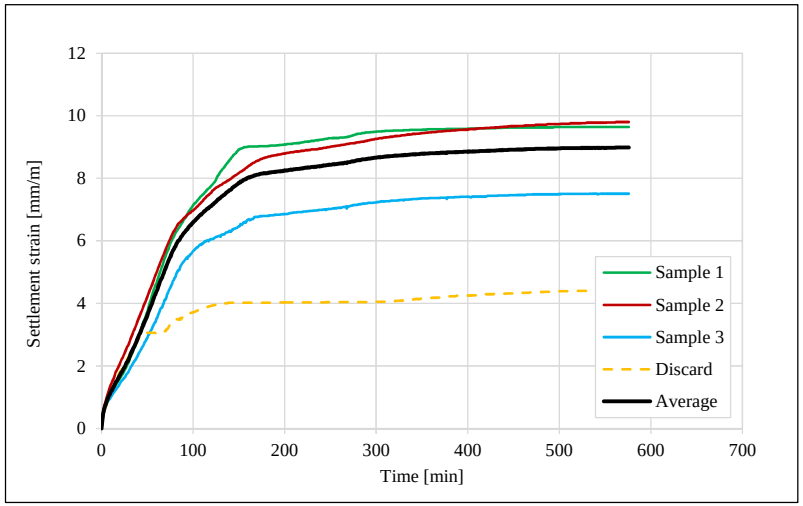

Figure 0.84 PL_Max settlement results

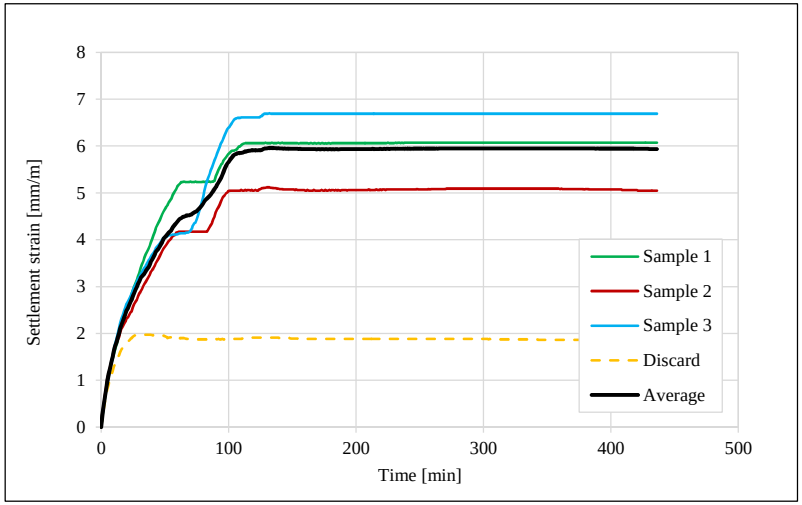

Figure 0.85 S_Min settlement results

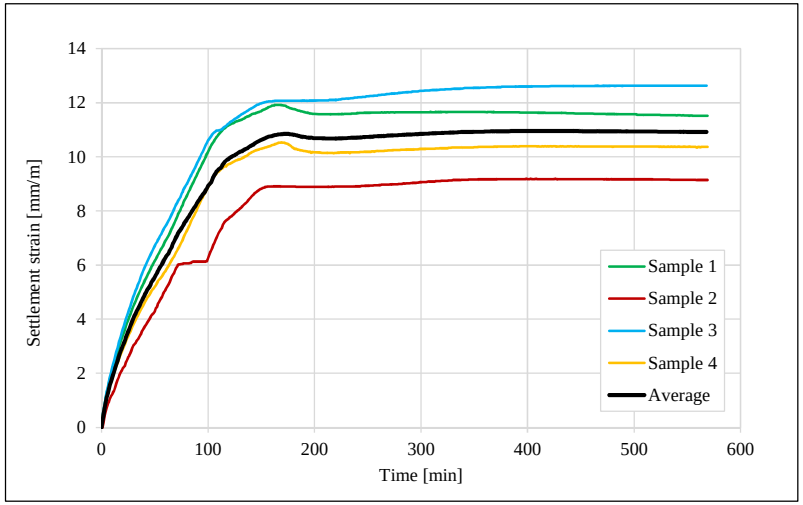

Figure 0.86 S_Min settlement results

APPENDIX B:

High flow concrete results

B.1. Crack area

The crack area results of the respective high flow concrete mixes are provided in this section. Four samples of each mix were tested simultaneously and calculated averages are provided accordingly. Measurements were conducted at 20 minute intervals. Measurement markers are only displayed once to avoid overly congested results.

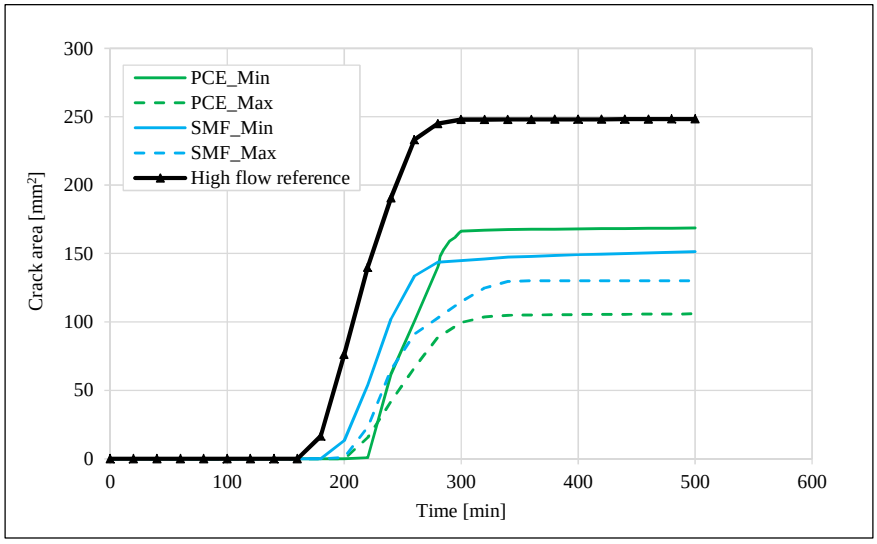

Figure 0.87 Crack area comparison of high flow mixes

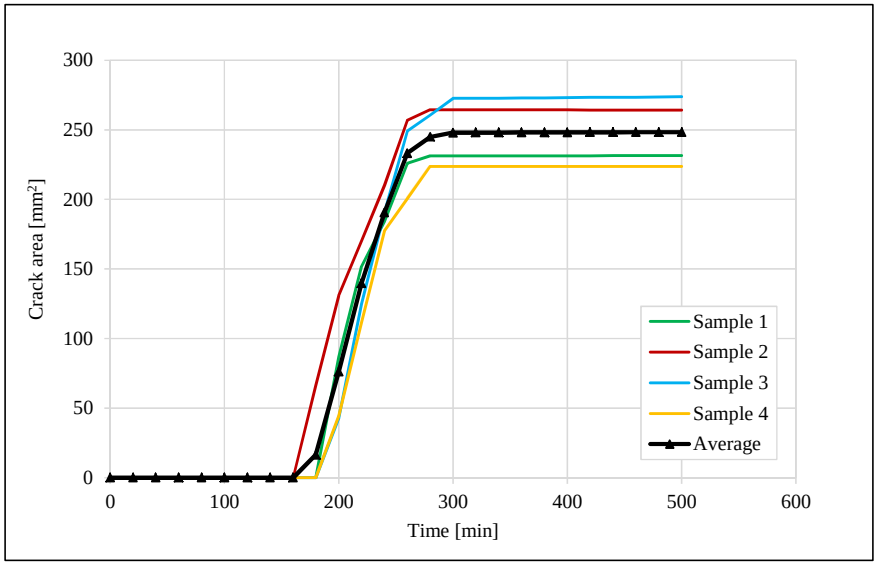

Figure 0.88 High flow concrete REF crack area results

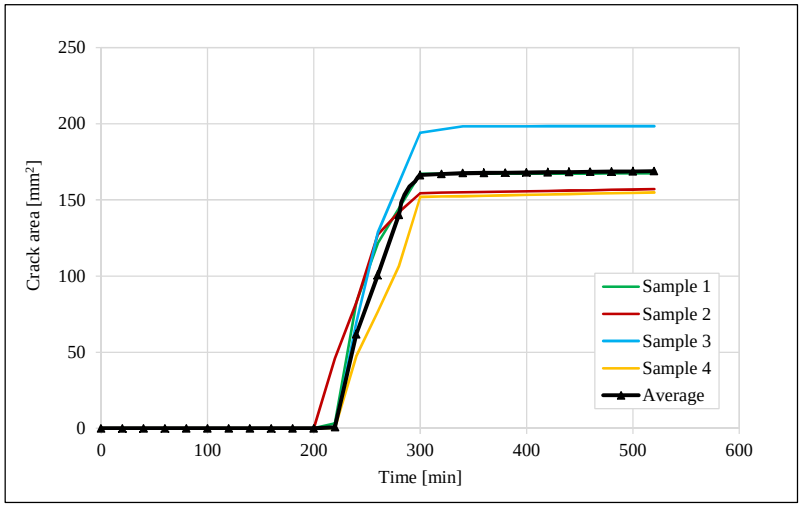

Figure 0.89 PCE_Min crack area results

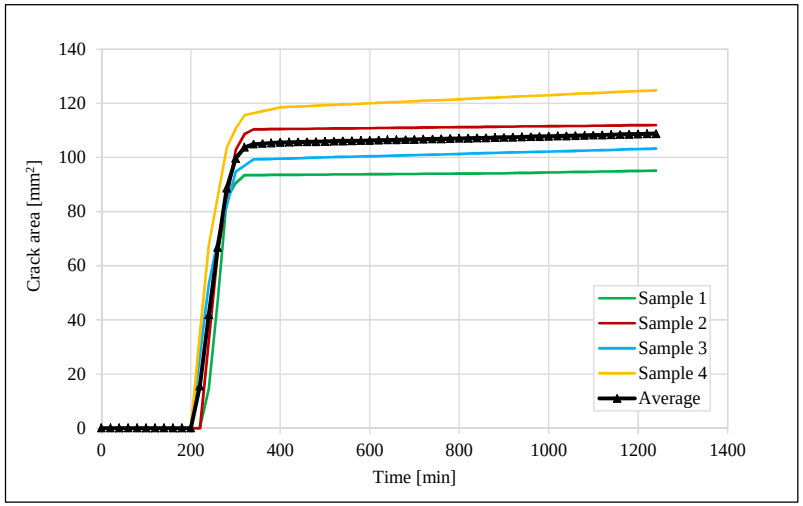

Figure 0.90 PCE_Max crack area results

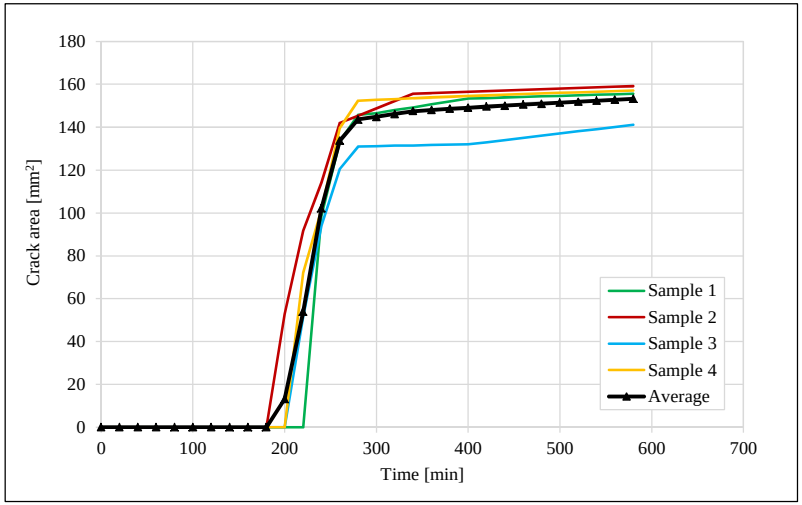

Figure 0.91 SMF_Min crack area results

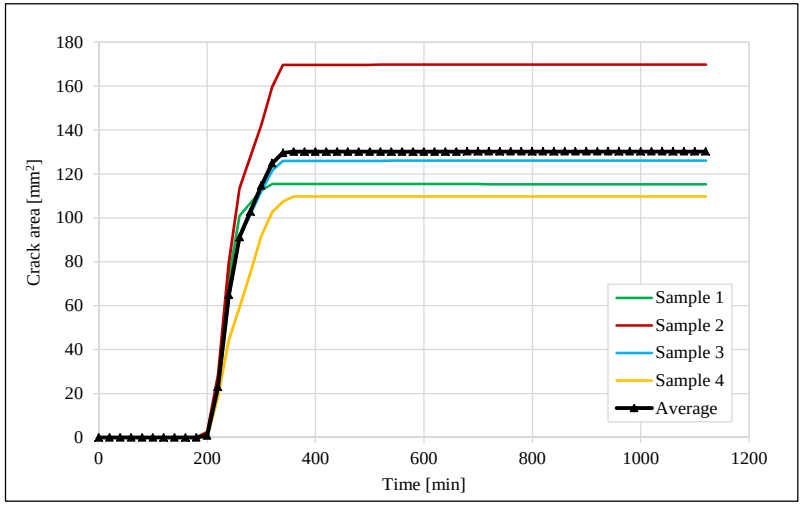

Figure 0.92 SMF_Max crack area results

B.2. Rapid crack growth period

The calculated rapid crack growth period of the respective high flow concrete mixes are provided in this section. The rate of crack growth is calculated as average growth during the 20 minute measurement intervals. Crack onset is defined as the first crack area measurement of which the measured crack area is greater than zero whereas crack stabilisation is defined as the time when the rate of crack growth became insignificant.

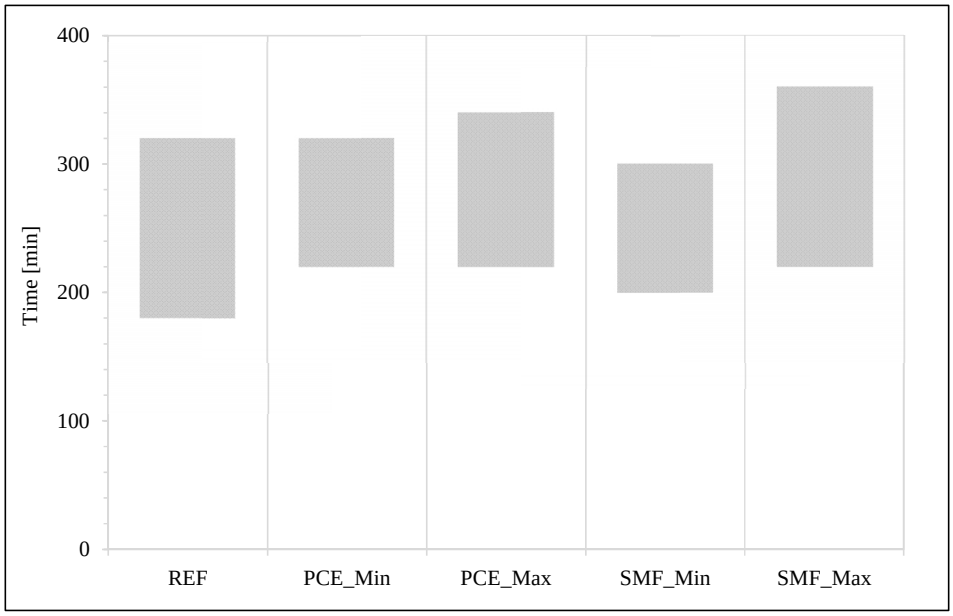

Figure 0.93 Comparison of rapid crack growth

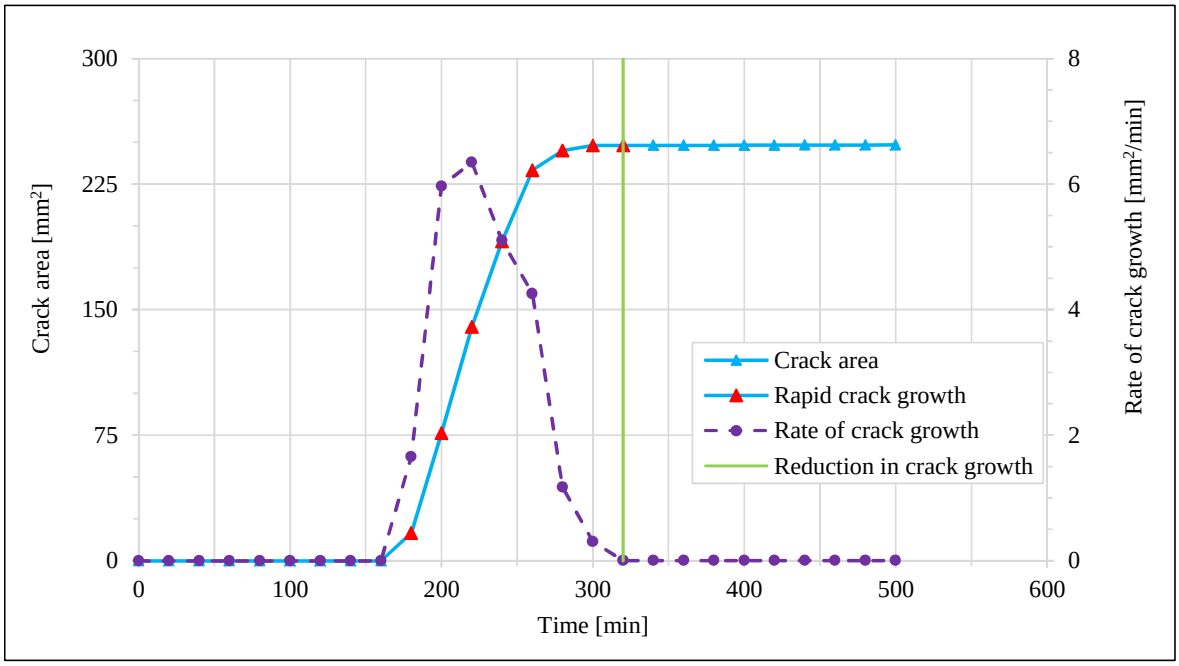

Figure 0.94 REF rapid crack growth

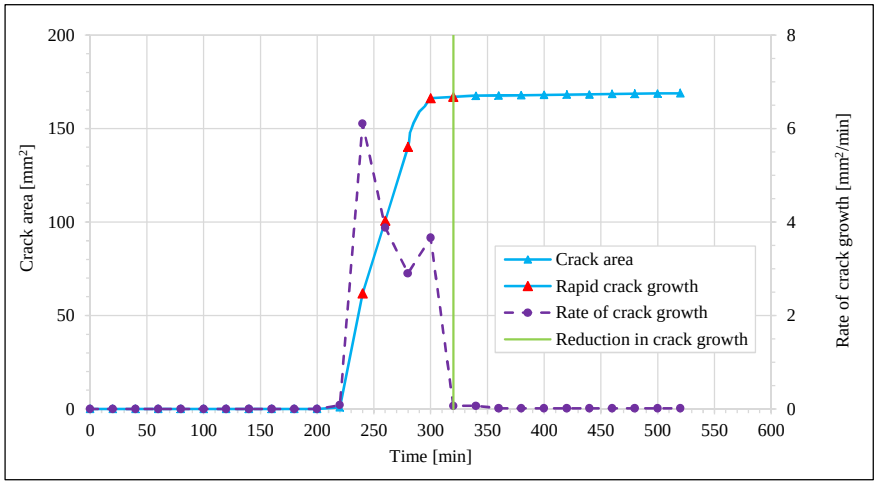

Figure 0.95 PCE_Min rapid crack growth

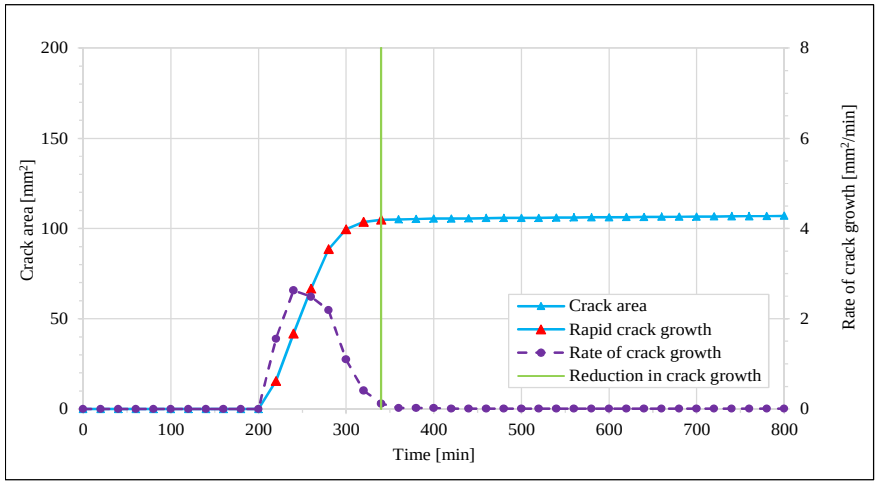

Figure 0.96 PCE_Max rapid crack growth

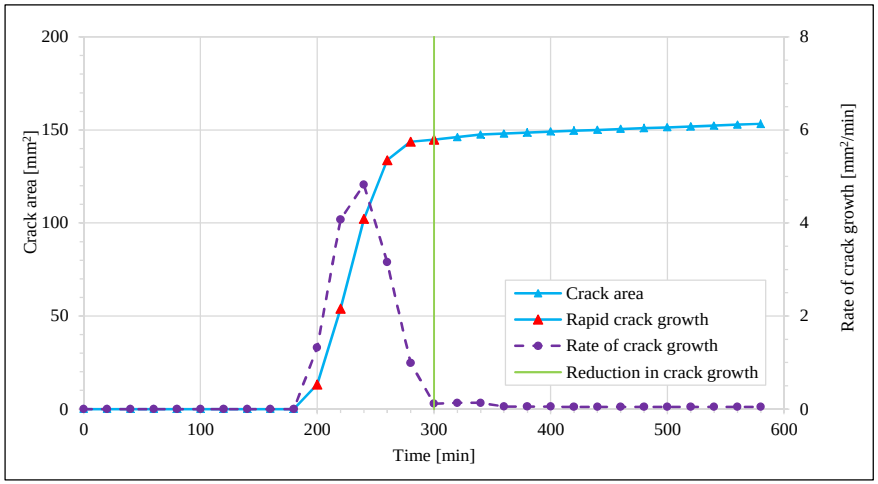

Figure 0.97 SMF_Min rapid crack growth

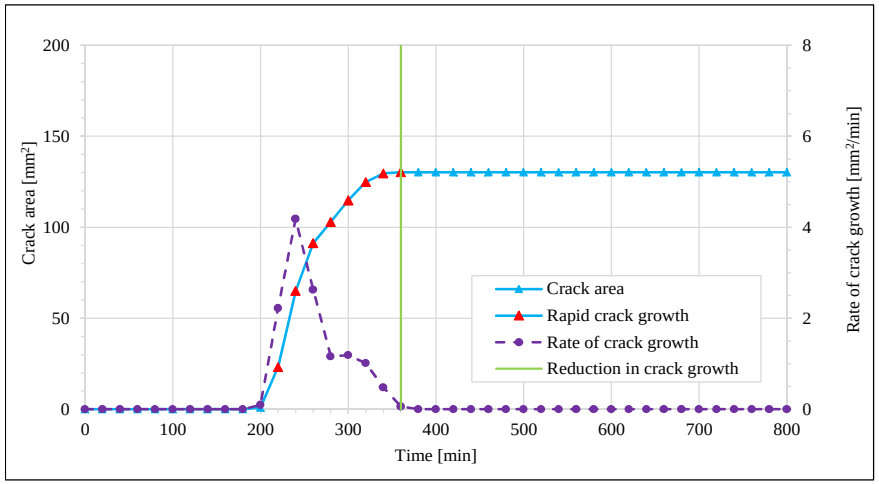

Figure 0.98 SMF_Max rapid crack growth

B.3. Setting time

The initial and final setting times of the respective high flow concrete mixes are provided in this section. Three samples of each mix were tested simultaneously and calculated averages are provided accordingly.

Table 0.2 Setting time results of respective high flow mixes

Mix	Initial setting time [min]	Final setting time [min]
REF	335	375
PCE_Min	480	540
PCE_Max	1180	1260
SMF_Min	550	615
SMF_Max	900	1005

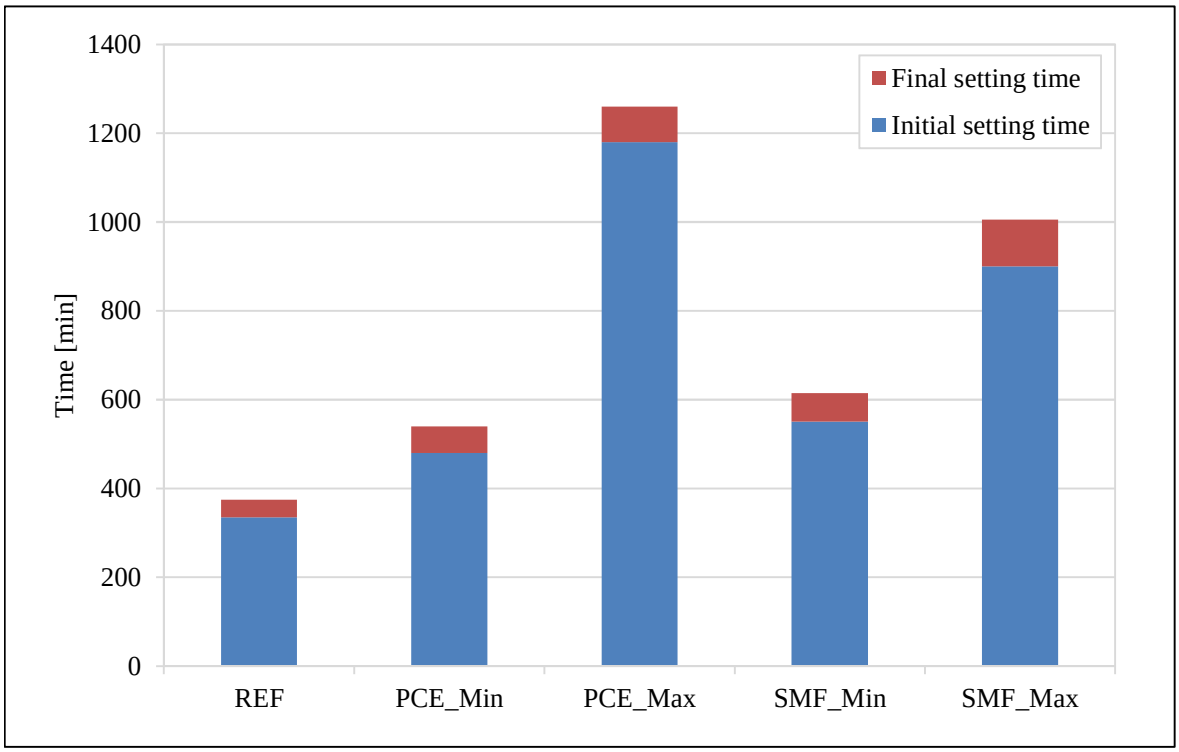

Figure 0.99 Setting time results of respective high flow concrete mixes

B.4. Bleeding

The bleeding results of the respective high flow concrete mixes are provided in this section. Four samples of each mix were tested simultaneously and calculated averages are provided accordingly. Accumulated bleed water was extracted in 20 minute intervals during the first 40 minutes after casting and 30 minute intervals thereafter until bleeding ceased. Measurement markers are only displayed for the calculated average to avoid overly congested results. As previously discussed, the self-levelling properties of SMF_Min, SMF_Max, and PCE_Max did not permit extraction of bleed water. Accordingly, bleeding tests were not performed for the aforementioned high flow mixes.

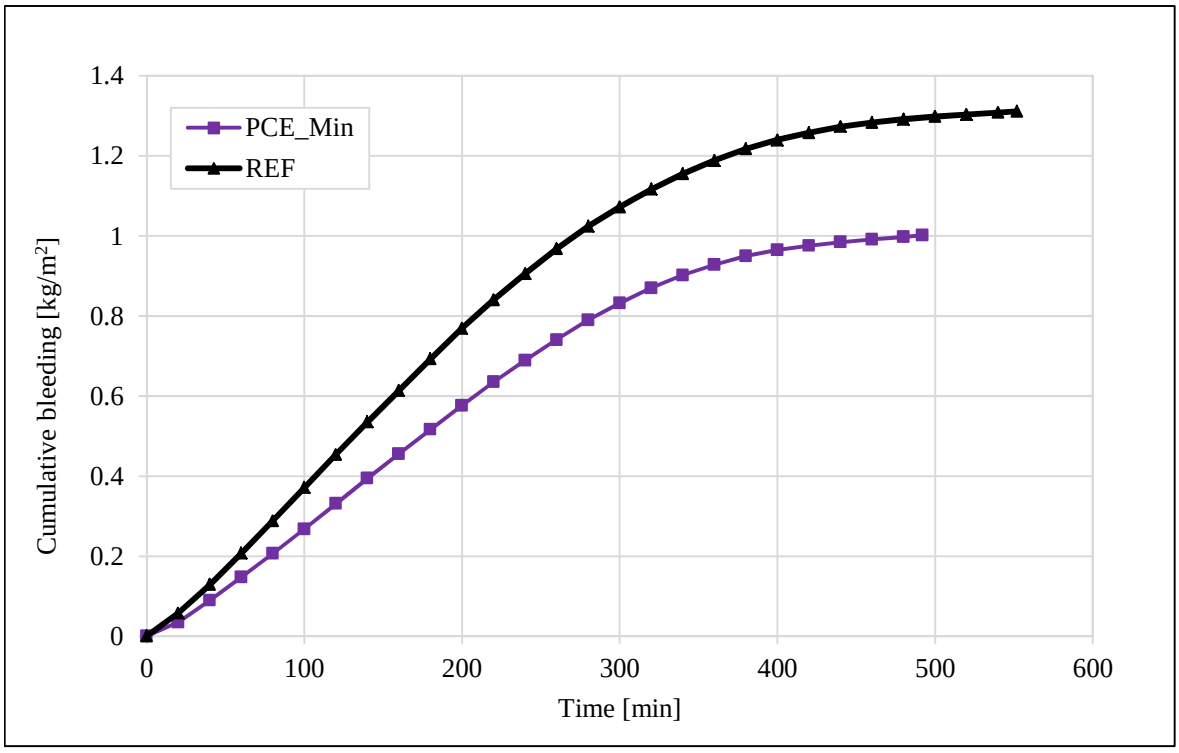

Figure 0.100 Bleeding comparison of high flow concrete mixes

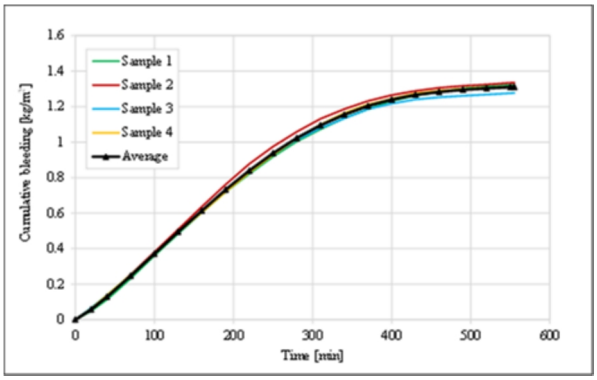

Figure 0.101 High flow REF bleeding results

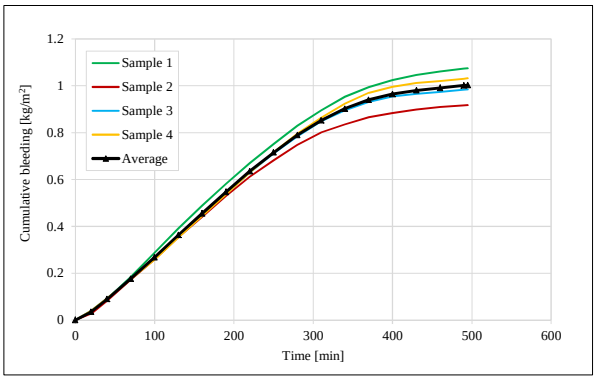

Figure 0.102 PCE_Min bleeding results

B.5. Evaporation

The evaporation results of the respective high flow concrete mixes are provided in this section. Four samples of each mix were tested and calculated averages are provided accordingly. Evaporation readings were conducted at 20 minute intervals during the first 40 minutes after casting and 30 minute intervals thereafter. Measurement markers are only displayed once to avoid overly congested results.

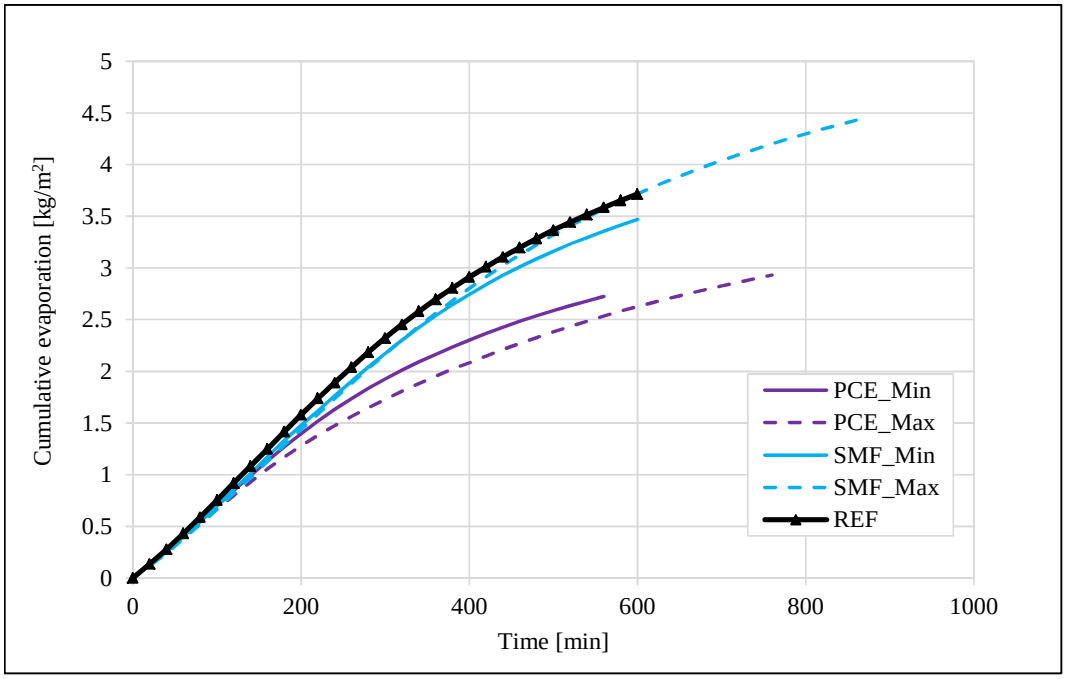

Figure 0.103 High flow concrete evaporation comparison

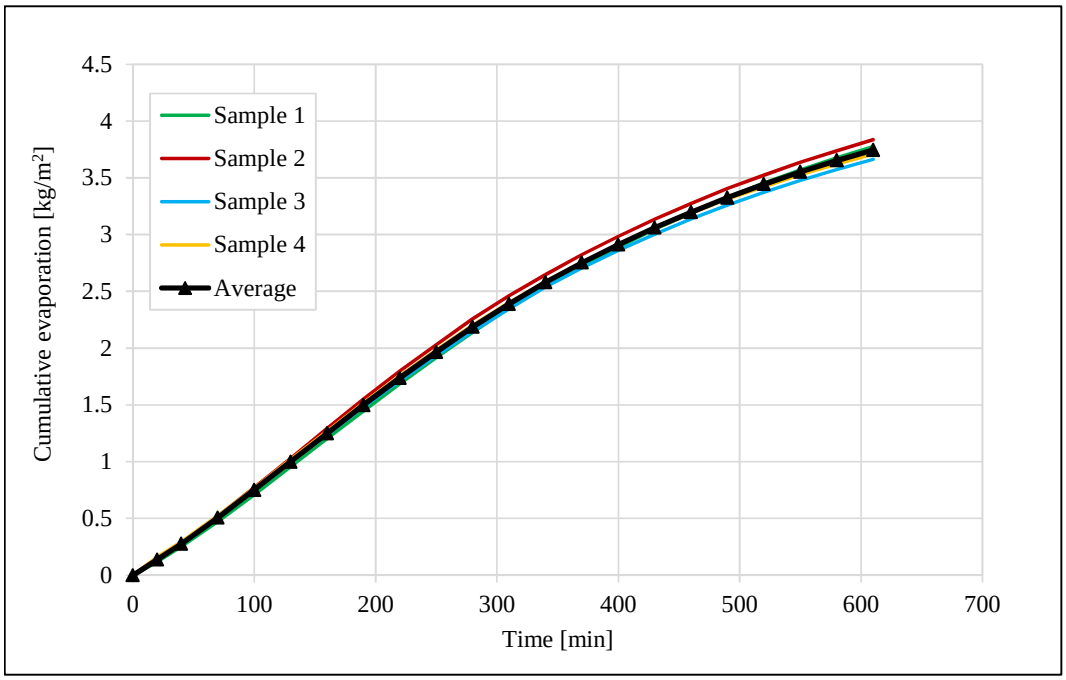

Figure 0.104 High flow REF evaporation results

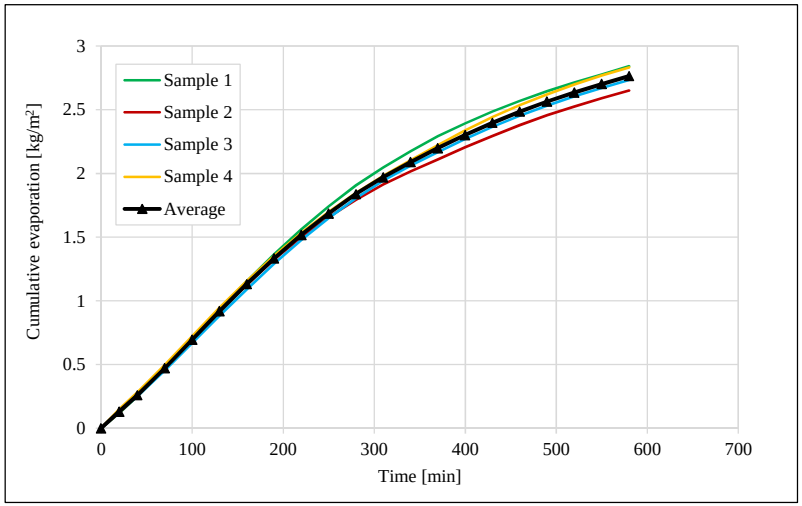

Figure 0.105 PCE_Min evaporation results

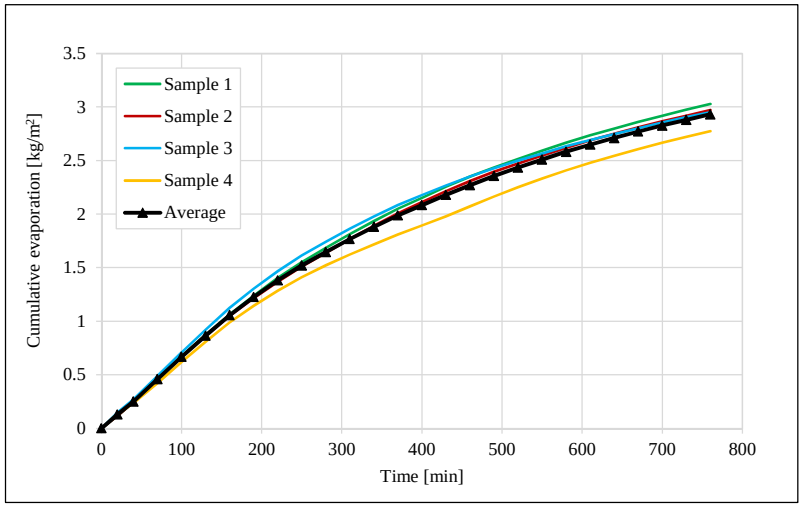

Figure 0.106 PCE_Max evaporation results

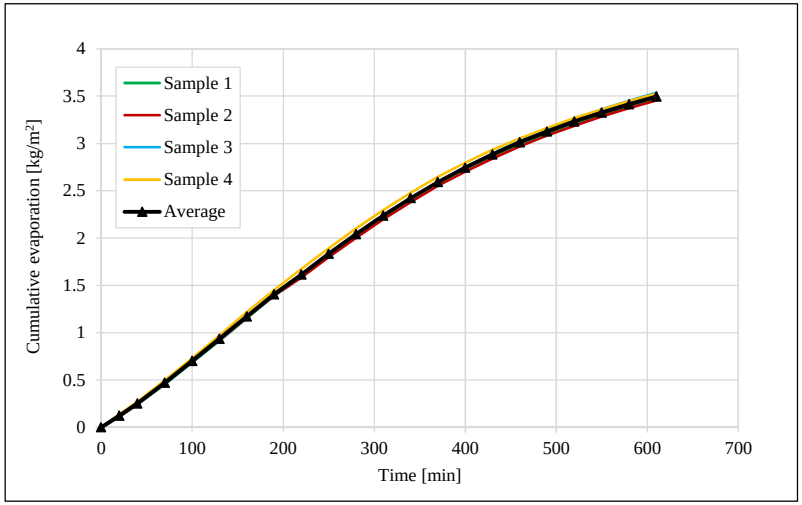

Figure 0.107 SMF_Min evaporation results

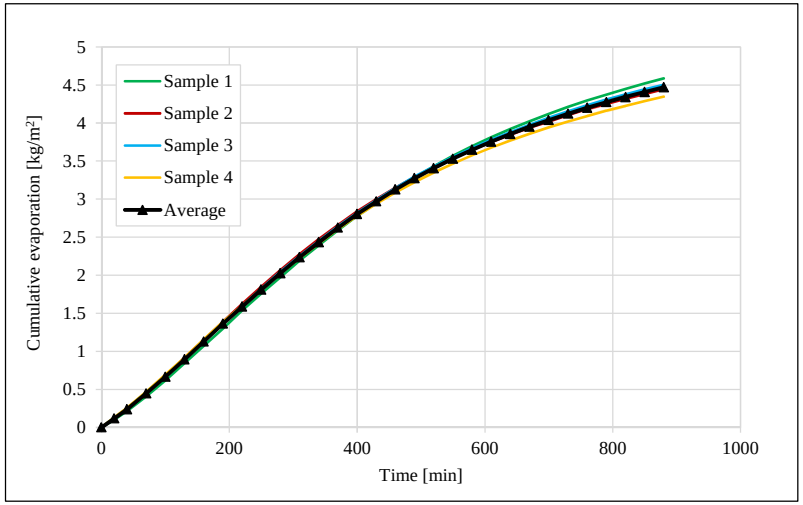

Figure 0.108 SMF_Max evaporation results

B.6. Capillary pressure

The capillary pressure results of the respective high flow concrete mixes are provided in this section. Capillary pressure measurements were fully automated and subsequent readings were taken every second. Due to the fact that air entry is considered to be arbitrary for different samples, only two samples of each mix were tested. Calculated results of the representative capillary pressure build-up are provided accordingly.

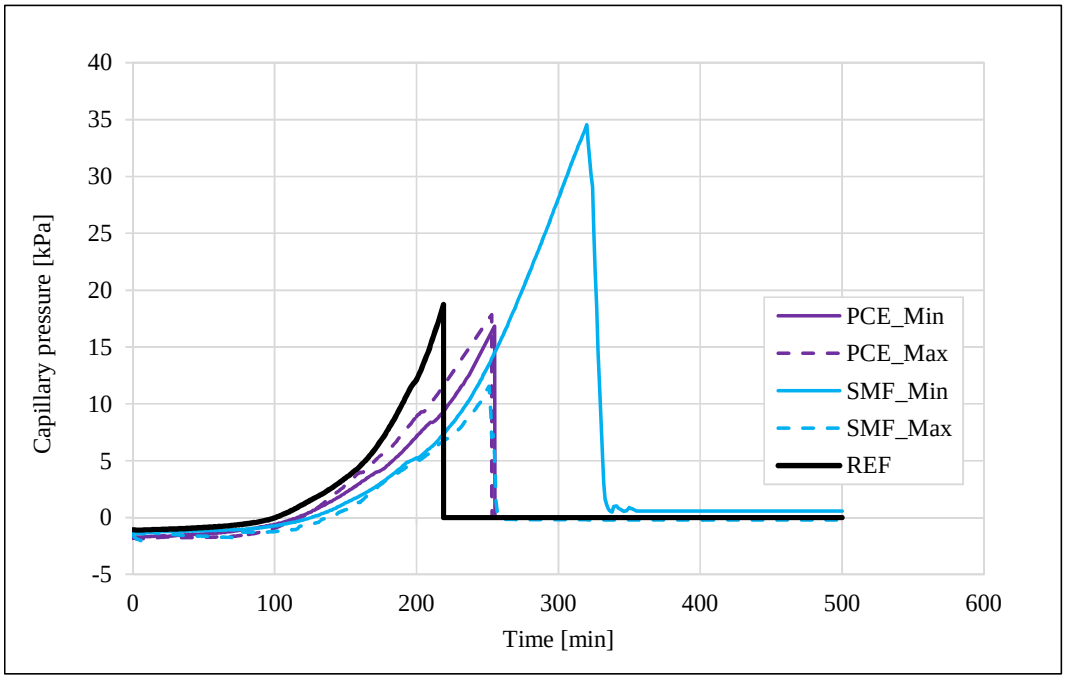

Figure 0.109 Capillary pressure comparison of high flow concrete mixes

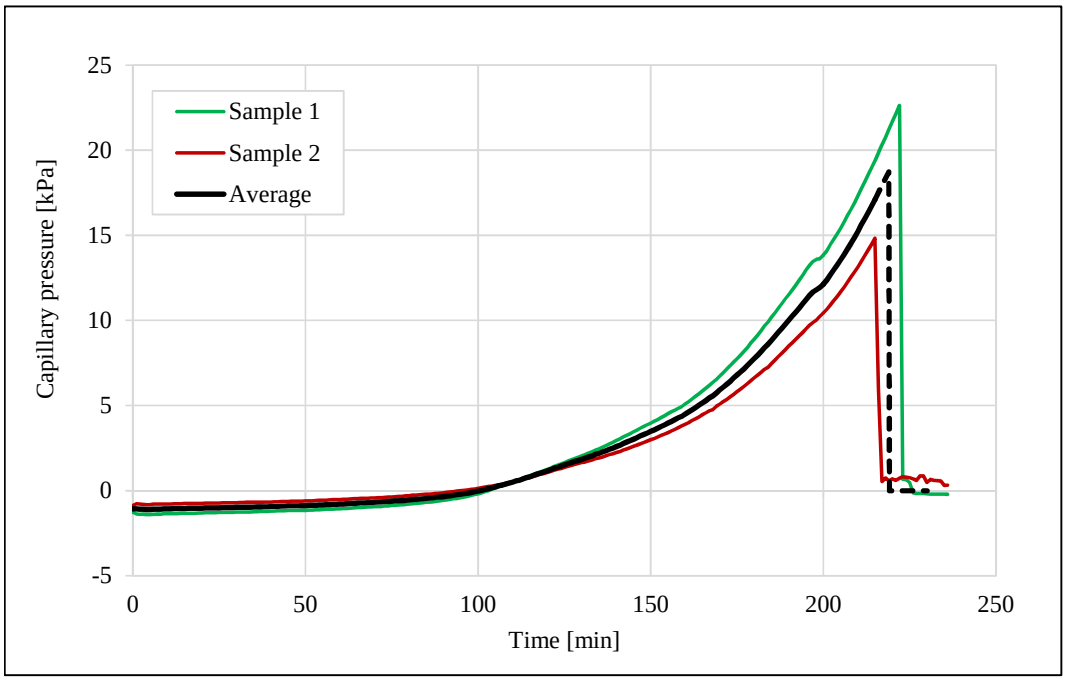

Figure 0.110 High flow REF capillary pressure results

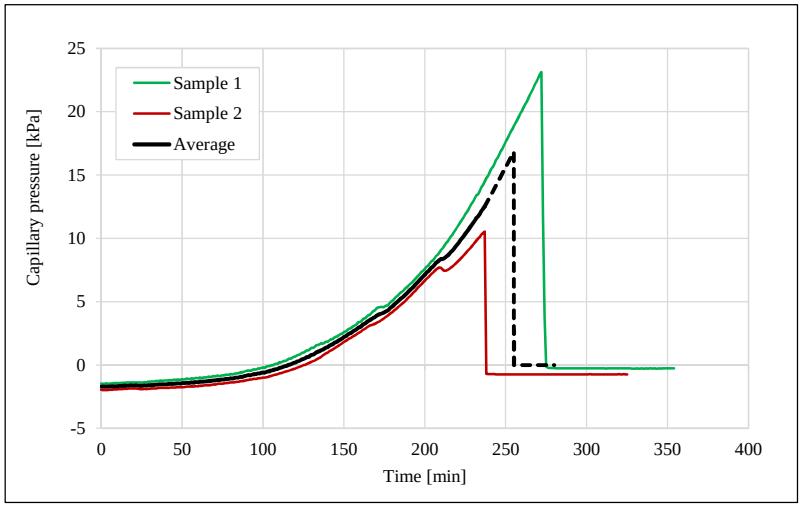

Figure 0.111 PCE_Min capillary pressure results

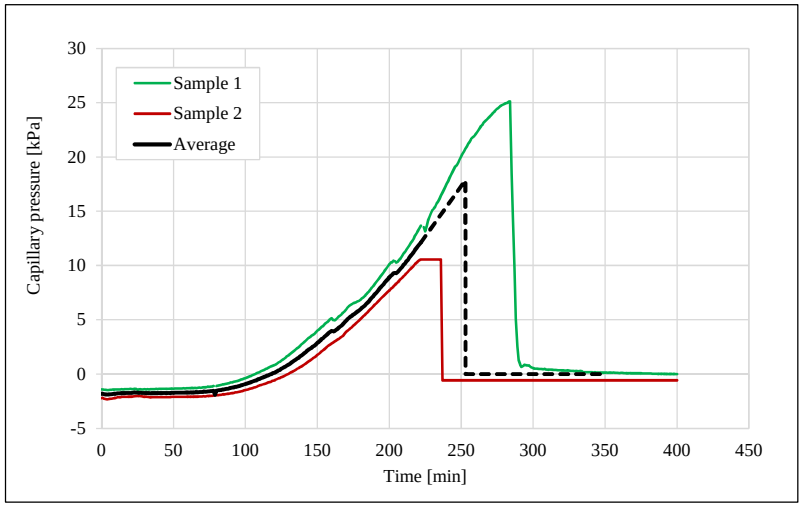

Figure 0.112 PCE_Max capillary pressure results

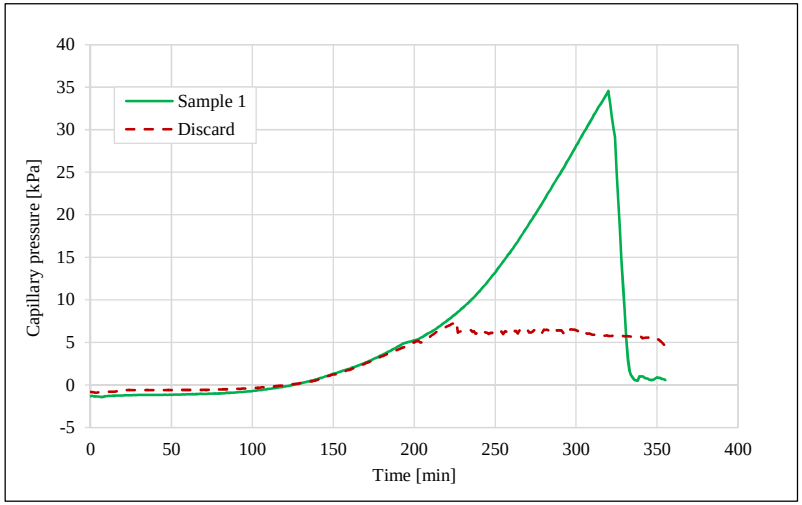

Figure 0.113 SMF_Min capillary pressure results

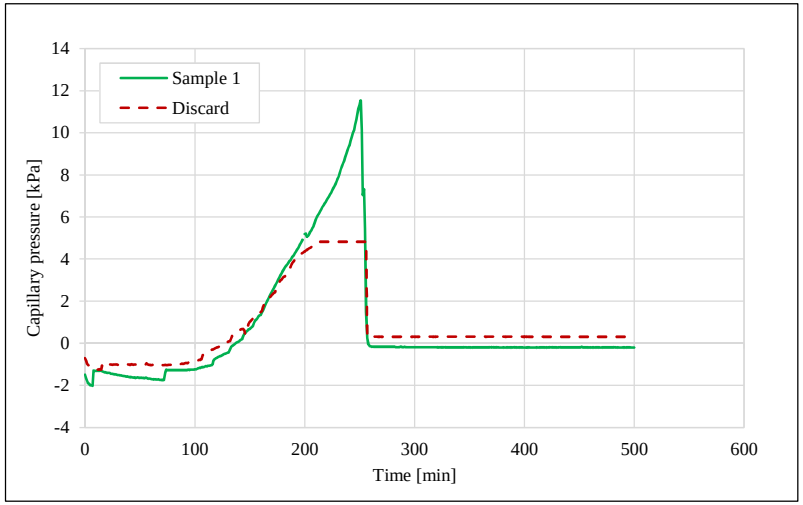

Figure 0.114 SMF_Max capillary pressure results

B.7. Shrinkage

The shrinkage results of the respective high flow concrete mixes are provided in this section. Shrinkage measurements were fully automated and subsequent readings were taken every second. Four samples of each mix were tested simultaneously and calculated averages are provided accordingly. As previously discussed in Section A.7, certain samples displayed reduced shrinkage measurements when compared to the corresponding samples of the same mix. This is attributed to increased friction at the contact surface due to an insufficient amount of grease applied to the guiding axis or ingress of concrete which obstructed displacement of shrinkage anchors. Shrinkage results of these samples are discarded, and include individual samples of PCE_Max and SMF_Min.

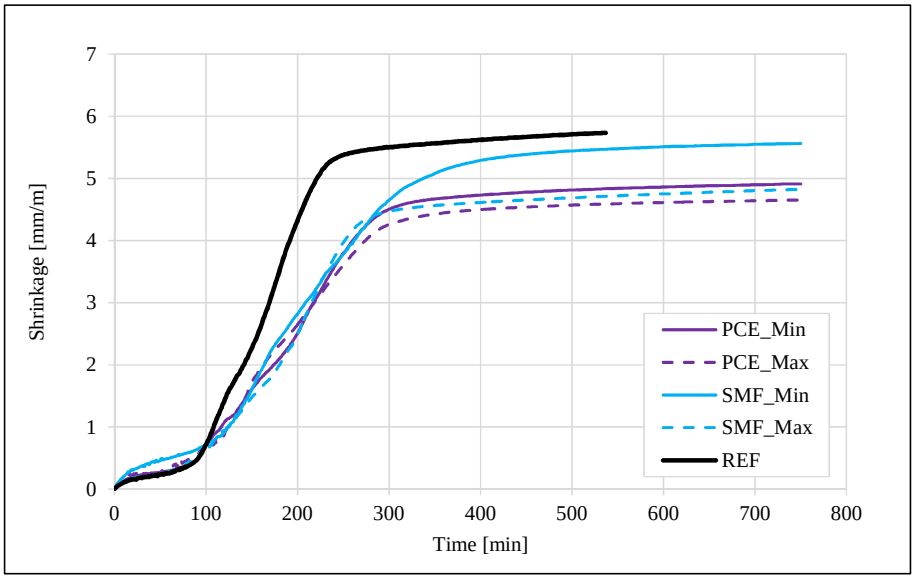

Figure 0.115 Shrinkage comparison of high flow concrete mixes

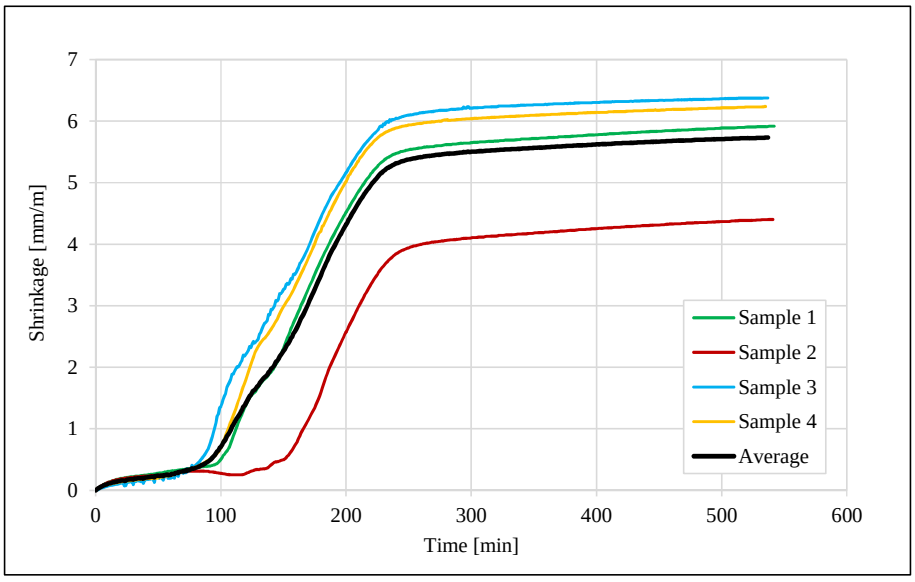

Figure 0.116 High flow REF shrinkage results

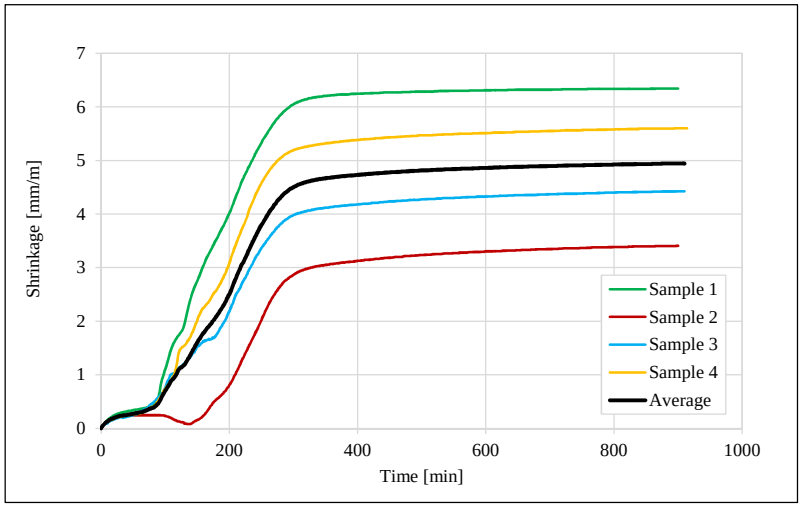

Figure 0.117 PCE_Min shrinkage results

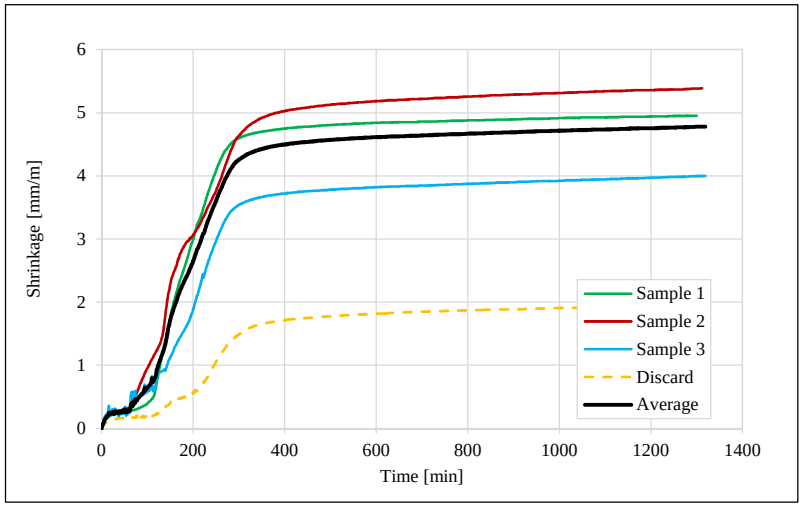

Figure 0.118 PCE_Max shrinkage results

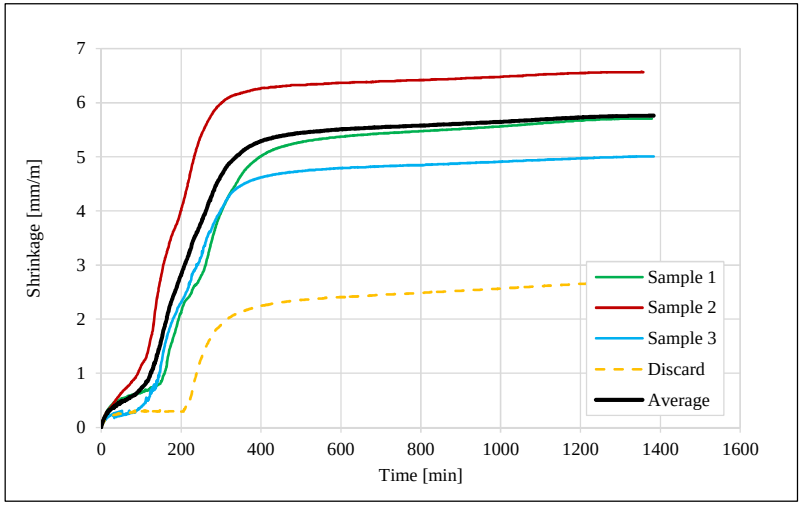

Figure 0.119 SMF_Min shrinkage results

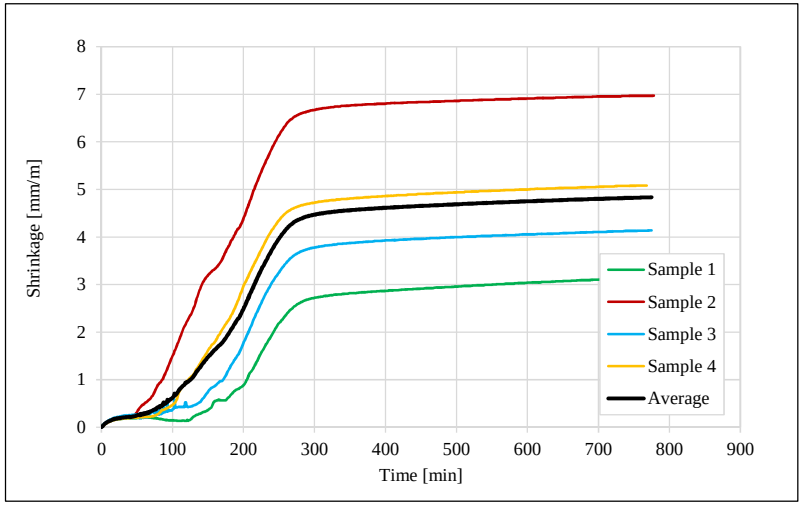

Figure 0.120 SMF_Max shrinkage results

B.8. Settlement

The settlement results of the respective high flow concrete mixes are provided in this section. Settlement measurements were fully automated and subsequent readings were taken every second. Four samples of each mix were tested simultaneously and calculated averages are provided accordingly. As previously discussed in Section A.8, settlement markers of certain samples were insufficiently bonded resulting in unrepresentative measurement of settlement. Settlement results of these samples are discarded, and include an individual sample of PCE_Min.

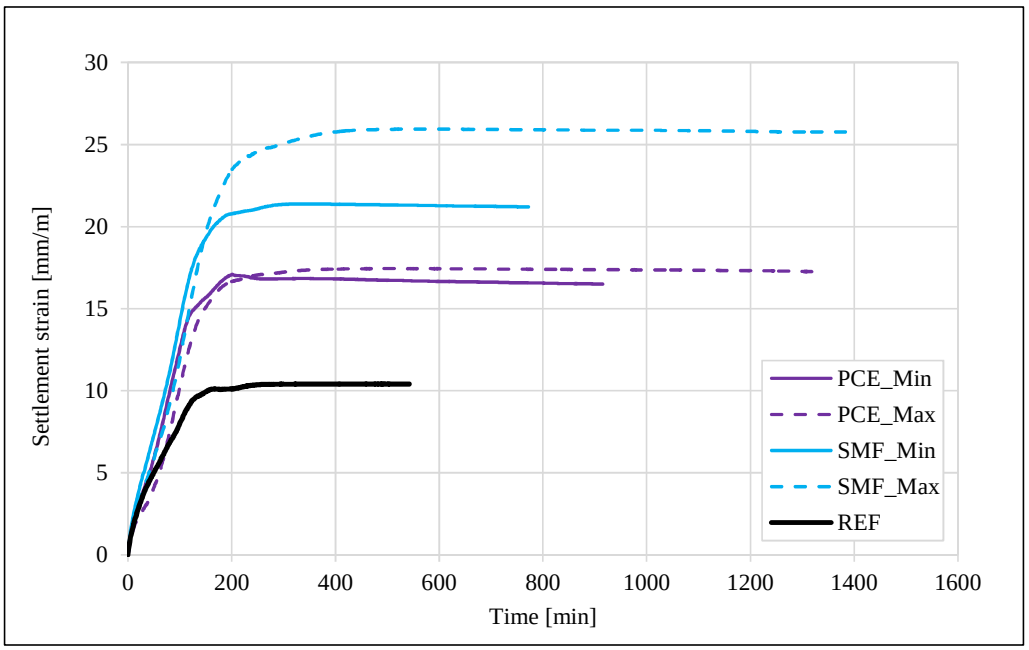

Figure 0.121 Settlement comparison of high flow concrete mixes

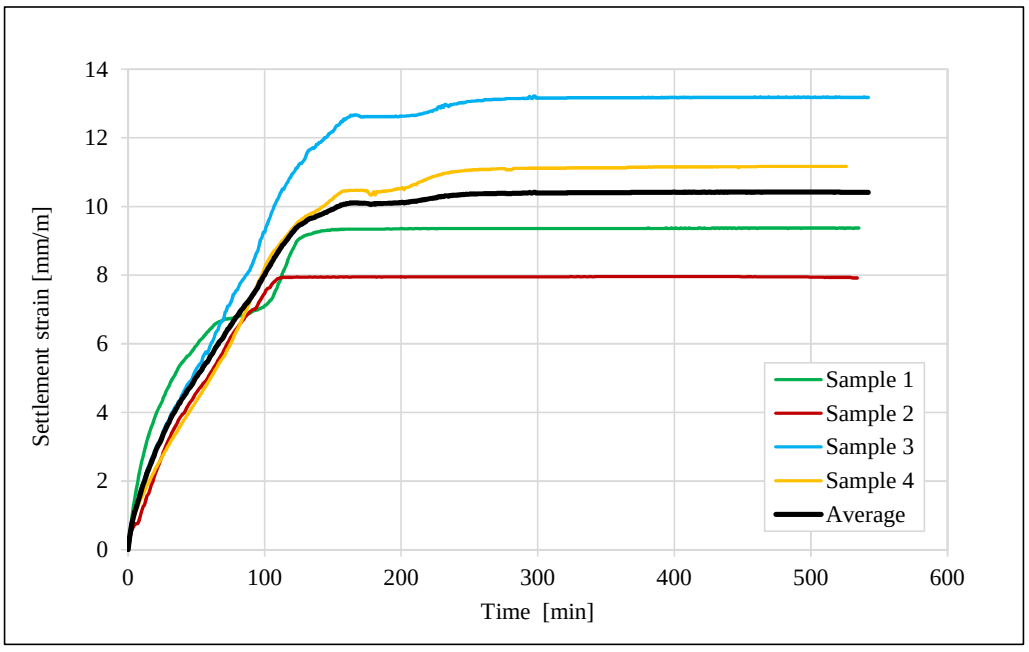

Figure 0.122 High flow REF settlement results

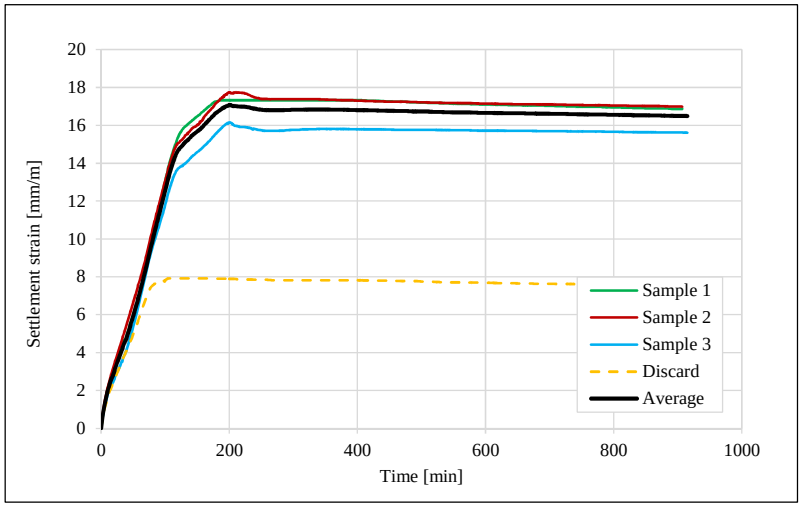

Figure 0.123 PCE_Min settlement results

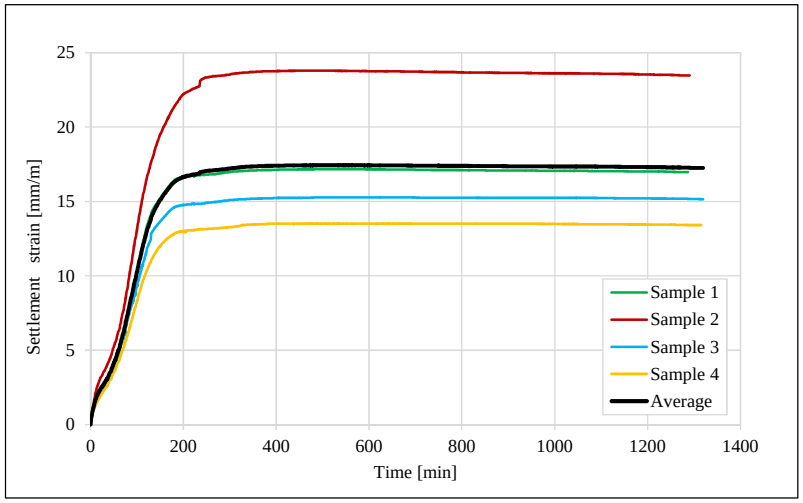

Figure 0.124 PCE_Max settlement results

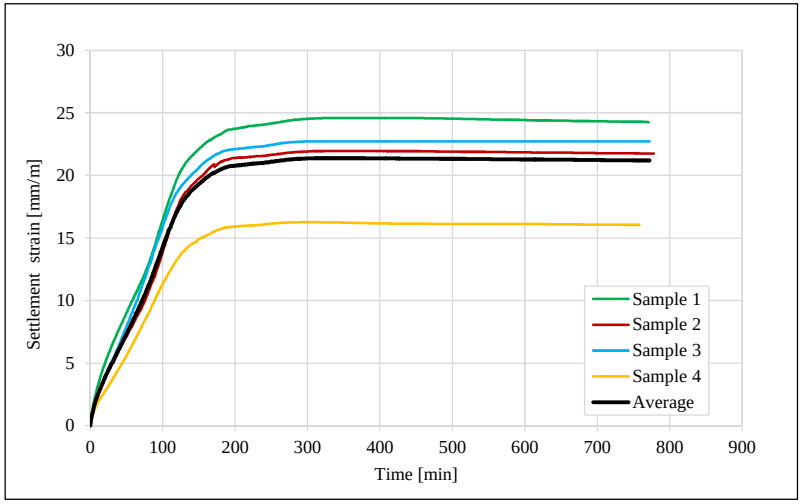

Figure 0.125 SMF_Min settlement results

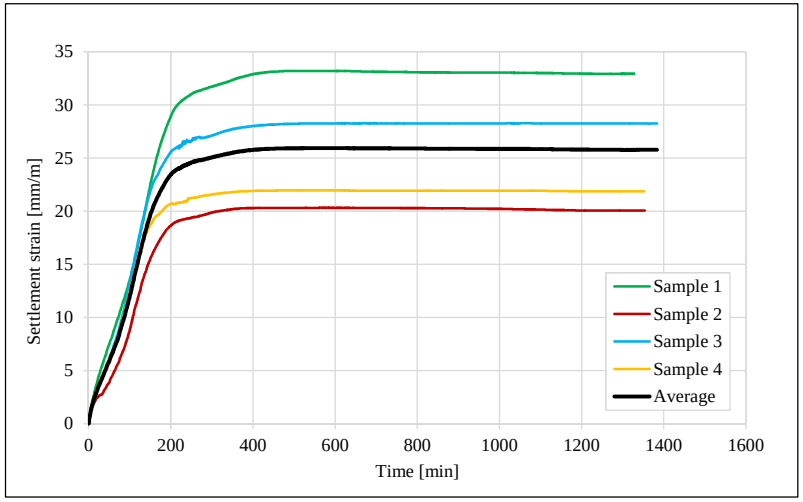

Figure 0.126 SMF_Max settlement results